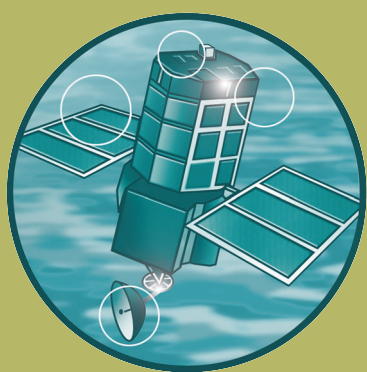


Understanding and Predicting Beach Morphological Change Associated with the Erosion of Cohesive Shore Platforms

R&D Technical Report FD1926/TR



Joint Defra/EA Flood and Coastal Erosion Risk
Management R&D Programme

Understanding and Predicting Beach Morphological Change Associated with the Erosion of Cohesive Shore Platforms

R&D Technical Report FD1926/TR

Produced: December 2007

Author(s): Royal Haskoning, British Geological
Survey, University of Sussex, Newcastle University

Statement of use

This report develops the science and suggests guidance to help flood and coastal erosion risk management policy makers and practitioners make better decisions on coastlines dominated by cohesive shore platforms. It should be noted that it does not constitute official government policy or guidance but provides information for understanding and predicting beach morphological change associated with the erosion of cohesive shore platforms. It will be of particular relevance for coastal managers and researchers engaged in developing understanding of these dynamic features.

Dissemination status

Internal: released internally External: released to public domain

Keywords: Beach; coastal processes; shore platforms; erosion.

Research contractor: Royal Haskoning, British Geological Survey, University of Sussex, Newcastle University.

Defra project officer: Jonathan Rogers (Mouchel Parkman), followed by Peter Allen Williams (Defra) followed by Stephen Jenkinson (Defra).

Publishing organisation

Department for Environment, Food and Rural Affairs
Flood Management Division,
Ergon House,
Horseferry Road
London SW1P 2AL

Tel: 020 7238 3000 Fax: 020 7238 6187

www.defra.gov.uk/environ/fcd

© Crown copyright (Defra) 2007

Copyright in the typographical arrangement and design rests with the Crown. This publication (excluding the logo) may be reproduced free of charge in any format or medium provided that it is reproduced accurately and not used in a misleading context. The material must be acknowledged as Crown copyright with the title and source of the publication specified. The views expressed in this document are not necessarily those of Defra or the Environment Agency. Its officers, servants or agents accept no liability whatsoever for any loss or damage arising from the interpretation or use of the information, or reliance on views contained herein.

Published by the Department for Environment, Food and Rural Affairs (Dec 2007). Printed on material that contains a minimum of 100% recycled fibre for uncoated paper and 75% recycled fibre for coated paper.

PB No 12807

Executive summary

Background Context

Cohesive shore platforms are developed in relatively non-resistant material and the irreversible erosion of these landforms plays a large part in controlling the functioning of the wider coastal system. In order to manage this coastal system most effectively, an improved understanding is required amongst coastal scientists and managers of the erosion and weathering processes governing the behaviour of these landforms, and also of their interactions with beaches and backing sea cliffs. This research project has aimed to improve our technical understanding of the roles of the different parameters and processes that contribute to the downwearing of cohesive shore platforms through:

- a detailed review of existing literature;
- innovative field work campaigns at two contrasting platform-beach sites in the UK;
- laboratory analyses of collected samples; and
- a series of numerical model tests.

The improved scientific knowledge gained from the study has been translated into preliminary 'best practice' guidance for coastal managers.

Literature Review

Cohesive shore platforms tend to be located in some of the most rapidly eroding parts of the UK, such as Holderness, Essex and Kent. The erosion and weathering of cohesive shore platforms has three often overlooked, but nonetheless critical, implications on the functioning of the wider coastal system since:

- (i) the platform tends to regulate wave energy impinging on the toe of a sea cliff and, over time, the rates of platform downwearing tends to govern the rates of cliff recession;
- (ii) platform morphology has an important relationship with beach form; and
- (iii) platform downwearing processes release significant volumes of sediment into the wider coastal system.

Previous literature has investigated the function of cohesive shore platforms within the wider coastal system. There is general agreement that the rate of platform downwearing is a key control on the long-term rate of cliff recession. Effectively, the whole profile is considered in many cases to retreat uniformly while maintaining a relatively uniform cross-shore shape. Since most profiles are steeper towards their upper limits, the rate of downwearing of the upper platform is often greater than at the mid and lower platforms.

Cohesive platform profiles with very little overlying beach have been identified in the literature as being similar in shape to profiles of completely sandy beaches along the same shoreline. Previous model tests have revealed the criticality of the ratio between beach sediment thickness and beach particle size on platform behaviour, with low ratio relationships leading to exposure of the underlying platform and high ratios resulting in more stable beaches.

Cohesive shore platform behaviour also has critical implications for the performance of coastal defence schemes since downwearing rates also potentially affect:

- (i) effective water depth at the toe of shoreline structures, leading to increased loading conditions and overtopping volumes; and
- (ii) undermining of the toe of defences.

The key control on all of the above behaviours and interactions is the rate of vertical lowering of the platform. This 'downwearing' rate, which integrates processes of marine erosion and subaerial weathering, is influenced by the geology and geotechnical properties of the material, the wave climate and tidal regime, the effect of beach sediment cover and the amount of biological activity. The literature reveals eight key processes which can contribute to the overall rate of platform downwearing:

1. Abrasion by mobile non-cohesive surface sediment - where sand or gravel is 'dragged' across the platform's surface by wave or tidal action;
2. Mechanical wave erosion - the extent of which is governed by the shear strength of the platform's material relative to the applied stress of the incoming waves;
3. Biological processes - with burrowing playing a role in weakening the platform surface prior to mechanical erosion;
4. Desiccation and weathering - where repeated wetting and drying causes expansion and contraction of the upper layers of the platform, resulting in tensional fatigue and fracturing;
5. Physio-chemical effects - which can help improve resistance against erosion between clay particles through enhanced net attractive forces, caused by an increase in salt concentration in surface pore water;
6. Freeze-thaw cycles - which leads to frost weathering and increased material fatigue;
7. Stiffening of the fabric due to removal of overburden - caused by 'unloading' effects associated with recession of backing sea cliffs and consequent 'swelling' of the foreshore;

8. Softening of the fabric due to pressure fluctuations induced by waves - due to cyclic loading and unloading related to the passage of waves, again leading to material fatigue.

Despite the importance of these platform downwearing processes, the literature reveals somewhat limited understanding of the relative importance of each process and a real paucity of data relating to their integrated effect in the form of measurements of actual downwearing rates. Whilst measurements have previously been undertaken on rocky shore platforms and on unconsolidated inter-tidal mudflats, downwearing of cohesive shore platforms is poorly researched. Due to the intention of this study in filling this gap in understanding, a review was undertaken of techniques previously used to measure downwearing rates in other environments and the best aspects of some of these approaches were incorporated into the subsequent design and construction of a device to measure cohesive platform downwearing as part of the present study.

Field and Laboratory Investigations

Due to the absence of data relating to downwearing processes and rates on cohesive shore platforms, field and laboratory investigations were undertaken at two contrasting sites in the UK, namely (i) Warden Point, Isle of Sheppey, Kent; and (ii) Easington, East Riding of Yorkshire. These investigations included measurements of platform downwearing, beach morphology and geotechnical and sedimentary properties and were supported by wave transformation modelling.

At Warden Point the platform is wider and shallower than at Easington, and is covered by a much narrower and thinner fringing beach, in contrast to Easington where large sand bars are present and are observed to migrate along the coast. Being relatively lower in the tidal frame, the Easington platform is covered by every tide (and is not uncovered by neap tides), whilst only the highest spring tides fully covered the platform at Warden Point.

The average downwearing recorded on the shore platform at Warden Point over the measurement year (July 2005 to July 2006) was 17.63mm. The upper platform exhibited the greatest average downwearing (30.59mm), the upper middle platform considerably less (13.75mm) and the lower-middle platform the least (8.5mm).

Downwearing at Warden Point was greatest during the February to May 2005 period and, when considering the micro-scale topography, downwearing was much greater on raised areas than in the depressions.

At the Easington shore platform, downwearing rates averaged 41.93mm per year between July 2005 and July 2006. This is considerably greater than the rate recorded at Warden Point and is likely to be influenced by the sand bar/ord migration along the coast. The average annual downwearing rate at the mid platform (43.4mm) was marginally greater than at the lower platform

(39.8mm). No measurements were possible at the upper platform location in July 2006 because the datum box was buried under >5m of beach sediment cover. It is postulated that such extensive beach material coverage is likely to have protected the platform against downwearing.

As at Warden Point, raised areas in the micro-relief experienced greater downwearing than depressions/micro-runnels.

At Warden Point five live fauna species were recorded, namely: American Piddock; Mud Shrimp; Bristle Worm; Sand Mason; and Acorn Barnacle. This is much less diversity than is typically recorded on platforms of other rock types (e.g. chalk and sandstone), but much greater than at Easington where only empty holes or dead shells of the White Piddock were observed (no live species were recorded during the life of the project). This lack of biological activity at Easington is presumably related to the volatility of the beach morphology, with the periodic covering by sand bars being a limiting factor on longevity of colonisation.

At Warden Point, the American Piddock and Mud Shrimp were found in greatest numbers. Peak colonisation of Mud Shrimp was found on the upper platform, with densities decreasing with seaward progression. In contrast, American Piddocks were observed in greatest numbers on the lower platform, near the MLWS mark. There was little difference in biological activity between the summer and winter surveys for all species except the Sand Mason, which declined in numbers in the winter.

The Mud Shrimp is likely to have weakened the upper platform at Warden Point, where it was recorded in greatest numbers, but only within the upper 1cm of platform surface. In contrast, the American Piddock, whilst coinciding with areas of lower downwearing rates, excavates far greater quantities of sediment and weakens the platform to a much greater depth (up to 10cm).

Although large quantities of algae were recorded on several surveys, the protection afforded to the platform is unlikely to have been great since most were attached to pebbles and not the platform surface itself.

No strong relationship could be found between cross shore variations in material strength and the field-measured downwearing rates, suggesting that whilst geotechnical properties are of importance other factors were more dominant controls on downwearing at the two field sites.

The profile surveying showed little change in beach and platform profile morphology at Warden Point between July 2005 and February 2006. In contrast, however, massive changes were recorded at Easington where, following the July 2005 survey, a sand bar covered the profile around November/December 2005, burying the platform over much of its length. The oblique shoreline-attached sand bars are separated along the Holderness coast by shoreline-oblique runnels known as 'ords'. The profile changes recorded between the July 2005, March 2006 and July 2006 surveys are consistent with the southward passage of an ord across the site.

The inshore wave climate at Easington is considerably greater than at Warden Point, with near shore significant wave heights of up to 3.5m modelled (compared with up to 1.5m at Warden Point).

At Warden Point, the greatest influences on platform downwearing were biological processes and mechanical wave action. At Easington, wave action and beach morphology changes were the principal influences. Due to this finding, numerical modelling tests were run to focus on the importance of biological process at Warden Point and beach/platform interactions at Easington.

Numerical Modelling

Numerical modelling offers the potential for deeper understanding of shore morphology than would be possible based on a study involving field observations alone. This is because, once set up, models can be used to simulate responses over a range of timescales to various input scenarios. In the present study, the Soft Cliff and Platform Erosion (SCAPE) model has been used for such scenario testing. This has included a model representation of the study sites at Warden Point and Easington to investigate the roles of biological processes and beach morphology changes, respectively, and to explore, at a generic level, more fundamental questions about cohesive shore platform dynamics.

SCAPE is a systems-based model of the processes and interactions through which the profiles of cohesive shore platforms emerge over long timescales. The foreshore and lower cliff is represented by a series of longshore sections, each of which is composed of a stack of horizontally aligned erodible elements. The underlying equation for the retreat of each element comprises parameters representing the breaking wave conditions, tidal variations, profile slope, and insitu material strength. The model links together modules representing the above parameters with cliff recession and talus formation, sediment transport and beach behaviour.

At Warden Point, the site-specific SCAPE model was run to generate an emergent shore profile. The introduction of a small volume of beach material (per metre run) caused the upper foreshore to steepen such that the resultant model profile was notably higher in the tidal frame than the measured profile at this location. Some process that removes material from the shore was thought not to be represented in the model to cause such a result. Consequently, the model was re-run to test the sensitivity of the profile response to biological activity, with results yielding a modelled profile that was much more closely matched to the measured profile. It can therefore be concluded that the direct material removal and, more importantly, fabric weakening caused by biological activity (burrowing) plays a significant role in shaping the foreshore over long timescales at Warden Point.

A similar site-specific SCAPE modelling exercise was undertaken at Easington, although the representation of a beach across the cohesive shore

profile was complicated by the atypical, perhaps unique, presence and cyclic behaviour of the oblique near shore sand bars and ords. Ultimately, the model represented the upper beach using a conventional empirical curve, with the sand bar represented by a bespoke vector fit to measured field data, with its migration represented by an annual antiphase sinusoidal fluctuation.

Whilst the modelling exercise did produce a reasonably good representation of the Easington foreshore, no firm conclusions could be drawn relating to the interaction between the beach, bar, ords and platforms. More success was achieved, however, with generic testing of beach/platform behaviour. In a series of model experiments a previously validated SCAPE model (developed at Walton-on-the Naze, Essex) was perturbed in various ways to explore the consequences for the profile and shoreline recession rate. The principal focus of these experiments was foreshore dynamic response to changes in beach volumes, caused either directly (e.g. replenished foreshores) or indirectly (e.g. foreshores managed through groynes) through management approaches.

Following introduction of a beach, the shoreline (measured by the cliff toe/upper platform junction) recession rate stopped initially, but then increased again over time. This was caused by the introduced beach material becoming progressively thinner and more widely dispersed across the profile. The benefits of (one-off) beach replenishment therefore were shown to diminish with time. A critical issue associated with this, therefore, is whether replenishment has any residual influence on the longer-term recession rates once its shorter-term benefits are expended. Through further model testing it was demonstrated that a highly non-linear relationship existed between beach volume and long-term recession rate. This means that engineering measures to increase beach volume will only have a lasting effect if the introduced volume is above a certain threshold, which is site-specific and dependent on tidal range, wave conditions and sea level rise.

Further model tests revealed that a decision to cease nourishment or allow groynes to fail, leading to reduced beach volumes, will result in an initially rapid rate of shoreline recession (i.e. 'catch-up'), with rates gradually returning over time to antecedent values. Consequently in these cases, the intervention works have no longer-term residual benefit once stopped or removed.

The effect of sea level rise on profile response was also investigated, with results indicating more rapid recession and an increasingly steep profile form for higher rates of sea level rise. This response is due to sea level rise progressively translating the portion of the profile that is subject to wave attack (and its profile flattening consequences) further landwards to higher elevations. Under higher rates of sea level rise, each elevation in the profile is flattened less as it is exposed to wave attack for shorter durations, meaning that the profile shape changes as it migrates landwards (in contrast to many widely applied assumptions that the form remains constant).

Conclusions and Preliminary Management Guidance

Previously, little work existed on the relative importance of erosion and weathering processes on cohesive shore platforms. The field investigations and laboratory tests in this study have yielded the first direct measurements of key processes and parameters in such detail in the UK. Results demonstrate that whilst a range of factors contribute to overall platform downwearing in some way, it is the incident wave energy and presence (or absence) of a beach that are by far the most significant factors. The tidal range, which influences where wave activity impinges on a profile and also influences wetting-drying cycles across the platform, and both biological activity and material strength are all processes of some importance (e.g. in resisting wave activity or in weakening the material strength in advance of mechanical erosion by waves). However, even these processes can be deemed of considerably lesser significance than the dominating wave conditions and nature of a covering beach.

From the field investigations, it is quite clear that interaction between the beach and the platform occurred at Easington, where migrating sand bars covered the platforms during part of the field campaign. The effect of this was two-fold. Firstly the upper platform was covered by an extensive volume of material which did not move significantly during the experiments. Here, the platform is likely to have been well protected by the beach. Lower down the platform, the more mobile sand bar coverage is likely to have contributed to the high downwearing rates through abrasion of the platform by the non-cohesive material.

Numerical model testing has further investigated these interactions and has demonstrated that the shore platform/beach interaction is an important regulator of landward shoreline recession.

Cohesive shore platforms are formed by processes of erosion. As this happens, material is released that constitutes an important, and often overlooked, component of the coastal sediment budget. These natural processes can, however, be problematic for coastal managers, who are faced with several issues related to the erosion of cohesive shore platforms. The erosion process can directly lead to loss of inter-tidal and sub-tidal habitat, which supports a range of faunal species, although it is recognised that such landforms are not as ecologically rich (in terms of either diversity or density) as other shore platform types (e.g. chalk, sandstone and other rock types) or other inter-tidal landforms (e.g. mudflats and salt marshes). Erosion processes can also expose and lead to the loss of sites of archaeological or geological importance. Further to this, erosion processes release material from the platform that constitutes an important, and often overlooked, component of the coastal sediment budget.

The erosion of cohesive shore platforms can also have negative consequences for coastal engineering interventions. Continued platform lowering, in the absence of a substantial protective beach, can lead to exposure and ultimately failure of the foundation of coastal defence

structures, for example. Elsewhere it is the consequences of the platform erosion on beach levels and cliff recession rates that are of concern to coastal managers.

In essence, the possible management responses to such problems are to:

- (i) Do nothing;
- (ii) Stop or limit the downwearing of the platform; or
- (iii) Manage the consequences of the platform downwearing.

The policy of 'managed realignment' (i.e. the removal of existing coastal defence structures) is also considered in the following discussion for completeness.

Do Nothing:

In situations where no cliff-top or foreshore assets are at risk from the processes, the irreversible downwearing of cohesive shore platforms does not necessarily cause a management concern, either directly or through its effects on beach levels or cliff recession rates. In such situations, the natural erosive processes should be allowed to continue since they release an important contribution of fine-grained material to the coastal sediment budget.

It is important to note that the adoption of a 'Do Nothing' policy will not, in the medium to long-term, necessarily result in a continuation of historic recession rates. This is because climate change, in particular accelerated sea-level rise, is expected to increase the erosion of cohesive shore platforms.

The use of predictive models, such as SCAPE, can provide managers with an indication of the scale of downwearing and cliff recession anticipated under different climate change scenarios so as to inform their decisions about whether or not the processes cause a longer-term risk to assets that are presently set-back from the current cliff edge. This predictive capacity can also be used to help inform land-use planning and development control activities.

Stop or Limit Downwearing of the Platform:

Where the downwearing of cohesive shore platforms, or the consequences of this process on beach levels or cliff recession, does cause a problem for cliff-top or foreshore assets, management efforts could be made to limit the downwearing rate. This is best achieved through the introduction of a protective covering of beach material across the platform. Such beach replenishment activities need to ensure a sufficient volume of material and regular maintenance (e.g. periodic 'top-up' replenishments) in order to remain protective and prevent enhanced erosion through processes of abrasion.

SCAPE modelling revealed that cohesive shore platforms respond dynamically to the introduction of a beach. This is important because it means that benefits seen shortly after beach building may not be sustained without increasing levels of investment. Over time the foreshore steepens, causing the beach to spread across it and become thinner. Ultimately the recession increases, and may return to pre-intervention rates.

The numerical models indicate that the critical threshold determining whether an artificial beach will reduce shoreline recession rates in the medium to long-term is how far it protects across the intertidal zone. If the beach provides some protection to the region between MLWN and MLWS and above then it will begin to have an effect on the equilibrium recession rate. If it does not extend this far then its benefits will only be transient. The further the beach extends beyond this level the more benefit it will bring.

Manage the Consequences of Platform Downwearing:

As an alternative to management of the platform downwearing process itself, a decision could be taken to manage its consequences using shoreline recession control structures. Typically, these may take the form of a seawall or revetment running along the toe of a sea cliff.

In such instances, it must be recognised that the downwearing of the fronting platform is likely to continue leading to:

- Increased wave loading on the defence structures as the water depth in front of them increases, due to both platform downwearing and sea level rise; and
- Decreased structural stability and increased risk of undermining of the foundations of the defence structures; and
- Narrowing of the intertidal zone, potentially leading to its disappearance.

When designing coastal defence structures, engineers incorporate an allowance in the design crest levels to account for predicted sea level rise over the design life of the scheme. Previous MAFF Flood and Coastal Defence Project Appraisal Guidance (MAFF, 1999) suggested an allowance be made of 6mm per year in the areas of the UK where cohesive shore platforms typically are located. More recent Defra Supplementary Guidance (Defra, 2006) has amended this linear allowance and recommends the following alternative arrangements for different future epochs for the east coast of England south of Flamborough Head (i.e. where both Easington and Warden Point are located):

- 1990 to 2025 4.0mm per year;
- 2025 to 2055 8.5mm per year;
- 2055 to 2085 12.0mm per year; and
- 2085 to 2115 15.0mm per year.

Such rates of sea level rise are often considered as significant when planning and designing coastal management responses, yet they are small in comparison to the rates of shore platform lowering measured at Warden Point and, particularly, Easington as part of the present study. Consequently, such downwearing rates should be incorporated into design aspects involving: (i) crest level design (e.g. through changes in overtopping volumes over time); (ii) calculation of wave loading forces on structures; and (iii) determination of foundation depths below existing, and predicted future, foreshore levels.

Managed Realignment:

If a decision is taken to cease or remove engineering interventions such as beach nourishment, groynes, seawalls or revetments to allow a coast to retreat the shoreline is likely to exhibit an initial 'catch-up'. Coastal managers should anticipate and account for these high rates of recession, which occur whilst a state of equilibrium with the governing processes is re-established.

When considering this question it is useful to first estimate the coastline's notional uninterrupted location, i.e. where it *would* be if the intervention had never been made. This can be found by multiplying the equilibrium recession rate prior to the intervention by the duration of the intervention. The numerical modelling work done within this study indicates the following:

- If the intervention protected the profile between MLWN and MLWS then the shoreline may not reach its uninterrupted location;
- If the intervention only protected higher elevations, *and* the coastal system is otherwise unchanged from its pre-intervention state then the shoreline is likely to catch up with its uninterrupted location; and
- The shoreline may retreat landward of its uninterrupted location if the coastal system has changed, for example if the beach volume has reduced, causing a more gently sloping foreshore.

The above issues are becoming increasingly relevant as the policy of managed realignment is now being more pro-actively considered in the second round of Shoreline Management Plans for the coastline of England and Wales.

CONTENTS

	Page
1 INTRODUCTION	1
1.1 Context of the Research Project	1
1.2 Aims and Objectives	2
1.3 Research Methodology	2
2. LITERATURE REVIEW	7
2.1 Background Context	7
2.2 Erosion and Weathering Processes	8
2.2.1 Abrasion by Mobile Non-Cohesive Surface Sediment	8
2.2.2 Mechanical Wave Erosion	10
2.2.3 Biological Processes	11
2.2.4 Desiccation and Wetting	12
2.2.5 Physico-Chemical Effects	13
2.2.6 Freeze-Thaw (Frost)	13
2.2.7 Softening of the Fabric Due to Removal of Overburden	13
2.2.8 Softening of the Fabric Due to Pressure Fluctuations Induced by Waves	14
2.3 The Platform-Beach-Cliff System	15
2.3.1 Cliff Recession-Platform Downwearing Relationship	15
2.3.2 Beach-Platform Interaction	16
2.3.3 Sea-Level Rise and Storminess	17
2.4 Measurements of Platform Downwearing	18
2.5 Summary of Key Findings from Literature Review	22
3 FIELD AND LABORATORY INVESTIGATIONS	24
3.1 Description of Field Sites	24
3.1.1 Warden Point	24
3.1.2 Easington	26
3.1.3 Comparison of Warden Point and Easington Field Sites	30
3.2 Method of Field Investigation	32
3.2.1 Platform Downwearing	32
3.2.2 Platform Biology	45
3.2.3 Profile Surveying	47
3.2.4 Geotechnical Properties	54
3.2.5 Wave Characteristics	61
3.3 Results	62
3.3.1 Warden Point	62
3.3.2 Easington	89

3.4 Interpretation	106
3.4.1 Warden Point	107
3.4.2 Easington	111
3.5 Summary of Key Findings from Field and Laboratory Investigations	113
4 NUMERICAL MODELLING	115
4.1 Introduction	115
4.2 The SCAPE Modelling Tool	115
4.3 Numerical Model Investigations of the Study Sites	118
4.3.1 Warden Point	118
4.3.2 Easington	122
4.4 Numerical Experiments into Beach/Platform Interaction	126
4.4.1 Response of a Foreshore to the Introduction of a Beach	127
4.4.2 Sensitivity of Equilibrium Recession Rate to Beach Volume	128
4.4.3 Consequences of Managed Retreat	131
4.5 Shore Profile Response to Accelerated Sea-level Rise	133
4.5.1 Equilibrium Profile Shapes	134
4.5.2 Equilibrium Recession Rates under Sea-level Rise	135
4.6 Summary of Key Findings from the Numerical Model Testing	138
5 CONCLUSIONS AND PRELIMINARY MANAGEMENT GUIDANCE	140
5.1 Erosion and Weathering Processes of Cohesive Shore Platforms	140
5.2 Platform/Beach/Cliff Interactions	142
5.3 Preliminary Management Guidance	143
6 REFERENCES	147

APPENDICES

- A BIOLOGICAL COUNTING RESULTS FROM WARDEN POINT – JULY 2005
- B BIOLOGICAL COUNTING RESULTS FROM WARDEN POINT – FEBRUARY 2006
- C BEACH SURVEY DATA FROM WARDEN POINT – JULY 2005
- D BEACH SURVEY DATA FROM WARDEN POINT – FEBRUARY 2006
- E BEACH SURVEY DATA FROM EASINGTON – JULY 2005
- F BEACH SURVEY DATA FROM EASINGTON – MARCH 2006
- G BEACH SURVEY DATA FROM EASINGTON – JULY 2006
- H TRIAXIAL STRESS-PATH PLOTS FROM WARDEN POINT
- I TRIAXIAL STRESS-PATH PLOTS FROM EASINGTON
- J PARTICLE SIZE ANALYSIS RESULTS FROM WARDEN POINT
- K PARTICLE SIZE ANALYSIS RESULTS FROM EASINGTON

LIST OF TABLES

Table		Page
2.1	Methods previously used to measure micro- to meso-scale downwearing of rocky shore platforms	18
2.2	Methods previously used to measure micro- to meso-scale lowering of estuarine mudflats	19
3.1	Summary of the principal differences between the Warden Point and Easington field sites	27
3.2	Summary of the results of the TEB reproducibility tests	33
3.3	Traversing Erosion Beam locations at Warden Point	34
3.4	Traversing Erosion Beam locations at Easington	36
3.5	Dates of TEB installation and measurements at Warden Point	37
3.6	Dates of TEB installation and measurements at Easington	38
3.7	Geotechnical samples	49
3.8	In-situ tests	50
3.9	Beach samples taken at Warden Point and Easington	50
3.10	Average daily downwearing rates for the 3 locations at Warden Point	54
3.11	Results of Geonor shear vane tests	70
3.12	Index test results corresponding to triaxial samples	72
3.13	Results of 100 mm CIU triaxial tests	73
3.14	Details of stress-path parameters at failure	74
3.15	Tide Levels at Sheerness	75
3.16	Offshore wind climate at Warden Point	75
3.17	Offshore wave climate at Warden Point	76
3.18	Offshore wave climate at Warden Point	77
3.19	Wave height – period relationship for the offshore wave data at Warden Point	78

3.20	Transformation matrices at Warden Point	78
3.21	Inshore wave climate at Warden Point	79
3.22	Piddock holes found at four sites on Easington shore platform	82
3.23	Results of Geonor shear vane tests	88
3.24	Index test results corresponding to triaxial samples	89
3.25	Results of 100 mm CIU triaxial tests	90
3.26	Details of stress-path parameters at failure	91
3.27	Tide Levels at Spurn Head	92
3.28	Offshore wind climate at Easington	92
3.29	Offshore wave climate at Easington	93
3.30	Offshore wave climate at Easington	94
3.31	Wave height – wave period relationship for the offshore wave data at Easington	95
3.32	Transformation matrices at Easington	95
3.33	Inshore wave climate at Easington	96
3.34	Estimated average wave conditions off the coast of Warden Point for the periods between downwearing measurements based on data from October 2001 to October 2005.	98
3.35	Bivalve borers in UK cohesive shore platforms	99
4.1	Parameter combinations tested	123
5.1	Relative importance of the factors involved in cohesive shore platform downwearing	129

LIST OF FIGURES

Figure	Page
1.1 Study site locations	3
1.2 Warden Point – General view	4
1.3 Easington – General view	5
2.1 Platform and cliff section	7
2.2 Bioerosion on cohesive shore platform	10
2.3 Polygons on cohesive shore platform	11
2.4 Platform downwearing-cliff recession relationship	14
3.1 Shore platform at Warden Point, 22 nd July 2005	21
3.2 Narrow thin beach at Warden Point, 23 rd July 2005	22
3.3 Shore platform at Easington, 25 th July 2005	23
3.4 Shore platform at Easington, 25 th July 2005	24
3.5 Gully erosion at Easington, 26 th July 2005	25
3.6 Armoured mud balls at Easington, 26 th July 2005	26
3.7 Morphology indicating direct erosion of the cliffs by waves at Easington, 26 th July 2005	27
3.8 The Traversing Erosion Beam (TEB)	29
3.9 The Traversing Erosion Beam in use at Warden Point	29
3.10 Distance from centre of steel datum box vs. difference between first and second measurements at Warden Point	33
3.11 Map showing TEB locations on the Warden Point platform	35
3.12 Map showing TEB locations on the Easington platform	36
3.13 Easington in March 2006	38
3.14 Saturated sand above the steel datum box at location C, Easington	39
3.15 Dissected block of cohesive shore platform	40

3.16	GPS measurement	41
3.17	Environment Agency benchmark P23006	42
3.18	Environment Agency benchmark P23007	42
3.19	Warden Point: GPS survey profiles measured on 22-23rd July 2005	43
3.20	Warden Point: GPS survey profiles measured on 3-4th February 2006.	44
3.21	Easington: GPS survey profiles measured on 25th-26th July 2005.	45
3.22	Easington: GPS survey profiles measured on 31st March 2006	46
3.23	Easington: GPS survey profiles measured on 14th July 2006	47
3.24	Preparation of U100 tube (triaxial) sample	48
3.25	Preparation of shear-box sample	48
3.26	Panda penetrometer test	49
3.27	Map showing sample and test locations at Warden Point, Isle of Sheppey	51
3.28	Map showing sample and test locations at Easington	51
3.29	Making repairs to the triaxial test specimen	52
3.30	GDS (Bishop & Wesley type) 100 mm automated stress-path triaxial system	53
3.31	Warden Point, location A1: seasonal change in platform elevation, July 2005 to July 2006	56
3.32	Warden Point, location A2: seasonal change in platform elevation, July 2005 to July 2006	56
3.33	Warden Point, location B1: seasonal change in platform elevation, July 2005 to July 2006	57
3.34	Warden Point, location B2: seasonal change in platform elevation, July 2005 to July 2006	57
3.35	Warden Point, location C1: seasonal change in platform elevation, July 2005 to July 2006	58

3.36	Warden Point, location C2: seasonal change in platform elevation, July 2005 to July 2006	58
3.37	America piddock	59
3.38	<i>Corophium volutator</i>	60
3.39	U-shaped burrows produced by <i>Corophium volutator</i>	61
3.40	Minute surface perforations produced by <i>Corophium volutator</i>	61
3.41	Head of <i>Nereis pelagica</i>	62
3.42	Tube constructed by <i>Lanice conchilega</i>	63
3.43	Acorn barnacle, <i>Semibalanus balanoides</i>	64
3.44	Summer distribution of organisms across the platform at Warden Point	65
3.45	Winter distribution of organisms across the platform at Warden Point	65
3.46	Warden Point, Profile 'bte', July 2005	68
3.47	Warden Point: Thin beach in July 2005	69
3.48	Warden Point site. Beach sediment	69
3.49	Warden Point: Beach sediment seen in February 2006	70
3.50	Panda penetrometer test profiles- Warden Point	71
3.51	Casagrande plasticity plot for triaxial samples	72
3.52	Particle size analysis grading curves matching triaxial samples	73
3.53	Mohr circle locus plots for triaxial tests	74
3.54	Wind rose at Warden Point	76
3.55	Offshore wave rose at Warden Point	77
3.56	Inshore wave rose at Warden Point	79
3.57	Easington, location B: changes in platform elevation, July 2005 to July 2006	81

3.58	Easington, location C: changes in platform elevation, July 2005 to July 2006	81
3.59	Scattered clusters of former piddock burrows at Easington	83
3.60	Easington: Narrow intertidal platform exposed at low water	84
3.61	Easington: Shore-normal profiles in July 2005	85
3.62	Easington: Cross-shore profile 'bpb' showing changes between July 2005 and July 2006	86
3.63	Easington: Profiles along top of beach July 2005-July 2006	87
3.64	Panda penetrometer test profiles	88
3.65	Casagrande plasticity plot for triaxial samples	89
3.66	Particle size analysis grading curves matching triaxial samples	90
3.67	Mohr circle locus plots for triaxial tests	91
3.68	Wind rose at Easington	93
3.69	Offshore wave rose at Easington	94
3.70	Inshore wave rose at Easington	96
3.71	Diagram showing the major factors influencing cohesive shore platform downwearing	97
4.1	Discretisation of the model foreshore profile	105
4.2	Flowchart of processes and interactions represented by SCAPE	106
4.3	One thousand years of Warden Point model profile evolution, in 100 year 'snapshots'	108
4.4	100 year snapshots of profile evolution over 1000 years following the introduction of a beach	109
4.5	Upper model foreshore and beach, and survey data	109
4.6	Profile obtained accounting for biological weathering	110
4.7	1000 years of Easington model profile evolution, in 100 year 'snapshots'	112

4.8	Surveyed beach profiles at Easington	113
4.9	Easington model profile	114
4.10	Shoreline recession with and without a beach	116
4.11	Shore profiles at three stages following the introduction of a beach (horizontally aligned by cliff toe)	117
4.12	Relationship between (normalised) equilibrium recession rate and beach volume	118
4.13	Relationship between (normalised) equilibrium recession rate and beach volume for three tidal ranges	119
4.14	Definition of Z_b	120
4.15	Relationship between normalised equilibrium recession rate and the normalised level of the seaward limit of the beach	120
4.16	Recession of a shore given 50 years of beach nourishment	121
4.17	Model shore profiles in 100 year timesteps before, during and after the temporary beach nourishment	122
4.18	Equilibrium profile sensitivity to rate of sea-level rise	123
4.19	Equilibrium recession rates of the parameter tests	124
4.20	Normalised rates of sea-level rise and equilibrium recession	125
4.21	Example model recession rates before and after a step change in sea-level rise from 2mm/a to 6mm/a at 6000 years	126
5.1	Exposure of sheet piling at the toe of a seawall	133

ACRONYMS AND ABBREVIATIONS

GPS	Global Positioning System
LiDAR	Light Direction and Range
OD	Ordnance Datum
SCAPE	Soft Cliff and Platform Erosion
SSSI	Site of Special Scientific Interest
TEB	Traversing Erosion Beam
UK	United Kingdom

GLOSSARY

Abrasion - the erosion caused by material carried by wind and water.

Armoured mudball – rolled masses of mud, the surfaces of which are covered with a protective layer of sand and/or gravel.

Backshore – area above high water but which can be affected by coastal processes.

Barton Clay - a geological formation of clays and silts exposed on the Hampshire and Isle of Wight coasts.

Beach - a deposit of non-cohesive material (e.g. sand, gravel) situated on the interface between dry land and the sea (or other large expanse of water) which results from the action of present-day hydrodynamic processes (i.e. waves, tides and currents) and sometimes of winds. Extends from the low water mark to the effective landward limit of storm waves.

Bedforms- topographic sedimentary features (e.g. sand waves, ripples) resulting from the movement of fluid over a non-cohesive substrate.

Bivalve – an aquatic animal living on or within the sediment with two protective calcareous shells (valves); relative of the snail.

Chalk - a geological formation of fine-grained calcareous limestone exposed as sea cliffs in southern and eastern England.

Clay - a fine-grained sediment with a typical particle size of less than 0.002 mm.

Cohesive sediment - sediment containing a significant proportion of clays, the electromagnetic properties of which causes the particles to bind together.

Consolidated - compacted by overburden to reduce pore space and increase density; applied to fine-grained sediment.

Cross-shore transport - the movement of sediment approximately perpendicular to the shoreline.

Diagenesis - the process of alteration of a sediment which take place after its deposition.

Diatom – microscopic single-celled plant.

Dynamic equilibrium - a state of balance between environmental forces acting on a landscape and the resisting earth material which fluctuates around an average that is itself gradually changing.

Episodic - composed of a series of discrete events rather than as a continual process.

Eocene – a period of geological time between 54 and 33 million years ago; during which time the London Clay and Barton Clay were deposited.

Erosion – the process of removal of material from the land or sea bed by the action of natural forces.

Flocculation - the aggregation of clay particles in suspension to form larger composite grains (flocs).

Foreshore - a morphological term for the part of the shore between mean low water and the landward limit of normal wave action.

Glacio-lacustrine - descriptive of lakes at the borders of glacial ice sheets.

GPS - Global Positioning System – an accurate navigational and positioning system by which the location of a position on or above the earth can be determined by interpreting signals received from a constellation of satellites.

Gravel (Pebbles)- loose, fragments of rock larger than sand but smaller than cobbles. Particles larger than 4 mm but less than 64 mm.

Holocene – a period encompassing the last 10,000 years of earth history.

Hydrodynamic - the process and science associated with the flow and motion in water produced by applied forces.

Impermeable - not allowing the passage of fluids.

Lag deposit - a deposit of coarser sediment left behind after the removal of finer material by water or wind transport.

Lithology - the general description of the material of a sediment or sedimentary rock.

London Clay - a geological formation of silts and clays found in southeast England and exposed along the coasts of Essex, Kent, Sussex, Hampshire and the Isle of Wight. Deposited during the Eocene period.

Longshore bar - an elongate ridge of sediment, occurring on the lower beach or shoreface parallel or sub-parallel to the shoreline.

Longshore transport - the movement of sediment approximately parallel to the shoreline predominantly as a result of wave action.

Mercia Mudstone - a geological formation of mudstones exposed along the coasts of Devon, Somerset and South Wales.

Mineral - a naturally occurring inorganic crystalline solid that has a definite chemical composition and possesses characteristic physical properties.

Mud - sediment with particles finer than sand (0.063mm). A term which encompasses both clay and silt.

Mudstone – a lithological term descriptive of consolidated or lithified mud.

Nearshore – the zone which extends from the surf zone to the position marking the start of the offshore zone.

Numerical modelling - the analysis of coastal processes using computational models.

Overconsolidated - a clay that has been compacted under overburden pressure greater than that existing at the present time. Implies that overburden has been removed at some time in the past.

Overtopping - the process where water is carried over the top of an existing defence due to wave action.

Pleistocene - an epoch of the Quaternary Period characterised by several glacial ages commencing approximately 1.6 million years ago.

Pore water - the fluid found in the interstitial spaces between sediment grains.

Sand - sediment particles, with a diameter of between 0.063 mm and 2 mm. Sand is generally classified as fine, medium or coarse.

Sea-level rise - the general term given to the upward trend in mean sea level resulting from a combination of local or regional geological movements and global climate change.

Shear strength - the maximum shear stress that can be applied in a particular direction. When exceeded the material can be said to have 'failed'.

Shear stress - the horizontal stress that results from a fluid passing over a sediment surface.

Shore platform - a platform of exposed bedrock exposed within the intertidal and subtidal zones.

Silt - sediment particles with a grain size between 0.002 mm and 0.063 mm, i.e. coarser than clay but finer than sand.

Sodium adsorption ratio – a relation between soluble sodium and soluble divalent cations, which can be used to predict the exchangeable sodium fraction of soil, equilibrated with a given solution.

Stratigraphy – the study of stratified rocks especially their sequence in time.

Subaerial - the portion of the environment above the water surface; subaerial processes due to atmospheric conditions (e.g. rainfall, temperature, pressure, etc.).

Surf zone - the zone within which waves break as they approach the shore.

Suspended sediment - fine-grained sediment transported in suspension.

Tertiary – a period of geological time between the untimely demise of Dinosaurs and the Pleistocene.

Till - poorly-sorted sediments deposited by a glacier.

Triassic - a period of geological time between 250 and 205 million years ago; during which time the Mercia Mudstone was deposited.

Unconsolidated - sediment particles packed in a loose arrangement. Relatively uncompacted or overconsolidated.

Undermining – erosion at the base, e.g. of a seawall or cliff, so that the feature above becomes unstable and is vulnerable to collapse.

Weathering – the process by which rocks are broken down and decomposed by the action of external agencies such as wind, rain, temperature changes, plants and bacteria.

1 Introduction

1.1 Context of the Research Project

Cohesive shore platforms are developed in relatively non-resistant, consolidated or partially consolidated cohesive sediments. The irreversible erosion of these platforms plays a large part in controlling the functioning of the wider coastal system, including beach form and shoreline recession, and poses significant problems for management. These features are typically found along the most rapidly eroding coastlines in the country, for example north Kent, Holderness and Essex, where sand and gravel beaches overlie cohesive clay materials, such as London Clay, glacial till and Holocene mud. The relative contributions from a variety of processes, which result in downwearing of the platform, and our present understanding of the interaction between the platform and non-cohesive beach sediments is insufficient to effectively inform the decision making process. Relatively little research has been undertaken to date that specifically addresses the issues of cohesive shore platform erosion, its interaction with beach behaviour and its consequences for coastal management. A lack of data and an under-developed understanding of the erosion processes of cohesive shore platforms have also handicapped numerical model development.

It is now generally accepted that the rate of vertical lowering of the shore platform is the key control in the long-term recession of cohesive shorelines over periods of decades. In turn, this lowering rate is probably dependent on the geology, strength of the cohesive material (and any strength changes due to weathering), rate of sea-level rise, wave climate, tidal regime and the effect of beach sediment cover. These parameters control the magnitude of the complex variety of weathering and erosion processes operating on the platform. Weathering processes such as desiccation and wetting, and physico-chemical (salt water) effects play a significant role in weakening the cohesive material prior to its erosion by marine processes, which include abrasion by mobile non-cohesive surface sediment and mechanical erosion by breaking and shoaling waves.

The relative magnitude of all these processes is poorly understood and has been debated for many years. Even more poorly understood is the role of biological activity, both in erosive and protective capacities, on and within the cohesive surface. A previous study (Royal Haskoning *et al.*, 2004) concluded, therefore, that further research should target answering the fundamental underlying principles of cohesive shore platform erosion, providing a baseline starting point for better strategic management.

1.2 Aims and Objectives

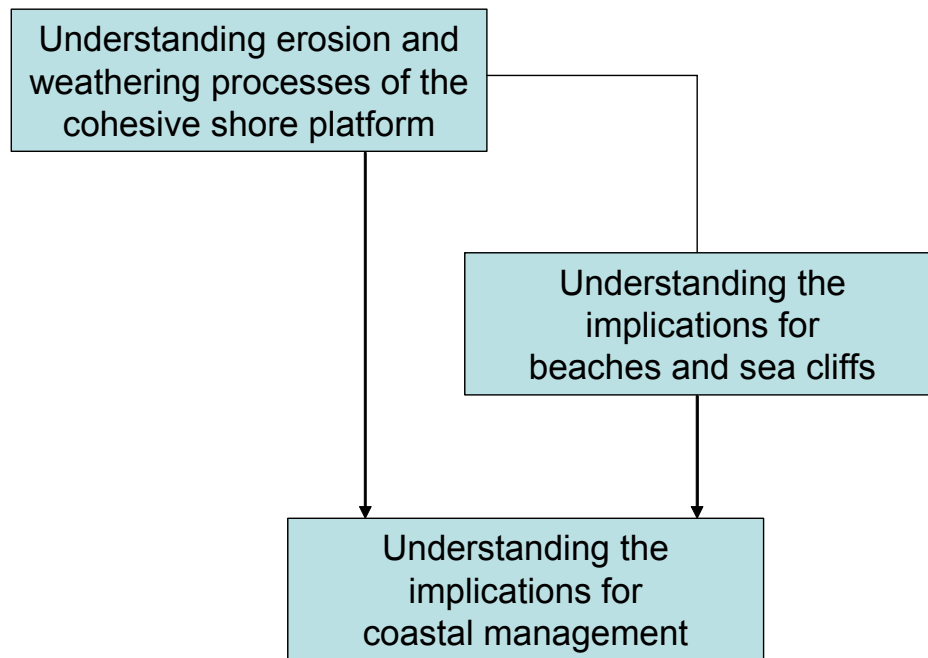
The aim of this research project is to examine and improve our technical understanding of the roles of the different parameters and processes that contribute to the downwearing of cohesive shore platforms.

Specific objectives include:

1. To design and implement field programmes at two contrasting platform-beach sites along the United Kingdom coast to collect samples and gather *in situ* data on downwearing rates, geology and biology;
2. To test the platform and beach samples in the laboratory for geotechnical, biological and textural parameters;
3. To interpret and integrate the field data and the results of the sample tests into an overall assessment of platform weathering and erosion, and their relationships with platform and beach morphology;
4. To collate current and historical data of the sites and neighbouring shorelines to describe their local geomorphological interactions and their role in larger coastal systems;
5. To use the data, geomorphological descriptions and interpreted results to produce models of the sites;
6. To produce a final report on the scientific results of the project and translate these into preliminary best practice guidelines regarding management of these shorelines; and
7. To draw conclusions relevant to practical shoreline management arising from the project, through cross-Theme exchange of results and an end user workshop.

1.3 Research Methodology

To deliver the overall aim and specific objectives of the research, the following methodology was adopted, aimed at understanding both: (i) the processes governing weathering and erosion of cohesive shore platforms; and (ii) the interaction of cohesive shore platforms with the neighbouring cliff and/or beach landforms within the context of a coastal geomorphological system. Both of these have been investigated with the aim of understanding the implications for coastal management, as illustrated overleaf.



Firstly a detailed **literature review** was undertaken to identify key previous research into the topics under investigation. Numerous documents were reviewed, including published papers and so-called ‘grey’ literature. This literature review aimed to collate existing information of the weathering and erosion processes of cohesive shore platforms, such as abrasion, wave action, biological processes, dessication and wetting, physico-chemical effects, freeze-thaw cycles, removal of overburden, and pressure fluctuations induced by waves.

This was followed by a **field measurement and sampling programme** at two contrasting sites in the United Kingdom, the first a platform of London Clay at Warden Point on the Isle of Sheppey, Kent, and the second a till platform at Easington on the East Riding of Yorkshire coast (Figure 1.1). These sites were chosen because they provide contrasting geological, geomorphological, geotechnical and biological make-ups.

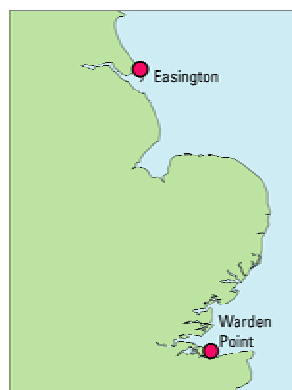


Figure 1.1. Study site locations

The site at Warden Point on the Isle of Sheppey lies at the foot of landslipped London Clay sea cliff. The cliff edge lies at approximately 48 metres OD. Cliff recession rates have averaged 1.93m/year (Nicholls et al., 2000). The tidal range on this section of coast is approximately 5.2 metres at mean spring tides. A broad, exposed, platform of London Clay is located in the intertidal zone at this point (Figure 1.2) which has been observed to have been continually exposed over several years prior to the commencement of this project. Adjacent coastlines also have an intermittently exposed platform, extending for several hundred metres southwards towards Leysdown and for more than a kilometre westwards towards Minster. A narrow beach exists at the cliff toe which ranged from 14 to 18 metres wide during the survey period.



Figure 1.2. Warden Point: General view of exposed London Clay platform with thin, narrow beach at foot of slipped London Clay sea cliff (July 2005).

The site at Easington lies at the foot of a section of unbroken cliffs just north of the Easington Gas Terminals. The cliff edge lies at approximately 20 metres OD. Cliff recession rates at this location have averaged 1.97m/year (East Riding Yorkshire Council data). The tidal range on this section of coast is approximately 5.7 metres at mean spring tides. An exposed platform of glacial till is located in the intertidal zone at this point (Figure 1.3) landward of a low sand bar which is slightly oblique to the line of the beach. A substantial mixed sand and gravel beach between 60 and 100 metres wide existed between the platform and the cliff toe during the survey period.



Figure 1.3. Easington: General view of study site showing glacial till platform (July 2005). Oblique sand bar visible at extreme right of picture.

The field campaign focussed on collecting the following data at each site:

- *In situ* measurements of platform geotechnical properties and collection of samples for further geotechnical testing (platform) and particle size analysis (beach) in the laboratory;
- Deployment of the Traversing Erosion Beam for *in situ* measurement of platform downwearing;
- Examination of *in situ* biological processes and sample collection for subsequent laboratory work;
- Surveying the platform and beach surfaces, and the location and elevation of point samples and measurements; and

- Site-specific and regional assessment of platform geology and geomorphology.

Two field campaigns were originally envisaged at each site, one to collect relevant data in the summer of 2005 and one in the winter of 2005/06, to enable seasonal comparisons to be made. In practice, however, this original plan needed to be revised at Easington because of particular beach morphology changes that were experienced. This meant that attempts at a winter 2005/06 campaign were initially delayed and then proven unsuccessful, with subsequent attempts further aborted. It was only in summer 2006 that the second campaign at Easington was successfully executed. In contrast, although only two campaigns were originally planned at Warden Point, five campaigns in total were successfully executed, thereby adding value to the study through improved data availability leading to improved downwearing understanding, being based on a seasonal basis throughout the course of a full year.

Finally a **numerical modelling** exercise was undertaken to investigate behaviour at both of the field sites and at a generic level of testing. This part of the study used the SCAPE (Soft Cliff And Platform Erosion) model, which adopts a systems-based assessment of the processes and interactions through which the profiles of cohesive shore platforms emerge. SCAPE investigated how the biological and morphological characteristics measured at Warden Point and Easington affected cohesive shore platform development and further investigated how management intervention, such as the introduction of a beach (e.g. through replenishment) influenced platform behaviour. The model was also used to investigate the sensitivity of the processes and interactions to tidal range, wave height and sea level rise.

Results from the above literature review, field measurement and sampling campaigns and numerical modelling exercises were then synthesised and interpreted to provide some preliminary best practice guidance in terms of the management of cohesive shore platforms and their interactions with beaches and sea cliffs

2. Literature Review

2.1. Background Context

Cohesive shore platforms are developed in relatively non-resistant, consolidated or partially consolidated cohesive sediments, such as Holocene mud, glacial till and soft mudrock. Commonly, an eroding cliff backs the platform; the cliff is the portion of the profile above the cliff toe and the platform extends from the cliff toe into deeper water (Figure 2.1). Hence, the platform may be lithologically and geotechnically closely related to the lower layers of the cliff. Many stretches of cohesive platform in the United Kingdom lie along the most rapidly eroding shorelines (Holderness, Essex and north Kent) and pose significant problems for management (Royal Haskoning *et al.*, 2004).

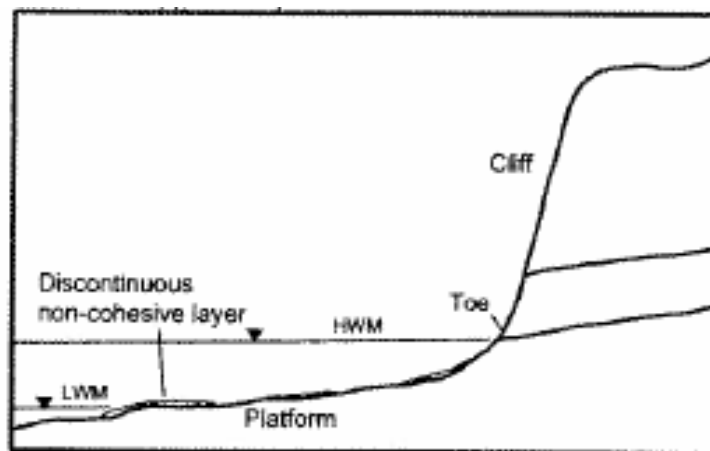


Figure 2.1. Platform and cliff section

The coastal engineers need to be better able to understand and manage cohesive platforms because of their importance in controlling the function of the wider coastal system, including cliff recession rates, beach form and sediment budgets. Indeed, many estimates of sediment yield from shoreline erosion ignore the important contribution made by the platform (see Balson *et al.*, 1998). Platform erosion produces fine sediment, and may produce coarse sediment into the coastal system. The coarser sediments tend to be moved along the shoreline by wave and tidal action influencing other areas as they pass whilst finer sediment is removed offshore in suspension.

In addition to being an important influence on the beach, the platform also acts as a regulator of cliff erosion. Over time, in a natural state, the rates of downwearing of the platform and retreat of the cliff tend to reach a state of equilibrium as the platform regulates the wave energy impinging on the cliff toe. Maximum observed rates of platform lowering can be surprisingly high, especially on shorelines developed in glacial tills or clays. This can become an important consideration in the long-term performance of coastal defence structures, especially if these structures have their foundations in the same formations.

The water depth in front of structures such as sea walls can increase significantly over their design life, affecting the overtopping performance and standard of protection as well as increasing the risk of undermining and failure. Rates of cliff retreat and platform lowering can also be severely affected by defensive structures erected on adjacent stretches of coastline that interfere with sediment supply and wave activity.

This literature review appraises previous research in the field of cohesive shore platform weathering and erosion. It examines how platform downwearing may affect the sustainability of adjoining beaches, the evaluation of any backing cliffs, and their influence on sediment budgets. Management techniques are described and examples are provided of management practices and experience along these types of shorelines in the United Kingdom. Finally, a review is provided of the techniques available to measure rates of downwearing of these features.

2.2. Erosion and Weathering Processes

The rate of vertical lowering of the platform is likely to be a key control in the long-term recession of cohesive shorelines over periods of decades. In turn, this is dependent on its geology, strength of the cohesive material (and any strength changes due to weathering), rate of sea-level rise, wave climate, tidal regime and the effect of beach sediment cover. These parameters control the magnitude of the complex variety of subaerial weathering and marine erosion processes operating on the platform (Royal Haskoning *et al.*, 2004). Weathering processes may be directly responsible for the actual break up of the cohesive material (or contribute to its weakening), which is then eroded by marine processes. Here follows a description of eight key processes.

2.2.1 Abrasion by Mobile Non-Cohesive Surface Sediment

Erosion of cohesive platforms may occur by abrasion as a result of the movement of sand and gravel by waves and currents across its surface (Davidson-Arnott and Askin, 1980; Kamphuis and Hall, 1983; Bishop *et al.*, 1993; Skafel and Bishop, 1994; Davidson-Arnott and Ollerhead, 1995).

Kamphuis and Hall (1983) and Kamphuis (1983, 1987, 1990) found that even a small amount of sediment in the eroding fluid substantially lowered the critical shear stress for erosion of cohesive clay. Kamphuis (1990) found that erosion rate increased by a factor of between three and eight when sand was present in the flow. Erosion in the presence of sand takes place by a general planing down of the surface as well as by formation of gulleys in the direction of flow which tend to coalesce and result in general lowering of the surface (Kamphuis, 1987, 1990). Long-term erosion rates with sand measured inside the surf zone peak at the zone of wave breaking, and decrease in an offshore direction (Bishop *et al.*, 1993; Skafel and Bishop, 1994).

Available wave energy and the hardness of the abrading sediment relative to the platform surface largely control the amount of abrasion. Kamphuis (1987) suggested a very strong relationship between cliff recession rate and wave

height, such that a 3 m high wave is more than 500 times more erosive than a 0.5 m high wave. Paradoxically, Trenhaile (1987) argued that extremely severe storms probably cause less abrasion than minor storms since the higher energy levels suspend or saltate most of the particles rather than dragging them across the platform surface.

For abrasion to occur, overlying sand or gravel in contact with the platform has to be moved over the surface by wave action. There is a critical thickness, that varies with the sediment size and wave energy, above which the sediment in contact with the surface can no longer be moved under wave action, and abrasion ceases (Davidson-Arnott and Ollerhead, 1995). Using a laboratory flume, Bishop et al. (1993) and Skafel and Bishop (1994) found that the continuous presence of a sand (particle size 0.51 mm in their experiments) layer 10 mm or more in thickness was sufficient to provide protection against erosion of the underlying till, for the wave conditions used in their tests.

A number of predictive models have attempted to evaluate the depth of the layer of sediment mobilised by waves but a definitive model has proved elusive. Sunamura and Kraus (1985) argued that mixing depth increases in an approximately linear fashion with the wave height, for breaking waves up to 1.5 m high. For greater wave heights, the rate of increase in the mixing depth decreases with increasing wave height. They also found that mixing depth is strongly related to wave period in the larger wave height region. Ferreira et al. (2000) defined the thickness of sand required to limit wave disturbance of the platform as exceeding one-fifth of the wave height.

The mobility of surface sediment is important, because if a beach is frequently changing position and thickness, the underlying cohesive sediments will be exposed to erosive situations more often. This can occur due to the migration of bedforms or the onshore offshore movement of sediment in nearshore bars and on the beach (Pringle, 1981, 1985). The presence of longshore bars can protect the underlying cohesive sediment from exposure and subsequent downwearing. As these bars migrate with changing wave and water level conditions, different areas of the underlying cohesive profile become exposed in the troughs between the bars (Pringle, 1981, 1985; Davidson-Arnott et al., 1999; Perez Alberti et al., 2002). Thus, over a period of years, all of the profile will be exposed to erosion. Where overlying sand or gravel forms a beach on the landward margin of a platform, evidence from soft, non-cohesive sediments such as chalk suggests that abrasion is concentrated in a zone on the seaward margin of the beach where there is an intermittent thin cover.

O'Brien et al. (2000) described a situation in the Severn Estuary where modern intertidal mudflat sediments overlie older consolidated Holocene muds. The thickness of modern sediment varies on a seasonal basis and erosion of the underlying Holocene material takes place when the mudflat has been removed by erosion. It was suggested that winter storm wave activity aided by freeze-thaw and ice scour were the main erosive agents.

2.2.2 Mechanical Wave Erosion

Particles may be eroded from the platform by the shear stresses associated with breaking and shoaling waves (Philpott, 1984). Erosion occurs with the formation of a pattern of fine cracks, created by pressure fluctuations at the boundary under turbulent flow. Detached particles are then prised from the surface (quarrying or plucking) and entrained in the flow, leaving a pitted surface. The spacing, orientation, aperture and persistence of discontinuities (e.g. joints and fractures) in the platform surface control its susceptibility to wave plucking processes and control the size of blocks removed by erosion processes. Erosion of the platform will continue due to wave action in an offshore direction until the closure depth is reached.

Philpott (1984), Nairn et al. (1986) and Kamphuis (1987) argued that the rate of platform lowering is strongly influenced by the rate of wave energy dissipation in the surf zone. They found rapid erosion rates where depth changes quickly and where reflected waves (from backing cliffs or seawalls) concentrate turbulent energy dissipation in shallow water. Skafel and Bishop (1994) suggested that where plunging breakers occur and the turbulence is able to penetrate to the cohesive surface, erosion rates in clear water (no sand) could be comparable to or even higher than those with sand outside the surf zone. Davidson-Arnott and Ollerhead (1995) and Amin and Davidson-Arnott (1997) showed that average annual total wave energy at the shoreline correlates positively with shoreline recession and is a good indicator of it. They argued that the significance of total wave energy as a predictor is greatest where beaches are narrow and there is limited protection from nearshore sediments.

Although mechanical wave erosion may be accomplished by a number of processes, few direct measurements have been made. The relative importance of these processes has usually been inferred from morphological evidence, which may be ambiguous.

2.2.3 Biological Processes

There is clear evidence that boring organisms make a significant contribution to the erosion of cohesive platforms, though not in every location.

Bioerosion may be negligible on rapidly eroding platforms, where there is little time for colonisation, whereas it may be more significant on slow eroding platforms where damaging organisms have time to colonise.

The distribution of the biological cover is also regulated by tides, which govern the duration of submersion and exposure of the platform, and hence the abundance of the flora and fauna. This factor may cause significant variations in cross-shore erosion thresholds due to biological factors.

Biological weathering processes, such as burrowing, are influential in weakening the platform surface (Figure 2.2), thus paving the way for larger-scale mechanical erosion.

Hutchinson (1986) provided an indication of the intensity of bio-erosion on a cohesive platform. He found crustaceans living in the top 9mm of the platform with a density of around 10,000 individuals per square metre, in burrows up to 1mm in diameter. He also identified boring bivalves, which were up to about 120mm long with burrows 10 - 30mm in diameter. The number and density of these burrows can greatly reduce the surface strength of the colonised rocks.

Not all organisms are destructive. Some can reduce the rates of erosion by protecting the surface of the platform. For example, the growth of seaweed during summer months may produce a dense mat which blankets a cohesive platform, reducing erosion. In winter, as the seaweed cover diminishes, erosion may increase.

The influence of organisms on the erosion dynamics of cohesive platforms has received little attention. Understanding the contribution of biological erosion relative to marine and subaerial processes, and the relative importance of the erosive and protective effects of the organisms themselves requires further research.



Figure 2.2. Example of bioerosion on the cohesive platform, Isle of Sheppey, north Kent

2.2.4 Desiccation and Wetting

Alternating phases of desiccation and wetting result in the thin upper layers of the cohesive sediment being cracked into polygons (10s of millimetres across, Figure 2.3).

Water attached to clay particles by quasi-crystalline bonds exerts pressures and repeated wetting and drying causes expansion and contraction, resulting in tensional fatigue and fracturing.

The surface of these polygons may then be removed as flakes by the sea. This process is probably confined to the intertidal zone, and is probably most active in well-drained areas and greater in summer than in winter. Wetting and drying can also occur as a result of rainfall episodes, although the erosive effect will be different to that caused by tidal cycles since there is an absence of salts.



Figure 2.3. Polygons on the surface of the cohesive shore platform on the Isle of Sheppey, north Kent.

2.2.5 Physico-Chemical Effects

Physico-chemical processes strongly influence the properties of the surface layers of cohesive platforms. Arulanandan et al. (1975) and Hutchinson (1986) argued that an increase in salt concentration in surface pore water from the intrusion of sea water may increase the net attractive forces between clay particles, increasing the degree of flocculation and hence improving the resistance of the clay to erosion. The degree to which this effect will occur will depend on the clay content and the chemical properties of the cohesive sediment. The mechanisms by which water enters the pores of cohesive platform sediments are complex (seepage and diffusion for example) and no specific work has been carried out.

2.2.6 Freeze-Thaw (Frost)

Frost weathering has been recognised as an important factor in the development of shore platforms in environments that are colder than the United Kingdom (Trenhaile and Rudakas, 1981; Matthews et al., 1986) and as a process formerly active during the cold conditions of the Late Glacial (Dawson, 1980; Larsen and Holtedahl, 1985).

Although the process is rare in the United Kingdom, during extreme winters there is evidence that freeze-thaw can cause severe damage to shore platforms. For example, Harris and Ralph (1980) described frost-induced lowering of the London Clay platform at Clacton by 0.3 m in a few weeks, during the hard winter of 1962/63.

Shore platforms are potentially susceptible to freeze-thaw conditions whenever air temperatures are below freezing, but the sea remains unfrozen. Each time the tide falls, the platform surface, saturated or nearly saturated with seawater, is exposed to freezing conditions. When the tide returns, submersion in seawater with its high thermal conductivity will quickly lead to thawing of any ice formed. Thus, low temperatures may only cause frost damage to shore platforms when they coincide with low-tide conditions. Rapid thawing by tidal inundation may increase the effectiveness of frost weathering. A higher number of freeze-thaw cycles will increase material fatigue.

2.2.7 Softening of the Fabric Due to Removal of Overburden

As the backing cliff retreats, the emerging platform experiences the effects of unloading. This causes a reduction in pore-water pressure to values below those associated with mean sea level. A process of swelling therefore takes place (particularly in overconsolidated materials) in which the pore-water pressures within the platform recover slowly to their long-term, fully equilibrated values. This reduces the strength of the platform material, as effective stresses diminish and water content increases. The magnitude of the strength reduction will depend upon clay content, mineralogy, degree of cohesion, and stress history of the platform.

Differential swelling will cause further weakening due to localised straining and the opening of fissures and joints. Parallel furrows may form, running normal to the cliff, typically around 0.1-0.2 m in width and depth (Hutchinson, 1986). Many of these features are likely to be eroded stress relief joints whereas others may be exposed shear surfaces.

Except for the work of Bromhead and Dixon (1984) and Hutchinson (1986), little attention has been paid to the depression of pore-water pressures on cohesive platforms. No accurate analyses of this phenomenon, linking the changes of geometry, and stress and strain with the generation and dissipation of depressed pore water pressures, have yet been made.

2.2.8 Softening of the Fabric Due to Pressure Fluctuations Induced by Waves

The strength of cohesive sediment may be reduced by softening of the surface layers caused by cyclic loading and unloading (pressure fluctuations) related to the passage of waves (Davidson-Arnott and Askin, 1980; Davidson-Arnott, 1986a, b; Davidson-Arnott and Ollerhead, 1995; Davidson-Arnott et al., 1999; Davidson-Arnott and Langham, 2000). The softening is manifested as the entry of water into the substrate pore system, leading to generation of positive pore water pressures, decreasing strength close to the surface. Lee and Focht (1976) tested clays under laboratory conditions, and found development of significant cyclic strains under pulsating stresses, and the strength after cyclic loading was less than the normal static undrained strength. Even if the passage of waves does not cause immediate erosion, it is capable of fatiguing the platform material leaving it more susceptible to erosion processes.

The softening process occurs in the top few centimetres of the cohesive sediment (Davidson-Arnott and Ollerhead, 1995; Davidson-Arnott and Langham, 2000) and can take place over a period of months (Skafel and Bishop, 1994). An increase in shear strength occurs with depth in the sediment indicating that softening proceeds from the surface downward. The process leads to the progressive development of soft patches reducing the shear strength to the point where direct erosion by fluid forces is feasible, particularly in deeper water where the cohesive sediment is exposed. As the process probably occurs at different rates across the platform, lowering could be highly variable in the short-term, depending on the degree of softening at any given point.

Davidson-Arnott and Langham (2000) found that the shear strength of the exposed cohesive substrate decreased during periods of low wave activity, whereas periods of high wave activity resulted in removal of a layer of softened material, thus exposing harder underlying cohesive sediment. They suggested that erosion during a storm may be related to the thickness of the softened layer that develops during non-storm periods. The softening process may be supported by field studies which have shown that significant erosion of a cohesive substrate can occur in water depths where wave induced shear stresses are well below the critical shear stress for erosion, and where there is

little coarse sediment available for abrasion (Coakley et al., 1986; Davidson-Arnott, 1986a, b).

Initial results on the process of softening in glacial till subject to erosion have been published (Davidson-Arnott and Langham, 2000). Further work is required to quantify the rate at which the softening process occurs, to ascertain the thickness of the layer involved in the process, to isolate the effects of softening from those of abrasion and to determine the relative significance of softening in platform downwearing.

2.3 The Platform-Beach-Cliff System

If a cohesive platform is associated with a beach and cliff then its downwearing is best understood in the context of a broader geomorphological system that includes all three morphological components. An understanding of the relationship between the platform, cliff and beach is critical to the implementation of strategies for management.

2.3.1 Cliff Recession-Platform Downwearing Relationship

It is generally agreed that the primary control on the long-term rate of cliff toe erosion is the rate of vertical lowering of the beach and platform (Davidson-Arnott and Askin, 1980; Philpott, 1984; Hutchinson, 1986; Kamphuis, 1987; Davidson-Arnott et al., 1999). Hutchinson (1986) suggested that cliff erosion follows at a rate that the platform erosion permits (Figure 2.4). While subaerial processes may dictate when and where a slope failure will occur, the frequency of failures over the long-term is strongly determined by the rate at which the platform is eroded.

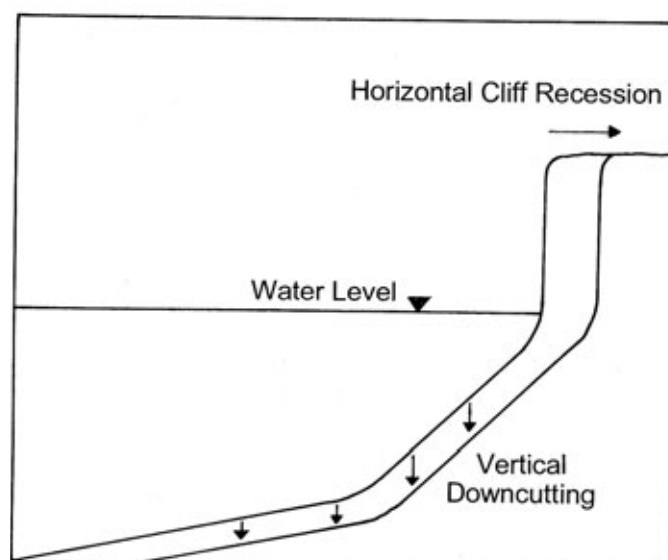


Figure 2.4. Platform downwearing-cliff recession relationship.

Where shoreline recession is rapid and long-shore transport removes coarser non-cohesive sediments, the whole profile retreats uniformly, while maintaining a relatively steady shape. Because the profile generally becomes steeper towards the cliff, this necessitates greater platform downwearing towards the shore to preserve the profile shape (Figure 2.4). The observation that the profile tends to retain its shape as it recedes suggests that toe erosion is in dynamic equilibrium with platform lowering and characteristic cohesive profile shape exists. The emergence of a dynamically stable profile form shows that the retreat rates of the cliff and platform tend to equalise and consequently the long-term rate of cliff retreat can be directly related to the rate of platform downwearing and the associated profile retreat, by the equation:

$$d = r.\tan(a)$$

where: d = vertical rate of platform lowering; r = corresponding horizontal rate of cliff erosion; a = platform gradient at a point.

If this equation is applied to the Holderness coast where $r \sim 2 \text{ myr}^{-1}$ and $\tan(a) \sim 0.01$, then a vertical platform erosion rate of about 0.02 myr^{-1} is calculated. For the long-term evaluation of the shore (over centuries) this represents a reasonable approximation. However, cliff recession is measured at the scale of decades, whereas platform lowering has often been measured over a period of a few years. Since platform development is thought to occur over long timescales (1000s of years), extrapolating short-term data may not provide a reliable estimate of rate of development. This problem is compounded by climate change, which means that future wave conditions and rates of sea level rise (and therefore recession) will be different to those acting during recent history.

2.3.2 Beach-Platform Interaction

If a non-cohesive beach is to provide adequate protection to a cohesive shore it must be high enough and wide enough that the cliff is beyond the reach of most extreme combinations of water level and wave action. The beach must also extend below water to the limiting depth for significant erosion of the underlying profile, which is related to water levels, incident wave power and the erosion resistance of the cohesive bed. The beach deposit must also be thick enough so that it is not fully mobilised by extreme events or dynamically influenced by the impermeable cohesive material beneath. This means that there must always be enough beach material in place to fully cushion the effects of wave pressure fluctuations including those that occur under breakers in the surf zone.

Generally, if a beach is present at a cohesive shore it is likely to be comprised of sediment released locally or moved in by longshore transport. If the platform and cliff are good sources of non-cohesive sediment then the material released will tend to increase the size of the beach. Larger beaches are capable of providing more protection against wave erosion, so this trend will act to reduce cliff retreat. If beach material were not removed by other means it would continue to build and cliff retreat would continue to reduce. In general, however, hydrodynamic processes remove beach material, deplete its volume,

reduce its protective capability and so promote erosion, shore retreat and the release of more sediment. If a beach remains then this tendency to remove sediment must be balanced by the supply of sediment, and in this way the local differential in sediment transport rate can be a strong determinant in shoreline retreat.

Platforms receive less protection from intermittent sparse beaches, and in this situation the relationship between shore retreat and transport differentials is less strong, but the beach can still exert a strong influence on the profile. Kamphuis (1990) demonstrated that cohesive platform profiles with very little overlying sand were similar in shape to profiles of completely sandy beaches along the same shoreline. In other words the eroded cohesive bed closely resembles the equilibrium shape that the overlying non-cohesive sediment would take in the absence of a cohesive substrate. Where the cohesive profile is lower than the natural profile for the non-cohesive sediment, the latter will deposit out of the fluid, into these depressions. Such deposited sediment then provides localised protection to the cohesive bed. When cohesive material protrudes through a beach, the non-cohesive sediment will be mobilised over the high spots, abrading them rapidly. By this process the eroded cohesive shore profiles eventually come to resemble stable profiles for the sand sizes overlying them.

Kamphuis (1983) found that the presence of an impermeable platform beneath the beach increased beach mobility. The impermeable layer prevented the complete dissipation of pore water pressures and caused a reduction in the net strength of the sand layer and its resistance to removal by waves. Powell (1990) conducted model tests on shingle beaches of varying thicknesses (up to 325mm) and particle sizes above an impermeable layer in a laboratory wave flume. He found that the effect of an underlying impermeable layer on the resultant beach profile could be categorised according to the ratio of the beach thickness and the median particular size. Shingle beaches with a ratio of less than about 30 generally led to exposure of the impermeable layer and the beach structure broke down. For ratios between 30 and 100 the profile was distorted but the effects confined mainly to horizontal displacements, and for ratios greater than 100 the beach profile was largely unaffected.

2.3.3 Sea-Level Rise and Storminess

Erosion at the base of a cliff is a critical factor in maintaining cliff instability, so the shore platform and its sediment cover ultimately control cliff retreat by dissipating energy. This cliff-platform relationship will be altered by potential future sea-level rise. Ray and Hooke (1997) recognised two different scenarios, each having a different response to sea-level rise:

- bare platforms that regulate erosion through their geometry. Typically, they erode and widen as sea-level rises.
- platforms covered by protective sediments that can accumulate to form beaches at the cliff toe. These can potentially build-up to preserve the profile morphology with rising sea level.

As a cliff retreats the platform may widen so that wave dissipation increases. At the same time the platform is being downcut and is gradually inundated by rising sea levels. For shores that mature to a state of dynamic equilibrium the wave dissipation and rate of sea-level rise produce a distribution of erosion that tends to maintain the profile shape. A change to incident wave conditions (and therefore wave dissipation) or rate of sea-level rise would be expected to produce different distributions of erosion and, consequently, different profile shapes and retreat rates.

Generally, higher rates of sea-level rise are expected to cause greater retreat rates. This is because, unless countered by enhanced sedimentation, sea-level rise should produce increasing nearshore water depths that allow waves to break further inshore. This is especially important over platforms with no beach. Higher sea levels would also reduce the return period of extreme sea levels produced by storm surges (i.e. increased storminess) and erosive events at the cliff toe would become more frequent. However the role of the shore profile is not fully understood; it appears to act as a regulator to the recession rate and may mitigate effects of climate change. In addition, higher recession rates imply increased beach volumes, which will tend to reduce erosion, so the response of a shore platform to sea-level rise and increased storminess must be considered in the context of the broader geomorphic system.

2.4 Measurements of Platform Downwearing

Since the rate of platform downwearing is dictated by a complex and time-varying combination of the processes described in Section 2.2, the measurement of downwearing rates is seen as a means of understanding the morphological integration of these processes at a particular site. Although cohesive shore platforms occur in many parts of the United Kingdom, there has been little attempt to measure rates of downwearing (Brew, 2004). In this regard, most focus has previously been on rocky shore platforms or inter-tidal mudflats.

The term 'downwearing' is used throughout this document to denote the wearing down of platform surfaces by either weathering or erosion. This is because consensus is lacking regarding the relative importance of different processes in shaping shore platforms in general and further study is required in order to ascribe downwearing rates to particular processes. From the limited information available it is difficult, if not impossible, to generalise about the rates of downwearing of cohesive shore platforms on UK coasts.

Although their material properties differ, cohesive shore platforms are subject to similar processes and share morphological characteristics with hard-rock shore platforms. They also share some similarities with unconsolidated estuarine mudflats. Consolidated clay, of which cohesive shore platforms are typically composed, is softer than most other rock types and erodes rapidly. As described in Section 2.2, it may also expand and contract with changes in water content and may expand due to pressure release, for example when cliff retreat removes the weight of overlying sediment. Eroded clay may also subsequently flocculate and be re-deposited as a layer of unconsolidated fluid mud on the

platform surface. In order to design an instrument to measure micro- to meso-scale downwearing of cohesive shore platforms as part of the present study, the methods that have previously been used on rocky shore platforms (Table 2.1) and estuarine mudflats (Table 2.2) were evaluated.

A range of techniques, including Laser Induced Direction and Range (LiDAR), satellite and aerial photogrammetry, and macro-scale laser scanning, are used to measure macro-scale changes in coastal environments (Brew, 2004). Standard surveying, using a total station or differential GPS, provides centimetre accuracy of vertical measurement. It does not, however, guarantee exact relocation on the horizontal surface, which has to be performed by a rover surveyor using “stake-out”. Elevation changes can, at best, be measured at meso-scale using this technique. The present study requires detailed measurement of platform downwearing to near millimetre accuracy and so none of these techniques were suitable.

Table 2.1 Methods previously used to measure micro- to meso-scale downwearing of rocky shore platforms

Method	Detail	Author(s)	Limitations for measuring micro to meso-scale downwearing on a cohesive shore platform
<u>Above Water Mechanical Devices</u> (Micro-Erosion Meter [MEM] and Traversing Micro-Erosion Meter [TMEM])	The triangular device is placed on three positioning screws, which have been previously installed into the platform surface. The legs of the device have flat, conical and wedges shapes so that when they are placed onto the positioning screws they are held firmly in a Kelvin grip, and the instrument can be accurately replaced for each re-measurement. A measurement probe is lowered onto the platform surface and a reading of the elevation taken from the attached engineer's gauge. The instrument is rotated on its screws and to give a total of 3 measurements. The TMEM allows more than three readings (typically ~ 30) per measurement site.	Askin and Davidson-Arnott (1981) High and Hanna (1970) Trudgill <i>et al.</i> 1981 Williams <i>et al.</i> 2000	Rapid downwearing (> 5 cm yr ⁻¹) quickly removes the positioning screws from the platform surface. Using longer screws or rods would counteract the high downwearing rates, but would leave the screws increasingly exposed to damage (bending or shearing) by the impact of shingle moved by the waves. The measurement probe may erode the surface to be measured. Soft cohesive sediment and spring-loading of the probe exacerbates this problem. Only small-scale downwearing (millimetres) is measured, not the removal of larger fragments (meso - macro change).
<u>Below Water Mechanical Devices</u> (Underwater Abrasion Table)	The Underwater Abrasion Table consists of a perspex grid, 70 x 70 cm, containing 36 measurement holes. It is mounted on three legs, which sit on three positioning studs or bolts fixed into the shore platform. Divers have to push measurement probes down through the grid to determine surface elevation.	Schrottke (2001) Schrottke (2003) Schwarzer <i>et al.</i> (2003)	The probes are not spring-loaded, but otherwise the problems are similar to those of the MEM.
<u>Laser-based Devices</u> (Laser Scanner)	The Laser Scanner uses a laser which is suspended from a portable aluminium frame and moved by stepping motors. The height from the laser to the platform surface can be measured every millimetre over an area of 40 x 40 cm in 2 hours. Within the measurement area small studs are glued into the platform and act as reference points for each successive scan. Detailed microtopographic maps are overlaid and downwearing rates calculated.	Williams <i>et al.</i> (2000) Swantesson <i>et al.</i> (2006)	Unsuitable for use on wet surfaces and therefore impossible to use on cohesive shore platforms with water and/or mud filled depressions and runnels.

Table 2.2 Methods previously used to measure micro- to meso-scale lowering of estuarine mudflats

Method	Detail	Author(s)	Limitations for measuring micro to meso-scale downwearing on a cohesive shore platform
Rods, canes and poles	Rods/canes/poles are sunk into the sediment. Topographic surveying can be used to measure the elevation of the sediment adjacent to the rod or the rod top or graduations inscribed along the side are assumed a set datum. Scour often occurs at the rod-platform junction. To avoid measuring the scoured area, measurements are often taken further away from the rod.	Bale <i>et al.</i> (1985) Frostick and McCave (1979) O' Brien <i>et al.</i> (2000)	Scour at the rod-platform junction may lead to an overestimation of platform downwearing. Thin protruding rods are exposed to damage from coarse sediment moved by waves which would make measurements impossible.
Buried plates	Plates of a variety of materials, from plastic to metal, have been buried in estuarine mud up to a depth of 20 cm, often in transects. A measurement probe is pushed down through the sediment to measure the depth from the surface to the buried plate, which acts as a marker horizon.	Amos <i>et al.</i> (1988) Allen and Duffy (1998)	Burying plates destroys the fabric of cohesive shore platforms. Sediment replaced on top of the plates would be significantly weaker than the surrounding platform surface and thus easily eroded to expose the plate. Plates must be buried very deeply to compensate for rapid downwearing (> 5 cm yr ⁻¹). It would then be difficult to push the probe through the sediment to the plate.
Mechanical gauges (Sedimentation-Erosion Table [SET])	The SET is a removable levelling arm, which, when in operation, is attached to a substantial stake sunk deep into the sediment. Nine lightweight measurement probes with shock absorbing tips are dropped into place on the sediment surface to measure the elevation.	Boumans and Day (1993) Cahoon <i>et al.</i> (2002)	Sinking a deep, immovable stake into the consolidated clay of a cohesive shore platform is not a simple task. The stake may attract vandals.
Optical devices (Argus Surface Meter IV [ASM] and the Photo-Electronic Erosion Pin [PEEP])	The ASM IV and PEEP both consist of a rigid rod with an array of optical sensors. The ASM also has a pressure sensor and built-in data logger.	Couperthwaite <i>et al.</i> (1998) Gutkuhn, (pers. comm.)	Only measures elevation change to a resolution of centimetres. Easily damaged on high-energy open coasts. Expensive: a separate device is needed to measure each point.

Method	Detail	Author(s)	Limitations for measuring micro to meso-scale downwearing on a cohesive shore platform
Acoustic devices (Scan Group Ltd's ARX II acoustic scour monitor and the Altus Altimeter)	The return sound of the sediment surface is used to measure the elevation relative to the device. The resolution is +/- 1 mm	Christie <i>et al.</i> (1999) Deloffre <i>et al.</i> (2005)	Measurements are collected only during inundation. Expensive: a separate device is needed to measure each point. Easily damaged on high-energy open coasts.

Of the measurement techniques listed in Tables 1 and 2, only the Sedimentation-Erosion Table (SET) showed potential for use on cohesive shore platforms. The installation of a single substantial foundation stake, although difficult, provides a set datum able to withstand damage in a high-energy open-coast environment enabling measurements to be made over more than a year. Features of Cahoon *et al.*'s (2002) SET were incorporated in the development of a new device designed and fabricated by the University of Sussex specifically for measuring downwearing of cohesive shore platforms as part of the present study (see Section 3.4.1 for further details).

2.5 Summary of Key Findings from Literature Review

Previous literature has investigated the function of cohesive shore platforms within the wider coastal system. There is general agreement that the rate of platform downwearing is a key control on the long-term rate of cliff recession. Effectively, the whole profile is considered in many cases to retreat uniformly while maintaining a relatively uniform cross-shore shape. Since most profiles are steeper towards their upper limits, the rate of downwearing of the upper platform is often greater than at the mid and lower platforms.

Cohesive platform profiles with very little overlying beach have been identified in the literature as being similar in shape to profiles of completely sandy beaches along the same shoreline. Previous model tests have revealed the criticality of the ratio between beach sediment thickness and beach particle size on platform behaviour, with low ratio relationships leading to exposure of the underlying platform and high ratios resulting in more stable beaches.

Cohesive shore platform behaviour also critical implications for the performance of coastal defence schemes since downwearing rates also potentially affect:

- (i) effective water depth at the toe of shoreline structures, leading to increased loading conditions and overtopping volumes; and
- (ii) undermining of the toe of defences.

The key control on all of the above behaviours and interactions is the rate of vertical lowering of the platform. This 'downwearing' rate, which integrates processes of marine erosion and subaerial weathering, is influenced by the

geology and geotechnical properties of the material, the wave climate and tidal regime, the effect of beach sediment cover and the amount of biological activity. The literature reveals eight key processes which can contribute to the overall rate of platform downwearing:

1. Abrasion by mobile non-cohesive surface sediment - where sand or gravel is 'dragged' across the platform's surface by wave or tidal action;
2. Mechanical wave erosion - the extent of which is governed by the shear strength of the platform's material relative to the applied stress of the incoming waves;
3. Biological processes - with burrowing playing a role in weakening the platform surface prior to mechanical erosion;
4. Desiccation and weathering - where repeated wetting and drying causes expansion and contraction of the upper layers of the platform, resulting in tensional fatigue and fracturing;
5. Physio-chemical effects - which can help improve resistance against erosion between clay particles through enhanced net attractive forces, caused by an increase in salt concentration in surface pore water;
6. Freeze-thaw cycles - which leads to frost weathering and increased material fatigue;
7. Stiffening of the fabric due to removal of overburden - caused by 'unloading' effects associated with recession of backing sea cliffs and consequent 'swelling' of the foreshore;
8. Softening of the fabric due to pressure fluctuations induced by waves - due to cyclic loading and unloading related to the passage of waves, again leading to material fatigue.

Despite the importance of these platform downwearing processes, the literature reveals somewhat limited understanding of the relative importance of each process and a real paucity of data relating to their integrated effect in the form of measurements of actual downwearing rates. Whilst measurements have previously been undertaken on rocky shore platforms and on unconsolidated inter-tidal mudflats, downwearing of cohesive shore platforms is poorly researched. Due to the intention of this study in filling this gap in understanding, a review was undertaken of techniques previously used to measure down-loading rates in other environments and the best aspects of some of these approaches were incorporated into the subsequent design and construction of a device to measure cohesive platform downwearing as part of the present study.

3 Field and Laboratory Investigations

Due to the absence of previous data relating to observed downwearing rates of cohesive shore platforms, field investigations were undertaken during this study at two contrasting sites on the east coast of England, namely Warden Point (Kent) and Easington (East Riding of Yorkshire). Some of the parameters under investigation were measured in situ in the field, with for others samples were taken and subject to laboratory testing. This section provides a description of the field sites and of the in situ and laboratory investigations undertaken at, and results derived from, each site during the course of the study.

3.1 Description of Field Sites

3.1.1 Warden Point

The cliffs and platform at the Warden Point study site consist of London Clay. The intertidal zone predominantly comprises a wide (100-500 m), low gradient (0.5° - 2°) undisturbed shore platform flanked by areas of disturbed deep-seated landslides (Figure 3.1). Seaward of low water is believed to be a wide shallow platform covered by sand.



Figure 3.1. Shore platform at Warden Point, 22nd July 2005. Study site is in the centre of photograph with disturbed landslides exposed to either side.

At the start of the field investigation, the shore platform was backed by a 20 m wide beach (Figure 3.2) at the base of highly unstable cliffs.

The surface of the beach comprised gravel, cobbles and boulders towards the lower part (including septarian nodules and rounded mud balls of London Clay).

The beach was also littered with anthropogenic material, such as bricks and other pieces of masonry. The beach fines towards the cliff toe becoming sand/gravel with numerous shell fragments. The beach was thin, only around 15 cm deep at the cliff toe thinning to 10 cm depth at mid level (see Figure 3.2).



Figure 3.2. Narrow thin beach at Warden Point, 23rd July 2005.

The platform at Warden Point is exposed all year round and there is little interaction with the beach. Biological activity and shrink-swell (in summer) may be mechanisms by which the platform weathers.

Nicholls *et al.* (2000) used 1:2500 County Series maps of the Ordnance Survey to measure coastal change using three shoreline indicators: mean low water, the cliff base/mean high water and the cliff-top. They showed that the cliffs at Warden Point have retreated at around 1.9 myr^{-1} between 1867 and 1998 producing large quantities of fine-grained sediment and small amounts of sand and gravel. The base of the cliff has retreated landward at a similar rate to the cliff top showing that the general cliff form has been conserved over time. However, mean low water moved 150 m shoreward between 1897 and 1966, suggesting a steepening of the shore platform (Nicholls *et al.*, 2000). However, the measurement of mean low water on older maps is not particularly reliable given the methods used to measure it prior to aerial photographs, the low slopes characterised by the platform and changes in vertical datum.

Nicholls *et al.* (2000) suggested that most of the sediment eroded from the Isle of Sheppey coast comes from the subaerial cliff.

The Warden Point study site forms part of the Sheppey Cliffs and Foreshore SSSI. It forms part of one of the best known Palaeogene (upper part of London Clay) sites in the United Kingdom. The stratigraphical and palaeoenvironmental significance of the site is a reflection of its extremely well preserved fossil fauna and flora. It is also important for its series of deep-seated, rotational landslips. Permission to carry out the invasive field methods was obtained from Lionel Solley at English Nature (now part of Natural England).

3.1.2 Easington

The East Riding of Yorkshire coast is an eroding cohesive coast with intermittent sand cover. The cliffs and platform are composed predominantly of glacial tills of differing character (Bell, 2002). At the time of the summer field work (25th-26th July 2005), the Easington study site (a few hundred metres north of the gas terminal) comprised of 14-m high till cliffs fronted by a 70 m wide, thick beach (around 4-5 m at the cliff toe) sloping down to a narrow exposed platform behind an oblique sand bar with a 'lagoon' between the bar and the platform (Figures 3.3 and 3.4). The beach is composed of sandy gravel with a thin veneer of mainly sand with some gravel. The platform is composed of decalcified till with a few pebbles and cobbles. It is a dynamic system where the degree of sediment cover may change due to the migrating sand bar and changes in beach dimensions. There is some biological activity, but significantly less than at Warden Point.



Figure 3.3. Shore platform at Easington, 25th July 2005. 'Lagoon' and sand bar in background. Exposed platform is about 30 m wide.



**Figure 3.4. Shore platform at Easington, 25th July 2005.
Exposed platform is about 30 m wide.**

Cliff erosion along the East Riding of Yorkshire coast is due to a combination of subaerial weathering and toe erosion by waves, which causes instability and results in frequent small slumps a few tens of metres wide (Balson *et al.*, 1996). Retreat of the cliffs is matched by the landward erosion of the platform which slopes at $0.5\text{-}0.75^\circ$ down to a depth of about 11-16 m below OD where a break of slope marks a change to a more gently sloping $0.05\text{-}0.2^\circ$ offshore platform (Balson *et al.*, 1996). The latter profile is effectively flat and the vertical erosion rate is low, whereas the former is actively eroding. This erosion causes a permanent lowering of the platform.

Erosion of the Easington platform may be partly controlled by features within the till. Closely spaced gullies perpendicular to the shoreline and to a depth of 0.5 m are common on the studied platform (Figure 3.5). As the tide ebbs, water exits the base of the beach and flows across the platform cutting gullies into it. This appears to be a significant process of erosion. Where the gullies are absent the till surface is smooth or irregularly undulating. However, some larger gullies are cut oblique to the general shore-perpendicular smaller gullies and are located along planes of weakness (disturbed areas of till). As the beach becomes thinner and narrower to the north of the study site, the gullying becomes less frequent and less deep. This may be related to the amount of water that can be released from storage in the beach.



Figure 3.5. Gully erosion at Easington, 26th July 2005.

Pringle (1985) suggested that during the summer, desiccation cracking may affect parts of the till surface which then breaks up into small flakes of till, which themselves form into short-lived till 'pebbles'. These types of pebbles were not seen during the summer field work.

Armoured mud balls often lie on the exposed till surface (Figure 3.6). They derive entirely from cliff fall debris, and concentrations of them indicate a period of local rapid cliff erosion.



Figure 3.6. Armoured mud balls at Easington, 26th July 2005. Mud ball in foreground is about 50 cm across.

Pringle (1981, 1985) argued for the presence of large coast-oblique depressions called ords, which allow increased wave energy to reach the cliff toe where the beach level is low. They have an important role in exposing the underlying till to erosion. Southward migration of the ords (around 500 myr^{-1}) allows the locus of scour to move along the shore locally increasing erosion and resulting in temporally-variable recession rates at any given point. Pringle (1985) showed that the reduction in beach level at the cliff toe associated with an ord was up to 3.9 m allowing high water neap tides to reach the cliff toe as compared to only some high water spring tides along the inter-ord beach. The lowering of the beach exposed the till platform to erosion.

There appears to be some support for Pringle (1981, 1985) at the Easington study site. It is likely that the water in the 'lagoon' covers part of an ord. The lagoon is therefore part of the ord system, along with the exposed shore platform at the study site, between the sand bar and the beach. Also, the backing cliffs where the beach is thinner have a morphology that indicates direct attack and erosion by waves in the form of 'fluting' up the cliff face (Figure 3.7). Where the beach is thicker the backing cliffs do not show such a distinct morphology.



Figure 3.7. Morphology indicating direct erosion of the cliffs by waves at Easington, 26th July 2005.

The study site at Easington partly falls within the southern limit of the Dimlington Cliff SSSI. It is a key site for Quaternary stratigraphy with a sequence of pre-Devensian and Late Devensian tills exposed in the cliffs. The cliffs provide evidence of palaeoenvironmental conditions and limiting dates for the maximum expansion of Late Devensian ice.

3.1.3 Comparison of Warden Point and Easington Field Sites

The primary differences between the Warden Point and Easington sites are summarised in Table 3.1.

Table 3.1 Summary of the principal differences between the Warden Point and Easington field sites

Feature	Warden Point	Easington
Cliff height (m)	48	20
Cliff retreat rate (m a ⁻¹)	1.93	1.97
Beach width (m)	8	80
Beach thickness (m)	0.1	5
Beach movement	Little	Extensive

Feature	Warden Point	Easington
Platform width (m)	300	60
Geology	London clay	Glacial till
Platform elevation (m ODN)	+0.53 -2.23	-1.71 -2.67

In essence, the main differences are:

- the Warden Point platform is wider and of a shallower gradient than at Easington;
- the beach at Warden Point is narrower, shallower and more of a ‘fringing’ feature than that at Easington, where large sand bars can periodically cover much of the platform to considerable thicknesses and their associated ‘ords’ (shallower areas between adjacent sand bars) are observed to migrate along the coast; and
- the Easington platform occupies a wider range of topographic elevations, with the platform being completely covered with water on every high tide. In contrast the upper platform at Warden Point is only covered by water on high spring tides.

3.2 Method of Field Investigation

This section describes the methods used to measure (or characterise) the following parameters at each of the two field sites:

- Platform downwearing rate;
- Beach morphology changes;
- Geotechnical properties of the platform; and
- Wave conditions.

Results from these investigations are presented in Section 3.3.

3.2.1 Platform Downwearing

(a) *General Background*

The instrument designed to measure platform downwearing rates for this project, the Traversing Erosion Beam (TEB), was constructed primarily of Flexlink Aluminium Structural System (FASS) standard components, which can be combined to form structures quickly and economically. Metal beams, incorporating continuous T-slots, were combined with framework connectors, sliding modules, enclosures and adjustable feet, to create the permanent structure of the TEB (Figures 3.8 and 3.9). The device is easily adjustable in the field using a minimum number of hand tools. The beams were made from anodised aluminium extrusions, which are corrosion resistant and sufficiently lightweight to:

- (i) allow the instrument to be carried by one person;
- (ii) prevent any compaction/destruction of the platform material when the instrument is in position in the field; and
- (iii) retain high stability and considerable torsional strength.

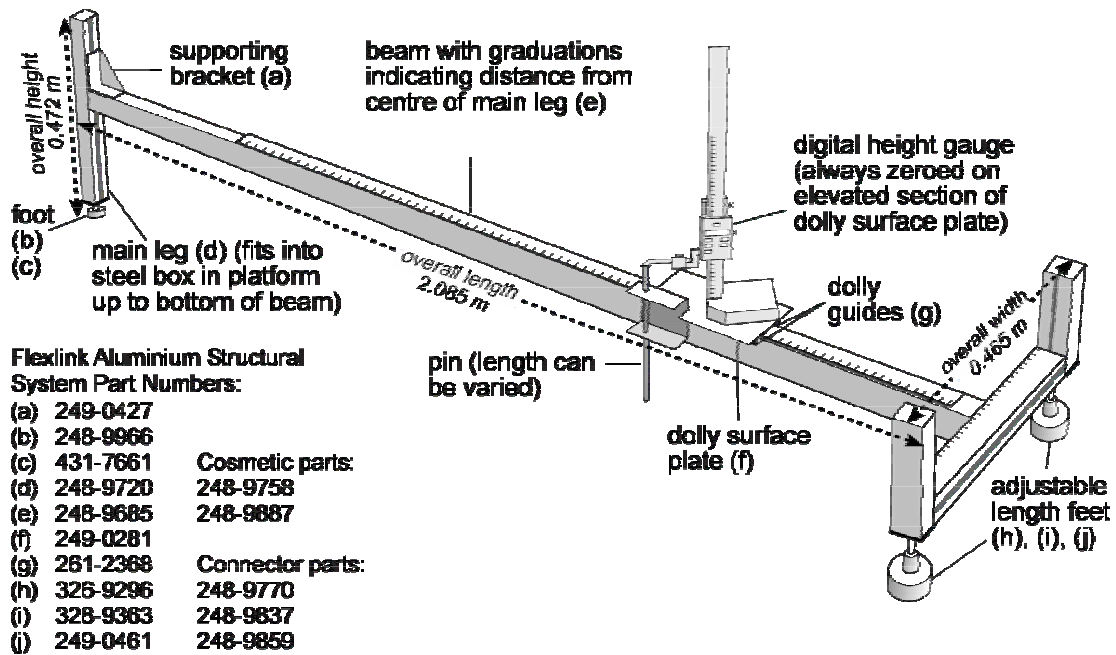


Figure 3.8. The Traversing Erosion Beam (TEB). Relevant Flexlink Aluminium Structural System part numbers are identified.



Figure 3.9. The Traversing Erosion Beam in use at Warden Point.

Note: The stainless steel datum box (shown without its lid in the inset) is on the left of the main picture, protruding from the platform surface. The spirit level was left in place across the two support legs to ensure that the device remained level whilst measurements were being made.

(b) *Use in the Field*

The TEB has a main leg at one end, which fits snugly into a 50 x 50 x 400 mm Marine Grade stainless steel box (inset of Figure 3.9) that has been fixed into the shore platform to act as a permanent datum. A horizontal beam (main beam) is rigidly attached to the main leg of the TEB and two further support legs are fixed at the opposite end. These have adjustable-length feet to allow the TEB to be set up so that the main beam and the beam that connects the two support legs are both perfectly horizontal when measurements are being made. The main beam has a longitudinal scale and a sliding 'dolly' module consisting of a surface plate and plastic guides. The dolly is moved along the beam at precise intervals on the scale. The topographic profile of the measurement surface is transferred to the dolly by a vertically sliding steel alloy pin (5 mm in diameter) from which the relative height differences are measured using a separate engineer's digital height gauge. Pins of length 250, 300 and 400 mm have been made to allow the instrument to be used on surfaces of different topography. An elastic band has been placed around the elevated section of the dolly surface plate to hold the pin in place when moving between measurement points.

The main leg of the TEB is square in cross section, as is the datum box into which it is inserted on the platform, and so the instrument can be rotated in four directions 90° apart. At any one measurement site, therefore, four topographic profile lines can be measured from the central datum box. The dolly can be moved along the scale in increments as small as one millimetre, which would yield 1500 readings per topographic profile line. In a tidal environment, where time is limited, such a high number of readings may be difficult to achieve. For the purposes of this project, to provide a suitable measurement density in the time available to perform measurements, the dolly was positioned at 50 mm intervals giving 28 readings per topographic profile line.

(c) *Construction of the Datum Box*

Each TEB measurement site needs to have a fixed datum point which is a Marine Grade stainless steel box that is embedded in the shore platform (the datum box). The upper end of this box is flanged with a 25 mm wide rim. A 100 mm square cap plate is bolted to this by four corner mounted M8 bolts. A neoprene waterproof gasket is sandwiched between the cap plate and the flange to give a waterproof seal. This protects the datum box between fieldwork sessions. The bottom end of the datum box is welded to the centre of a 100 mm², 3 mm thick, 316 plate that has a M6 threaded stud in the centre protruding downwards. This allows the box to be attached to a tapped hole in the reinforced head of a 1000 mm long rebar rod. The other end of the rod is sharpened to a point and fitted with simple one-way wire barbs. The datum box has an expected lifetime well in excess of one year because of its substantial design and fitting.

(d) Installation of the Datum Box

Some simple purpose-built tools and general tools and materials are needed to install the datum box: an alignment insert (1500 mm long section of 44 x 44 mm FASS beam milled to fit inside the fixed datum box and with attachment points at the upper end for four adjustable guy ropes); a 150 mm diameter screw auger; a rebar extension rod (40 mm tube approximately 600 mm long with a hammering surface at one end and an indent capable of accepting the head of a rebar rod at the other); a sledge hammer; cement/concrete mix with a rapid hardener additive; buckets and trowels; spirit levels; four short metal stakes; small flags on thin wire rods.

Once the location of the TEB measurement sites has been selected, care must be taken to ensure that the profile lines are not trampled during the installation procedure. One way of doing this is to mark out the measurement profile lines using small flags so that no-one accidentally walks over them. At the centre of the chosen location a 400 mm deep hole is dug with the auger and the material taken well away from the measurement site to prevent wave action transporting the material back onto the measurement profile lines. The rebar rod is placed in the centre of the hole and hammered vertically downward, using the rebar extension rod, until only 100 mm protrudes above the base of the hole. This protrusion gives sufficient flexibility to allow precise vertical alignment of the stainless steel box. The datum box is then screwed onto the top of the rebar rod and the alignment insert fitted inside the box. The box is rotated so that the sides are parallel to the intended profile lines, normally shore parallel and shore normal. The top of the box must be checked to ensure that it sits a few centimetres higher than the adjacent platform surface. Then, using the levels and the adjustable guy ropes attached to the four metal stakes, the datum box is temporarily aligned perfectly vertical and the hole filled with rapid setting concrete. Once the concrete has hardened the alignment insert is removed and the steel datum box capped.

The height and location of the steel boxes need to be checked periodically throughout the period of TEB measurements (e.g. every six months) with standard surveying techniques (e.g. total station or GPS) to ensure that the entire platform is not experiencing mass movement (e.g. uplift, distortion or rotation). If required, measurements from the TEB can be adjusted to real-world elevations.

(e) Performing Measurements

Ideally, two people are needed: an operator to raise and lower the pin onto the platform surface and a data recorder to make clean, legible notes and offer cleaning equipment to the operator when required. For each measurement site the procedure listed in Box A should be followed.

Box A: TEB Measurement Procedure (17 steps)

- I. Unscrew the corner mounted M8 bolts, remove the lid and gasket and clean the inside of the box and flange and lubricate with WD40.
- II. Taking care not to damage the platform surface that is to be measured, position the TEB along the first longitudinal profile line. Lower the main leg (also cleaned and lubricated) carefully into the steel box until the main beam sits flush with the top flange.
- III. To make the lengthways direction approximately level: place a spirit level along the surface of the main beam and adjust the feet on the two support legs.
- IV. To make the widthways direction of the end beam level: place the spirit level across the top of the two support legs and adjust the feet in unison to ensure that the lengthways direction is not brought off-plum.
- V. Finally, reposition the spirit level along the surface of the main beam and adjust the feet to make the lengthways direction completely level. Leave the spirit level across the top of the two support legs during measurements to ensure that the end beam remains perfectly level in the widthways direction.
- VI. Clean and lubricate the surface of the main beam and move the dolly into position at the first measurement point.
- VII. Insert the aluminium pin, of known length, into the supporting holes (both of which are lubricated) in the elevated section of the dolly plate. Use the elastic band to hold the pin above the platform surface whilst moving the dolly.
- VIII. Clean the dolly surface plate and the base of the digital height gauge before placing the digital height gauge in position.
- IX. Zero the digital height gauge on the elevated section of the dolly surface plate.
- X. Gently lower the aluminium pin onto the platform surface, taking extreme care to avoid damage to the rock/sediment. Take care when reapplying the grip of the elastic band that the pin doesn't spin and dig into the platform surface as this would give a false reading.
- XI. Gently lower the digital height gauge onto the top of the pin and record the reading together with any observations of the platform surface at that point (e.g. presence of shell fragments, extremely soft sediment or puddle).
- XII. Raise the digital height gauge and then the pin (again avoid any spinning of the pin when releasing the grip of the elastic band).
- XIII. Move the dolly along the selected interval (50 mm in the present study) to the next measurement point.
- XIV. Repeat steps X to XIII until the end of the scale is reached. The length of the aluminium pin can be varied during measurements but it must be noted and taken into account in the post-field calculations. Frequent checks should be made to ensure that the digital height gauge returns to zero on the elevated section of the dolly surface plate.
- XV. Gently raise the TEB out of the datum box and clean and dry the digital height gauge to prevent malfunction.

Box A: TEB Measurement Procedure (17 steps)

XVI. Repeat steps II to XV for each longitudinal profile line remaining.

XVII. Replace the datum box cap together with a new neoprene gasket and screw the corner mounted M8 bolts back into place.

When the measurements were completed, the TEB was cleaned and lubricated, with particular attention paid to the digital height gauge, as corrosion or clogging with sediment would have been highly detrimental to future measurements.

(f) Accuracy and Reproducibility of Measurements

The digital height-gauge used in an ordinary laboratory context yields data of better than millimetre accuracy. As far as the TEB is concerned, the gauge is only a minor source of error. Determining the point of contact of the pin with the ground surface can be troublesome if the platform surface is somewhat liquid, but provided care is taken the mean error in readings ought not to exceed a millimetre. The main source of inaccuracy with the TEB measurements appears to be imperfect or imprecise levelling of the beam each time measurements are recorded.

Experiments have been carried out by repeating measurements at the same TEB location to check the overall reproducibility. Following completion of a full set of measurements, the TEB has been removed completely from the steel datum box, and the set-up procedure repeated, including readjustment of the feet, before taking a new set of measurements. The differences between the two sets of measurements have then been calculated. Table 3.2 summarises the results:

Table 3.2. Summary of the results of the TEB reproducibility tests.

Parameter	Test A	Test B	Test C		
	1st & 2nd set-up	1st & 2nd set-up	1st & 2nd set-up	1st & 3rd set-up	2nd & 3rd set-up
Mean difference in the measurements	0.860	2.053	0.104	1.210	1.314
Absolute mean difference	0.952	2.053	0.228	1.214	1.314
Standard deviation of the differences	0.749	0.909	0.263	0.649	0.454
Correlation between the differences and distance from the box	0.799	0.697	0.854	0.900	0.789

The differences in the measurements do not sum to zero. In other words, the differences tend to be in the same direction and do little to cancel each other out. This is because the beam can be almost exactly relocated close to the steel datum box (due to its tight fit), but further away the relocation errors increase almost certainly because of lack of horizontality of the beam. This is demonstrated by the correlation that exists between the differences in the two sets of measurements and distance from the box. The increase in differences with distance from the box appears to follow a linear relationship (Figure 3.10), which suggests that errors of levelling are more significant than possible slight flexure of the beam.

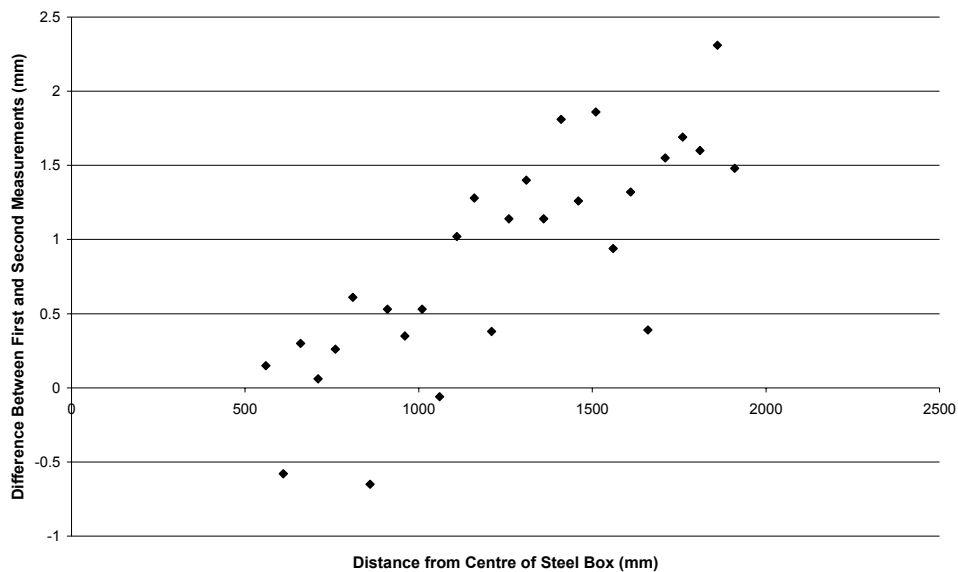


Figure 3.10. Distance from centre of steel datum box vs. difference between first and second measurements (mm) at Warden Point.

The reproducibility tests suggest that differences in TEB readings between successive visits that average less than about 2.5 mm are likely to be due to instrument error and should be ignored. Greater trust can be placed on differences measured close to the steel box than on differences measured towards the far end of the beam.

(g) Deployment Locations

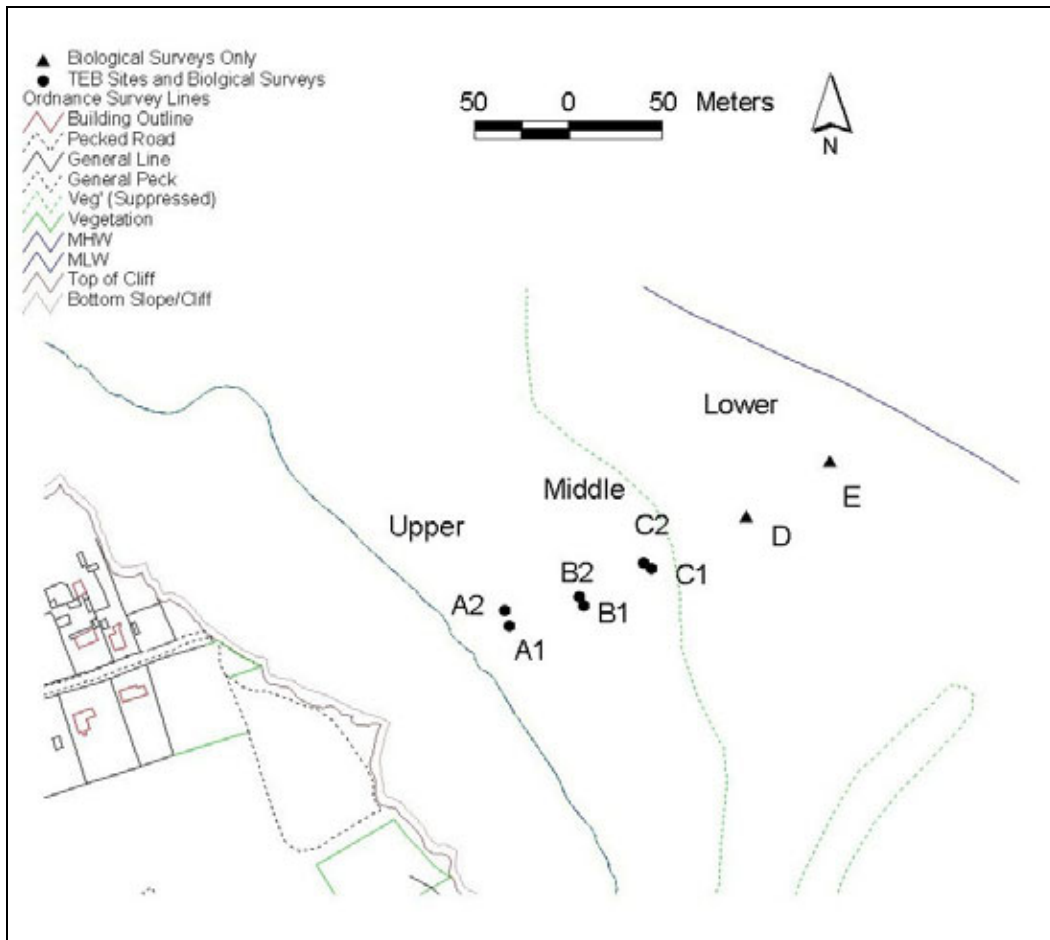
The TEB locations at Warden Point and Easington were selected to represent three different surface elevations as well as the micro- and meso-morphology of the shore platform. The measurement sites at all locations were at a high enough elevation on the shore platform to allow time to install the equipment and record measurements during a near-spring low tide. They were sufficiently far from both the cliff and the beach to minimise the risk of being covered by flows of unconsolidated material.

Warden Point:

At Warden Point, the shore platform is smooth, planar and slopes very gently seaward. Beach development is limited, consisting of a small amount of shingle (mainly far travelled flints and broken septarian nodules of local origin) mixed with rubble from collapsed WW2 defence structures on the cliff and with unconsolidated mud. Because of the gentle slope of the platform small changes in low tide elevation result in large variations in the area of the platform that is exposed. At the start of the summer field campaign on the 21st July 2005, three days before the spring tide, the area available at low tide was much more restricted than that on the 24th July 2005. Even on the 24th of July the lowest part of the platform was uncovered for such a short a period of time that it was impossible to install TEB measurement sites close to the spring low tide mark. As a result, the three sites selected for TEB measurements were located on the upper and middle part of the shore platform (Table 3.3 and Figure 3.11). Two replicate TEB datum boxes were installed at each of the three selected locations.

Table 3.3. Traversing Erosion Beam locations at Warden Point.

Location on the platform	Code	Replicate	Ordnance Survey Coordinates		
			Easting	Northing	Elevation
Close to top of platform	A	1	601996	172496	-0.03
		2	601993	172506	-0.12
Upper middle platform	B	1	602043	172509	-0.92
		2	602040	172514	-0.84
Lower middle platform	C	1	602085	172532	-1.37
		2	602080	172536	-1.30



© Crown copyright Ordnance Survey. An EDINA Digimap/JISC supplied service.

Figure 3.11. Map showing TEB locations on the Warden Point platform. NB: Biological survey locations are also plotted for reference.

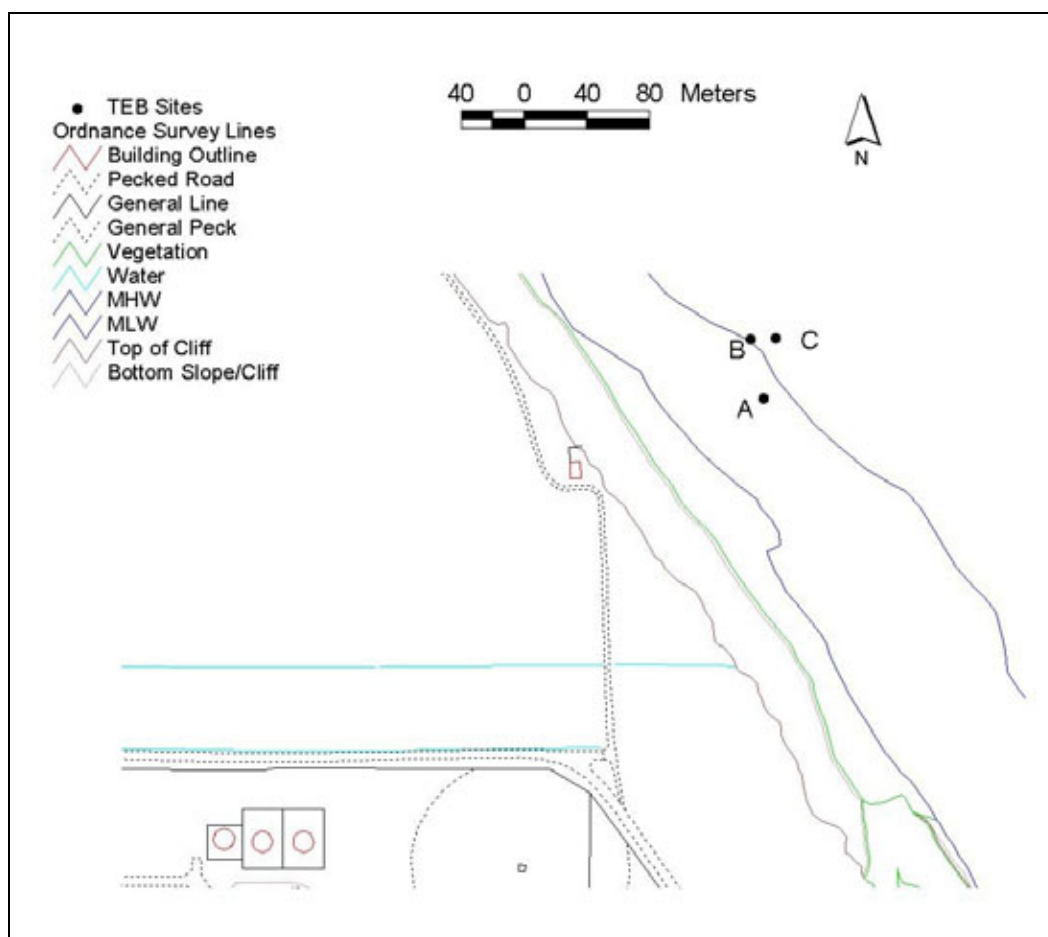
Easington:

The glacial till at Easington is much harder than the London Clay at Warden Point. The shore platform surface is dissected by runnels that run perpendicular to the cliff and of a similar morphology to those found on chalk shore platforms. A clearly defined sand and shingle beach covers the upper platform, concealing the cliff-platform interface. A sand bar exposed at low tide conceals the lowest part of the shore platform. At low tide, water remains trapped on the lower shore platform behind the ord. As a result, the area available for study, in effect the mid-platform, is much narrower and around a metre lower in elevation than the area of platform studied at Warden Point. The period of time available for instrument installation and measurements at this site was severely restricted.

The three locations selected for TEB measurements were: (A) near the edge of the beach; (B) in the centre of the exposed platform; and (C) near the low water spring tide mark (Table 3.4 and Figure 3.12). The location near the low water spring tide mark was situated close to a well-developed runnel in order to assess relative downwearing rates on the platform surface and within the runnel. Due to tidal constraints, there was insufficient time to install replicate TEB sites and therefore only one datum box was installed at each location.

Table 3.4. Traversing Erosion Beam locations at Easington.

Location on Shore Platform	Code	Landmarks	Ordnance Survey Coordinates		
			Easting	Northing	Elevation
Near beach	A	-	539828	420826	-1.96
Centre	B	-	539820	420864	-2.19
Near low water mark on a spring tide	C	Next to a well-developed runnel	539836	420864	-2.38



© Crown copyright Ordnance Survey. An EDINA Digimap/JISC supplied service.

Figure 3.12. Map showing TEB locations on the Easington platform.

(h) *Survey Dates*

It was originally intended to take downwearing measurements twice at each site, once in summer 2005 and once in winter 2005/06. However, this plan changed during the course of the study due to the reasons explained in the following sections.

Warden Point:

Following installation in July 2005, it was identified that added value could be brought to the study by making measurements on a seasonal basis (approximately every 3 months) throughout the course of one year, rather than only twice as originally planned. All steel datum boxes and their shore-normal axes were successfully measured at Warden Point on the dates listed in Table 3.5.

Table 3.5. Dates of TEB installation and measurements at Warden Point.

	Dates	Measurements conducted
Installation	21 & 22 July 2005	-
Survey 1: First summer 'base' measurements	22 & 23 July 2005	All
Survey 2: Autumn measurements	19 & 20 October 2005	All
Survey 3: Winter measurements	3 & 4 February 2006	All
Survey 4: Spring measurements	26 May 2006	All
Survey 5: Second summer measurements	13 & 14 July 2006	All

Easington:

After successful installation and an initial summer 2005 survey at Easington, problems in undertaking a second set of downwearing measurements were encountered. These problems were associated with the low platform elevation, shallowing of the beach profile in the winter and movement of the sand bars across the site, as shown in Figures 3.13 and 3.14. This meant that it was not possible to make measurements during the February 2006 visit and a subsequent planned visit was aborted when it was reported that the sand bar was still covering the site. It was only in July 2006 that a second survey was successfully undertaken, although even then location A could not be measured during this survey because the end of the sand bar still covered this part of the site.

Table 3.6. Dates of TEB installation and measurements at Easington.

	Dates	Measurements conducted
Installation	25 & 26 July 2005	-
Survey 1: First summer 'base' measurements	26 July 2005	All except the southern axis of site C where measurements in the runnel and adjacent platform were recorded.
Survey 2: Attempt 1	5 February 2006	None. Platform covered by a sand bar. TEB measurements not possible.
Survey 2: Attempt 2	31 March 2006	None. The sites were covered by a sand bar. Visit was aborted ¹ .
Survey 2: Attempt 3	15 July 2006	B and C. Sand cover over A too deep.

¹ The beach morphology was successfully surveyed on this date.



Figure 3.13. Easington in March 2006.

Note: The sand bar joined the main beach, covering the three TEB datum boxes. Although some of the platform was exposed elsewhere (e.g. to the left of the picture), no measurements could be made at the TEB locations.



Figure 3.14. Saturated sand above the steel datum box at location C, Easington in March 2006.

Note: The bottom of the spade was touching the lid of the steel box but because the sand was saturated it was impossible to uncover the datum box.

3.2.2 Platform Biology

(a) Field Study

Quadrats (50 x 50 cm, divided into 100 cells) were thrown semi-randomly around the TEB measurement sites at Warden Point, and at two sites on the lower platform, very close to the spring low tide mark (Figure 2.11). Particular attention was paid to burrowing organisms, as these affect the geotechnical properties of the platform. Identification of seaweed species belonging to the genera *Ulva* and *Enteromorpha* is very difficult, especially in the field, and has not been attempted.

Organisms living on boulders and pebbles scattered on the shore platforms were not monitored because they have little or no relevance to the study of cohesive platform downwearing. At Warden Point, most of the boulders were covered in barnacles and/or *Fucus vesiculosus*. Rippled, re-deposited mud,

which is not representative of the consolidated clay platform surface, was avoided during sampling. This mud was found mostly on the lowest parts of the shore platform at Warden Point.

No measurements were performed at Easington due to the absence of any significant biological activity from the cohesive shore platform.

(b) *Laboratory Study*

Two blocks each, approximately 30 cm x 30 cm x 15 cm, were removed from the upper, middle (between sites B and C) and lower (between sites D and E) platform at Warden Point for laboratory analysis of the burrowing organisms. The density of piddocks in each block was estimated. In the laboratory the blocks were firstly trimmed and their precise dimensions measured. Each block was then examined by slicing 2 cm layers from the upper surface using a cheese wire (Figure 3.15). A scale diagram was made of each successive fresh surface and the following recorded: location and diameter of each live piddock, dead piddock, position of a former piddock's body (but now containing little to no shell material), open hole, infilled hole or back-filled plug or base of a hole. Complete shells were removed and their lengths measured. The depth of the bottoms of piddock boreholes was recorded. Volume calculations were based on the assumption that the blocks were perfectly rectangular. Piddock shells were assumed to be cylindrical and their volume calculated using their measured length. Infilled holes were assumed to be cylindrical and their volume calculated based on the assumption that they extended from one 2 centimetre slice to the next. The bottoms of the boreholes were assumed to be cone-shaped and their volume calculated using their measured depth.



Figure 3.15. Dissected block of cohesive shore platform used to estimate piddock and borehole density.

Note: The view is onto the upper surface of the block from which a 2 cm layer has been removed. Piddock shells, open boreholes and infilled boreholes are clearly visible.

3.2.3 Profile Surveying

(a) Background

Field surveys were carried out using RTK DGPS with an expected accuracy of ± 2 cm in x, y and z measurements. In practice at Warden Point it was found that measurements were only reproducible to ± 5 cm. At the Warden Point site, surveys were conducted on 22-23 July 2005 and 3-4th February 2006. At the Easington site surveys were conducted on the 25-26th July 2005, 31st March 2006 and the 14th July 2006.

The Leica Geosystems Differential GPS System 500 comprises a 24-channel, dual-frequency, survey receiver with on-board Real Time Kinematic capability (Figure 3.16). The SR530 receiver can be used either as a reference or rover. Real time range will usually be about 8 km in normal conditions. Longer ranges are possible depending on the transmitter strength. The instrument is used to derive point measurements with accuracies in the region of 0.01 m in a horizontal plane and 0.02 m in the vertical. The British Geological Survey uses this equipment where engineering survey accuracies are required or where

repeat surveys will involve deriving the precise movement or change in elevation of a specific point.



Figure 3.16. GPS measurement.

At each study site a beach monitoring network was installed, which consisted of a base station set up on the lower part of the cliff at Warden Point, its position marked with a yellow Perma-Mark™ survey pin; and a base station set up on the beach (day 1) and cliff top (day 2) at Easington. The GPS network was used to accurately survey key geomorphological and instrument test sites, including platform profiles, beach profiles (shore-normal and shore-parallel), base of cliff, TEB sites, triaxial test sites, cone penetrometer test sites, beach sediment sample locations, and other beach morphology features. At Warden Point, two Environment Agency benchmarks (P23006 and P23007) (Figures 3.17 and 3.18) were also occupied using the rover (P23007) and static observations (P23006), providing a control for the data. At Easington, a nearby Ordnance Survey benchmark (TA 3831 2068) provided control.


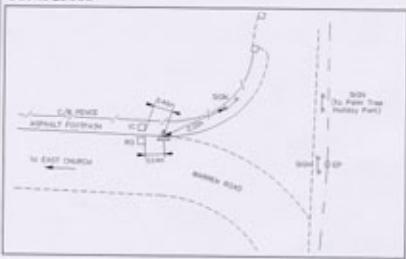

 ENVIRONMENT AGENCY		E2 GPS STATION DESCRIPTION <small>REVISED 04/01/05</small>																					
STN: P23006		WITNESS DIAGRAM																					
																							
O.S. GRID REFERENCE: TR 0023 7252 <small>(9 FIGURES)</small> LOCATION: Top of kerb on sharp bend on Warden Road, Swanley Farm, East Church, Isle of Sheppey. DESCRIPTION: EA Brass Bolt SURVEYED BY: L&B DATE SURVEYED: 23/12/2002 JOB NUMBER: SESSION TIME: <small>(BASED ON ACTIVE NETWORK)</small>		<table border="1"> <tr> <td>NETWORK BASED ON ACTIVE O.S. GPS STATIONS</td> <td>OSGB36 CO-ORDINATES: <small>(CONVERTED BY OSTN02/OSGM02)</small></td> </tr> <tr> <td>1. 3. 5.</td> <td>EASTING: 600228.764</td> </tr> <tr> <td>2. 4. 6.</td> <td>NORTHING: 172523.230</td> </tr> <tr> <td>ALTITUDE COMPARISON BASED ON EXISTING BENCHMARKS</td> <td></td> </tr> <tr> <td>1. type: OSBM</td> <td></td> </tr> <tr> <td>ALTITUDE FROM OLD BM SYSTEM <small>(m)</small> ODN</td> <td></td> </tr> <tr> <td>ETRS89 CO-ORDINATES</td> <td>ALTITUDE (m) ODN: 41.228</td> </tr> <tr> <td>LATITUDE: 51° 24' 58.894804"N</td> <td>(GPS ORTHOMETRIC HEIGHT)</td> </tr> <tr> <td>LONGITUDE: 00° 52' 41.404287"E</td> <td></td> </tr> <tr> <td>ELLIPSOIDAL HEIGHT (m): 85.9515</td> <td></td> </tr> </table>		NETWORK BASED ON ACTIVE O.S. GPS STATIONS	OSGB36 CO-ORDINATES: <small>(CONVERTED BY OSTN02/OSGM02)</small>	1. 3. 5.	EASTING: 600228.764	2. 4. 6.	NORTHING: 172523.230	ALTITUDE COMPARISON BASED ON EXISTING BENCHMARKS		1. type: OSBM		ALTITUDE FROM OLD BM SYSTEM <small>(m)</small> ODN		ETRS89 CO-ORDINATES	ALTITUDE (m) ODN: 41.228	LATITUDE: 51° 24' 58.894804"N	(GPS ORTHOMETRIC HEIGHT)	LONGITUDE: 00° 52' 41.404287"E		ELLIPSOIDAL HEIGHT (m): 85.9515	
NETWORK BASED ON ACTIVE O.S. GPS STATIONS	OSGB36 CO-ORDINATES: <small>(CONVERTED BY OSTN02/OSGM02)</small>																						
1. 3. 5.	EASTING: 600228.764																						
2. 4. 6.	NORTHING: 172523.230																						
ALTITUDE COMPARISON BASED ON EXISTING BENCHMARKS																							
1. type: OSBM																							
ALTITUDE FROM OLD BM SYSTEM <small>(m)</small> ODN																							
ETRS89 CO-ORDINATES	ALTITUDE (m) ODN: 41.228																						
LATITUDE: 51° 24' 58.894804"N	(GPS ORTHOMETRIC HEIGHT)																						
LONGITUDE: 00° 52' 41.404287"E																							
ELLIPSOIDAL HEIGHT (m): 85.9515																							
<small>Environment Agency logo and text</small>		VALIDATED: <input type="checkbox"/>																					
K.M. Square: TR 0073																							

Figure 3.17. Environment Agency benchmark P23006.

 ENVIRONMENT AGENCY		E2 GPS STATION DESCRIPTION <small>REVISED 04/01/05</small>																					
STN: P23007		WITNESS DIAGRAM																					
																							
O.S. GRID REFERENCE: TR 0237 7181 <small>(9 FIGURES)</small> LOCATION: Top of steps adjacent to waterfront car park in Warden Village, Isle of Sheppey. DESCRIPTION: EA Brass Bolt SURVEYED BY: L&B DATE SURVEYED: 24/12/2002 JOB NUMBER: SESSION TIME: <small>(BASED ON ACTIVE NETWORK)</small>		<table border="1"> <tr> <td>NETWORK BASED ON ACTIVE O.S. GPS STATIONS</td> <td>OSGB36 CO-ORDINATES: <small>(CONVERTED BY OSTN02/OSGM02)</small></td> </tr> <tr> <td>1. 3. 5.</td> <td>EASTING: 602368.769</td> </tr> <tr> <td>2. 4. 6.</td> <td>NORTHING: 171805.055</td> </tr> <tr> <td>ALTITUDE COMPARISON BASED ON EXISTING BENCHMARKS</td> <td></td> </tr> <tr> <td>1. type: OSBM</td> <td></td> </tr> <tr> <td>ALTITUDE FROM OLD BM SYSTEM <small>(m)</small> ODN</td> <td></td> </tr> <tr> <td>ETRS89 CO-ORDINATES</td> <td>ALTITUDE (m) ODN: 7.602</td> </tr> <tr> <td>LATITUDE: 51° 24' 32.944516"N</td> <td>(GPS ORTHOMETRIC HEIGHT)</td> </tr> <tr> <td>LONGITUDE: 00° 54' 30.570288"E</td> <td></td> </tr> <tr> <td>ELLIPSOIDAL HEIGHT (m): 52.3100</td> <td></td> </tr> </table>		NETWORK BASED ON ACTIVE O.S. GPS STATIONS	OSGB36 CO-ORDINATES: <small>(CONVERTED BY OSTN02/OSGM02)</small>	1. 3. 5.	EASTING: 602368.769	2. 4. 6.	NORTHING: 171805.055	ALTITUDE COMPARISON BASED ON EXISTING BENCHMARKS		1. type: OSBM		ALTITUDE FROM OLD BM SYSTEM <small>(m)</small> ODN		ETRS89 CO-ORDINATES	ALTITUDE (m) ODN: 7.602	LATITUDE: 51° 24' 32.944516"N	(GPS ORTHOMETRIC HEIGHT)	LONGITUDE: 00° 54' 30.570288"E		ELLIPSOIDAL HEIGHT (m): 52.3100	
NETWORK BASED ON ACTIVE O.S. GPS STATIONS	OSGB36 CO-ORDINATES: <small>(CONVERTED BY OSTN02/OSGM02)</small>																						
1. 3. 5.	EASTING: 602368.769																						
2. 4. 6.	NORTHING: 171805.055																						
ALTITUDE COMPARISON BASED ON EXISTING BENCHMARKS																							
1. type: OSBM																							
ALTITUDE FROM OLD BM SYSTEM <small>(m)</small> ODN																							
ETRS89 CO-ORDINATES	ALTITUDE (m) ODN: 7.602																						
LATITUDE: 51° 24' 32.944516"N	(GPS ORTHOMETRIC HEIGHT)																						
LONGITUDE: 00° 54' 30.570288"E																							
ELLIPSOIDAL HEIGHT (m): 52.3100																							
<small>Environment Agency logo and text</small>		VALIDATED: <input type="checkbox"/>																					
K.M. Square: TR 0272																							

Figure 3.18. Environment Agency benchmark P23007.

(b) *Warden Point*

GPS profiles were measured along a frontage of approximately 75 metres and consisted of shore normal profiles from the cliff toe, across the beach and out to the low water mark at the time of survey together with coast parallel profiles across the platform. Profiles were also obtained along the top and base of the beach (Figure 3.19). All surveys were conducted during low water spring tides.

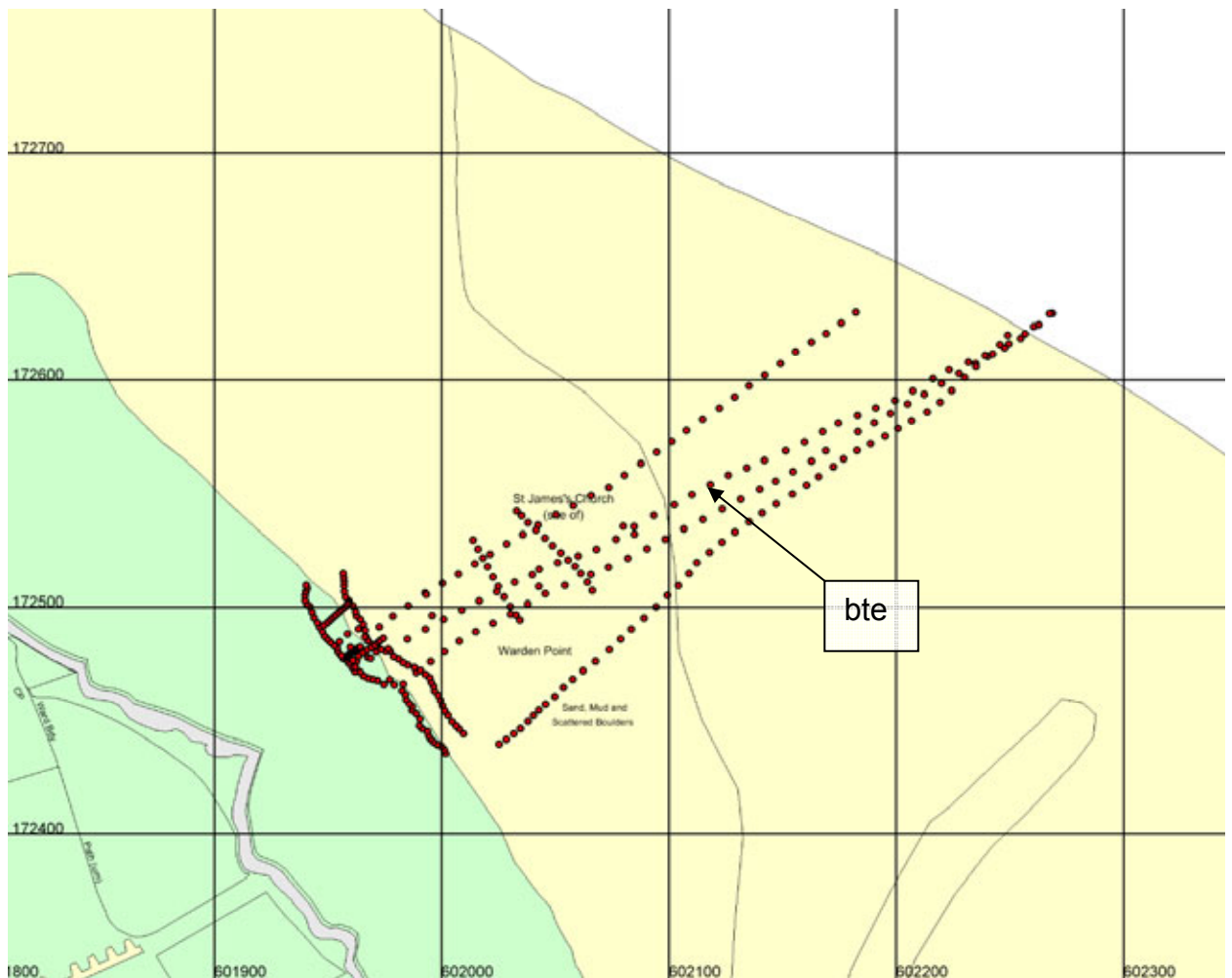


Figure 3.19. Warden Point: GPS survey profiles measured on 22-23rd July 2005. Profile 'bte' labelled (see Figure 3.45).

During the repeat surveys on 3-4th February 2006 the same profiles were measured as far as was practicable in order that any changes to the beach profile could be quantified (Figure 3.20).

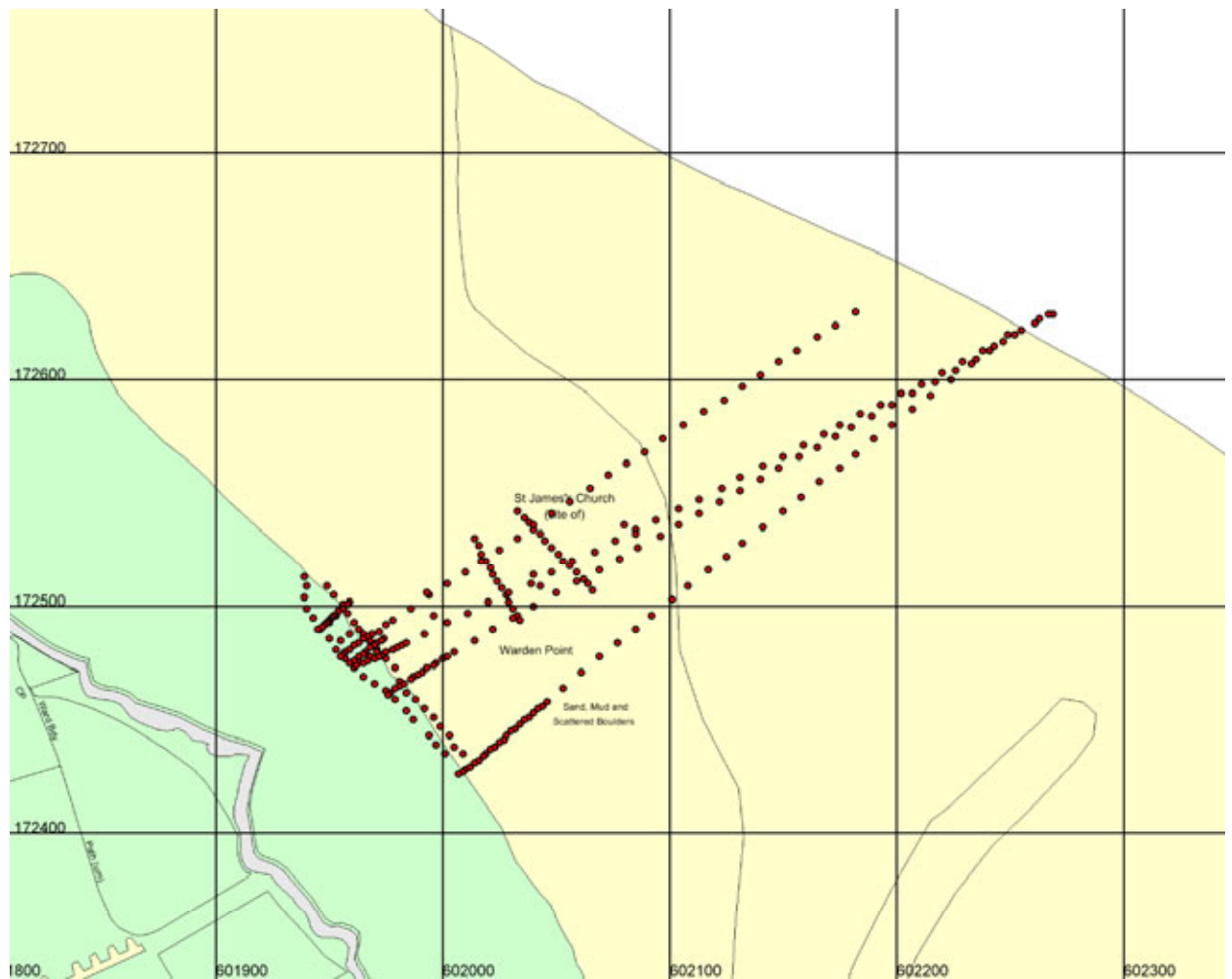


Figure 3.20. Warden Point: GPS survey profiles measured on 3-4th February 2006.

(c) *Easington*

In July 2005 three shore-normal profiles were measured across the beach covering an alongshore section of approximately 100 metres (Figure 3.21). Due to tidal constraints these profiles were not continuous across the platform and several shorter shore-normal profiles were measured across the exposed platform. Also, the top of the beach and base of the beach were measured for the studied frontage with extensions both to the north and south. Additional profiles were measured in July 2005 across a section where almost no beach sediments were present approximately 350 metres to the north of the study site.

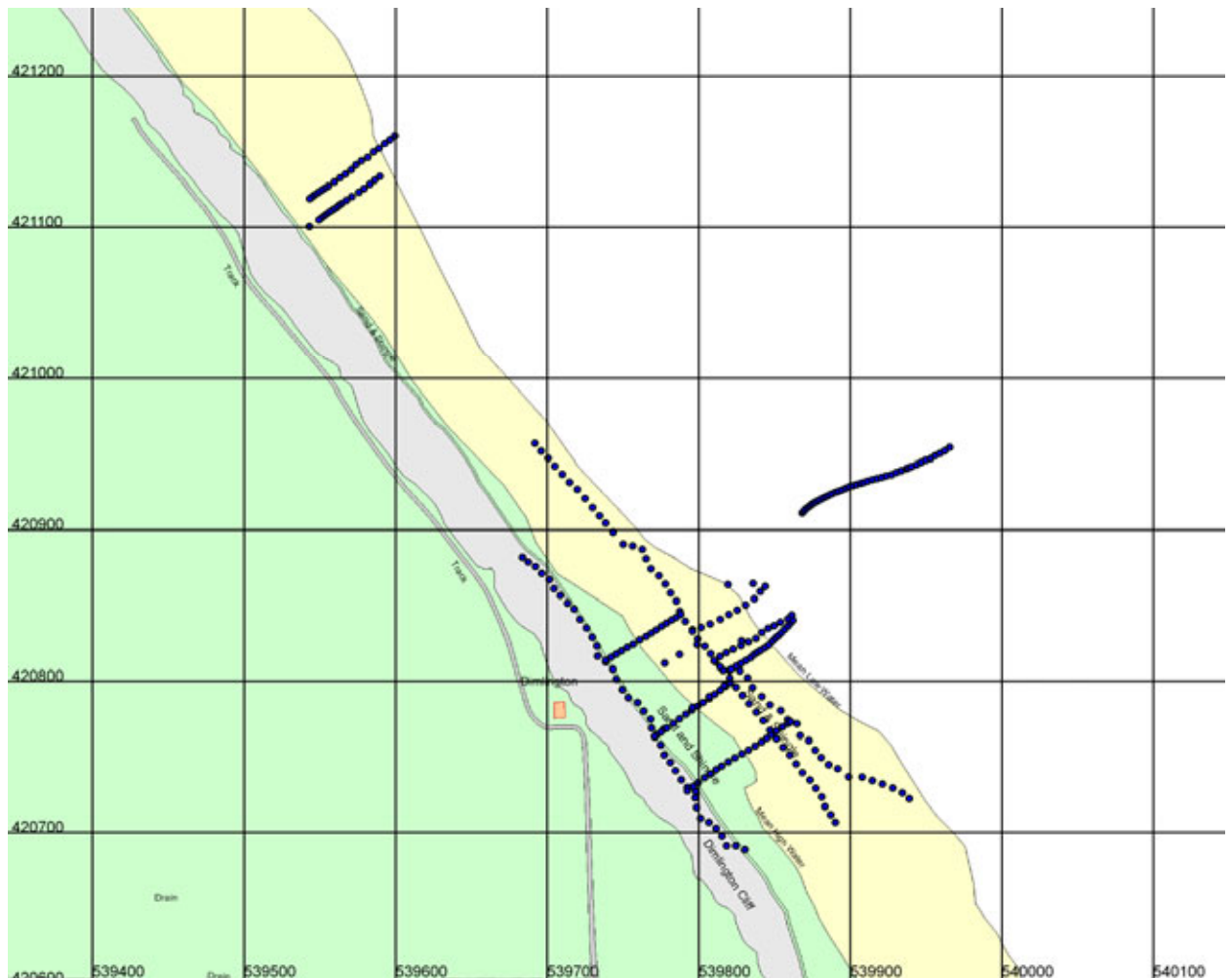


Figure 3.21. Easington: GPS survey profiles measured on 25th-26th July 2005.

In March 2006 (Figure 3.22) and July 2006 (Figure 3.23) the three cross-shore beach profiles were re-measured and continued across the platform. Also, the top of beach and base of beach profiles were re-measured and one of the additional cross-shore profiles to the north of the site was re-measured in each of the two subsequent surveys.

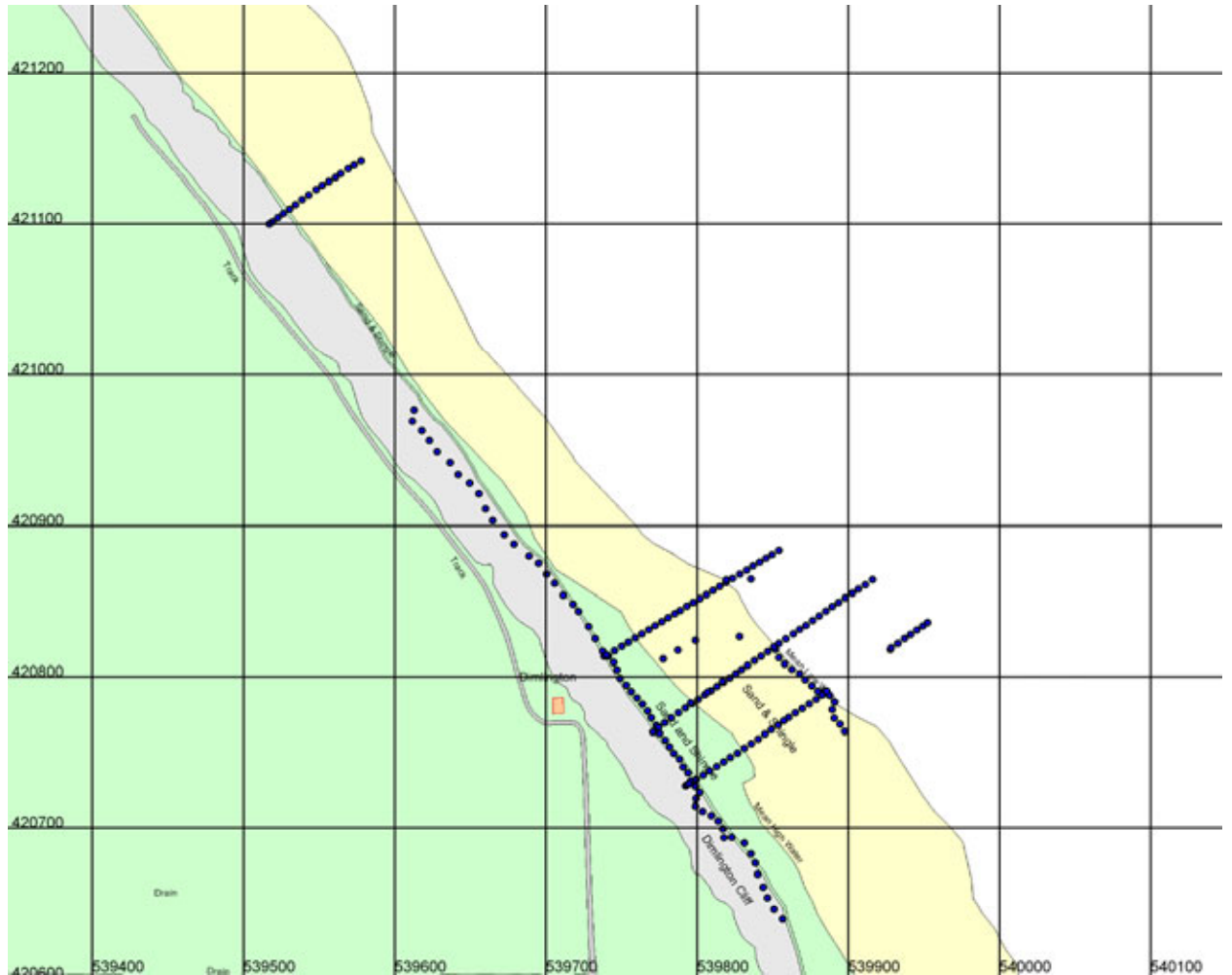


Figure 3.22. Easington: GPS survey profiles measured on 31st March 2006.

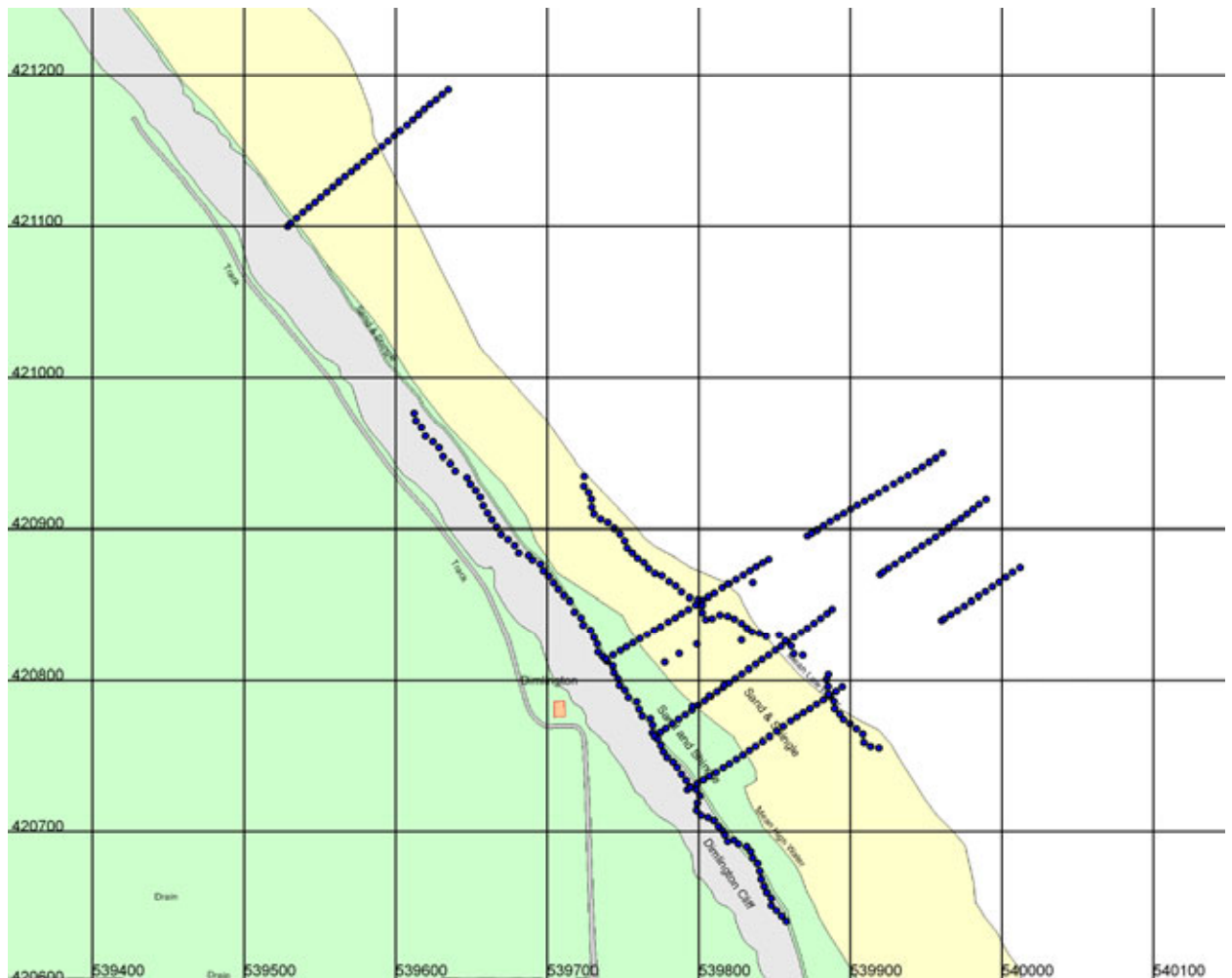


Figure 3.23. Easington: GPS survey profiles measured on 14th July 2006.

3.2.4 Geotechnical Properties

(a) Geotechnical Sampling

Three U100 (100mm diameter undisturbed) samples were taken at each sampling location for triaxial testing in the geotechnical laboratories at BGS, Keyworth. Two of each group of three were taken close together in the upper part of the exposed platform, whilst the third was some distance to seaward of the first two. Data from the two closely spaced samples was used to demonstrate repeatability and determine the extent of natural heterogeneity within the material. The third sample in each case was used to determine any cross-profile variability. In addition, three 100 mm square shear-box samples were taken adjacent to the U100 samples. Bag samples of loose disturbed material were also taken at each location, for the purpose of laboratory index testing at BGS, Keyworth.

The U100 samples were taken using a technique of hand trimming so that the final sample was contained within a rigid plastic tube of the correct size for the

triaxial test (Figure 3.24). This was done within the wall of a shallow pit. This minimised any sample disturbance caused by the subsequent extrusion and trimming normally associated with triaxial specimen preparation from block samples or drill core. The tube was pre-cut and lightly greased on the inside. The steel cutters used had a 1mm relief on the inside diameter to further reduce friction. A tripod device was used to steady the cutter and ensure verticality. When the tube was full, the cutter was separated from the tube, and the material within the cutter saved as a bag sample (disturbed). The U100 sample was sealed with plastic end caps, which were taped to the tube. On return to the laboratory, the samples were stored in a temperature and humidity controlled room.



Figure 3.24. Preparation of U100 tube (triaxial) sample

The shear-box samples were prepared in a similar way to the U100's, that is by hand trimming, but without a guidance device. The 100 x 100 x 30 mm aluminium 'pastry' cutter device had sharpened edges (Figure 3.25). The final samples were separated from the ground using a spatula, and the box capped and sealed with tape. Again these were intended to be the correct size for the shear box test, thus minimising the need for re-trimming.



Figure 3.25. Preparation of shear-box sample

All samples were finally sealed and packed in airtight crates for transport to the laboratory at BGS, Keyworth. A list of undisturbed sample reference numbers is shown in Table 3.7.

Table 3.7. Geotechnical samples

Location	U100	Shear-box
Warden Point	SHEP1 (TX)	SHEP1 (SHBX)
	SHEP2 (TX)	SHEP2 (SHBX)
	SHEP3 (TX)	SHEP3 (SHBX)
Easington	EAS1 (TX)	EAS1 (SHBX)
	EAS2 (TX)	EAS2 (SHBX)
	EAS3 (TX)	EAS3 (SHBX)

(b) In Situ Tests

Two types of in-situ test were carried out at both sites: the Panda ultra-lightweight penetrometer and the Geonor shear vane.

The Panda ultra-lightweight penetrometer is a large hand-operated cone penetrometer which uses a hammer to drive in a 2 or 4 cm² (area) cone, and measures cone penetration resistance versus depth (Figure 3.26).



Figure 3.26. Panda penetrometer test

The Geonor shear vane is a small hand-held shear vane used near surface which measures undrained shear strength directly.

Panda penetrometer tests were carried out at Warden Point at twelve locations along two lines perpendicular to the coast and spaced at 5m and 10 m intervals. At Easington nine Panda penetrometer tests were carried out along two lines, one parallel and one perpendicular to the coast at 10 m spacings. Each Panda location had a corresponding Geonor shear vane test, each consisting of three determinations (Table 3.8).

Table 3.8. In-situ tests

Location	Panda	Shear vane
Warden Point	SHEP CP1 – CP14	12 (x 3)
Easington	EAS CP1 – CP9	9 (x 3)

The Panda penetrometer test provides an almost continuous profile of cone penetration resistance with depth. This may be correlated with undrained shear strength using empirical relationships. Each Panda test was to a depth of 1.0m. The average measurement interval for Sheppey was 5.0 mm and for Easington 5.6 mm. The Geonor shear vane provided a value for undrained shear strength at a fixed depth of 60mm below the surface.

(c) *Beach Sediment Sampling*

Bag samples were taken of the beach sediments at both sites in order to characterise the beach lithology. At Warden Point six samples were taken along two shore normal profiles (3 from each). At Easington a similar strategy was adopted along two shore normal profiles. In addition samples were taken from the nearshore bar and two samples were taken from the patchy veneer of mobile sediment on the platform. A total of 18 samples were therefore obtained for subsequent particle size analysis.

Table 3.9. Beach samples taken at Warden Point and Easington.

Location	Label	Position
Warden Point	E1 (east transect)	Upper beach, 2 m from cliff toe
	E2	Mid beach, 9 m from cliff toe
	E3	Lower beach, 14 m from cliff toe
	W1 (west transect)	Upper beach, 2 m from cliff toe
	W2	Mid beach, 8 m from cliff toe
	W3	Lower beach, 14 m from cliff toe
Easington	N1 (north transect)	Seaward edge of beach, 67 m from cliff toe
	N2	52 m from cliff toe
	N3	38 m from cliff toe

Location	Label	Position
	S1	Seaward edge of beach, 67 m from cliff toe
	S2	52 m from cliff toe
	S3	37 m from cliff toe

(d) *Sample and Test Locations*

Warden Point:

Figure 3.27 shows the sample and in situ test locations at Warden Point. The triaxial, shear box, penetrometer and beach sediment locations are depicted.

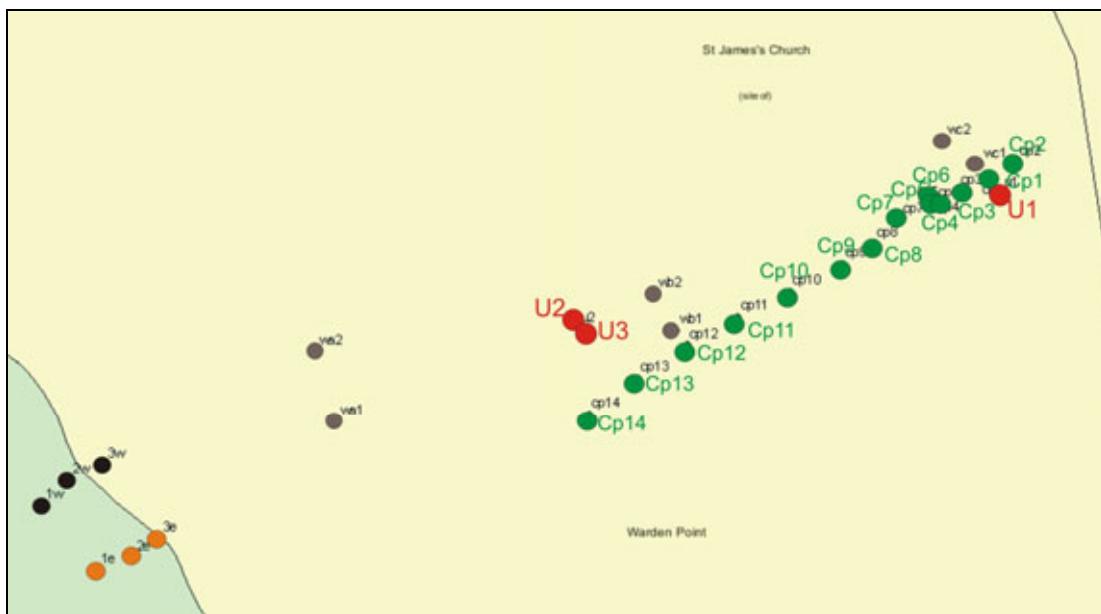


Figure 3.27. Map showing sample and test locations at Warden Point, Isle of Sheppey (U = triaxial and shear-box, Cp = Panda penetrometer).

Easington:

Figure 3.28 similarly shows the sample and in situ test locations at Easington.

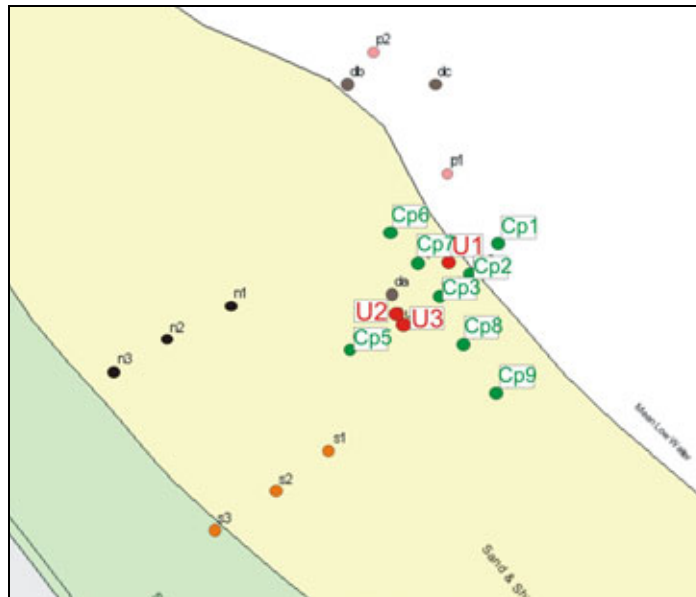


Figure 3.28. Map showing sample and test locations at Easington (U = triaxial and shear-box, Cp = Panda penetrometer).

(e) Laboratory Testing (Triaxial Tests)

A total of six 100 mm multi-stage CIU triaxial tests were carried out at the BGS's Keyworth laboratories. Specimens were taken from the store and the ends trimmed flat and parallel using a hacksaw and the plastic tube ends as guides. The outer plastic tube was then removed, the 1 mm rebate in the cutting shoe allowing all the samples to be removed without cutting the tube and without extrusion. Any large holes in the specimen were repaired at this point using trimmings (Figure 3.29). This was necessary to prevent significant air-pockets developing during the test. The specimen was then weighed using a digital balance, and its length and diameter measured using digital calipers; each dimension determination being the average of three measurements at different locations on the specimen.



Figure 3.29. Making repairs to the triaxial test specimen.

Standard vertical filter drains and porous discs (with filter discs) were then applied to the specimen and a standard rubber membrane fitted. The layout of the filter drains was such that they were all in contact with each other and with the filter discs at each end of the specimen. Whilst the fittings used throughout were 100 mm diameter, the specimen produced by the tube method was slightly larger than this.

The specimen was then placed in the computer-controlled 100 mm GDS (Bishop & Wesley) stress-path triaxial cell (Figure 3.30), which was then filled with de-aired water and subject to the 3-stage, saturated, isotropically-consolidated, undrained (CIU) triaxial test (BS1377:Part 8: 1990). This test method (also described in Head, 1987) allowed a single test specimen to be saturated by increasing pore and cell pressures, then consolidated at three different effective confining pressure stages (50, 100, & 200 kPa) taking the elevated back pressure (typically 350 kPa) as datum, at the end of each of which the specimen was compressed axially so that shear failure occurred. This method produces the same result as a test on three separate specimens, provided that certain procedures are followed (Head, 1987). Throughout the test, pore pressures at each end of the specimen were monitored, thus allowing effective stress parameters to be determined under undrained conditions. During the first two stages, complete shear failure was prevented by arresting the stage at peak shear stress or maximum principle effective stress ratio, whichever was most appropriate to the material under test.



Figure 3.30. GDS (Bishop & Wesley type) 100 mm automated stress-path triaxial system.

3.2.5 Wave Characteristics

For each of the sites, offshore Meteorological Office wind and wave data was used with astronomical tide levels in an offshore to nearshore wave transformation derived from the SWAN 1D model, to give an inshore wave climate. Results from this modelling exercise, together with results from the field work and laboratory testing, are presented in Section 3.3.

3.3 Results

3.3.1 Warden Point

This section presents results from the field investigations, laboratory testing and numerical wave modelling undertaken at Warden Point. It deals with each of the following parameters of relevance in turn, before the results are interpreted in Section 3.4:

- Platform downwearing rates;
- Platform biology;
- Beach and platform morphology (profile surveying);
- Geotechnical testing; and
- Wave climate.

(a) Platform Downwearing Rates

The average downwearing recorded by the TEB on the shore platform at Warden Point over the measurement year (July 2005 to July 2006) was 17.63 mm (standard deviation of 12.62). The upper platform showed the greatest downwearing (30.59 mm), the upper middle platform considerably less (13.75 mm) and the lower middle platform the least (8.55 mm). The time intervals between successive measurements were unequal (October to February is 5 months whereas May to July is only 3 months) and so daily rates were calculated to facilitate seasonal comparisons (Table 3.10). Downwearing was greatest during the winter to spring period (February to May; 0.066 mm/day) which was also the only period when downwearing of the lower middle platform exceeded that of the upper middle platform. Downwearing rates during spring to summer were only marginally lower (May to July; 0.060 mm/day). Surprisingly, despite more stormy conditions, the autumn to winter period 2005 had the lowest downwearing rate (October to February; 0.033 mm/day).

Table 3.10 Average daily downwearing rates for the 3 locations at Warden Point.

Period	Platform Downwearing Rates (mm/day)			
	Upper Platform	Upper Middle Platform	Lower Middle Platform	Average Across Platform
July 05 to October 05	0.080	0.038	0.013	0.044
October 05 to February 06	0.049	0.033	0.015	0.033
Feb. 06 to May 06	0.103	0.044	0.052	0.066

Period	Platform Downwearing Rates (mm/day)			
	Upper Platform	Upper Middle Platform	Lower Middle Platform	Average Across Platform
May 06 to July 06	0.135	0.043	0.002	0.060
Annual average	0.084	0.038	0.023	0.048

The micro- to meso-topography of the Warden Point shore platform TEB sites changed throughout the year, and higher downwearing rates on the upper platform were clearly evident (Figures 3.31 to 3.36). The daily averages used in Table 3.10 mask the fact that, in some cases, parts of the platform recorded a brief rise in elevation as can be seen, for example, on Figure 3.35 where some of the platform surface depressions increased in elevation between May and July 2006. Usually less than half of any profile line was affected and it is likely that these apparent rises were due to either or both instrument error or the presence of fluid mud recorded as an actual rise in elevation.

On the upper platform, extensive areas of fluid mud were present in July 2005, but these were greatly reduced in the succeeding autumn and winter. Unfortunately, when the TEB base measurements were recorded in July 2005 no note was made of the occurrence of very soft areas of sediment under the alloy pin. Detailed notes of the nature of the platform surface began in October 2005. Measurement points located on consolidated clay could then be differentiated from those on fluid mud in order to test their influence on downwearing rates. For the data collected in May and July 2006 separate lists of 18 differences in elevation were created for the two surface types. The difference in means was 3.127 mm, yielding a value of Student's *t* of 2.126 with 34 degrees of freedom. The associated two-tailed probability is only 0.04, indicating that the difference in means cannot reasonably be explained by chance sampling. Downwearing on the very soft areas appears to be greater than on the consolidated mud.

The graphs indicate that downwearing (or accretion) has been greater on locally raised areas of the platform surface than in depressions. In order to test this, the data, starting in July 2005, were split into two sets of 36 measurements representing raised areas and depressions. Over this period, the raised areas recorded a mean of downwearing of 5.78 mm and the depressions just 0.73 mm. The value of Student's *t* is 2.362 with 70 degrees of freedom, and the associated two-tailed probability is less than 0.001. The difference in means cannot reasonably be dismissed as chance sampling.

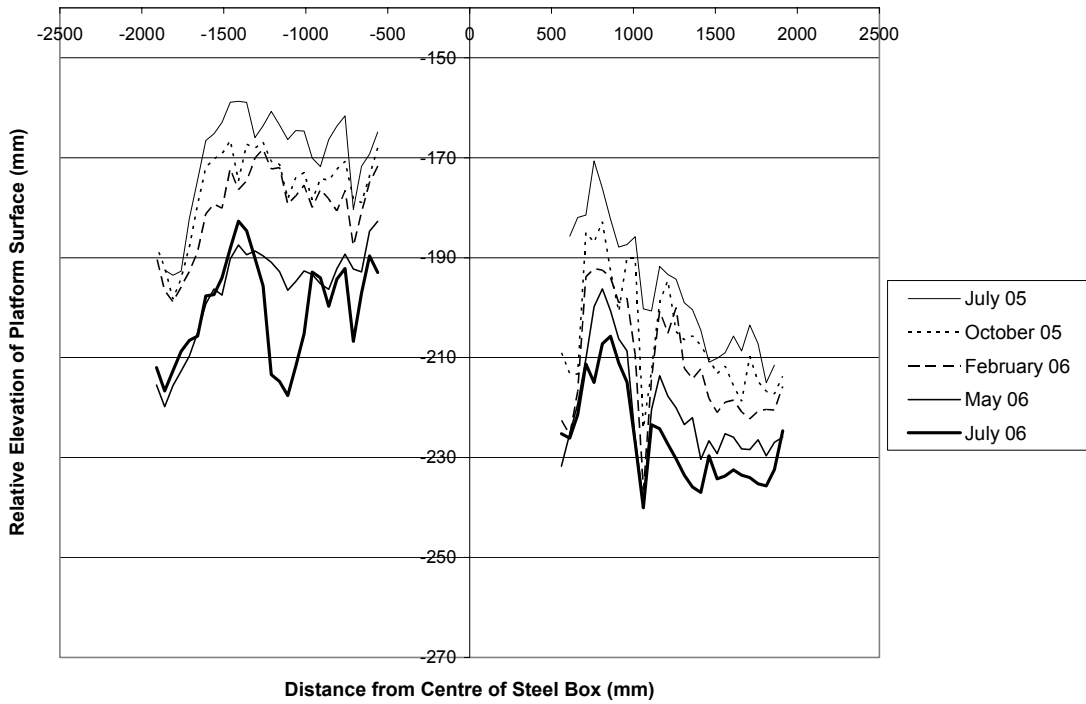


Figure 3.31. Warden Point, location A1: seasonal change in platform elevation, July 2005 to July 2006.

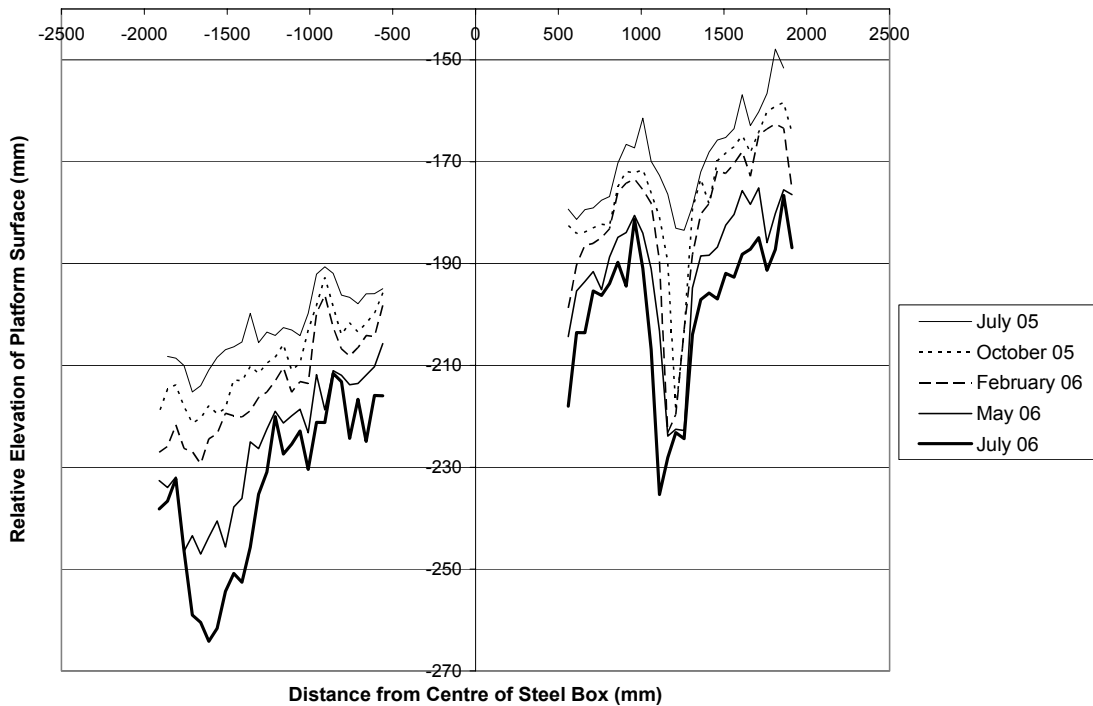


Figure 3.32. Warden Point, location A2: seasonal change in platform elevation, July 2005 to July 2006.

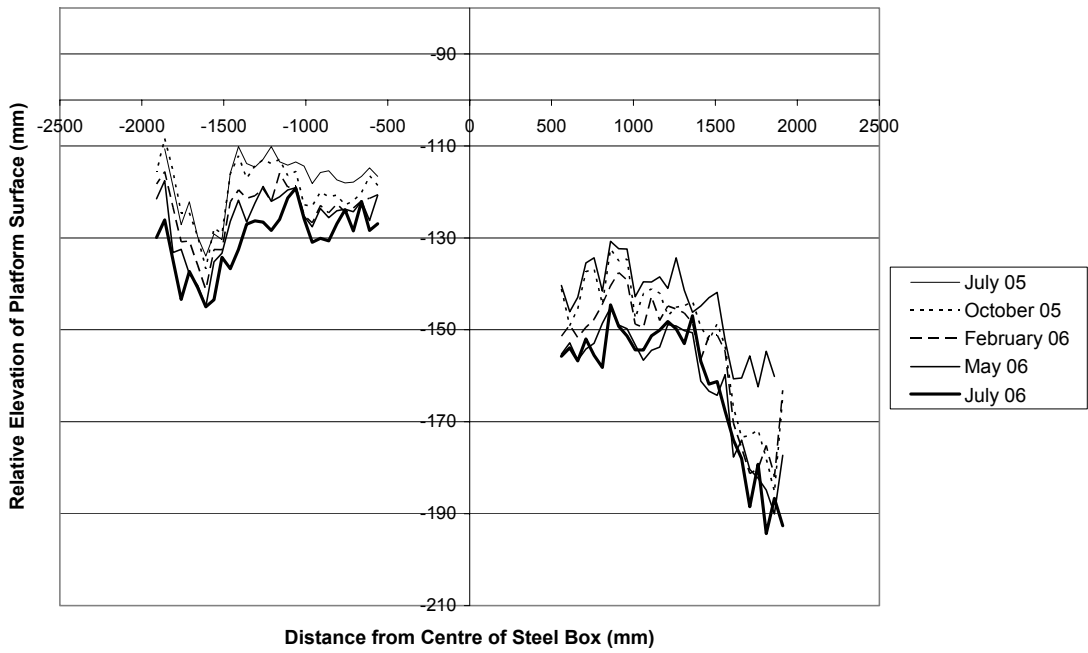


Figure 3.33. Warden Point, location B1: seasonal change in platform elevation, July 2005 to July 2006.

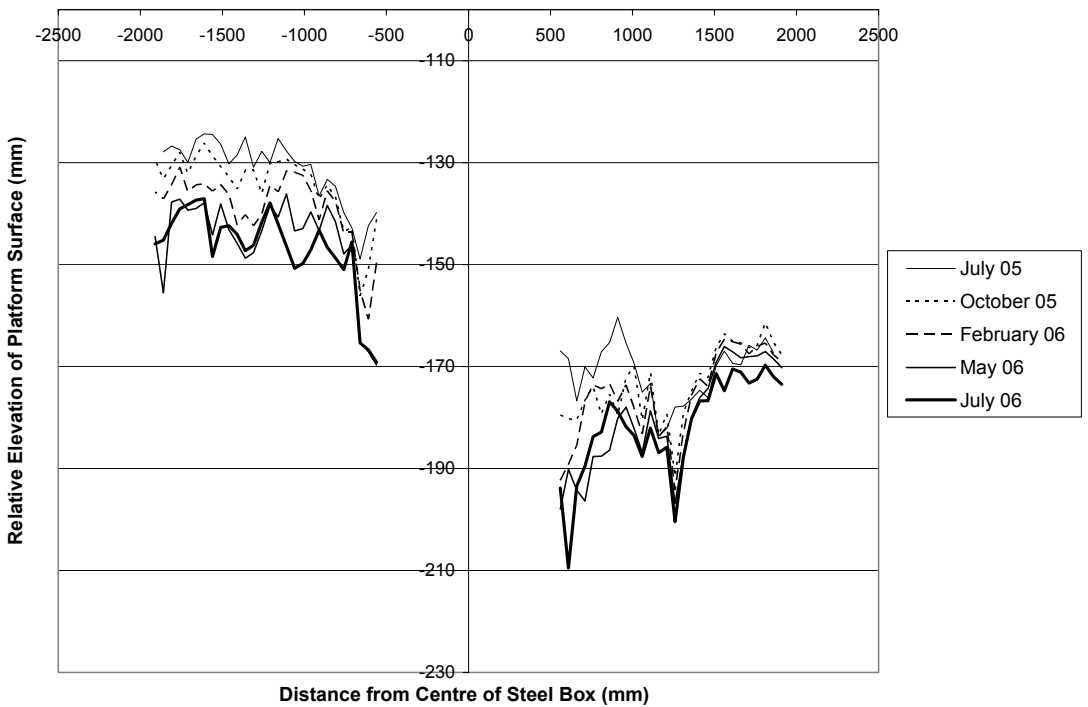


Figure 3.34. Warden Point, location B2: seasonal change in platform elevation, July 2005 to July 2006.

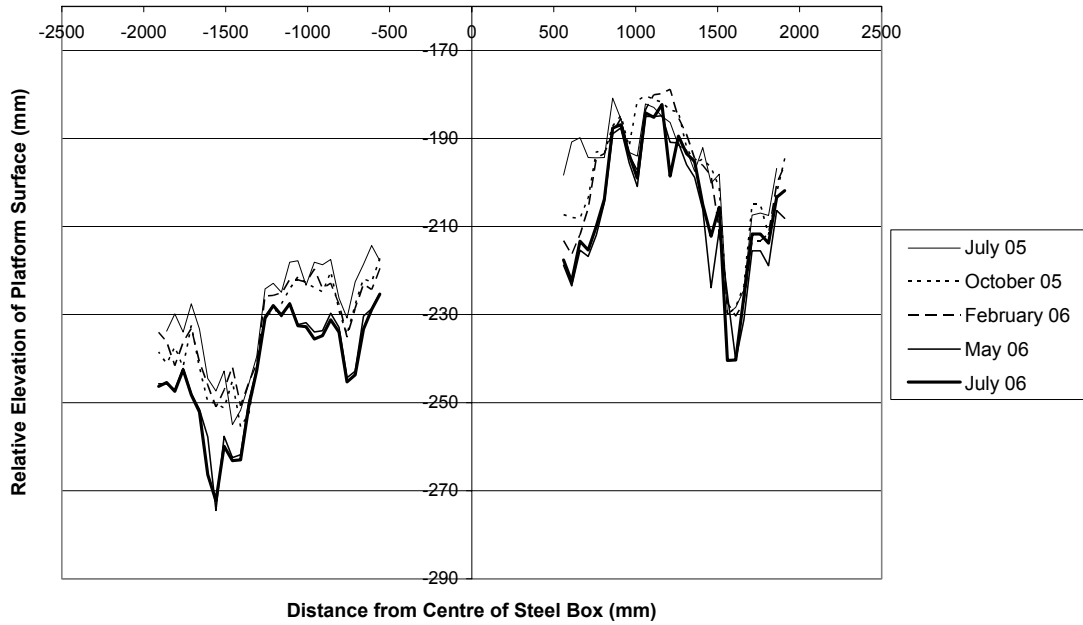


Figure 3.35. Warden Point, location C1: seasonal change in platform elevation, July 2005 to July 2006.

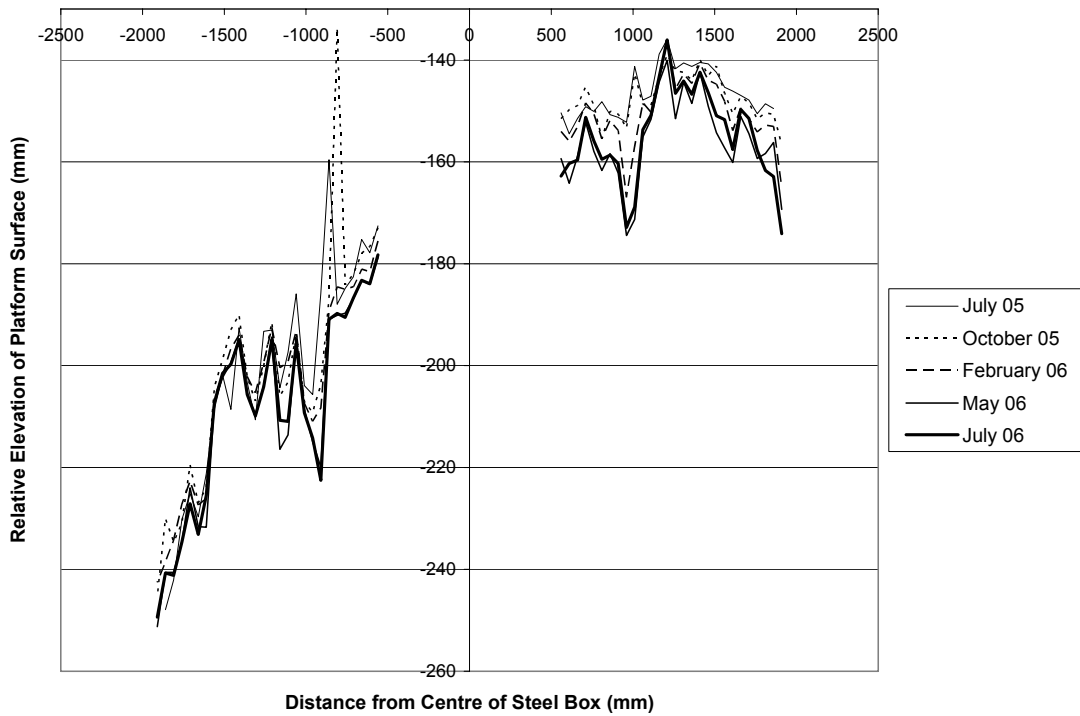


Figure 3.36. Warden Point, location C2: seasonal change in platform elevation, July 2005 to July 2006.

(b) Platform Biology

The biodiversity of the Warden Point clay shore platform is much less than that of platforms formed of other rock types e.g. chalk and sandstone. Of the live fauna, five species have been identified:

Species 1: American piddock *Petricola pholadiformis*

Phylum	Class	Order	Family	Genus	Species
Mollusca	Bivalvia	-	Petricolidae	Petricola	pholadiformis

The paired shells (valves) of the American piddock are thin, brittle and elongate-oval in outline, up to 65 mm long. They are white or fawn in colour with a darker brown periostracum. The surface of the shell is crossed by concentric ridges, which are believed to record the annual growth of the animal (Duval, 1963), and by radiating ridges, which are most strongly developed on the anterior part (blunt end) of the shell (Figure 3.37).

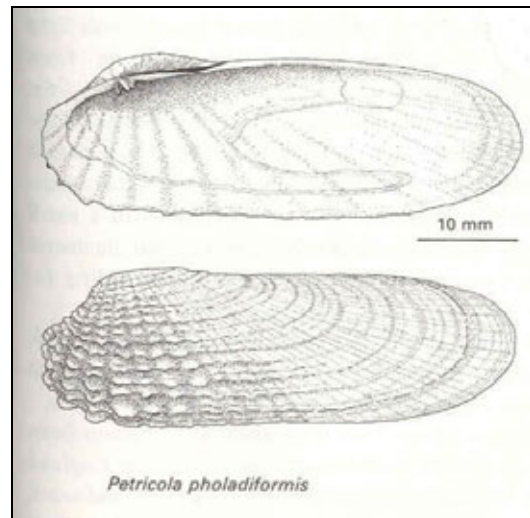


Figure 3.37. America piddock *Petricola pholadiformis* (Hayward et al, 1995b).

The species was first found in Britain in the River Crouch in Essex in 1890. A native of eastern North America, it may have been introduced accidentally with a shipment of American oysters used to stock local oyster beds (Tebble, 1966).

Now very abundant throughout the Thames estuary, it has spread along the coast of southern England to Lyme Regis in Dorset, as well as north to Lincolnshire. Isolated colonies have been reported from Cornwall and Wales.

Petricola is a mechanical borer, using its sharp edged valves to “chisel” its way into mud, peat and soft rocks such as London Clay, Thanet Sandstone and Chalk (Duval, 1963; Yonge and Thompson, 1976). The excavated material mixed with mucous forms a sludge, which is passed back up the vertical burrow to the top, where it forms a plug, through which the siphons emerge. The mollusc is apparently unable to bore into Gault Clay, which is appreciably harder than London Clay (Duval, 1963).

Duval (1963) suggests that the age of *Petricola* specimens can be estimated from their shell length. Exceptionally large individuals, between 5-6 cm in length, may be 6-10 years old. Individuals that reach 4.5 cm in length may be as much as 5-7 years old. Most of the shells found at Warden Point are shorter

than 4.5 cm, suggesting that the population at this site is less than 5-7 years old. During their lifetime, the piddocks must continually excavate their burrows to compensate for the foreshore lowering.

A shell living at a depth of 4-8 cm in the London Clay at Warden Point would, judged on our downwearing measurements, begin to be exposed within 4-5 years if it stopped excavating its burrow. One reason why piddocks are absent from the upper shore may be that the surface lowering is too rapid to allow the animals to colonise.

Species 2: *Corophium volutator*

Phylum (Subphylum)	Class	Order (Suborder)	Family	Genus	Species
Arthropoda (Crustacea)	Malacostraca	Amphipoda (Gammaridea)	Corophiidae	Corophium	volutator

Sometimes known as the Mud Shrimp, this crustacean grows to 8 mm in length, and is whitish with brown markings (Figure 3.37). Found in the intertidal environment throughout the British Isles, it creates semi-permanent U-shaped burrows (Figure 3.38), typically in estuarine muds (Hayward et al., 1995a). This results in numerous pairs of minute surface perforations (Figure 3.40) up to 1 cm in depth. At Warden Point the perforations tend to be most numerous on slightly raised areas of the platform. It is unclear whether variations in the numbers of perforations cause, or result from, variations in surface relief.

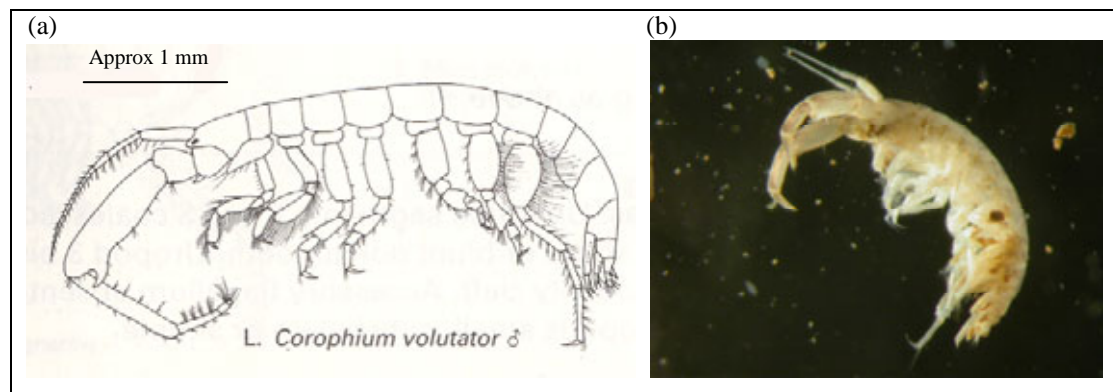


Figure 3.38. *Corophium volutator*: (a) Identification diagram (source: Hayward et al., 1995(a)) and (b) photograph of a specimen from Warden Point.



Figure 3.39. U-shaped burrows produced by *Corophium volutator*, lower-middle shore platform, Warden Point. (Yellow lines highlight the burrows. The right hand sample shows two adjacent burrows.)



Figure 3.40. Minute surface perforations produced by *Corophium volutator*, upper shore platform, Warden Point.

Species 3: Bristle worm *Nereis pelagica*

Phylum	Class	Order	Family	Genus	Species
Annelida	Polychaeta	Phyllodocida	Nereidae	Nereis	pelagica

Between 60 and 210 mm long, this very active bristle worm is red with a smooth, cylindrical body. It is found throughout the British Isles in the intertidal environment, typically amongst algae or kelp and mussel beds (Knight-Jones, et al., 2005; Figure 3.41).

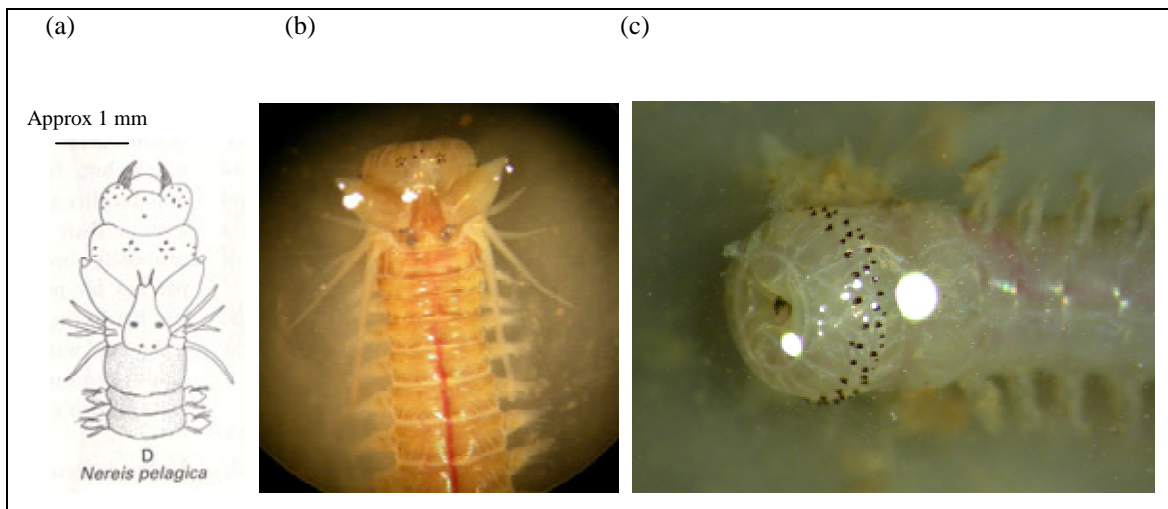


Figure 3.41. Head of *Nereis pelagica*: (a) Identification diagram (source: Knight-Jones et al., 1995) and photographs taken under microscope from (b) same angle and (c) detail on the mouth parts (retracted).

Species 4: Sand mason *Lanice conchilega*

Phylum	Class	Order (Suborder)	Family	Genus	Species
Annelida	Polychaeta	Canalipalpata (Terebellida)	Terebellidae	Lanice	conchilega

This species is up to 250-300 mm long (Figure 3.42). Its lower section is soft and fragile making it particularly difficult to obtain intact samples. The samples collected had whitish bodies, suggesting that they were in breeding condition (the body is normally pink, yellowish or brownish). The tube, characteristically built of cemented sand and shell fragments with a ragged fringe at the mouth end, and was seen at Warden Point protruding around half a centimetre above the platform surface. The Sand Mason is found most commonly on sandy beaches but also occurs on mud where wave action is moderate.

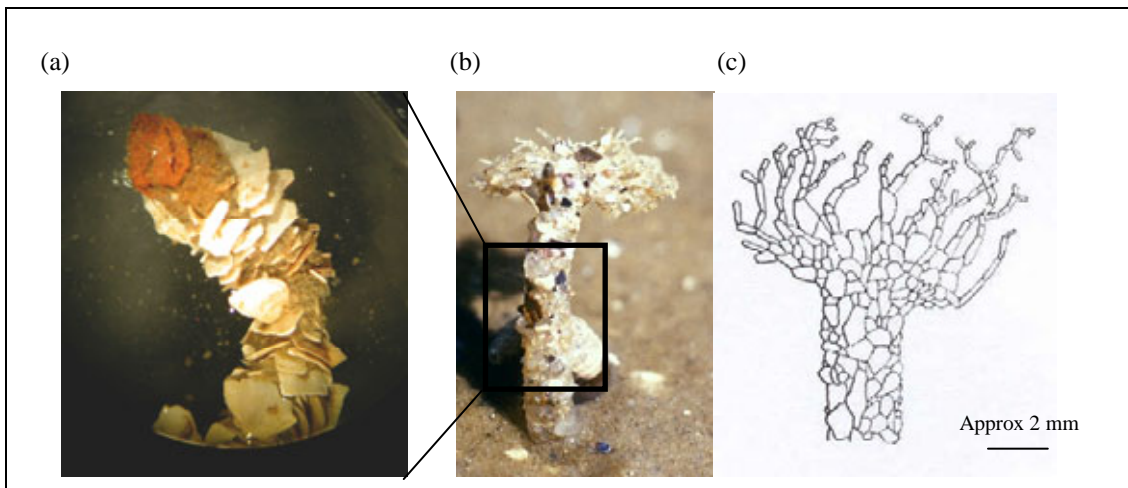


Figure 3.42. Tube constructed by *Lanice conchilega*. (a) Segment photographed under the microscope, (b) specimen in field conditions showing ragged fringe (source: Jassesnee.de web page, 2006), (c) identification diagram (source: Hayward et al, 1995a).

Species 5: Acorn barnacle *Semibalanus balanoides*

Phylum	Class (Subclass)	Order	Family	Genus	Species
Arthropod	Crustacea (Cirripedia)	Thoracica	Balanidae	Semibalanus	balanoides

Up to 5-10 mm in diameter and growing up to, but rarely as tall as, 15 mm in height, this crustacean has a white or cream to grey-brown shell (Figure 3.43). It is the most common barnacle found on the mid-shore rocky environments of the British Isles. At Warden Point the barnacles were confined to pebbles.

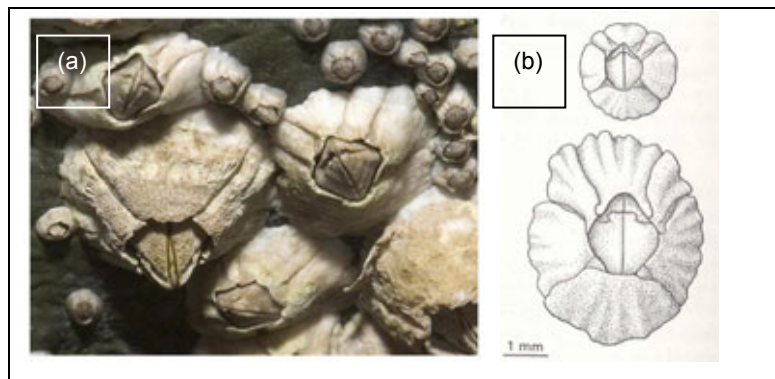


Figure 3.43. Acorn barnacle, *Semibalanus balanoides*. (a) Photograph showing different ages (source: Seawater.no web page, 2006). (b) Identification diagram (source: Hayward et al, 1995a).

Field-derived distribution and density:

The platform at Warden Point has been found to support generally large populations of *Corophium* and piddocks (Figure 3.44 and Figure 3.45).

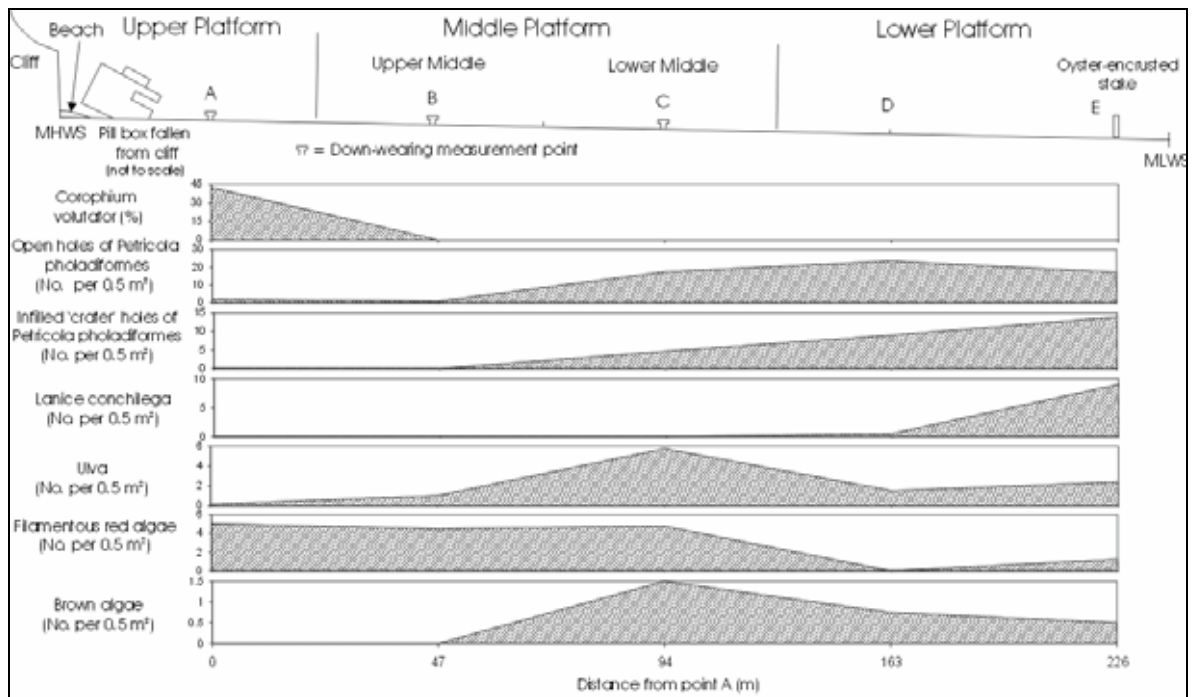


Figure 3.44. Summer distribution of organisms across the platform at Warden Point. Note the differences in the density (Y axis) scales. Percentages are the number of 1 cm² within 100 cm² quadrats containing that organism.

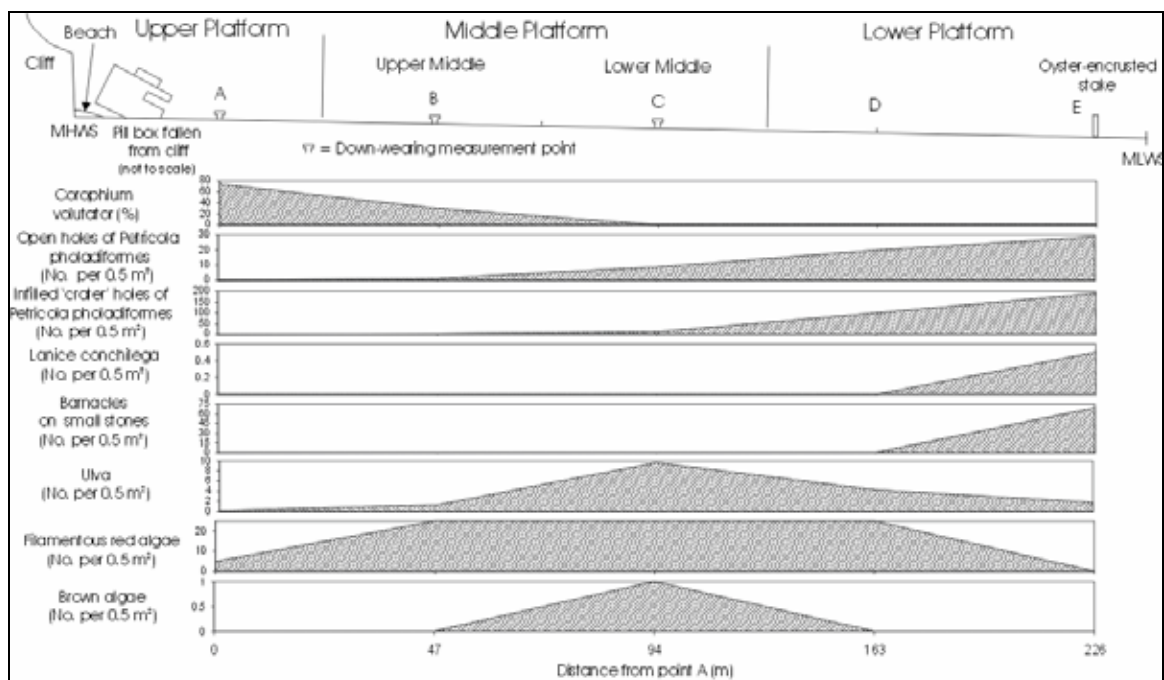


Figure 3.45. Winter distribution of organisms across the platform at Warden Point. Note the differences in the density (Y axis) scales and the addition of Barnacles which were not counted in the summer (Figure 3.43).

Corophium are found in their largest numbers on the upper platform. In July 2005, the following densities were recorded: 37, 38, 45, 33, 53, 39, 33, 55 and 58 round holes or "slits" per 5 x 5 cm cell.

This suggests that the maximum density is 50-60 perforations per 25 cm². As the organisms occupy U-shaped tubes, the number of individuals is 25-30 per 5 x 5 cm cell. The presence of fluid mud in the summer, which smothered many such holes, makes this figure less certain.

Corophium numbers decline in a seaward direction towards the upper middle platform where piddocks become more dominant. Piddocks have been found in their largest numbers on the lower platform, near the MLWS mark. The field-derived figures referring to open holes and infilled 'crater' holes (raw data are displayed in Appendix A and Appendix B) give an indication of the relative densities of near-surface and deeper-buried piddocks but not absolute densities. The laboratory-derived figures below give absolute densities albeit at a lower resolution across the platform. All excavations have uncovered only vertical piddocks.

The sand mason and barnacle have been found in their largest numbers on the lower shore platform. The sand mason, however, has also been encountered around the TEB sites on the lower middle platform.

The red, brown and green algae all peaked on the lower middle platform, forming a clearly visible zone and thought to be associated with the stones and rubble at this location, to which the algae attach themselves.

The summer and winter densities and distribution of fauna are thought to be very similar. The only organism with a distinct seasonal difference is the lower platform dwelling sand mason which decreased from 9 individuals per 0.5 m² in the summer to 0.5 individuals per 0.5 m² in the winter. Occasional individuals were also seen on the lower middle platform in the summer. As for the other burrowing organisms, the differences displayed between Figure 3.44 and Figure 3.45 may be due to a combination of platform geomorphology and sampling error. The fluid mud that was present on the platform in July 2005 masked many burrows and made counting difficult. The mud was agitated using a spade so that some piddocks expelled water through their siphons, clearing previously unseen, mud-blocked holes. However, the absence of this fluid mud in February 2006 clearly increased the count of burrowing and tube-building organisms. On the upper platform Corophium holes increased from an average of 43 % of 1 cm² quadrat cells in summer to 74 % in winter. It is doubtful that the population actually increased as one would have expected numbers to decrease due to the stormier and colder weather. On the lower platform the numbers of piddock holes increased from an average of 14 individuals per 0.5 m² in summer to 191 individuals per 0.5 m² in winter. The mollusc's slow growth rate, longevity and inability to change location rule out a population increase on this scale; the observed increase in holes must have been due to greater visibility, perhaps caused by increased scouring of the platform. It may also be the case that the experience gained in the summer counting inadvertently increased the counted numbers in the winter through 'better training of the eye'.

All algae increased in numbers in winter, the most conspicuous being the filamentous red algae, which are so prolific on the middle and upper lower platform that numbers could not be counted and instead the word 'abundant' was substituted.

Laboratory-derived calculations of piddock density:

Neither of the two blocks of mud from the upper platform contained any piddocks nor showed any evidence that piddocks were once present.

Of the two blocks from middle platform, only one contained live piddocks (8 individuals) between 2 and 6 cm depth beneath the surface. It also had 17 dead piddocks, at depths of between 0 and 8 cm beneath the surface. Some infilled holes were also present as deep as 10 cm into the block showing that piddocks are capable of living to this depth on the middle platform. The block devoid of live piddocks held 9 dead individuals between 2 and 8 cm beneath the surface.

The middle platform has been found to have a highly variable piddock density with some areas containing no live piddocks at all. Averaging the results from both blocks, the surface 10 cm contains 0.1% live piddocks, 0.51% dead piddocks, 0.72% infilled holes which would have once been a burrow or a piddock's body and 0.03% void spaces used for feeding and breathing. Thus an average of 1.36% of the middle platform has been bored by piddocks to a depth of 10 cm.

Both blocks from the lower platform contained live piddocks (8 in one and 31 in the other). The block containing the larger number of live piddocks had a greater range of depths with individuals occurring between 2 cm and 10 cm beneath the surface. The other block had live piddocks only between 4 cm and 8 cm beneath the surface. The block with the greater number of live piddocks also had a greater number of dead piddocks, with 18 empty shells recorded between the surface and 10 cm beneath. The other block contained only 13 dead individuals between the surface and 8 cm depth. As with the middle platform, some infilled holes were found as deep as 10 cm into the block (in both blocks) showing that piddocks are capable of living to this depth on the lower platform.

The lower platform also recorded a highly variable piddock density and depth distribution. Piddocks appear to be able to live deeper below the surface on this section of the platform. Averaging the results from both blocks, the surface 10 cm contains 1.69% live piddocks, 1.56% dead piddocks, 2.56% infilled holes which would have once been a burrow or a piddock's body and 0.32% open burrows or spaces used for feeding and breathing. Thus an average of 6.13% of the lower platform, to a depth of 10 cm, has been bored by piddocks.

The number of piddocks per 50 cm² of platform surface can be estimated as follows:

Lower platform:		
1 st block = 12 x 18.5 cm	8 live piddocks	= 90 per 50 cm ²
2 nd block = 17 x 19 cm	31 live piddocks	= 240 per 50 cm ²
		Average = 165 per 50 cm ²
Middle platform:		
1 st block = 18 x 26 cm	8 live piddocks	= 43 per 50 cm ²
2 nd block = 21 x 21 cm	No live piddocks	= 0 per 50 cm ²
		Average = 21.5 per 50 cm ²
Upper platform:		
	No live piddocks in either block	
		Average = 0 per 50 cm ²

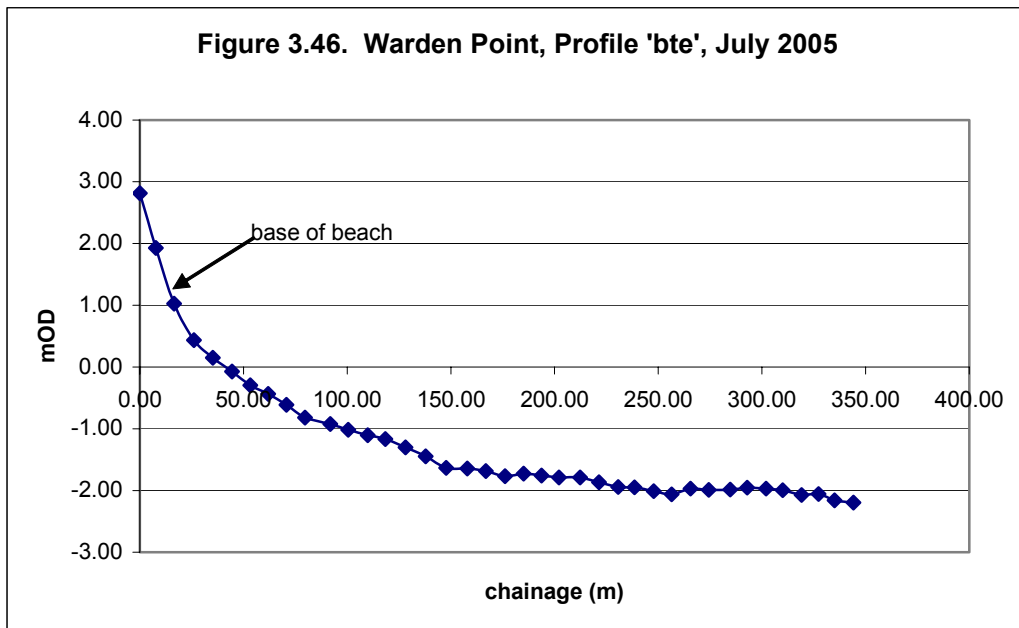
Results from the middle and lower platform have been averaged to give 93 per 50 cm². Further along the coast at Whitstable, Duval (1963) reported densities of 43 per 50 cm² at The Street, but only 12 per 50 cm² off Wave Crest, where conditions for growth were less favourable.

(c) Profile Surveying

One of the summer shore-normal profiles (bte) is shown in Figure 3.46 (see Figure 3.19 for location). The beach is approximately 16 metres wide on this profile (chainage 0 = toe of cliff). The exposed platform extends from the seaward edge of the beach to the low water mark a distance of around 320 metres. The beach face can be seen to be relatively steep with a gradient of 6.13° or approximately 1:9. The platform has a gentler gradient which appears to consist of two distinct parts separated by a slight break of slope. From the base of the beach to approximately 148 metres chainage the platform has a gradient of 0.97° or approximately 1:59. From 148 metres chainage to the low water mark the platform has a very low gradient of only 0.17° equivalent to 1:344. All three of the erosion pin sites lie on the segment of platform between the base of the beach and 148 metres chainage so lie on the segment of platform with an approximate gradient of 1:59.

The base of the beach lies at an elevation of approximately +1 metres OD with the top of the beach/toe of cliff at around +2.8mOD. The lowest part of the platform seen was at approximately -2.27mOD (Profile bte in February 2006). The break of slope in mid platform mentioned above occurs at approximately -1.8mOD.

Mean high water springs (MHWS) reach an elevation of around +2.9 metres OD (based on data from the tide gauge at Sheerness) which is close to the elevation of the top of the beach sediments/cliff toe. The mean low water spring level (MLWS) is -2.23 metres OD which is close to the measured minimum elevation height measured by the GPS survey. The mid platform break of slope occurs close to the elevation of mean low water neap tides (MLWN) at -1.4 metres OD.



The beach at Warden Point in July 2005 was found to be very thin. A veneer of sand-sized sediment consisting mostly of abraded shell fragments was found to be approximately only 10 cm thick resting directly on the London Clay (Figures 3.47 and 3.48).

Other beach sediment consisted of pyritic sand and pebble-sized sediment including pyritised wood and other fossils derived from the erosion of the London Clay.

The beach also included scattered phosphatic pebbles, cobbles and boulders of limestone which originated as septarian concretions within the London Clay, together with a variety of anthropogenic debris including bricks and concrete many of which were derived from the erosion of WW2 military defences at this site. These larger scattered clasts rested directly on the underlying clay platform. There were also numbers of rounded lumps of clay and armoured mudballs derived from the direct erosion of the London Clay.



Figure 3.47. Warden Point: Thin beach in July 2005 consisting of shell debris (light coloured sediment) and scattered blocks of clay and limestone.



Figure 3.48. Warden Point site.

Note: Beach sediment with abundant shell debris and scattered limestone pebbles (coin is 22mm diameter) (July 2005).

The February 2006 inspection found that the thin veneer of sand had been largely removed leaving only scattered pebbles and cobbles with the platform clearly exposed between individual clasts (Figure 3.49).

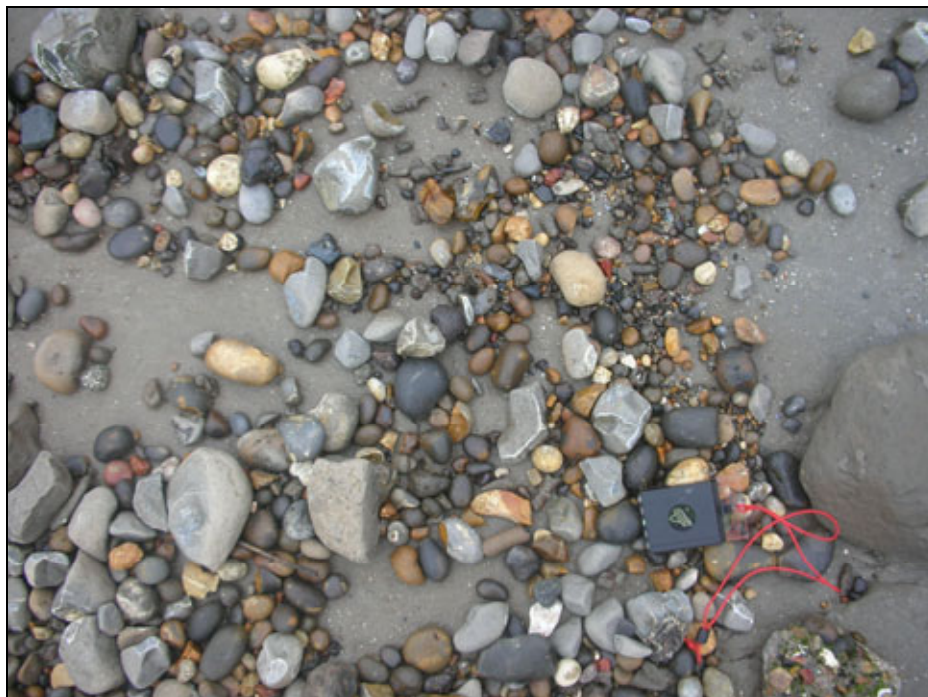


Figure 3.49. Warden Point: Beach sediment seen in February 2006 with lag gravel resting directly on London Clay platform.

Platform profile 'bte' was measured again in February 2006 but showed no measurable change compared with the July 2005 profile within the accuracy of the GPS method.

(d) *Geotechnical*

In Situ Tests: The Geonor shear vane results for Warden Point, representing the undrained shear strength, s_u , at a depth of 60 mm, show a range from 75 to 108 kPa (Table 3.11).

Table 3.11. Results of Geonor shear vane tests.

Site	Location	Su (kPa)	Location	Su (kPa)
Warden Point (Isle of Sheppey)	Cp1	82	Cp7	101
	Cp2	78	Cp8	81
	Cp3	90	Cp9	89
	Cp4	95	Cp10	80
	Cp5	102	Cp11	75
	Cp6	108	Cp12	76

This result classifies all the material tested as 'stiff' according to BS5930 (1999). The higher values cluster in an area close to triaxial sample location U1; this triaxial test having produced the highest value of undrained cohesion, c_u .

The Panda penetrometer test results for Warden Point (Figure 3.50) show that overall cone resistance lies in the range 1 –2 MPa with variations above 0.15 m. At depths shallower than 0.15 m variability may be caused in part by bioturbation and the presence of shells. Below this depth the principal deviations are seen in soundings Cp7 and Cp8, which tend to increase significantly, though not uniformly, with depth and reach penetration resistances in excess of 5 MPa and, in the case of Cp8, 10 MPa. The reason for these anomalies is unclear. Their overall form suggests that they were not formed by individual obstructions. It may be that they indicate the presence of layers of nodular claystones or other stronger lithologies within the London Clay Formation due for example to cementation, though why such layers should not have been penetrated by the other profiles is unclear, if the assumption that the study area represents previously unslipped London Clay is correct (Dixon & Bromhead, 2002). Two zones of decreased penetration resistance are seen for Cp12 and Cp14 at 0.3 and 0.6 m depth, respectively. These may represent the interception of individual joints within the London Clay Formation or the presence of sandy lenses or layers.

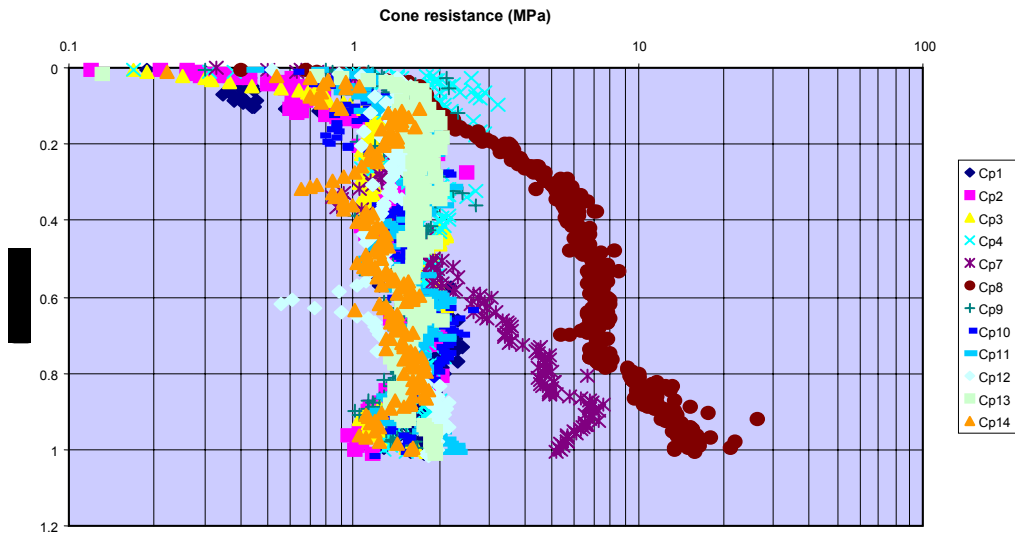


Figure 3.50. Panda penetrometer test profiles- Warden Point

Laboratory Tests: The results of index tests (Atterberg and linear shrinkage) carried out on disturbed (bag) samples matching the triaxial test samples are shown in Table 3.12.

Table 3.12. Index test results corresponding to triaxial samples. LL=Liquid limit, PL=Plastic limit, PI=Plasticity index, LS=Linear shrinkage, Ac = Activity.

Sample	LL (%)	PL (%)	PI (%)	LS (%)	CLAY (%)	SILT (%)	SAND (%)	Ac
SHEP1 (U1)	89.7	33.2	56.5	15.2	63.1	35.3	1.6	0.90
SHEP2 (U2)	75.8	29.4	46.4	15.0	58.7	39.4	1.9	0.79
SHEP3 (U3)	75.0	28.2	46.8	14.9	59.3	38.9	1.8	0.79

The plasticity data are shown in the form of a Casagrande plot in Figure 3.51. This shows that the Sheppey samples are classified as ‘very high’ plasticity. All three samples plot above the A-line, indicating that they are neither predominantly silty nor metastable. The samples taken close together (SHEP2 and SHEP3) show good agreement in terms of index data, and differ significantly from the remote sample (SHEP1).

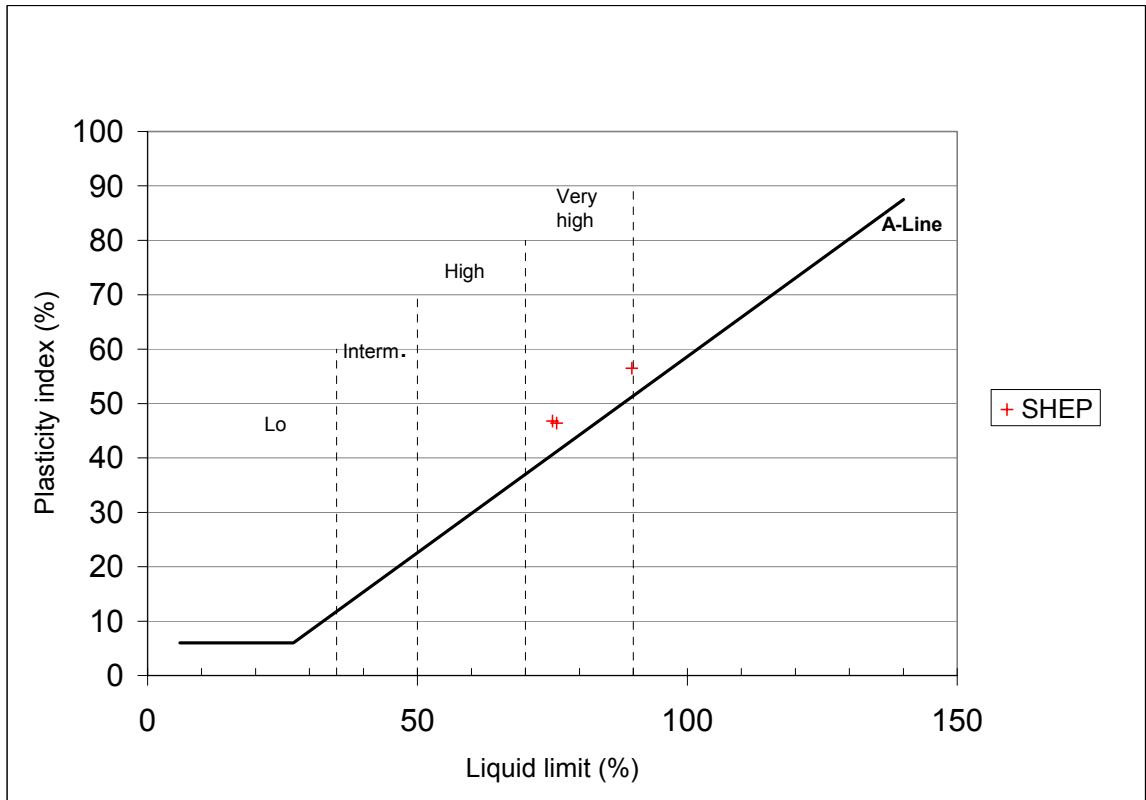


Figure 3.51. Casagrande plasticity plot for triaxial samples.

Activity, A_c , is defined as the plasticity index divided by the clay fraction. Values are quoted in Table 3.12. This indicates the relative contribution of clay minerals to overall plasticity. The Warden Point samples could be described as ‘normal’.

It should be noted that all samples contained saline pore water. Salinity has a small effect on plastic behaviour, and may be expected to have influenced the tests non-uniformly. That is, the wetter remoulded (liquid limit test) sub-samples will have contained water of reduced salinity compared with the drier sub-samples. No correction has been applied to water content determinations as a result of salts remaining within the pores during oven drying.

The results of particle-size determinations for samples matching the triaxial tests are shown in Figure 3.52. The results show that SHEP2 and SHEP3 have similar grading curves. The Warden Point curves are closely grouped and are considered typical of the London Clay Formation.

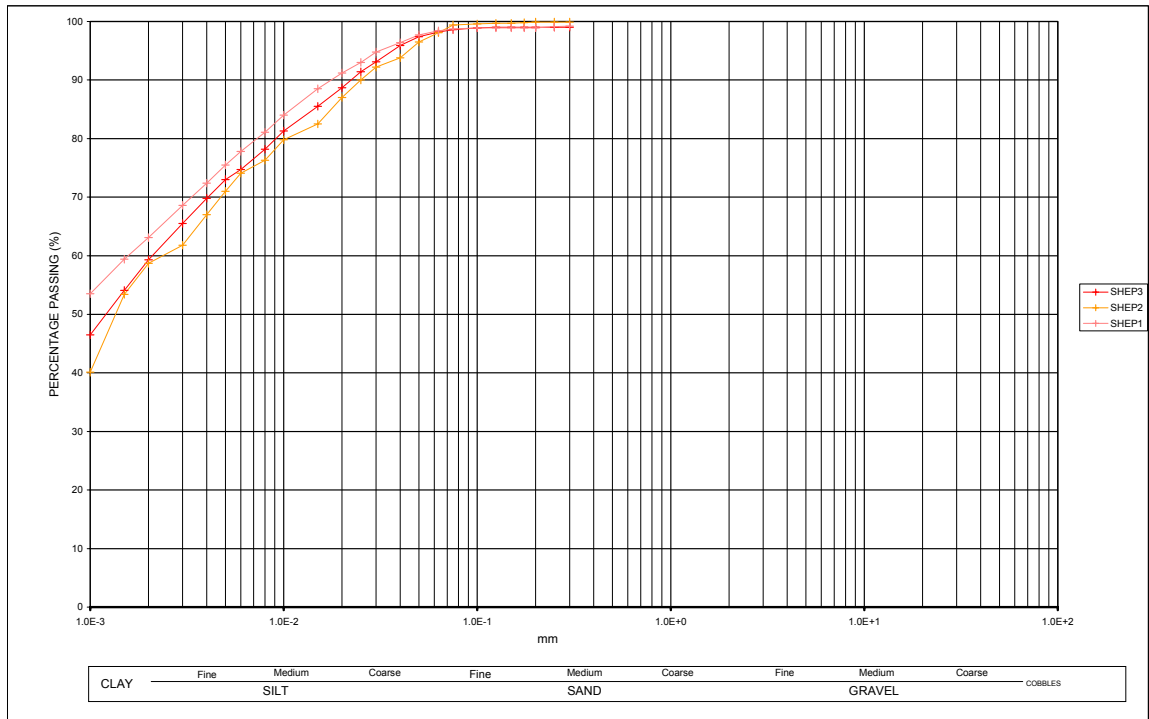


Figure 3.52 Particle size analysis grading curves matching triaxial samples.

From the triaxial tests results the Mohr-Coulomb failure envelope for each specimen was determined and the values for effective cohesion, c' and effective internal friction angle, ϕ' calculated. The results are shown in Tables 3.13 and 3.14, and plotted in Figure 3.52.

Table 3.13. Results of 100 mm CIU triaxial tests (effective strength).

Sample No.	c'	ϕ'
	(kPa)	(degrees)
Shep 1	25.7	24.3
Shep 2	18.7	43.7
Shep 3	7.06	28.03

Table 3.14. Details of stress-path parameters at failure (effective parameters) (Mean effective stress, s' , maximum effective shear stress, t').

Sample	Stage 1		Stage 2		Stage 3	
	s' (kPa)	t' (kPa)	s' (kPa)	t' (kPa)	s' (kPa)	t' (kPa)
Shep1	41.77	39.17	72.09	54.99	154.02	86.22
Shep2	38.11	37.71	74.82	68.42	149.16	115.56
Shep3	30.42	19.62	68.70	40.00	128.76	66.16

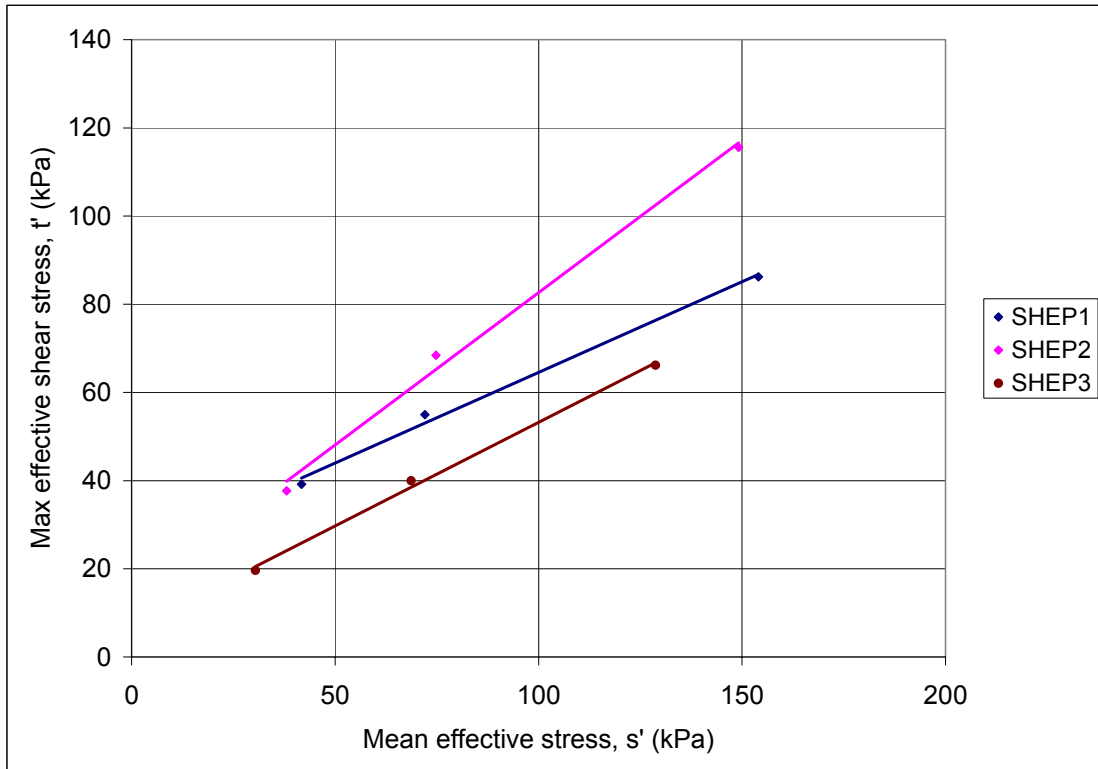


Figure 3.53. Mohr circle locus plots for triaxial tests (effective strength).

Samples SHEP1 and SHEP3 show similar effective friction angle, ϕ' , but with SHEP3 having a lower effective cohesion, c' . Sample SHEP2 stands out as having a relatively high effective friction angle, ϕ' , compared with the other Warden Point samples (and also compared with the Easington samples). This does not appear to be explained by the particle-size grading, but may be due to shell content. The index test results show that sample SHEP1 is significantly more plastic, and has a higher clay fraction, than the other samples. This explains the higher effective cohesion and lower effective friction obtained for this sample in the triaxial test.

The stress-path plots for the triaxial tests show similarities between SHEP1 and SHEP3, both behaving as 'normally consolidated' throughout the stress range of the test (with the possible exception of SHEP1's Stage 1). However, sample SHEP2 behaves as 'over consolidated' in all 3 stages. This same sample has the highest effective friction angle. 'Normally consolidated' and 'over consolidated' type behaviours, as described above, are sometimes referred to as 'wet of critical' and 'dry of critical', respectively when used in a critical state context.

(e) *Wave Climate*

Offshore Wave Data: Meteorological Office wind and wave data availability for a grid point offshore from Warden Point is summarised below:

Location: 51.5°N, 1.1°E, water depth 7 m

Data Range: 07/1988 to 10/2005

Wind Data: Three-hourly time series of wind direction (degrees true) and wind speed (knots)

Wave Data: Three-hourly time series of wave direction (degrees true), resultant (mean) wave period (seconds) and resultant (significant) wave height (metres)

Water Level: Table 3.15 summarises astronomical tide levels for the Standard Port of Sheerness. The MHWS level of +5.8 m CD is used in the numerical transformation of the offshore wave data to the coast at Warden Point.

Table 3.15. Tide Levels at Sheerness (m CD)

LAT	MLWS	MLWN	MSL	MHWN	MHWS	HAT	Spring Range	Neap Range
-0.1	+0.6	+1.5	+3.0	+4.7	+5.8	+6.3	5.2	3.2

Offshore Wind Climate: The offshore wind time series data was transformed into a frequency table shown in Table 3.16 (note wind speed in knots) and a wind rose shown in Figure 3.54.

Table 3.16. Offshore wind climate at Warden Point

Direction °N	0	30	60	90	120	150	180	210	240	270	300	330
Wind Speed knots												
0	0	0	0	0	0	0	0	0	0	0	0	0
1.0-3.0	147	161	205	170	195	169	153	195	212	202	199	166
4.0-6.0	471	445	556	542	487	485	515	650	727	718	560	480
7.0-10.0	816	980	1178	972	818	724	967	1533	1984	1485	1098	817
11.0-16.0	891	1234	1340	835	515	644	1079	2219	3033	1919	1240	1010
17.0-21.0	333	494	512	288	137	192	536	1347	1592	905	519	450
22.0-27.0	107	197	220	79	28	49	266	843	910	462	180	161
28.0-33.0	11	23	17	12	5	9	101	281	308	110	24	21
34.0-40.0	3	4	0	0	1	0	19	58	51	39	9	1
41.0-47.0	0	1	0	0	0	0	0	17	19	11	1	0
48.0-55.0	0	0	0	0	0	0	0	1	5	4	1	0
56.0-63.0	0	0	0	0	0	0	0	0	0	2	0	0
>63	0	0	0	0	0	0	0	0	0	1	0	0

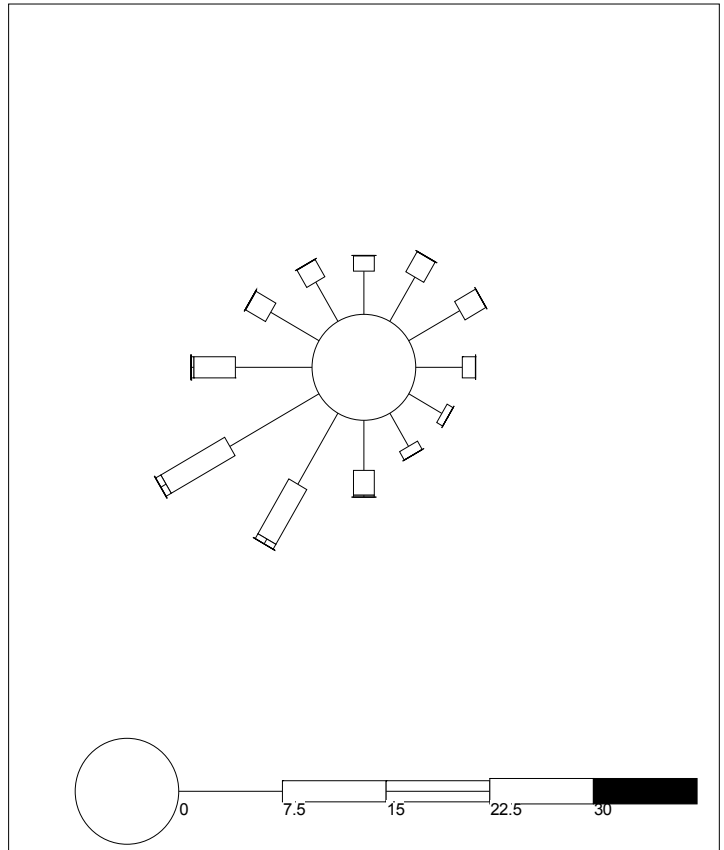


Figure 3.54. Wind rose at Warden Point. Scale is in ms^{-1} .

The wind data has been used to derive average wind speeds from each sector that were used in the wave transformation.

Direction °N	0°	30°	60 (55)°	90(80)°
Wind speed ms^{-1}	5.1	5.4	5.3	4.8

Offshore Wave Climate: The offshore wave time series data was used to create the frequency tables shown in Tables 3.17 and 3.18, and the wave rose shown in Figure 3.55.

Table 3.17. Offshore wave climate at Warden Point

Period s	2.1-3.0	3.1-4.0	4.1-5.0	5.1-6.0	6.1-7.0	7.1-8.0	8.1-9.0	9.1-10.0	10.1-11.0	11.1-12.0	12.1-13.0
Wave Height H_s m											
0-0.5	0	15176	3704	1011	249	101	31	12	3	1	7
0.6-1.0	0	18421	3898	352	104	23	2	2	1	0	0
1.1-1.5	0	875	5213	251	21	4	3	0	0	0	0
1.6-2.0	0	0	544	239	7	1	1	0	0	0	0
2.1-2.5	0	0	28	77	16	4	0	2	0	0	0
2.6-3.0	0	0	1	13	12	2	0	0	0	0	0
3.1-3.5	0	0	0	0	7	1	0	0	0	0	0
3.6-4.0	0	0	0	0	1	2	0	0	0	0	0

Table 3.18. Offshore wave climate at Warden Point

Direction °N	0	30	60	90	120	150	180	210	240	270	300	330
Wave Height Hs m												
0-0.5	452	2458	5073	2032	1386	1481	1206	1584	1985	1366	791	481
0.6-1.0	840	1668	3626	1598	1269	1054	1417	2887	3663	2258	1458	1065
1.1-1.5	166	346	777	414	197	214	612	1261	1271	609	262	238
1.6-2.0	8	73	93	39	10	7	81	188	156	114	17	7
2.1-2.5	0	4	13	7	15	6	10	34	15	20	2	0
2.6-3.0	0	0	0	4	10	7	2	1	1	3	0	0
3.1-3.5	0	0	0	5	1	2	0	0	0	0	0	0
3.6-4.0	0	0	0	3	0	0	0	0	0	0	0	0

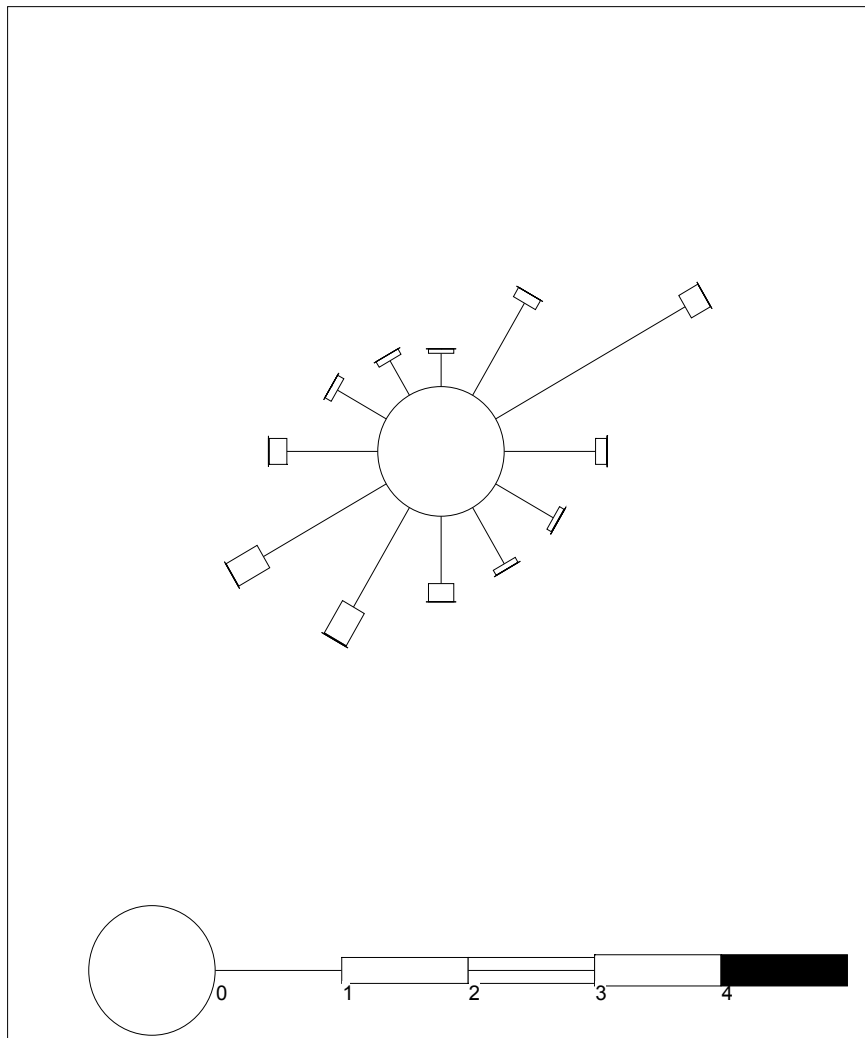


Figure 3.55. Offshore wave rose at Warden Point. Location 51.5°N, 1.1°E. Period July 1988 to October 2005. Scale is in metres

Table 3.17 has been used to derive a wave height-wave period relationship that was used in the wave transformation (Table 3.19).

Table 3.19. Wave height – period relationship for the offshore wave data at Warden Point

Height	Period
0.5	4.92
1	5.29
1.5	6.01
2	6.72
2.5	7.47
3	8.19
3.5	8.96
4	9.69

The dominant wave direction is from the north-east sector with significant contribution to the wave climate from the south-west sector. These dominant wave energies reflect the exposure to waves directly from the North Sea approaching in to the Outer Thames Estuary.

Nearshore Wave Climate: The nearshore wave climate at Warden Point at the 0m CD contour close to the shore platform study site was derived using the SWAN 1D model. The transformation matrices for Warden Point derived from the SWAN 1D model is shown in Table 3.20.

Table 3.20. Transformation matrices at Warden Point. Table at top shows output wave heights at 0 m CD contour (5.8 m water depth = MHWS). Table at bottom shows output wave directions at same location.

Input Hs (m)	Direction			
	0	30	60	90
0	0.00	0.00	0.00	0.00
0.5	0.52	0.54	0.51	0.46
1	0.78	0.76	0.71	0.57
2	1.42	1.32	1.13	0.86
4	2.16	2.19	1.89	1.54

Input Hs (m)	Direction			
	0	30	60	90
0	0.0	30.0	60.0	90.0
0.5	359.9	29.8	59.8	89.8
1	359.8	29.6	59.2	89.1
2	359.9	30.0	60.0	89.9
4	353.6	25.5	55.1	87.6

The inshore wave climate derived from the model results is shown in Table 3.21 and Figure 3.56.

Table 3.21. Inshore wave climate at Warden Point

Direction °N	0	30	60	90	120	150	180	210	240	270	300	330
Wave Height Hs m												
0 - 0.5	630	2315	5029	3102	2860	2759	3324	5951	7101	4363	2531	1790
0.6 - 1.0	827	2173	4483	968	0	0	0	0	0	0	0	0
1.1 - 1.5	30	116	61	10	0	0	0	0	0	0	0	0
1.6 - 2.0	0	0	0	0	0	0	0	0	0	0	0	0
2.1 - 2.5	0	0	0	0	0	0	0	0	0	0	0	0
2.6 - 3.0	0	0	0	0	0	0	0	0	0	0	0	0
3.1 - 3.5	0	0	0	0	0	0	0	0	0	0	0	0
3.6 - 4.0	0	0	0	0	0	0	0	0	0	0	0	0
4.1 - 4.5	0	0	0	0	0	0	0	0	0	0	0	0

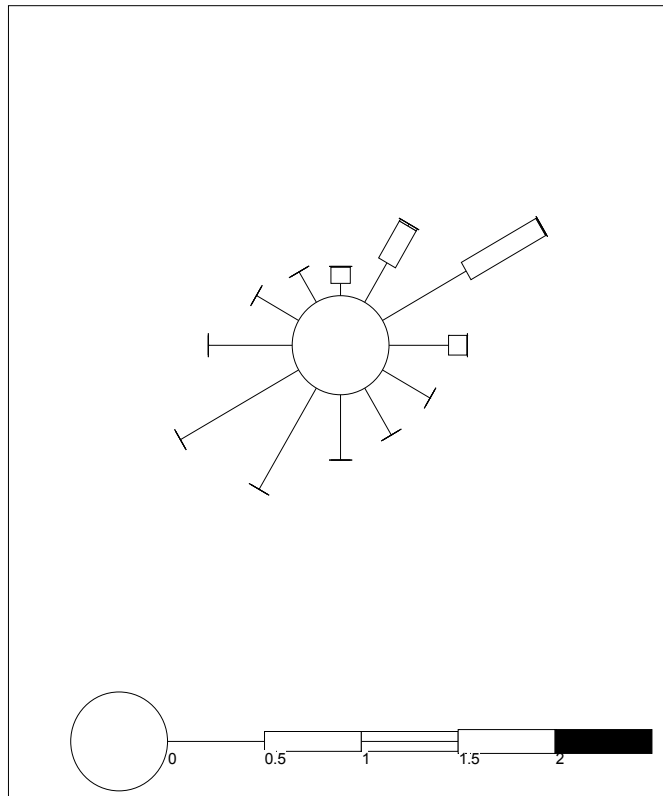


Figure 3.56. Inshore wave rose at Warden Point. Scale is in ms^{-1} .

3.3.2 Easington

This section presents results from the field investigations, laboratory testing and numerical wave modelling undertaken at Easington. It deals with each of the following parameters of relevance in turn, before the results are interpreted in Section 3.4:

- Platform downwearing rates;
- Platform biology;
- Beach and platform morphology (profile surveying);
- Geotechnical testing; and
- Wave climate.

(a) Platform Downwearing Rates

Platform downwearing results from locations B and C at Easington are presented in Figures 3.57 and 3.58 respectively. The mean annual downwearing recorded by the TEB from July 2005 to July 2006 was 41.93 mm (standard deviation 14.29). This was almost two and a half times higher than at Warden Point and it is possible that the sand and shingle in the beach and the ord at the Easington site contributed to this higher rate. Of the measured results, the middle platform downwearing over the 1 year period was 43.4 mm and the lower platform downwearing was only very marginally lower at 39.8 mm.

Beyond the TEB locations however, towards the head of the beach, the shingle depth was >5 m for the entire measurement period and this probably protected the platform surface on this section of the profile from downwearing.

As with the Warden Point measurements, the graphs indicate that downwearing may have been different in areas of positive and negative microrelief. This is particularly apparent on the southern side of site C where the raised areas recorded seemingly much greater downwearing than the hollow or runnel. To test this, the data from July 2005 onwards were divided into two sets of 11 measurement points representing raised areas and depressions. The raised areas gave a mean of 51.24 mm and the depressions just 30.16 mm. The value of Student's *t* is 3.385 with 20 degrees of freedom, yielding a two-tailed probability of only 0.003, which strongly suggests that the difference in the means is not due entirely to chance sampling. As at Warden Point, it is reasonable to conclude that downwearing rates vary with microrelief and that slightly raised areas wear down faster than depressions.

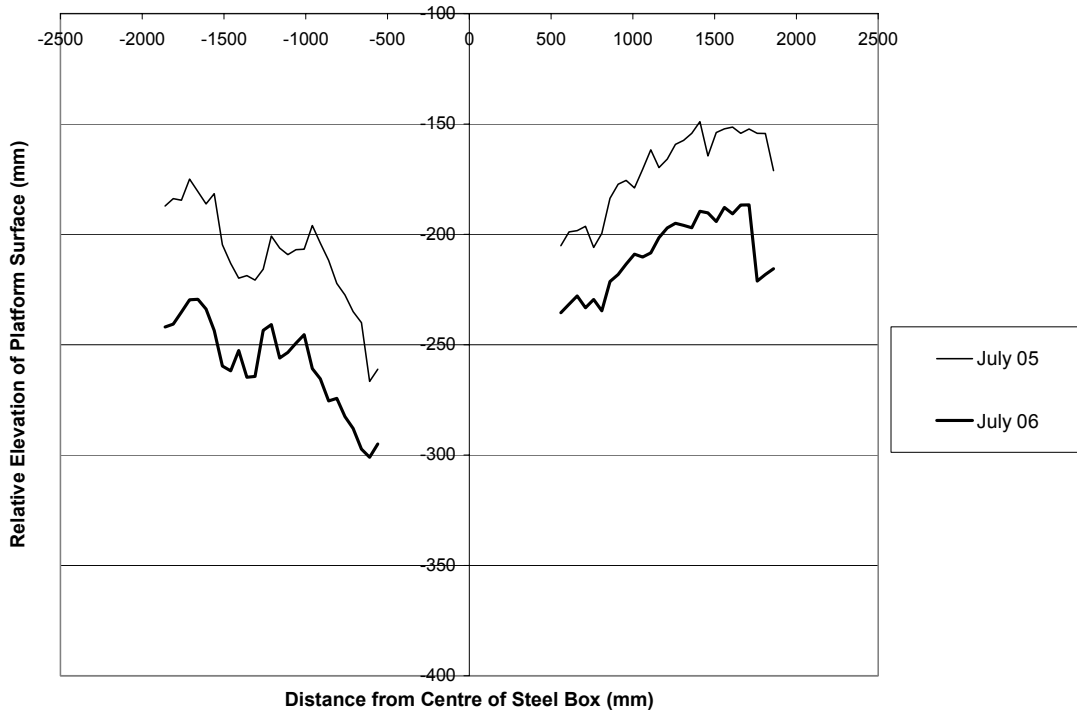


Figure 3.57. Easington, location B: changes in platform elevation, July 2005 to July 2006. Southern profiles on the left hand side, northern profiles on the right hand side.

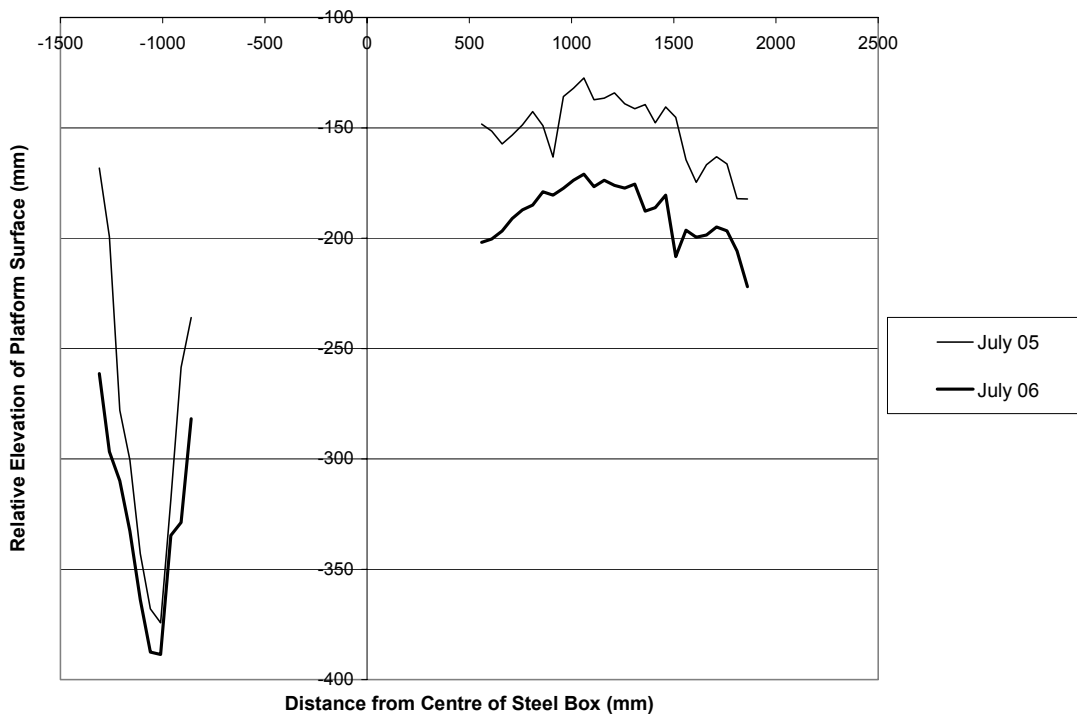


Figure 3.58. Easington, location C: changes in platform elevation, July 2005 to July 2006. Southern profiles on the left hand side, northern profiles on the right hand side.

(b) Platform Biology

The shore platform at Easington is very exposed and, at a casual glance, seemingly devoid of life. This is in great contrast to the Warden Point site where there exists considerable biological activity. No seaweeds grew on the platform at the time of the summer survey. The only animal species noted was the white piddock:

Species 1: White piddock *Barnea candida*

Phylum	Class	Order	Family	Genus
Mollusca	Bivalvia	Pholadidae	Barnea	Barnea

This piddock has white, oval valves up to 6.5 cm long, with a light brown periostracum. A native, it is widely distributed around the British Isles, but is most common in the south. According to Irving (1998, p. 105), it is “found from mid-shore to a depth of less than 10 m.” Both Irving and Tebble (1966, p. 181) claim that the burrows “tend to be horizontal”, but Duval (1963) reported near vertical burrows at Whitstable and the burrows at Easington are mostly vertical, though a few are conspicuously horizontal. White piddocks bore mechanically into peat, clays and shales, chalk and sand. Little seems to be known about their life span.

Near the TEB sites at Easington, there were only small scattered clusters of piddock holes. No live individuals could be found. All the holes were empty or contained only dead shells. The rounded mouths of the holes suggest that downwearing of the shore platforms has occurred since the death of the piddocks. The following densities were noted:

Table 3.22. Piddock holes found at four sites on Easington shore platform

Number of Holes	Area (cm ²)
19	750
11	500
12	375
43	500

On an astronomical spring tide, high densities of eroded burrows filled with dead piddocks could be seen at the extreme low water mark (Figure 3.59). Shells are both more numerous and more complete, indicating that the piddocks had recently died or the platform had been less heavily eroded.



Figure 3.59. Scattered clusters of former piddock burrows at Easington.

Piddocks have evidently succeeded in colonising the Easington platform when the beach and sand bars were more stable. They presumably died when moving sand and shingle buried the colonies. Except near extreme low water mark, there is little evidence that they have played a significant role in platform downwearing and for this reason the biological observations made at Easington were reduced compared to the Warden Point site where biological activity was considerably greater.

(c) Profile Surveying

In July 2005 the beach was approximately 60-65m wide at the study site. The beach face had a gradient of around 5.7° or approximately 1:10. An extensive intertidal platform of glacial till was exposed seaward of the beach up to 60m wide. A shoreline-oblique sand bar was lying separated from the seaward edge of the exposed platform by a narrow water-filled runnel which was open to the sea to the south. This runnel remained full of water even at the lowest state of the tide.

In March 2006 the beach was much wider and flatter than when seen the previous July. The beach was now up to 100m wide and the beach face gradient was approximately 2.5° or 1:22. The increase in beach width meant that all of the three erosion pins had become buried and no measurements of platform downwearing were possible. Observations from field inspections made over the winter suggest significant widening of the beach and the burial of the erosion pins occurred in November/December 2005. The bar appeared to have become attached to the lower beach face at the northern end of the study site increasing the beach width to over 175m, which accounts for the overall widening of the beach at this time.

By July 2006 the beach was still wider than in the previous summer and had steepened slightly when compared to the March profile with a beach face gradient of 3.2° or approximately 1:18. A bar was lying offshore from the platform which was attached to the beach to the north of the study site. It is possible that the bar which had become attached to the beach at the study site over the winter had migrated southwards and that the bar seen in the July 2006 survey was a different bar which had migrated southwards into the study section over the intervening 4 months.

These oblique shoreline attached bars are separated by shoreline-oblique runnels known as 'ords' and are a characteristic of the Holderness coast. The runnels are characterised by an absence of beach sediment and exposure of the underlying till platform (Figure 3.60). These features have been shown to move southwards at an average rate of 500 metres per year (Pringle, 1985). Many of the beach/platform morphological changes witnessed within the study period July 2005/July 2006 are consistent with the southward passage of an ord across the study site.



Figure 3.60. Easington: Narrow intertidal platform exposed at low water between low angle beach and nearshore shore-oblique bar (March 2006).

The cross-shore profiles measured in July 2005 (Figure 3.61) show the lowering of the profile in a northwards direction, bpc being the profile at the southern edge of the frontage and bpa at the northern edge. The data in Figure 13 indicates a consistent lowering over the whole of the beach profile of approximately 1 metre over the 100 metres of frontage. Profile btna was taken 350 metres further north where the beach lowering within the ord had caused the till platform to be exposed up to the foot of the cliff. Armoured mudballs were abundant across this exposed platform. If the exposed platform profile seen in btna is typical of the platform profile buried beneath the beach at the study site, a maximum beach thickness of around two metres is suggested at the study site.

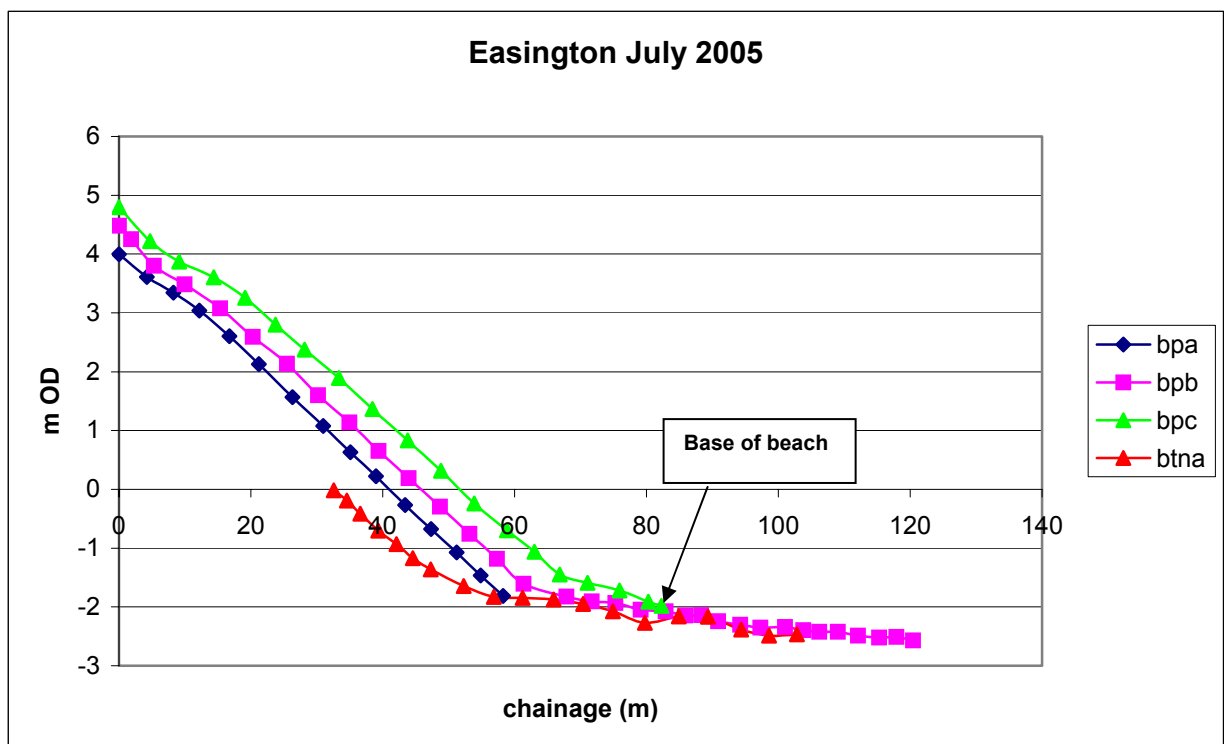


Figure 3.61. Easington: Shore-normal profiles in July 2005 showing reduction in elevation of beach profile from south (bpc) to north (btna).

Figure 3.62 shows the changes in cross-shore profile bpb over the three surveys. The beach profile shows the steep profile of July 2006 is similar to that seen one year earlier although with the addition of an 'apron' of sediment in the lower part of the profile serving to obscure part of the till platform. The presence of a bar close to the toe of the beach is apparent in the March 2006 profile which appears to migrate offshore by July 2006. It is possible that the bar in the latter survey is a different bar which has migrated from the north and may therefore appear to attach to the beach at the study site in the ensuing months as it too migrates through the site.

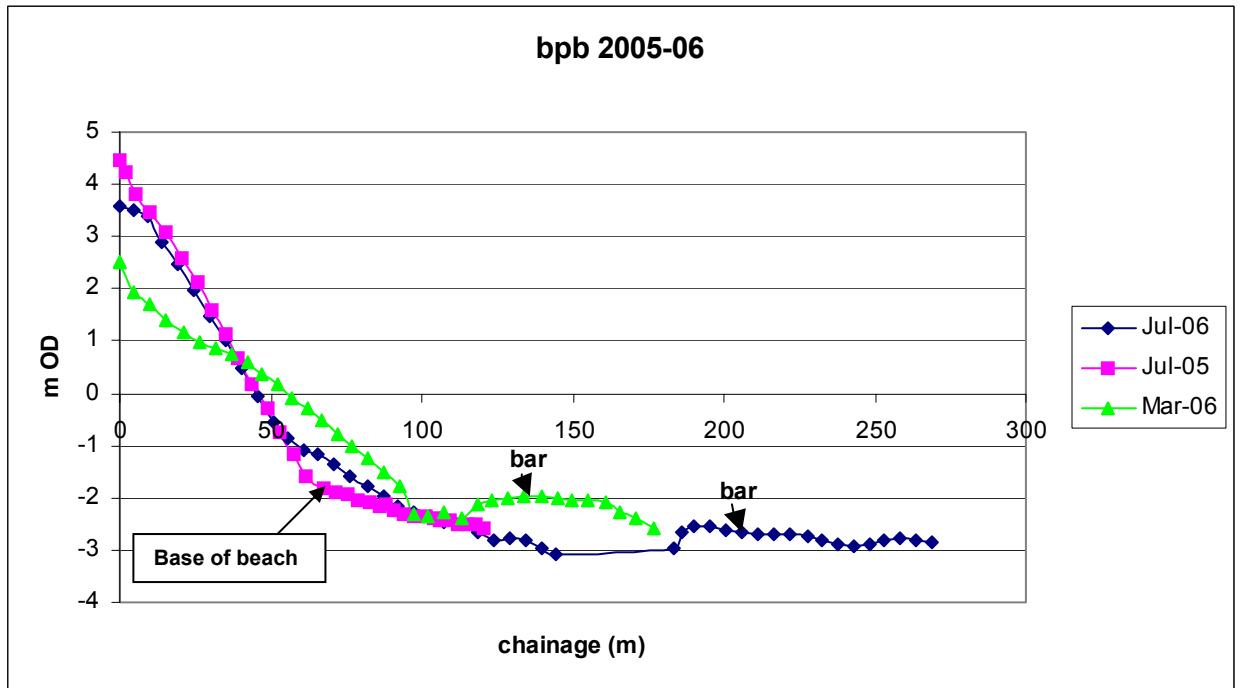


Figure 3.62. Easington: Cross-shore profile 'bpb' showing changes between July 2005 and July 2006.

Figure 3.63 shows the alongshore variation in elevation of the top of the beach. In July 2005 the beach has a high elevation through the study site with a slight slope from south to north of approximately 0.5 metres over the 100 metres between profiles bpc and bpa. By March 2006 the beach has dropped over 2 metres reflecting the general flattening of the beach profile already mentioned. It appears that the study site is within a 'trough' in the alongshore beach elevation. By July 2006 the beach elevation has built up again although not to the levels seen in the summer before. The study site now appears to coincide with a 'crest' in beach elevations. These observations appear to confirm that a rhythmic 'wave' in the alongshore beach morphology has passed from north to south during the period of survey.

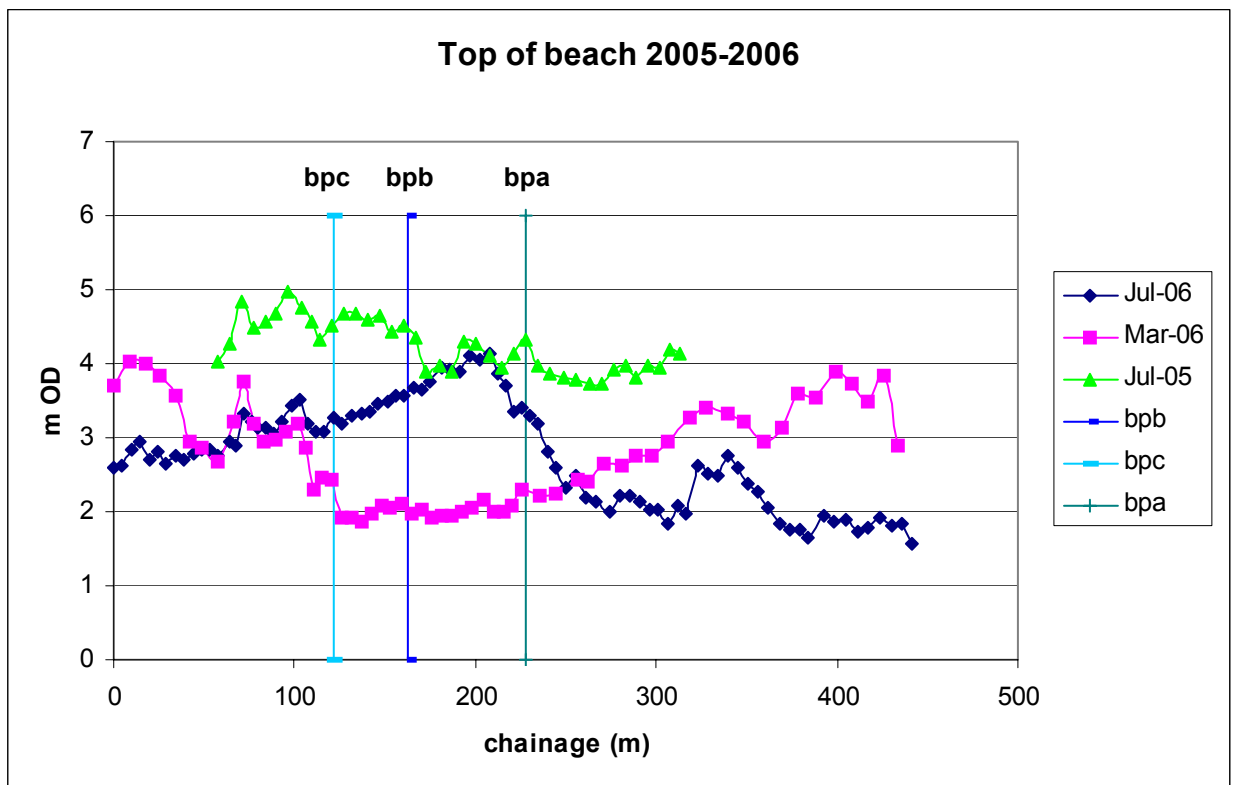


Figure 3.63. Easington: Profiles along top of beach July 2005-July 2006. Intersections with shore normal profiles bpa, bpb and bpc indicated.

Rates of platform downwearing appear to be high with an observed lowering relative to the project erosion pins and a wooden stake installed in summer 2005 showing approximately 9cm lost over the 12 month period of the field campaign.

The exposed intertidal platform at Easington lies between -2.0 metres OD and low water. Mean tide level is at around $+0.2$ m OD and mean low water neaps (MLWN) is at -1.2 metres OD. Consequently during neap tides the platform will not be uncovered at any time during the tide and its duration of exposure to the air is therefore much less than the platform at Warden Point.

(d) Geotechnical Properties

In Situ Tests: The Geonor shear vane data for Easington are patchy due to the refusal of the instrument at many locations. These materials may probably be classified as at least 'stiff' (and possibly 'very stiff'), with the exceptions of Cp1 and Cp8 which are 'firm'.

Table 3.23. Results of Geonor shear vane tests.

Site	Location	Su (kPa)
Easington	Cp1	66
	Cp2	>108
	Cp3	>108
	Cp4	>108
	Cp5	>108
	Cp6	>108
	Cp7	78
	Cp8	63
	Cp9	>108

Results of the Panda penetrometer test are shown plotted on a log scale in Figure 3.63. Whilst not being strictly a continuous log, each plot represents a large number of readings of penetration resistance with depth. The results are probably unreliable at depths shallower than 50 mm.

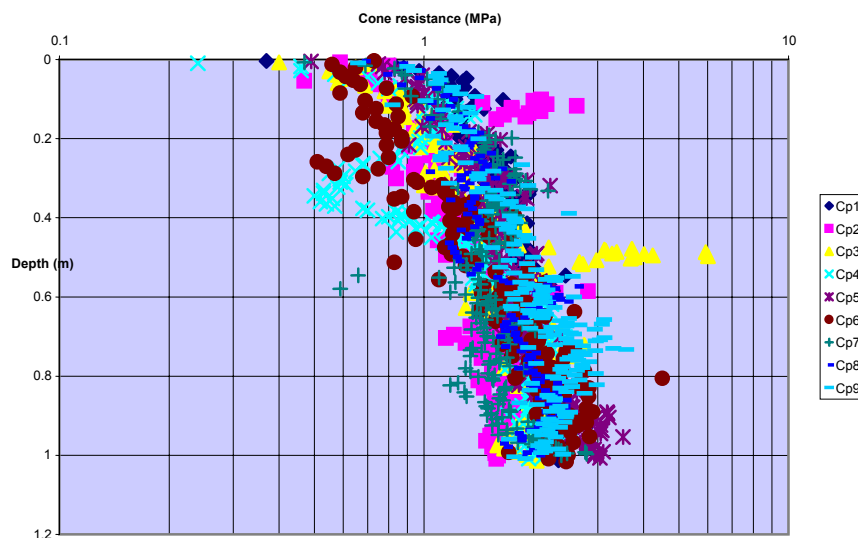


Figure 3.64. Panda penetrometer test profiles

The Panda test results for Easington show that overall penetration resistance increases linearly with depth. This trend appears to become established below a depth of about 0.1 m. High spikes in the data are seen in Cp2, Cp3, and to a lesser extent Cp9. These may represent individual obstructions, due for example to clasts within the till or a change in lithology. Some low spikes are

also seen. Whilst the profiles taken together suggest an overall linear depth profile, some individual soundings show considerable variation with depth. Below about 0.3 m most readings are above 1 MPa and attain values of between 2 and 3 MPa between 0.3 and 1.0m.

Laboratory Tests: The results of index tests (Atterberg and linear shrinkage) carried out on disturbed (bag) samples matching the triaxial test samples are shown in Table 3.24.

Table 3.24. Index test results corresponding to triaxial samples. LL=Liquid limit, PL=Plastic limit, PI=Plasticity index, LS=Linear shrinkage, Ac = Activity.

Sample	LL (%)	PL (%)	PI (%)	LS (%)	CLAY (%)	SILT (%)	SAND (%)	Ac
EAS1 (U1)	43.8	21.5	22.3	11.1	49.69	37.64	12.67	0.45
EAS2 (U2)	36.5	18.8	17.7	9.4	47.36	32.39	20.25	0.37
EAS3 (U3)	38.5	20.2	18.3	9.9	52.01	33.09	14.9	0.35

The plasticity data are shown in the form of a Casagrande plot in Figure 3.65. This shows that the Easington samples may be classified as ‘intermediate’ plasticity. All three samples plot above the A-line, indicating that they are neither predominantly silty nor metastable. The samples taken close together (EAS2 & EAS3) at Easington show good agreement in terms of index data, and differ slightly from the remote sample (EAS1).

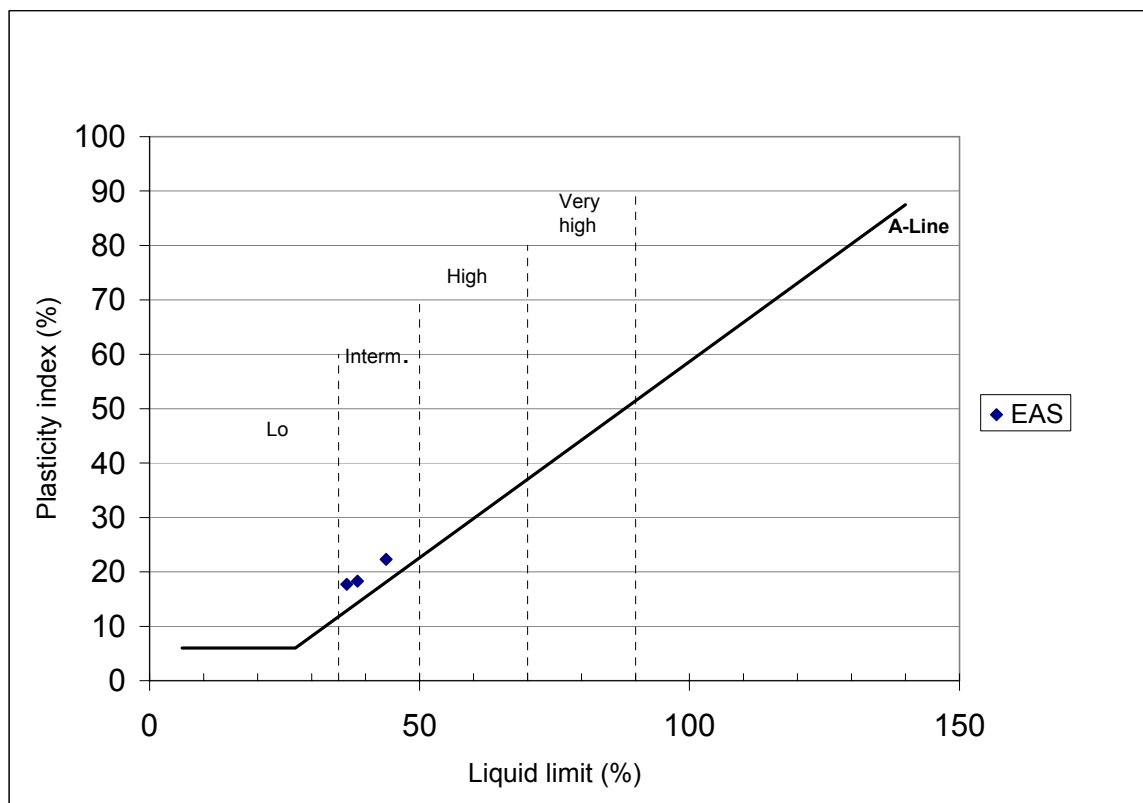


Figure 3.65. Casagrande plasticity plot for triaxial samples.

Activity, A_c , is defined as the plasticity index divided by the clay fraction. Values are quoted in Table 3.24. This indicates the relative contribution of clay minerals to overall plasticity. The Easington samples have a lower activity than the Warden Point samples and may be described as 'inactive'.

It should be noted that all samples contained saline pore water. Salinity has a small effect on plastic behaviour, and may be expected to have influenced the tests non-uniformly. That is, the wetter remoulded (liquid limit test) sub-samples will have contained water of reduced salinity compared with the drier sub-samples. No correction has been applied to water content determinations as a result of salts remaining within the pores during oven drying.

The results of particle-size determinations for samples matching the triaxial tests are shown in Figure 3.67. The results show that EAS2 and EAS3 have similar curves featuring a single gap-grade, whilst EAS1 appears to have a double gap-grade. The results show that the particle-size analysis has not captured the coarsest 10% of material in the case of the Easington samples. This can be assumed to consist of clasts coarser than medium sand-size. The plots are considered typical of the till found at Easington.

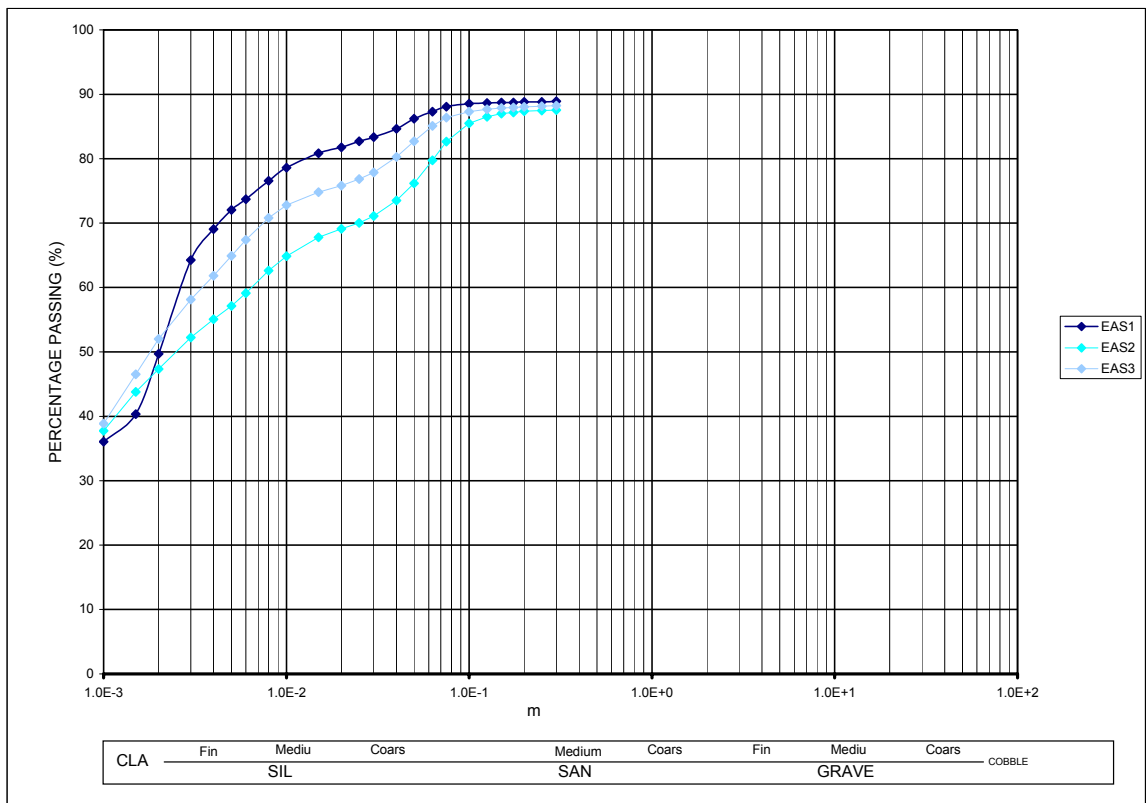


Figure 3.66. Particle size analysis grading curves matching triaxial samples.

The results of the triaxial tests are shown in Tables 3.25 and 3.26 and are plotted in Figure 3.68.

Table 3.25. Results of 100 mm CIU triaxial tests (effective strength).

Sample No.	c'	ϕ'
	(kPa)	(degrees)
Eas 1	17.9	22.2
Eas 2	26.0	25.7
Eas 3	28.2	23.1

Table 3.26. Details of stress-path parameters at failure (effective parameters) (Mean effective stress, s' , maximum effective shear stress, t').

Sample	Stage 1		Stage 2		Stage 3	
	s' (kPa)	t' (kPa)	s' (kPa)	t' (kPa)	s' (kPa)	t' (kPa)
Eas 1	37.12	29.12	86.54	51.54	165.28	77.98
Eas 2	67.4	52.3	191.34	106.74	315.67	159.77
Eas 3	86.06	57.56	149.87	87.97	269.7	130.5

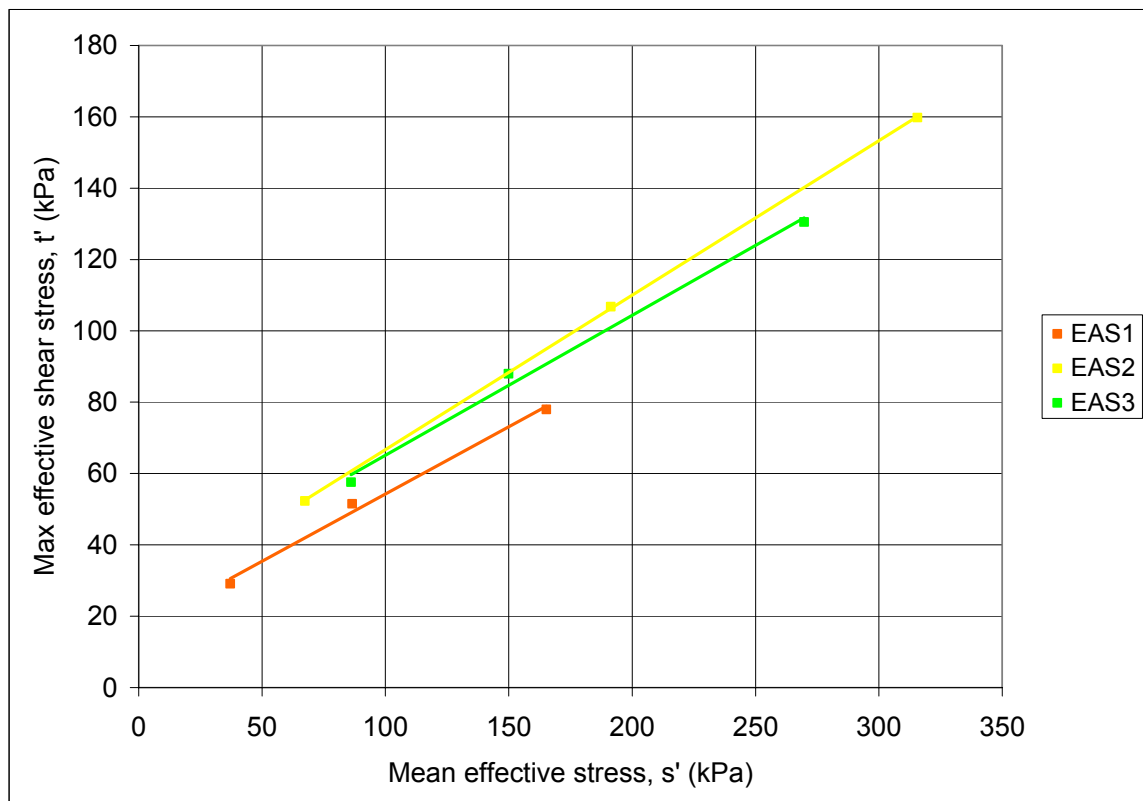


Figure 3.67. Mohr circle locus plots for triaxial tests (effective strength).

The triaxial test results (Table 3.25) show a good agreement between adjacent samples EAS2 and EAS3, whilst remote sample EAS1 has a lower effective cohesion, c' . Samples EAS2 and EAS3 have the lowest plasticity, whilst sample EAS2 has the highest sand fraction and also the highest effective friction angle. It is notable that the behaviour of the London Clay and Easington Till does not differ significantly in the triaxial test.

The stress-path plots (Appendix I) for the triaxial tests show samples EAS2 and EAS3 have similar 'over-consolidated' behaviour, whereas sample EAS1 has 'normally consolidated' behaviour. This same sample has reduced effective cohesion. 'Normally consolidated' and 'over consolidated' type behaviours, as described above, are sometimes referred to as 'wet of critical' and 'dry of critical', respectively when used in a critical state context.

(e) Wave Climate

Offshore Data: Meteorological Office wind and wave data availability for a grid point offshore from Easington, is summarised as follows:

Location: 53.8°N, 0.3°E, water depth 26 m

Data Range: 07/1988 to 10/2005

Wind Data: Three-hourly time series of wind direction (degrees true) and wind speed (knots)

Wave Data: Three-hourly time series of wave direction (degrees true), resultant (mean) wave period (seconds) and resultant (significant) wave height (metres)

Water Level: Table 3.27 summarises astronomical tide levels for the Standard Port of Spurn Head. The MHWS level of +6.9 m CD is used in the numerical transformation of the offshore wave data to the coast at Easington.

Table 3.27. Tide Levels at Spurn Head (m CD)

LAT	MLWS	MLWN	MSL	MHWN	MHWS	HAT	Spring Range	Neap Range
+0.3	+1.2	+2.7	+4.1	+5.5	+6.9	+7.7	5.7	2.8

Offshore Wind Climate: The offshore wind time series data was transformed into a frequency table shown in Table 3.28 (note wind speed in knots) and a wind rose shown in Figure 3.68.

Table 3.28. Offshore wind climate at Easington

Direction °N	0	30	60	90	120	150	180	210	240	270	300	330
Wind Speed knots												
0	0	0	0	0	0	0	0	0	0	0	0	0
1.0-3.0	163	156	173	123	140	153	146	144	174	173	153	177
4.0-6.0	382	381	357	351	429	488	450	476	486	507	430	413
7.0-10.0	780	703	629	670	806	901	1099	1161	1308	1152	886	801
11.0-16.0	1152	882	813	782	853	1051	1413	2013	2300	2013	1253	1196
17.0-21.0	560	373	338	385	380	476	731	1398	1592	1234	716	685
22.0-27.0	341	158	133	202	138	189	474	1061	1031	823	432	436
28.0-33.0	84	41	39	55	26	53	169	330	367	340	126	135
34.0-40.0	10	15	1	6	2	6	36	58	64	101	41	27
41.0-47.0	2	0	0	0	3	1	4	2	10	20	7	2
48.0-55.0	0	0	0	0	0	0	0	2	2	2	0	0
56.0-63.0	0	0	0	0	0	0	0	0	0	1	0	0
>63	0	0	0	0	0	0	0	0	0	0	0	0

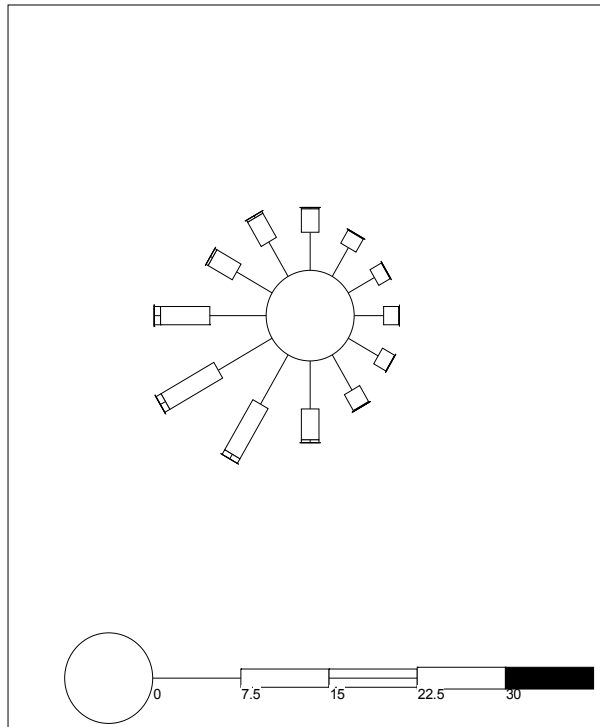


Figure 3.68. Wind rose at Easington. Scale is in ms^{-1} .

The wind data has been used to derive average wind speeds from each sector that were used in the wave transformation.

Direction °N	0°	30°	60°	90°	120°
Wind speed ms^{-1}	6.0	5.5	5.3	5.7	5.3

Offshore Wave Climate: The offshore wave time series data was used to create the frequency tables shown in Tables 3.29 and 3.30, and the wave rose shown in Figure 3.69.

Table 3.29. Offshore wave climate at Easington

Period s	2.1-3	3.1-4	4.1-5	5.1-6	6.1-7	7.1-8	8.1-9	9.1-10	10.1-11	11.1-12	12.1-13	13.1-14	14.1-15
Wave Height H_s m													
0-0.5	0	5672	1994	616	230	123	25	7	13	2	2	0	0
0.6-1.0	0	8411	6628	1869	501	179	54	28	17	9	0	1	1
1.1-1.5	0	655	8765	1899	583	125	21	12	4	0	0	0	0
1.6-2.0	0	73	2220	3774	349	64	16	2	0	0	0	0	0
2.1-2.5	0	1	25	2717	376	18	0	4	1	0	0	0	0
2.6-3.0	0	0	1	375	1047	17	1	0	0	0	0	0	0
3.1-3.5	0	0	0	2	513	96	0	0	0	0	0	0	0
3.6-4.0	0	0	0	0	43	202	0	0	0	0	0	0	0
4.1-4.5	0	0	0	0	2	57	2	0	0	0	0	0	0
4.6-5.0	0	0	0	0	1	6	11	0	0	0	0	0	0
5.1-5.5	0	0	0	0	0	0	6	0	0	0	0	0	0
5.6-6.0	0	0	0	0	0	0	2	1	0	0	0	0	0

Table 3.30. Offshore wave climate at Easington

Direction °N	0	30	60	90	120	150	180	210	240	270	300	330
Wave Height Hs m												
0-0.5	1194	2709	591	489	574	395	458	567	571	435	411	290
0.6-1.0	1834	5156	1002	965	824	695	1061	1500	1599	1248	1113	701
1.1-1.5	921	3315	772	640	537	530	838	1256	1194	824	723	514
1.6-2.0	534	1303	472	363	268	356	564	819	656	461	312	390
2.1-2.5	341	557	347	307	214	184	217	239	259	202	125	150
2.6-3.0	256	322	186	93	55	101	118	63	59	53	66	69
3.1-3.5	109	172	107	43	22	20	33	15	14	31	24	21
3.6-4.0	65	74	38	16	10	1	2	4	3	11	16	5
4.1-4.5	6	33	10	5	0	0	2	0	0	0	1	4
4.6-5.0	1	11	2	0	0	0	0	0	0	1	0	3
5.1-5.5	1	1	0	0	0	0	0	0	0	0	0	4
5.6-6.0	0	3	0	0	0	0	0	0	0	0	0	0

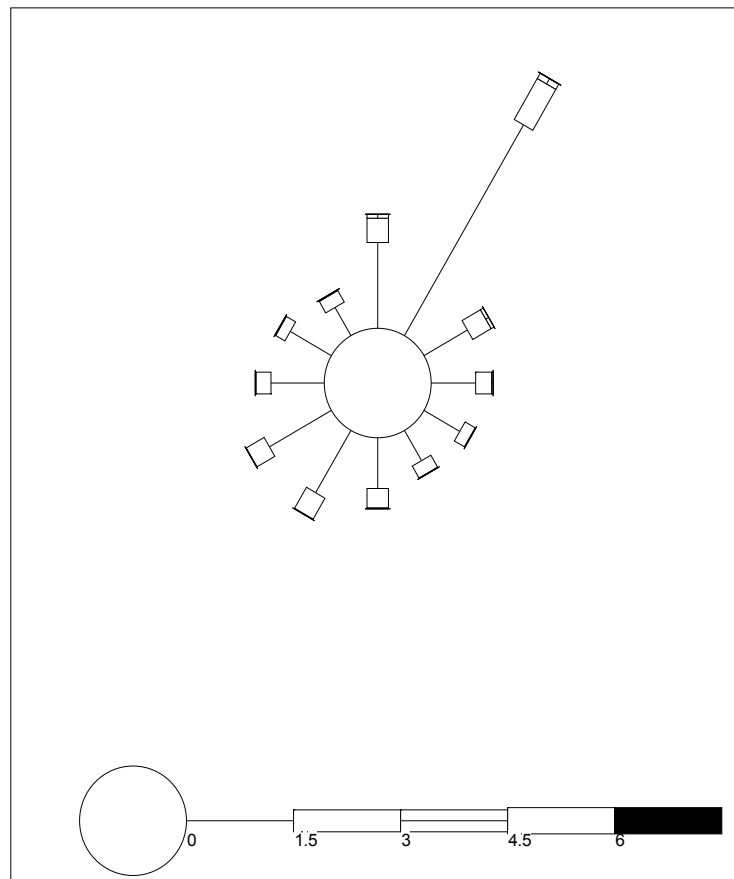


Figure 3.69. Offshore wave rose at Easington. Location 53.8°N, 0.3°E. Period July 1988 to October 2005. Scale is in metres

Table 3.31 has been used to derive a wave height-wave period relationship that was used in the wave transformation.

Table 3.31. Wave height – wave period relationship for the offshore wave data at Easington

Height (m)	Period (s)	Height (m)	Period (s)
0.5	5.39	3.5	9.1
1	5.85	4	9.64
1.5	6.48	4.5	10.11
2	7.05	5	10.76
2.5	7.72	5.5	11.27
3	8.39	6	11.86

The dominant wave direction is from the north-east sector with a significant contribution to the wave climate from the northern sector. These dominant wave energies reflect the exposure to waves directly from the northern North Sea.

Nearshore Wave Climate: As waves propagate into the nearshore their height and direction is influenced by interaction with the sea bed (shoaling and refraction). The nearshore wave climate at Easington at the 0m CD contour close to the shore platform study site was derived using the SWAN 1D model. The transformation matrices for Easington derived from the SWAN 1D model are shown in Table 3.32.

Table 3.32. Transformation matrices at Easington.

Table at top shows output wave heights at 0 m CD contour (6.9 m water depth = MHWS). Table at bottom shows output wave directions at same location.

Input Hs (m)	Direction (°)				
	0	30	60	90	120
0	0.00	0.00	0.00	0.00	0.00
0.5	0.68	0.63	0.63	0.67	0.63
1	0.94	0.93	0.93	0.92	0.87
2	1.50	1.59	1.59	1.42	1.32
4	2.91	3.15	3.16	2.70	2.49
6	3.56	4.01	4.14	3.73	3.28

Input Hs (m)	Direction (°)				
	0	30	60	90	120
0	0.0	30.0	60.0	90.0	120.0
0.5	359.4	29.8	59.2	90.1	120.0
1	360.0	29.9	59.8	89.9	120.0
2	359.8	30.0	60.0	89.5	119.9
4	0.1	30.0	60.0	90.1	120.0
6	358.4	27.3	58.0	90.4	120.6

The inshore wave climate derived from the model results is shown in Table 3.33 and in Figure 3.69.

Table 3.33. Inshore wave climate at Easington

Direction °N	0	30	60	90	120	150	180	210	240	270	300	330
Wave Height Hs m												
0 - 0.5	1013	2118	463	367	520	2236	3290	4461	4355	3264	2790	2069
0.5 - 1.0	2690	6411	1297	1287	1408	45	0	0	0	0	0	96
1.0 - 1.5	1020	3594	974	858	464	0	0	0	0	0	0	0
1.5 - 2.0	384	903	474	308	96	0	0	0	0	0	0	0
2.0 - 2.5	157	358	207	71	15	0	0	0	0	0	0	0
2.5 - 3.0	50	156	91	15	0	0	0	0	0	0	0	0
3.0 - 3.5	5	66	20	0	0	0	0	0	0	0	0	0
3.5 - 4.0	0	5	0	0	0	0	0	0	0	0	0	0
4.0 - 4.5	0	0	0	0	0	0	0	0	0	0	0	0

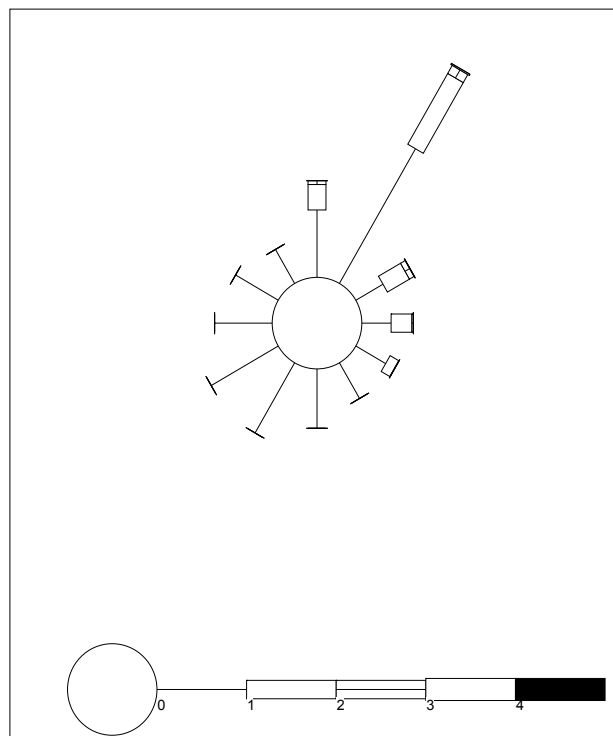


Figure 3.70. Inshore wave rose at Easington. Scale is in ms^{-1} .

3.4 Interpretation

In interpreting the results at Warden Point and Easington, it is useful to consider as many factors as possible which may affect downwearing rates and form, over time, the resultant cliff and platform of known width, gradient and elevation (Figure 3.71).

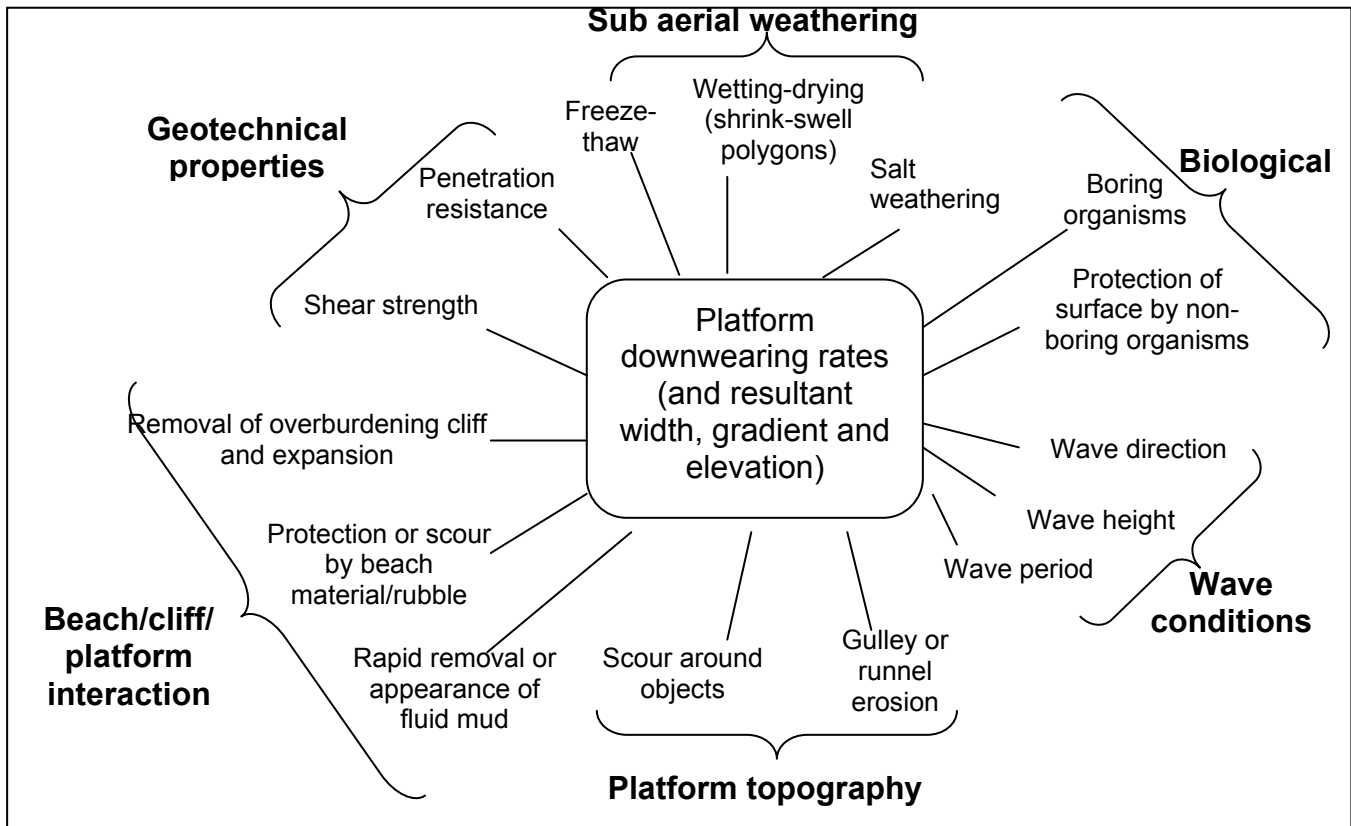


Figure 3.71. Diagram showing the major factors influencing cohesive shore platform downwearing.

Relevant processes and findings are summarised for each site in the following sections, which cover:

- Wave conditions;
- Biological processes;
- Platform geomorphology;
- Geotechnical properties;
- Beach/cliff/platform interactions; and
- Downwearing and platform topography.

3.4.1 Warden Point

(a) Wave Conditions

UK Metrological Office data for wave conditions up to 10 October 2005 off the coast of Warden Point have been examined. These cover only the summer to autumn measurement period (23 July 2005 to 20 October 2005). Extensive records of back-dated data were also available and data from October 2001 were used to estimate average wave conditions for the other three measurement periods (3.34).

Table 3.34. Estimated average wave conditions off the coast of Warden Point for the periods between downwearing measurements based on data from October 2001 to October 2005.

Dates	Season	Average wave height (m)	Average wave period (seconds)	Average wave direction (degrees)
23 July to 20 October	Summer to Autumn	0.57	3.71	154.67
20 October to 4 February	Autumn to Winter	0.74	3.87	182.32
4 February to 26 May	Winter to Spring	0.66	3.81	150.80
26 May to 14 July	Spring to Summer	0.52	3.60	172.18

With a coastline facing a direction of approximately 45° , it is only waves with a direction of between 130° and 320° that affect the shore platform at Warden Point. The most destructive waves are likely to have an angle of approximately 225° , both normal to the coastline and having a long fetch across the North Sea. It would be expected that the autumn-winter period, with an estimated mean wave direction of 182° and the highest waves, should have the highest downwearing rates. However, the 2005/2006 downwearing data showed that the autumn to winter period in fact had the lowest downwearing rate. One explanation may be that the estimated wave period was greater at this time such that there were fewer, albeit higher and more erosive, waves breaking on the platform. Alternatively, it may have been the case that wave directions and heights were anomalous during the measurement period. During the winter-spring period, waves with an estimated mean direction of 151° would have been expected to hit the Warden Point platform nearly parallel to the angle of the coastline. Such waves are likely to have originated from within the Thames estuary and therefore have a much more limited fetch than those of the autumn-winter. Despite this apparently ineffective approach angle, downwearing rates were highest in the 2006 measurement period. The apparently anomalous relationship between wave conditions and downwearing rates remains difficult to resolve without access to real time wave data for the measurement period.

(b) *Biological Processes*

The presence of *Corophium volutator* on the upper platform coincided with the highest rates of downwearing, but this does not necessarily explain why the rates are high. However, due to its high densities in some areas, it is likely to weaken the platform surface. When such areas dry they tend to fragment easily. The burrow depth of around 1 cm means that the platform more than 1 cm beneath the surface is unlikely to be affected by *Corophium*. In comparison, the American piddock, found in its highest densities on the lower platform but which is also fairly prolific on the lower middle platform where downwearing rates were measured, coincides with lower downwearing rates. However, the piddock excavates far greater quantities of sediment and weakens the platform to a much greater depth (up to 10 cm) than *Corophium*. It is likely that downwearing on the lower platform is more catastrophic (occurring less frequently but in larger sized fragments) due to presence of piddocks. The surface of the platform occupied by piddocks is often much smoother and complete, as their burrows are so deep and their breathing/feeding holes so small.

Despite the larger number of algae counted in February 2006, most were not attached to the platform surface and it is unlikely that they protected the surface from downwearing. Few individuals were found on the TEB sites and therefore their influence would not be reflected in the downwearing measurements.

The Warden Point site is somewhat exceptional in the British context in having high densities of the introduced American piddock. However, piddocks of one species or another are to be expected on almost all cohesive shore platforms except where: (i) the downwearing is very rapid; (ii) there is very soft or liquid mud; (iii) the rock is exceptionally hard; or (iv) the foreshore is periodically buried under a beach, smothering the piddocks. The range of potential piddock species on British foreshores is indicated in Table 3.35.

Table 3.35. Bivalve borers in UK cohesive shore platforms.

Name	Family	Shell Length (Max.)	Type Of Burrow	Vertical Range	Geographical Distribution	Notes
<i>Petricola pholadiformis</i> American piddock	Petricolidae	6.5 cm	Vertical	Midtide level to a depth of at least 8.2 m ("4½ fathoms") (1)	Mostly from the Humber estuary to Lyme Regis, Dorset. Isolated occurrences elsewhere. Particularly common in the Thames estuary.	Introduced. First found 1890 in Essex. Life span maximum of about 10 years (1)
<i>Hiatella arctica</i> Wrinkled rock borer	Hiatellidae	4 cm	Often horizontal. Also lives in pre-existing holes, crevices etc.	Lower shore to depths of about 50 m (2)	Common around the British coast, except between the Humber and the Thames, where it is scarce or absent.	

Name	Family	Shell Length (Max.)	Type Of Burrow	Vertical Range	Geographical Distribution	Notes
<i>Gastrochaena dubia</i> Flask shell	Gastrochaenidae	2.5 cm	Often horizontal	No information found	South and south-west England	
<i>Pholas dactylus</i> Common piddock	Pholadidae	15 cm	Vertical	Lower shore to a depth of 35 m (3)	Mostly southern England and Wales. Isolated occurrences in the Lake District. Yorkshire and Northumberland	Britain's largest piddock. Life span up to 14 years (3)
<i>Barnea candida</i> White piddock	Pholadidae	7 cm	Vertical (1) or horizontal (4)	Mid-shore to a depth of less than 10 m (4)	Mainly southern Britain, rare in the north	
<i>Barnea parva</i> Little piddock	Pholadidae	4 cm	No information found	Mid-shore to a depth of less than 10 m (4)	South and south-west England	
<i>Zirfaea crispata</i> Oval piddock	Pholadidae	10 cm	Vertical	Lower shore to a depth of 7-8 m (5 & 6)	Widely distributed on British coasts	
<i>Pholadidea loscombiana</i> Paper piddock	Pholadidae	4 cm	No information found	Low water to a depth of about 8 m (6)	South and south-west England	

(Sources: 1-Duval, 1963; 2- Carter, 2003; 3- Hill, 2006; 4- Irving, 1998; 5- Tebble, 1966 and 6- Yonge and Thompson, 1976).

(c) *Platform Geomorphology*

At Warden Point a broad low-angle platform cut into the London Clay was exposed at low water during this study. This platform has been observed to have been present at this location for many years previously. The site is a relatively low energy site when compared to the site at Easington. The beach is extremely thin and consists dominantly of materials derived from the London Clay cliffs and platform (pyritic grains and pebbles, phosphatic pebbles, limestone pebbles, cobbles and boulders), biogenic grains from the comminution of shells and anthropogenic materials (bricks, concrete etc.) local to the site. Much of the finer grained and less dense sediment (shell fragments and quartz sand) appear to have been winnowed from the beach before the winter survey, presumably as the result of wave action. The more dense (e.g. pyritic fragments) or larger (cobbles, boulders) clasts remained on the beach and platform as a lag deposit. No observations were made however to confirm whether the thin beach re-formed during the summer of 2006 to show whether the removal was part of an annual cycle. The highest point of the exposed platform lies at around + 1 metre OD which is 0.8 metres above mean tide level (+ 0.2 metres at Sheerness).

(d) *Geotechnical Properties*

The Panda penetrometer and Geonor shear vane test sites Cp 13 and Cp 1, and the triaxial and shear-box sample sites U2/3 and U1, coincided well with the locations of the TEB sites B and C respectively. The Panda penetrometer and Geonor shear vane test sites Cp 12, Cp 13 and Cp 14 and the triaxial and shear-box sample sites U2 and U3 were close to the TEB site B. Likewise, Cp 1, Cp 2, Cp 3 and U1 coincided well with the location of the TEB site C.

The triaxial tests have shown that the lower platform is stronger, requiring 25.7 kPa to fail, compared to the middle platform, which failed at an average of 12.9 kPa. The lower platform has a higher clay content, which increases the liquid limit, plastic limit, plasticity index and linear shrinkage, and may account for its greater strength. Likewise, the Genor Shear Vane stress tests have shown that the lower platform is made of material which shears slightly less readily (at 82K kPa) than the middle platform (at 76 kPa). Both these tests help to explain the higher downwearing rates measured on the middle platform. However, the Panda penetrometer test has shown that the resistance between the middle and lower platform is almost identical. The high surface resistance occurs to a marginally greater depth on the lower platform, which may be linked to the presence of a greater number of Piddock shells there.

(e) *Beach/Cliff/Platform Interaction*

It is possible that the entire section of platform used for downwearing measurements has been distorted by mass movement of the London Clay during the study period. Further detailed surface surveys are needed in order to know if this really is the case, but these are beyond the scope of the present project. The beach at the Warden Point site is limited in extent and so unlikely either to actively erode or protect the platform. Unfortunately, detailed notes on

the occurrence of fluid mud were made only after it was first observed in the base measurements in July 2005. The summer to autumn downwearing measurements cannot be statistically tested for any differences caused by this fluid mud. As discussed earlier, the statistical test of the spring to summer 2006 TEB measurements showed no difference between downwearing of the very soft areas and the 'normal' consolidated clay.

(f) Downwearing and Platform Topography

Shrink-swell polygons are clearly visible on the upper platform and fragment easily under foot. No evidence of freeze-thaw weathering was found during the study period. As already discussed, downwearing has been shown to be greater on slightly raised areas than in shallow depressions and puddles.

3.4.2 Easington

(a) *Wave Conditions*

As only one annual measurement of downwearing was obtained at Easington, temporal analysis of the influence of wave conditions was not worthwhile.

(b) *Biological*

The very limited biological activity at Easington is unlikely to affect downwearing rates except perhaps at LWM and beyond.

(c) *Platform Geomorphology*

At Easington a relatively narrow intertidal platform was exposed at low water within a large-scale, shore-oblique runnel known locally as an ord. The site is a relatively high energy site and the beach very dynamic with large amounts of beach sediment being moved both alongshore and across the beach profile in relatively short periods of time. The longshore movement of shore-oblique bars mean that the runnel location and consequently the location of the exposed platform changes during the year. In this study this meant that during the winter 2005-spring 2006 period much of the study site was buried beneath beach sediments as a bar passed over it. The exposed intertidal platform at Easington lies between around -2 metres and -2.7 metres and is therefore relatively much lower in the tidal frame compared to the platform at Sheppey. The upper part of the platform at Sheppey is consequently inundated for a much briefer period during high tides than the platform at Easington.

The beach sediments at Easington originate largely from erosion of the glacial till cliffs and platform which, unlike the London Clay at Sheppey, contains a large proportion of beach building sediment. Beach building sediment supply is therefore much greater at Easington than at Warden Point.

(d) *Geotechnical Properties*

The triaxial and shear-box sample sites U2/3 were close to the TEB site A. Further down the shore, sample site U1 was the same distance from the cliff/sea as the TEB site B, but the latter was displaced a short distance from the general line of transect in order to measure runnel downwearing. Unfortunately, TEB location A was covered with sand when the annual downwearing measurements were made at the other locations. The shore-normal transect of Panda penetrometer and Geonor shear vane test sites Cp 5, Cp 3, Cp 2 and Cp 1 provide the most useful comparison with the downwearing results obtained from TEB sites B and C.

The triaxial tests have shown that the upper platform is stronger, requiring an average of 27.1 kPa to fail, compared to the middle platform, which fails at 17.9 kPa. This is despite the higher clay content of the middle platform, which results in a higher liquid limit, plastic limit, plasticity index and linear shrinkage. The Geonor shear vane test supported the triaxial test results, showing that the middle to lower platform is made of material that shears more easily (at 66 kPa) than the upper platform (at > 108 kPa). Likewise, the Panda penetrometer test has shown that the resistance of the upper platform (at Cp 5) is marginally higher than the rest of the platform. However, none of these results support the TEB data which have shown that the middle platform experiences slightly greater downwearing than the lower platform (though there are no replicate measurements for the Easington TEB locations).

(e) *Beach/Cliff/Platform Interaction*

Surveying has proven that the platform has not uplifted on the macro-scale during measurements. The movement of the extensive beach and sand bars are significant factors in the downwearing of the platform. It would appear that they do not protect the platform surface although some protection would be expected at the top of the platform where beach depth is greatest. No fluid mud was found.

(f) *Downwearing and Platform Topography*

No evidence of wetting-drying or freeze-thaw has been noted at Easington. As with the shallow depressions and raised areas at Warden Point, downwearing has been found to be statistically greater on the ridges than in the runnels at Easington. Stones present in the glacial till actively promote scour around them producing a pedestal of sediment underneath.

3.5 Summary of Key Findings from Field and Laboratory Investigations

The average downwearing rate recorded on the shore platform at Warden Point over the measurement year (July 2005 to July 2006) was 17.63mm. The upper platform exhibited the greatest downwearing (30.59mm), the upper middle platform considerably less (13.75mm) and the lower-middle platform the least (8.5mm).

Downwearing at Warden Point was greatest during the February to May 2005 period and, when considering the micro-scale topography, downwearing was much greater on raised areas than in the depressions.

At the Easington shore platform, downwearing rates averaged 41.93mm per year between July 2005 and July 2006. This is considerably greater than the rate recorded at Warden Point and is likely to be influenced by the sand bar/ord migration along the coast. The average annual downwearing rate at the mid platform (43.4mm) was marginally greater than at the lower platform (39.8mm). No measurements were possible at the upper platform location in July 2006 because the pin was buried under >5m of beach sediment cover. It is postulated that such extensive beach material coverage is likely to have protected the platform against downwearing.

As at Warden Point, raised areas in the micro-relief experienced greater downwearing than depressions/micro-runnels.

At both sites, the downwearing rate of the shore platform has been found to increase with distance from the sea up the platform. This has been found on a number of shore platforms (e.g. Foote et al., 2006; Henaff et al. 2006) and is thought to be necessary in order to keep the steeper, more recently uncovered upper platform moving landwards and downwards to match the cliff retreat.

At Warden Point five live fauna species were recorded, namely: American Piddock; Mud Shrimp; Bristle Worm; Sand Mason; and Acorn Barnacle. This is much less diversity than is typically recorded on platforms of other rock types (e.g. chalk and sandstone), but much greater than at Easington where only empty holes or dead shells of the White Piddock were observed (no live species were recorded). This lack of biological activity at Easington is presumably related to the volatility of the beach morphology, with the periodic covering by sand bars being a limiting factor on longevity of colonisation.

At Warden Point, the American Piddock and Mud Shrimp were found in greatest numbers. Peak colonisation of Mud Shrimp was found on the upper platform, with densities decreasing with seaward progression. In contrast, American Piddocks were observed in greatest numbers on the lower platform, near the MLWS mark. There was little difference in biological activity between the summer and winter surveys for all species except the Sand Mason, which declined in numbers in the winter.

The Mud Shrimp is likely to have weakened the upper platform at Warden Point, where it was recorded in greatest numbers, but only within the upper 1cm of platform surface. In contrast, the American Piddock, whilst coinciding with areas of lower downwearing rates, excavates far greater quantities of sediment and weakens the platform to a much greater depth (up to 10cm).

Although large quantities of algae were recorded on several surveys, the protection afforded to the platform is unlikely to have been great since most were attached to pebbles and not the platform surface itself.

The profile surveying showed little change in beach and platform profile morphology at Warden Point between July 2005 and February 2006. In contrast, however, massive changes were recorded at Easington where, following the July 2005 survey, a sand bar covered the profile around November/December 2005, burying the platform over much of its length. The oblique shoreline-attached sand bars are separated along the Holderness coast by shoreline-oblique runnels known as 'ords'. The profile changes recorded between the July 2005, March 2006 and July 2006 surveys are consistent with the southward passage of an ord across the site.

At Warden Point, the greatest influences on platform downwearing were biological processes and mechanical wave action. At Easington, wave action and beach morphology changes were the principal influences. Due to this finding, numerical modelling tests were run to focus on the importance of biological process of Warden Point and beach platform interactions at Easington.

4 NUMERICAL MODELLING

4.1 Introduction

Numerical modelling offers the potential for deeper understanding of shore morphology than would be possible with a study based only on site observations. This is because such models can, in principle, resolve long periods of time, quantify complex processes and interactions, and deal with systemic change such as accelerated sea-level rise. For these reasons a numerical model investigation was undertaken to compliment the fieldwork campaign as part of the present study.

In practice shore morphological models tend to deal with periods of time that are short, relative to coastal management decisions, and are normally restricted to the representation of beach dynamics, neglecting *in situ* foreshore erosion. Two models that do deal with erosion of cohesive shores and their interaction with beaches are COSMOS (Nairn & Southgate, 1993) and SCAPE (Walkden & Hall 2005). COSMOS describes processes in much more detail than SCAPE, however its application is restricted to periods of storm activity since it does not simulate beach building during relatively calm conditions. It is also relatively computationally demanding, which limits the spatial and temporal scales over which it can be applied. In contrast SCAPE uses relatively abstract process descriptions and employs more behavioural descriptions than COSMOS. However, these abstractions mean that it can be used to represent century scale morphology. This advantage makes it more appropriate for this study which is intended to inform coastal management decisions, which typically have implications over these longer timescales. The processes and interactions described by SCAPE are given in more detail in Section 4.2.

This study includes specific representations of the study sites, Warden Point and Easington, which are described in Section 4.3, and simulations of general beach/ cohesive shore interaction (Section 4.4). Whereas construction of the site specific models tested the modelling tool, revealed data requirements and informed interpretation of the dominant processes at Easington and Warden Point, the generic tests allowed exploration of more fundamental questions about cohesive shore/ beach dynamics. Response to sea-level rise is considered in Section 4.5 and a discussion of key results is presented in Section 4.6.

4.2 The SCAPE Modelling Tool

The SCAPE (Soft Cliff and Platform Erosion) model was developed with EPSRC funding at the University of Bristol drawing on a detailed investigation of the shore morphology of the Naze peninsula in Essex (Walkden & Hall, 2002, 2005). It was subsequently used to model the development of 35 km of the North Norfolk coast for the Overstrand to Walcott strategy study (HR Wallingford 2003). The success of this regional model led to its inclusion in the Regional Coastal Simulator of the Tyndall Centre for Climate Change Research,

where it is being used to represent 50km of coastal morphology over 200 years (Dickson et al, in press).

SCAPE is a systems-based model of the processes and interactions through which the profiles of cohesive shore platforms emerge. It is not an equilibrium model since the equilibrium form of the profile emerges from the modelling process, rather than being pre-defined. The process descriptions are relatively abstract so that model run times are short, which allows simulation of long periods.

The foreshore and lower cliff is represented by a series of alongshore sections, each of which is discretised into a stack of horizontally aligned erodeable elements, as illustrated in Figure 4.1.



Figure 4.1. Discretisation of the model foreshore profile.

The expression for the erosion of each element, which was developed by Walkden & Hall (2005) drawing on previous work by Kamphuis (1987) and Skafel (1995), is:

$$\frac{dy}{dt} = \frac{H_b^{13/4} T^{3/2}}{S} f_1(f_3(t) - z) \tan(f_2(z))$$

Equation 1

Where y is the horizontal recession, t represents time, H_b is the breaking wave height, T is the wave period, f_1 , f_2 , and f_3 are functions representing, respectively, the distribution of erosion under a breaking wave passing through the surf zone, tidal variation in water level, and the local slope. The strength of the *in situ* rock is represented by S , which is a calibration term. SCAPE also includes a one-line beach module which allows interaction between adjacent shore profiles.

Other modules include representation of cliff failure, talus formation and erosion, wave transformation, and cross-shore sediment transport. A flowchart of the model's component modules is shown in Figure 4.2.

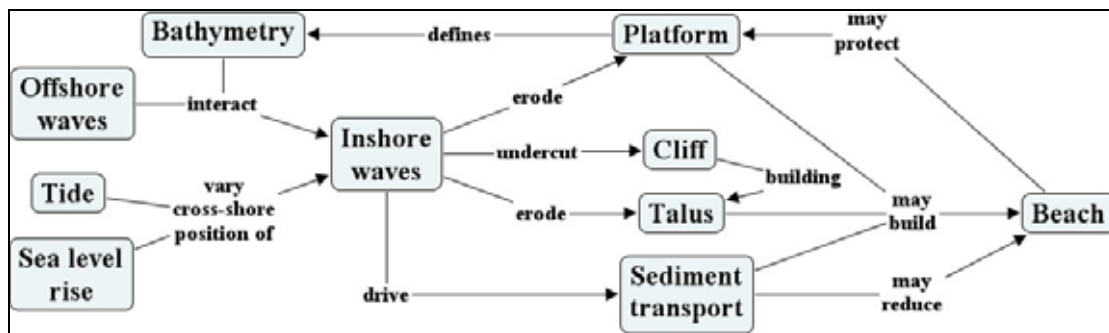


Figure 4.2. Flowchart of processes and interactions represented by SCAPE.

SCAPE was developed to be holistic and represents some processes that are relatively unknown such as cross shore sediment motion during low wave activity and the capability of a beach to protect an underlying foreshore. To achieve this it uses some empirical data and behavioural descriptions. The beach, where sufficiently thick, provides protection to the foreshore. The literature contains almost no guidance on erosion protection as a function of beach depth, and so this aspect of the model is based on a single study in which it was found that beaches were only disturbed to a depth of $0.25H$ (where H is the wave height). In SCAPE this was assumed to represent the maximum depth to which a wave can erode an underlying foreshore. Protective capability was assumed to vary linearly for beach depths less than $0.25H$. Although the cohesive foreshore is treated as an emergent form, the beach profile shape is defined as a Bruun curve (Bruun, 1954) below a gently sloping (1:100) berm. This shape was chosen as an appropriate representation of the long-term average beach surface. Although the upper surface shape is defined, the beach's width and lower surface (in contact with the foreshore) emerge as model output.

The model receives, as site specific input, wave climate, tidal conditions and sea-level rise. In addition, for quasi 3D applications, a coefficient of longshore sediment transport is calibrated, although this study was restricted to 2D simulations.

SCAPE models require a process of 'winding-up' in which they are run to achieve a state of dynamic equilibrium with the applied loading (waves, tides and sea-level rise). They are then calibrated by adjusting the material strength term (S) until the correct recession rate is obtained. Confidence in model performance (validation) is based in the similarity between the emergent profile form and the site being modelled. For quasi 3D applications further validation is possible by examination of longshore variation in recession rates (e.g. Dickson et al, in press).

4.3 Numerical Model Investigations of the Study Sites

The purpose of the site specific models is to explore the processes of erosion at Warden Point and Easington, and to trial the numerical model. In both cases the aim was to model the form of the shore profile whilst making the minimum number of assumptions.

4.3.1 Warden Point

Warden Point forms part of the coastline of the Isle of Sheppey and is composed of London Clay. The site faces North East along the outer Thames estuary and it is from this direction that the dominant waves arrive. The shore is fronted by the Kentish Flats, a large shallow platform covered in sand which limits inshore wave heights. Warden Point sea cliff is not artificially protected and is eroding at approximately 1.9 m/annum (Nicholls et al, 2000). The beach is mixed and small, apparently due to the presence of a drift divide and covers the upper foreshore from the cliff toe to approximately mean sea level. The spring tidal range is around 5m and the local rate of relative sea-level rise is approximately 2.13 mm/a (Dixon and Tawn, 1997).

(a) Model Input Data

Seventeen years of offshore hindcast wave data was purchased from the Met Office (July 1988 – October 2005, gridpoint 51.50N, 1.14E). Copies of some sections were made to patch gaps. Where patching was necessary appropriate months were selected to retain seasonality. The data were then classified by direction and distributions were fitted to the extreme values in each class. These distributions were used to generate synthetic extremes. The data was then extended to create a 1000 year timeseries by:

1. splitting the original data into its constituent months,
2. constructing one thousand years of data by randomly selecting appropriate months in turn (e.g. one January, followed by one February, and so on), and
3. replacing the extreme values with synthetic data taken from the fitted distributions.

Step 2 preserved seasonality, whilst step 3 was done to represent long return period events not in the original data. Nearshore wave data was then calculated using the extended time series and a transformation matrix, generated through SWAN modelling.

Twenty four years (1980-2004) of tide gauge data recorded at Sheerness was obtained from the British Oceanographic Data Centre, and was assumed to represent the tidal conditions at Warden Point. This data was extended to represent a 1000 year time series using the same approach applied to the wave data. The extreme value distributions were based on analysis presented by Dixon and Tawn (1997).

(b) Model Set-up and Operation

The wave, tide and sea-level rise data were input to a SCAPE model that was run until the emergent shore profile had reached dynamic equilibrium. Figure 4.3 illustrates the first thousand years of profile development from a vertical initial condition.

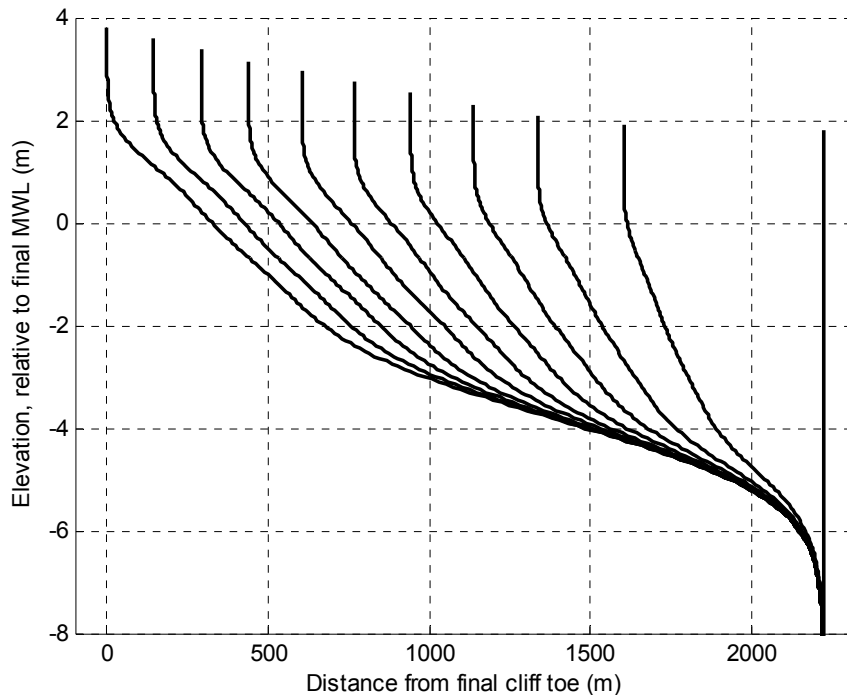


Figure 4.3. One thousand years of Warden Point model profile evolution, in 100 year ‘snapshots’

Over this model period the characteristic wide intertidal zone emerges, seaward of which is a flatter shoreface.

At this stage a beach was introduced, with an assumed volume of $3\text{m}^3/\text{m}$. The beach surface was represented with a Bruun curve of form:

$$d = ax^{2/3} \tag{Equation 2}$$

where d is the water depth, and x the distance from the water line. A value of 0.35 for the Bruun constant (a) was found to provide the best fit to the surveyed profiles.

The effect of the beach on the on the overall profile shape can be seen in Figure 4.4.

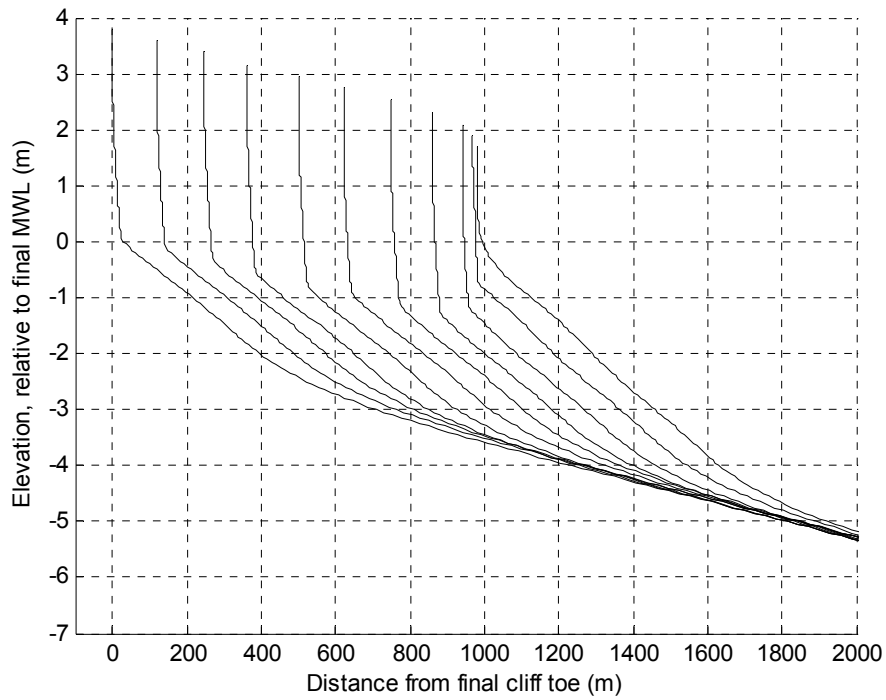


Figure 4.4. 100 year snapshots of profile evolution over 1000 years following the introduction of a beach.

It can be seen that the beach causes the upper foreshore to steepen. The final profile is also shown in Figure 4.5, along with survey data.

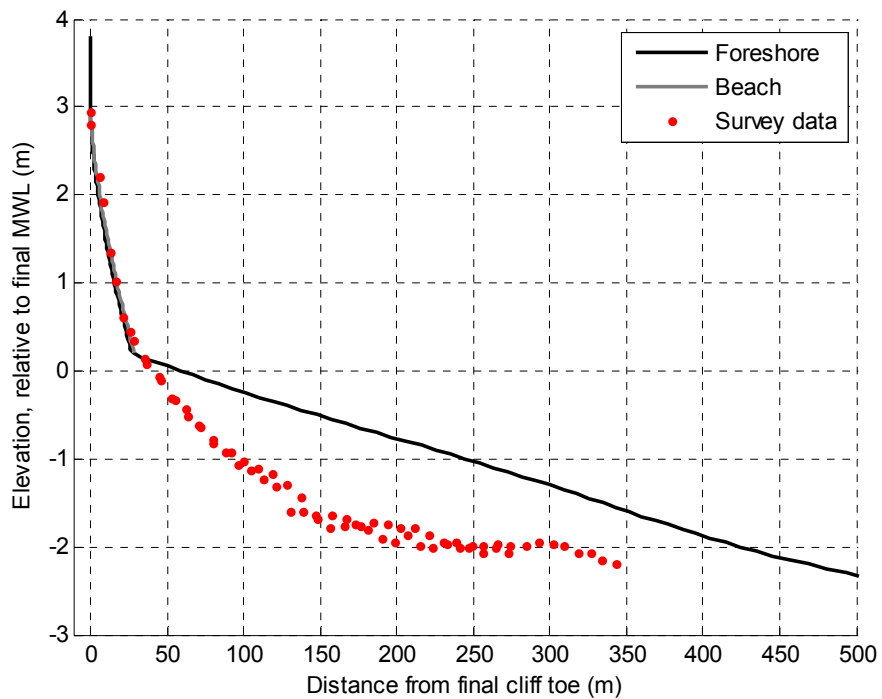


Figure 4.5. Upper model foreshore and beach, and survey data.

It can be seen in Figure 4.5 that the foreshore level is too high, by as much as 1.2 m. Clearly some process that removes material from the shore is not represented in the model. Site investigations identified a high level of biological activity, principally piddocks boring into the foreshore. Clearly this process removes foreshore material directly and may also weaken its fabric. It was therefore decided to conduct a series of numerical experiments to explore foreshore sensitivity to biological weathering.

Survey results showed a linear increased in piddock density from the mean water level to a depth of 2m, where the creatures were found to occupy approximately 4% of the surface clay.

In the sensitivity tests it was assumed that:

- piddocks remove material from the range at which they were observed (-2m to 0m)
- The distribution of the erosion was the same as the distribution of their observed population density (i.e. triangular, zero at mean water level and maximum (k) at -2m)
- Material was removed at a steady rate, i.e. the same amount each tide.

Tests were then conducted to explore the relationship between profile shape and the maximum erosion (k) per tide. It was found that a value for k of 150 μm produced a realistic profile, as shown in Figure 4.6.

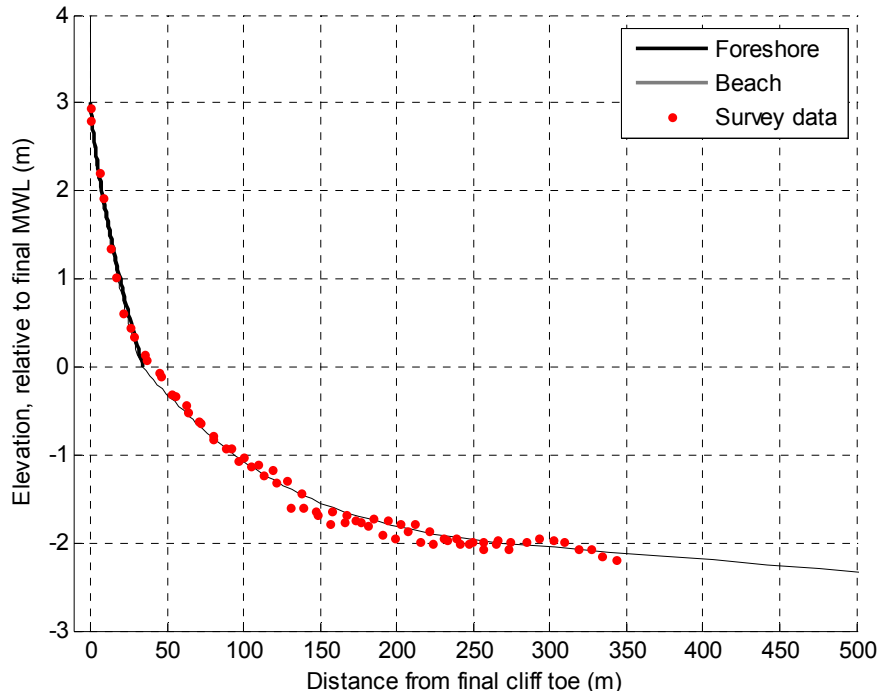


Figure 4.6. Profile obtained accounting for biological weathering ($k = 150 \mu\text{m}$).

(c) Discussion

In order to model the profile of the Warden Point foreshore it was necessary to simulate the effect of biological weathering. It therefore seems likely that direct removal of foreshore material and fabric weakening through piddock boring plays a significant role in shaping the foreshore. The maximum amount of lowering per tide, $150\ \mu\text{m}$ equates to approximately $100\ \text{mm/annum}$ of lowering, which seems quite large, however this should be considered in the context of the high recession rates of this site ($2\ \text{m/annum}$). Also, $150\ \mu\text{m}$ is the maxima of a triangular distribution, so the average rate is half this ($75\ \mu\text{m/ tide}$ or $50\ \text{mm/annum}$).

The shore recession rate was found to be sensitive to the value adopted for k , such that values of $50\ \mu\text{m/tide}$, $100\ \mu\text{m/tide}$ and $150\ \mu\text{m/tide}$ produced recession rates of $1.24\ \text{m/annum}$, $1.81\ \text{m/annum}$ and $2\ \text{m/annum}$ respectively. It therefore seems likely that biological weathering has a direct impact on recession rates.

The assumed triangular distribution of piddock weathering was derived directly from the survey data. However, these surveys were limited to the intertidal zone so it was not possible to establish whether the piddock communities extended beyond the low water line. If this is the case then biological weathering will remove material from a wider swath of the foreshore and so would have more influence on shore recession rates. Under those circumstances k would have to be reduced to maintain a model recession rate of $2\ \text{m/annum}$.

4.3.2 Easington

The Easington cliffs and shore are composed of relatively soft Holocene deposits and are exposed to the southern North Sea towards the south of the Holderness coast. The regional wave climate is aggressive and as a consequence local cliff recession rates are high, averaging around $1.5\ \text{m/a}$ (Royal Haskoning, 2005). The dominant wave direction is from the North East, which drives a southerly longshore transport. Pringle (1985) provides a description of the geomorphic behaviour around Easington, describing in particular the presence of nearshore oblique bars, and gaps between them referred to as 'ords' which migrate with the longshore transport. Since the beach protects the cliff and foreshore these waves introduce an oscillation in recession, such that low erosion happens at the sandwave crest and high erosion occurs where the trough or 'ord' is present. The beach at Easington is unusual in that it does not conform to a typical equilibrium profile. Instead the beach profile is essentially split into two sections, one relatively steep overlying the upper section of the foreshore, the other (over the oblique bars) is quite flat and occupies the section of the foreshore around low water. Beyond the low water line the water depths increase rapidly compared with most cohesive foreshore sites. There appears to be no significant biological weathering.

(a) Model Input Data

Seventeen years of offshore hindcast wave data was purchased from the Met Office (July 1988 – October 2005, gridpoint 53.75N, 0.34E). The data was patched, analysed and extended using the same methods applied to the Warden Point wave files.

Twenty four years (1980-2004) of tide gauge data recorded at Immingham was obtained from the British Oceanographic Data Centre, and was assumed to represent the tidal conditions at Easington. This data was extended to represent a 1000 year time series using the same approach applied to the wave data. The extreme value distributions were based on analysis presented by Dixon and Tawn (1997).

Current relative sea level rise is approximately 1.09 mm/annum (Dixon and Tawn, 1997). In reality the rate of sea level rise has changed drastically over the time that the nearshore bathymetry at Holderness has developed. This changing rate was identified (Shennan, 2000) and used during early model investigations to explore its role on the shoreface. Although it was found that the variable sea-level did have an effect on the shoreface, generally causing it to be lower, the results were highly sensitive to initial profile conditions. For this reason the rate of sea-level rise was assumed to be historically constant and it was noted that this would tend to make the offshore profiles rather shallow.

(b) Model Set-up and Operation

The wave, tide, and sea-level rise data were input to a SCAPE model, which was then run until the emergent shore profile had reached dynamic equilibrium. Figure 4.7 illustrates the first thousand years of profile development from a vertical initial condition.

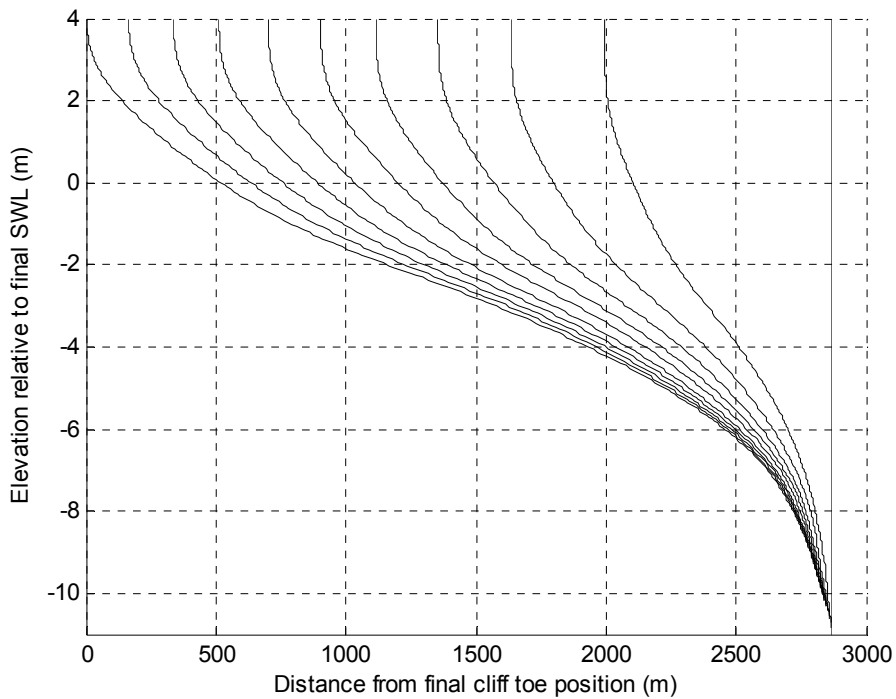


Figure 4.7. 1000 years of Easington model profile evolution, in 100 year 'snapshots'.

Simulation of the beach was complicated by the atypical presence of the oblique nearshore sandbars. These were represented with two different vectors derived from the field surveys shown in Figure 4.8.

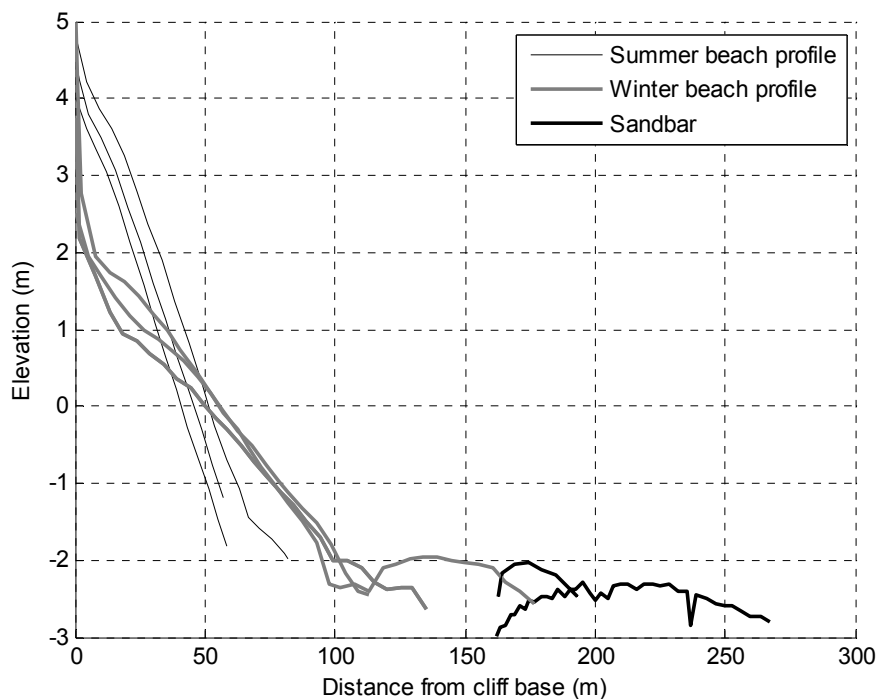


Figure 4.8. Surveyed beach profiles at Easington.

The beach was adequately represented with a Bruun curve (Equation 2) with a constant (a) of 0.325, whilst the bar was represented with a vector fitted to the observed bar profiles.

The beach volume at the site is unknown since the boundary between the foreshore and beach could not be surveyed. An additional problem was that the field trips only provided 'snapshots' of the beach, which in reality exhibit large the cyclic variations referred to above. Consequently rough estimates of average volumes were used ($100 \text{ m}^3/\text{m}$ for the beach and $300 \text{ m}^3/\text{m}$ for the bar). The large scale longshore migration of the beach and the passage of ords were represented by applying annual antiphase sinusoidal fluctuations to the beach and bar. Clearly this representation of the beach involves several major assumptions; these will be discussed further below.

Model calibration involved adjusting the model's material strength parameter (S) until the correct recession rate was obtained. The resulting shore profile can be seen in Figure 4.9.

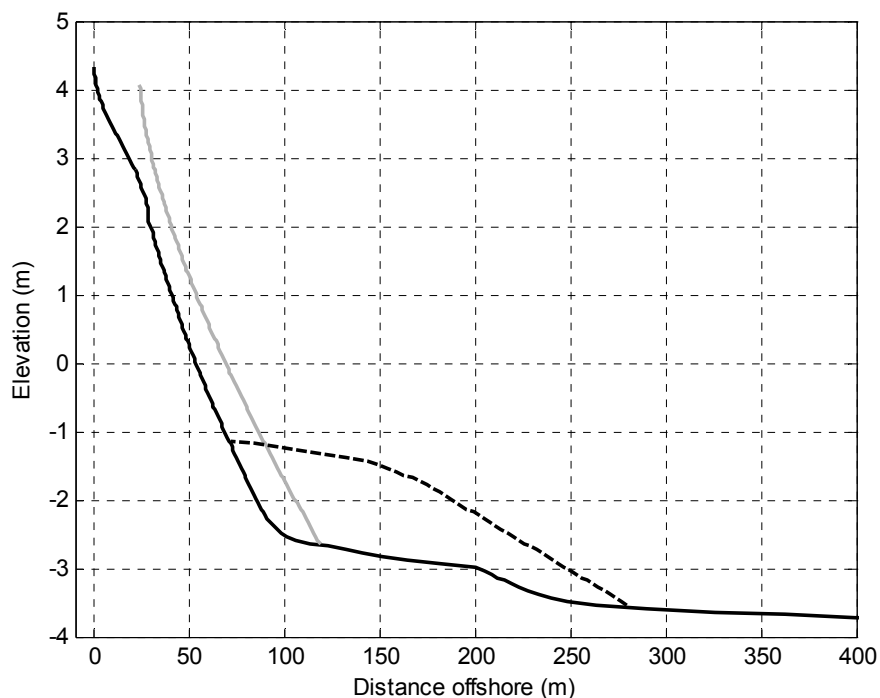


Figure 4.9. Easington model profile.

(c) Discussion

The modelling exercise did produce a reasonably good representation of the Easington foreshore. However, this was only possible after making several major assumptions about the volume and behaviour of the beach and bar.

Consequently confidence in the Easington model was not high and the modelling exercise reveals areas where the both the model and foreshore monitoring could be improved, including:

1. Surveying the surface of the foreshore below the beach,
2. Understanding in more detail the migration of the sandwave/ord systems
3. Investigating the shore profiles at the start of the Holocene transgression.

The first point above is a general issue for cohesive shore platforms with beaches, but is particularly a modelling problem for shores with substantial beaches, like Easington. The second point may be specific (in the UK) to the Holderness coast, whilst the third point is a generic problem for all cohesive foreshore sites.

4.4 Numerical Experiments into Beach/Platform Interaction

A series of numerical experiments were also run to explore generic beach/platform interaction and the consequences for shoreline recession rates. Clearly such models should represent realistic conditions without being too site specific. For this reason it was decided not to use the models developed to describe either of the study sites since Easington proved to be dominated by unusual beach forms and Warden Point was significantly influenced by biological weathering. Instead the model constructed by Walkden & Hall (2005) to describe the Naze shore was used. This held the advantages of being the simplest of the three in process terms and was the most successfully validated. In these generic tests the Naze model was perturbed in various ways to explore the consequences for the profile and shoreline recession rate. Here the shoreline is defined as the junction of the cliff and foreshore.

Decisions to protect cohesive shore platforms often involve increasing beach volume either directly (through nourishment), indirectly (through groyne construction) or both. Consequently the main focus of these experiments was foreshore dynamic response to changes in beach volumes. Relatively long-term behaviours were explored to inform understanding of sustainability. The consequences of managed retreat were also investigated, since this is becoming increasingly viable as a management option. The implications of sea-level rise were also explored, since coastal engineering decisions are now made under the assumption of accelerated sea-level rise.

In this work a distinction is made between recession rate (R) and equilibrium recession rate (ε) since:

- R changes constantly due to natural variation in loads and systems state, whilst
- ε represents a long-term average that depends on, *inter alia*, the wave climate, tidal characteristics and long-term average beach volume.

Any engineered modification of beach volume is likely to affect R in the short-term and ε in the long-term. Questions of sustainability will depend largely on ε .

4.4.1 Response of a Foreshore to the Introduction of a Beach

A model with no beach was run to observe the shoreline retreat over a long period. The model was then rerun, with the addition of a beach assuming that:

- The new berm was formed around the highest surge level,
- The beach fluctuates about a constant volume ($25 \text{ m}^3/\text{m}$), and
- The surface of the new beach immediately assumes a Bruun form (equation 2).

The shoreline retreat observed in both models is shown in Figure 4.10. The land 'saved' through the addition of the beach is equal to the vertical distance between the lines.

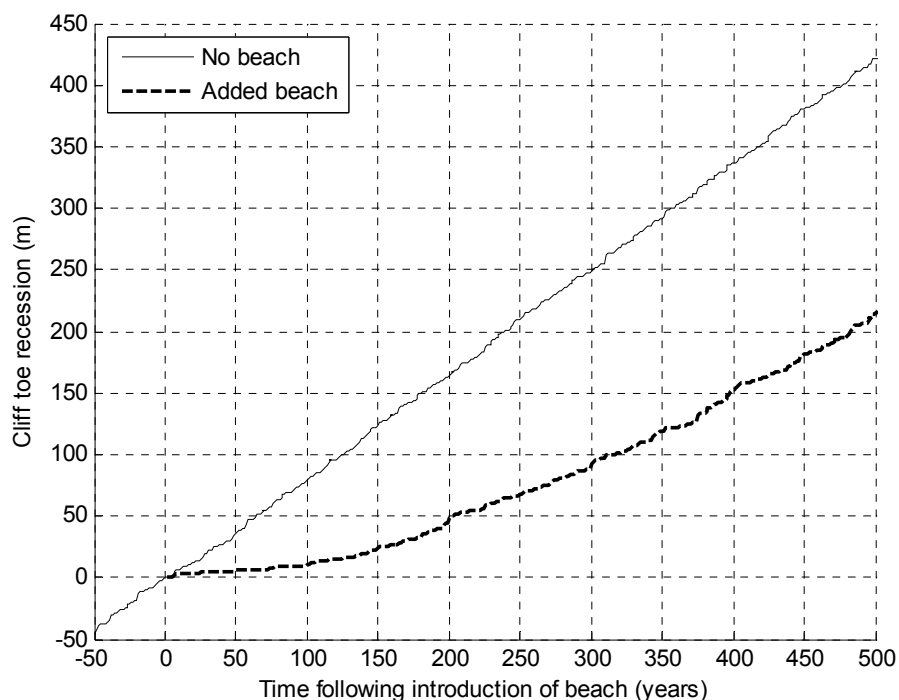


Figure 4.10. Shoreline recession with and without a beach.

It can be seen that the beach temporarily causes recession to stop, but over time the retreat rate increases. This happens because of morphological interaction between the beach and the foreshore, as demonstrated in Figure 4.11, which shows profiles from the 'with beach' model. The profiles have been horizontally aligned by cliff toe.

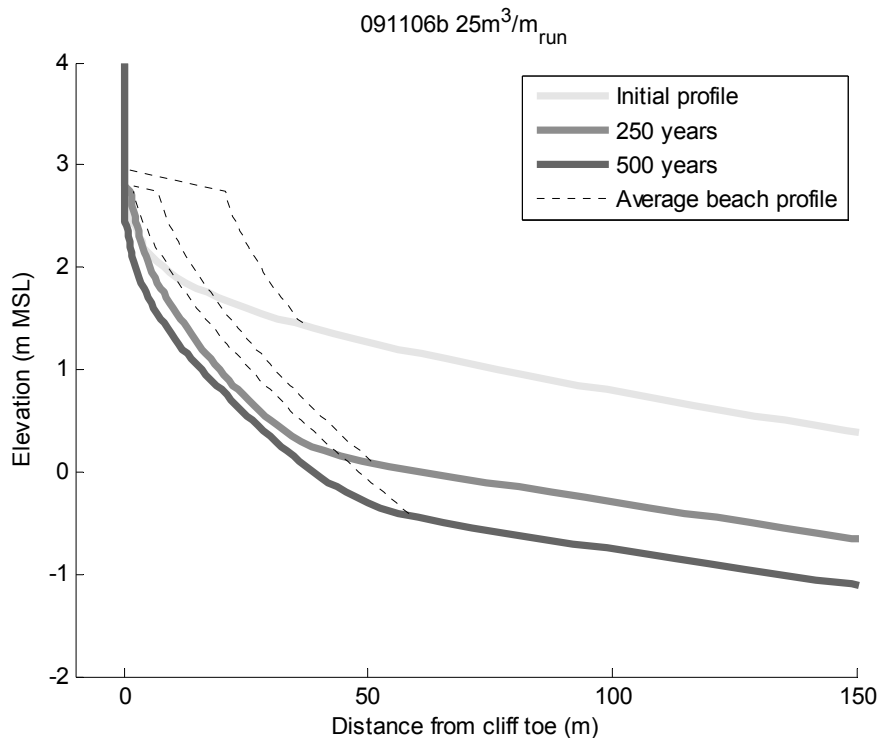


Figure 4.11. Shore profiles at three stages following the introduction of a beach (horizontally aligned by cliff toe).

Initially the beach sits high up the profile, protecting the toe of the cliff and the narrow width of foreshore on which it rests. This protection coupled with continued lowering of the foreshore seaward of the beach causes the profile shape to change. Overall the foreshore steepens, with the upper section mimicking the beach profile (See Kamphuis 1987 and Walkden & Hall 2005 for fuller descriptions). This foreshore adaptation causes the beach to spread and become thinner, reducing its protective capability. Ultimately the beach thins to the extent that erosion can occur through it and the shore recession rate increases.

This behaviour is significant because it implies the benefits of beach building diminish with time. The next question that was addressed was whether, ultimately, beach building has any influence on the equilibrium recession rate.

4.4.2 Sensitivity of Equilibrium Recession Rate to Beach Volume

In these experiments the average beach volume was varied from 5 to 300 m³/m in 5 m³/m steps. As before, although the average volume was held constant the actual volume varied every timestep. For each average beach volume the model was run until dynamic equilibrium had been reached, at which point ε was recorded and the average beach volume was incremented to the next value. In Figure 4.12 the beach volumes are plotted against equilibrium recession rates normalised against the 'no beach' rates.

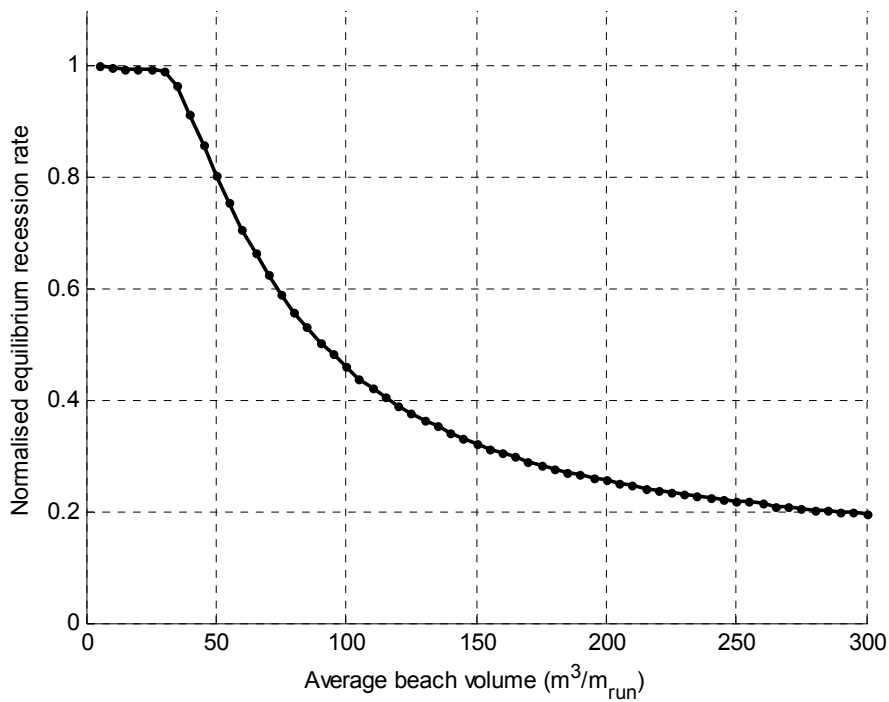


Figure 4.12. Relationship between (normalised) equilibrium recession rate and beach volume.

It can be seen that the relationship is highly non-linear and that there is a threshold below which the beach volume does not influence ε . This result is significant because it indicates that engineering measures to increase beach volume will only have a lasting benefit if the introduced volume is above a certain threshold. The value of the threshold ($30 m^3/m$ in Figure 4.12) is specific to the model conditions tested. When the experiment was repeated with other tidal ranges, different thresholds were found, as demonstrated in Figure 4.13.

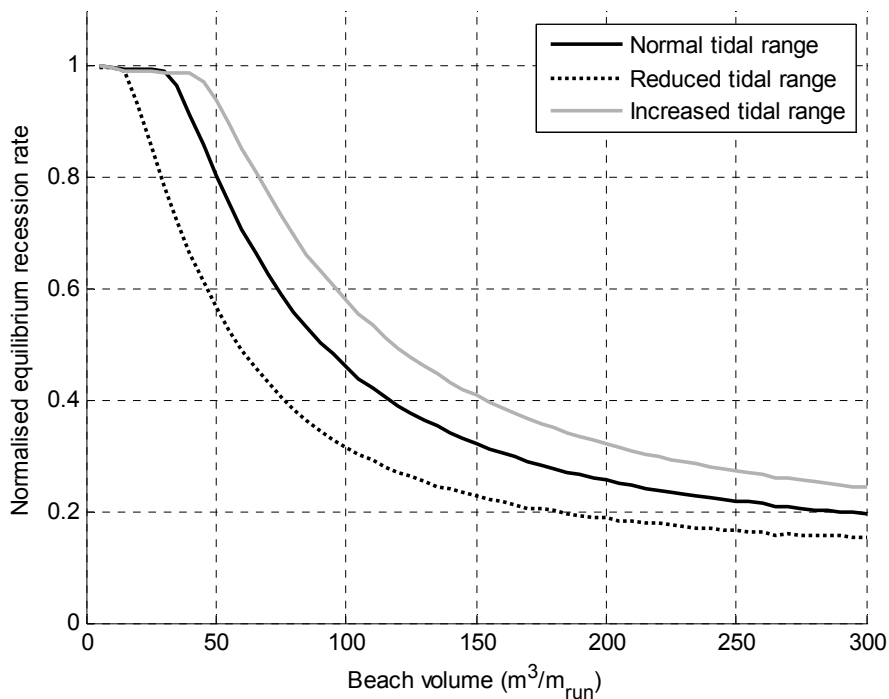


Figure 4.13. Relationship between (normalised) equilibrium recession rate and beach volume for three tidal ranges

The results in Figure 4.13 were analysed to find a general threshold definition. It was found to depend on the depth through the intertidal zone of the seaward edge of the beach (Z_b , see Figure 4.14). This is illustrated in Figure 4.15, in which the same equilibrium recession rates have been plotted against Z_b , normalised to the mean level of low water neap tides (MLWN).

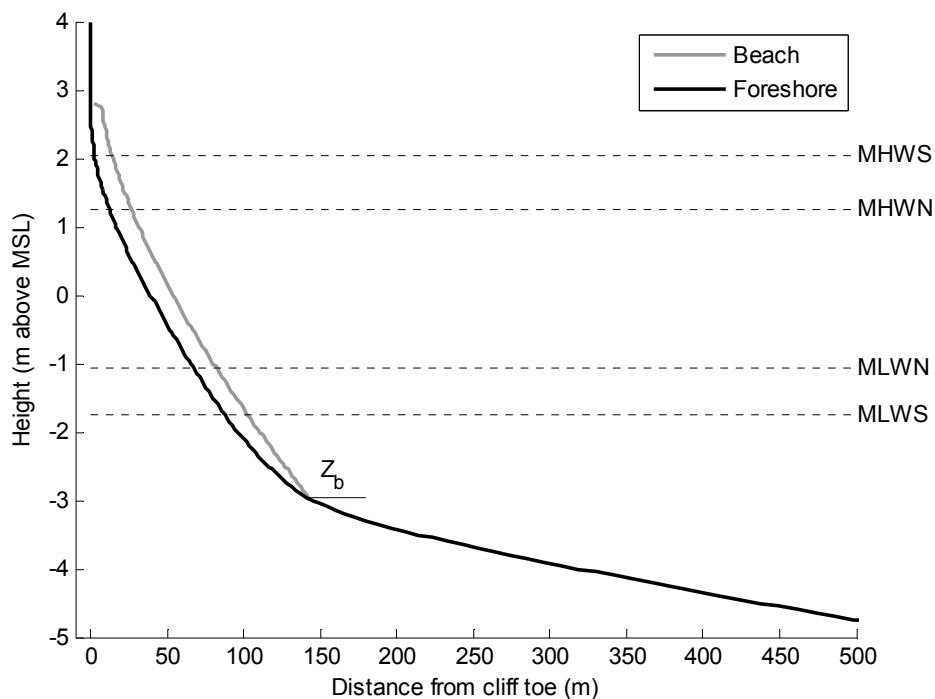


Figure 4.14. Definition of Z_b

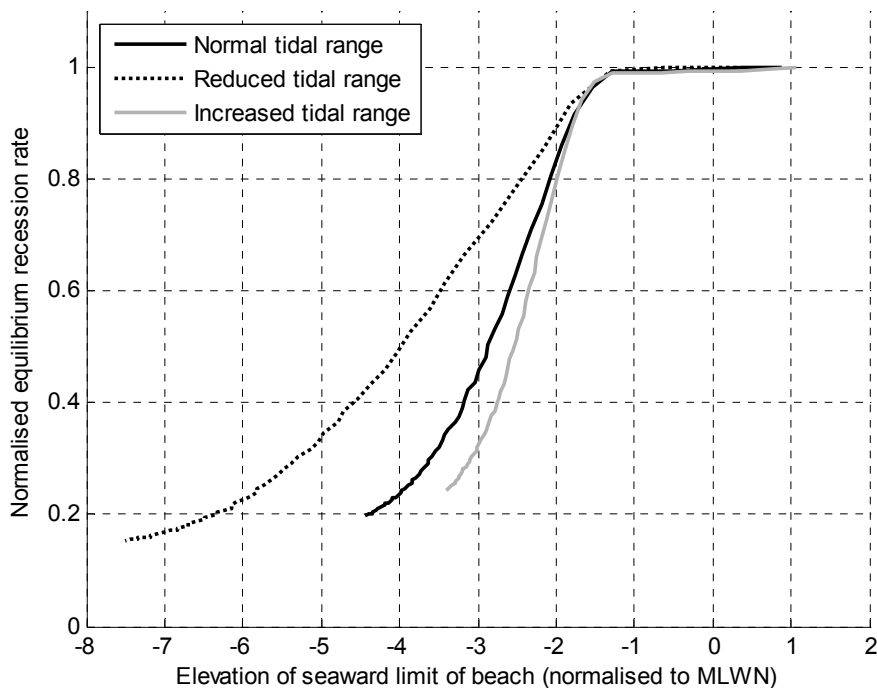


Figure 4.15. Relationship between normalised equilibrium recession rate and the normalised level of the seaward limit of the beach.

The convergence of these lines indicates that when Z_b is higher than approximately -1.5MLWN , it has no influence on ε . The reasons for this will be considered in the discussion section.

4.4.3 Consequences of Managed Retreat

Generally speaking coast protection measures require maintenance, without which shoreline erosion will resume. Observations of coastal recession at Happisburgh (Norfolk) over the last decade reveal that once a decision is taken to cease protection, the subsequent recession may be severe. At Happisburgh it appears that the coastline has now retreated to at least as far as, and possibly beyond the line that it would have reached if structures had never been built, i.e. there is no residual benefit from the original coast protection.

The question of whether an intervention at the coast will provide residual benefit once maintenance has ceased is pertinent to the assessment of both the sustainability of new interventions and whether to retreat a previously defended coast. A series of experiments were therefore conducted to explore the residual benefit of beach building. Firstly modified versions of the experiments described in Section 4.1 were conducted in which the added beach was removed after 50 years. Two average beach volumes were tested ($25\text{m}^3/\text{m}$ and $50\text{m}^3/\text{m}$) and the resulting shoreline recession is shown in Figure 4.16.

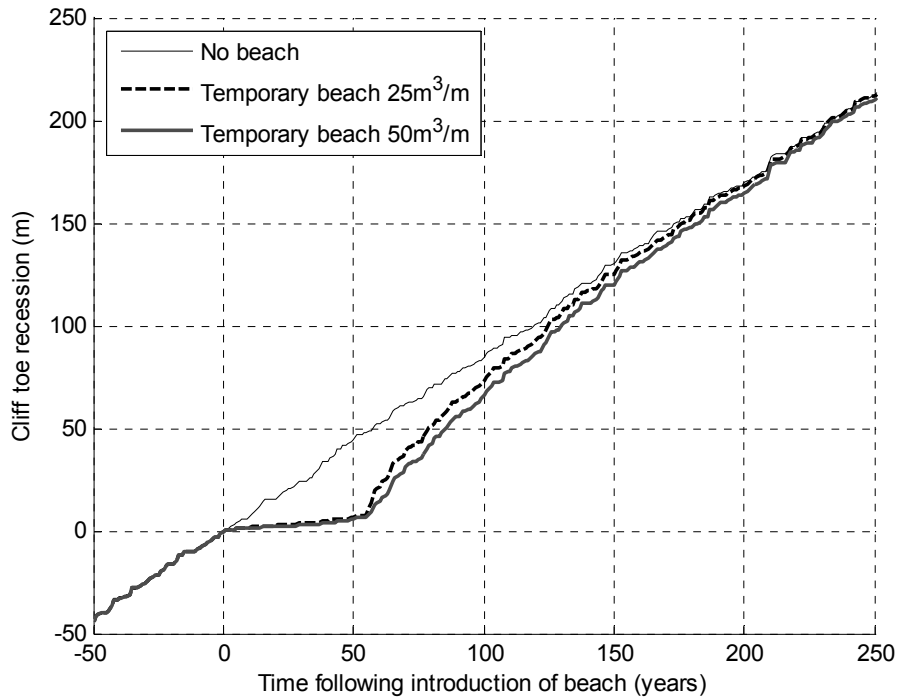


Figure 4.16. Recession of a shore given 50 years of beach nourishment.

In this experiment both beach volumes provided no residual benefit, although in each case it took a long time for the coastline to reach the position it would have been at if nourishment had never been introduced.

This result is significant because it implies that a decision to cease nourishment (or allow groynes to fail) will result in a period of shoreline recession greater than the original pre-nourishment retreat. The reasons for this coastal 'catch-up' were explored through further analysis.

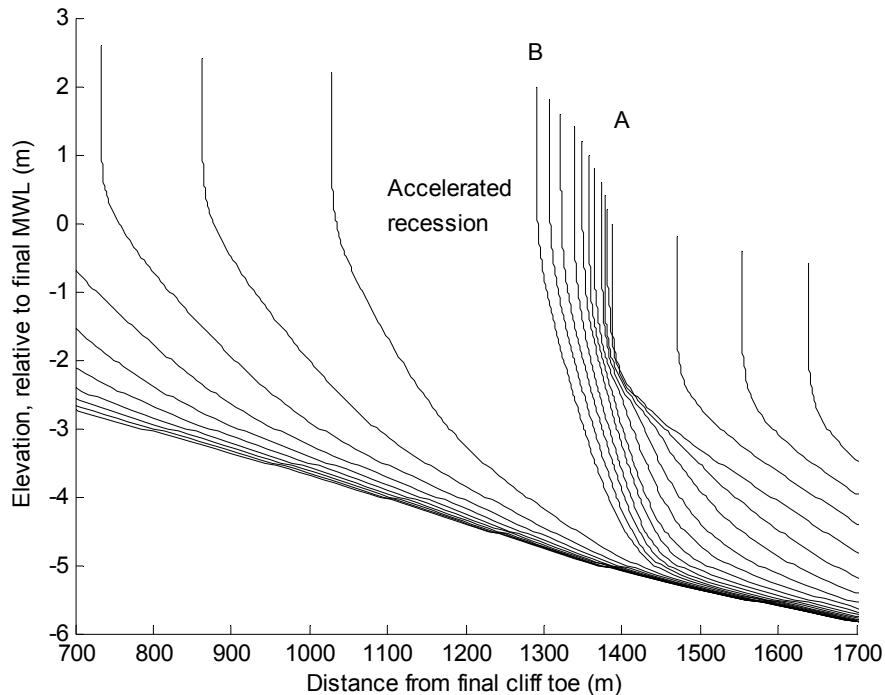


Figure 4.17. Model shore profiles in 100 year timesteps before, during and after the temporary beach nourishment.

In Figure 4.17 a series of shore profiles are shown (progressing from right to left) representing model development with no beach (to the right of point 'A') whilst a beach is maintained (between 'A' and 'B') and after the beach is removed (to the left of 'B'). It can be seen that the beach causes the foreshore to steepen, and the recession rate to drop, as previously seen in Figures 4.10 and 4.11. However, once the beach is removed, the original profile shape reforms (at a higher elevation due to sea-level rise). It does this from the bottom up and this causes a period of accelerated shoreline recession.

Although this explains the process of shoreline 'catch-up' it is still unclear whether a residual benefit will remain after the foreshore has returned to its equilibrium form. This issue is closely related to the threshold behaviour described in Section 4.2 and will be considered in the discussion.

4.5 Shore Profile Response to Accelerated Sea-level Rise

A series of numerical experiments were conducted to explore the response of cohesive shores to accelerated sea-level rise. To simplify the problem attention was restricted to low beach volume shores, i.e. shores where the beach was not large enough to influence the equilibrium recession rate.

A range of model parameters were perturbed using the amplification factors shown in Table 4.1. For each amplification factor the equilibrium recession rate was found for a range of rates of sea-level rise. In addition, more extensive sea-level rise rates were tested on the basic Naze model without parameter modification.

Table 4.1. Parameter combinations tested.

Parameter	Amplification Factors	Rates of Sea-level rise, mm/annum	No. Combinations
Rock strength (R)	0.25, 0.5, 1, 2, 4	2, 4, 6, 8, 10, 12, 14, 16	40
Tide range (TR)	0.5, 1, 1.5	2, 4, 6, 8, 10, 12, 14, 16	24
Wave height (H)	0.5, 1, 1.5	2, 4, 6, 8, 10, 12, 14, 16	24
Wave period (T)	0.75, 1, 1.25, 1.5	2, 4, 6, 8, 10, 12, 14, 16	32

4.5.1 Equilibrium Profile Shapes

The results show a strong relationship between sea-level rise and profile shape. This can be seen in Figure 4.18, which shows equilibrium profile shapes resulting from different rates of sea-level rise that emerged from a baseline test series in which all the amplification factors were set to 1.

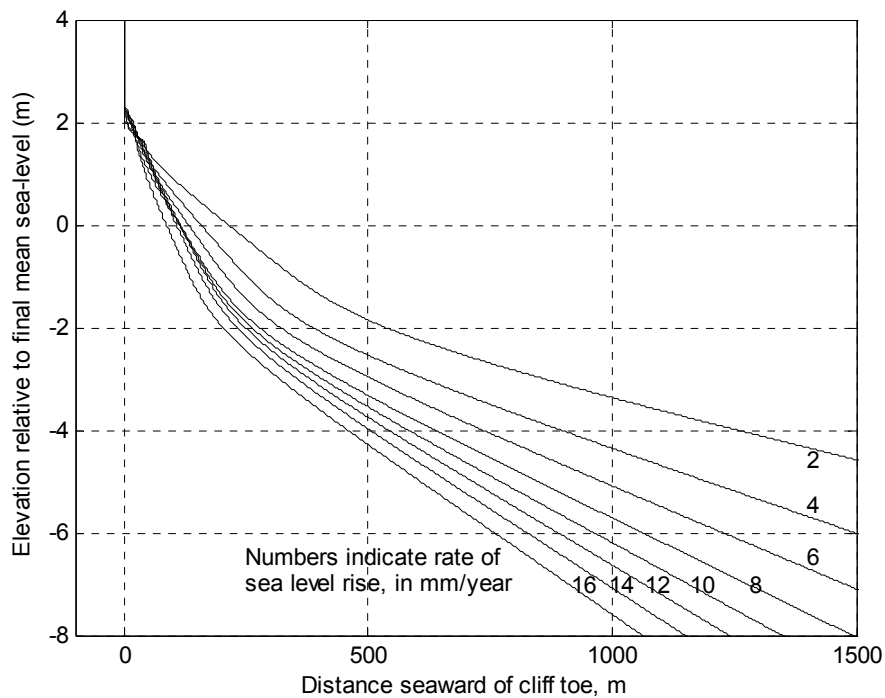


Figure 4.18. Equilibrium profile sensitivity to rate of sea-level rise.

Figure 4.18 shows emergent modelled equilibrium shapes at rates of sea-level rise of between 2 mm/year and 16 mm/year. It is apparent that the equilibrium profiles become increasingly steep for higher rates of sea-level rise.

This behaviour can be understood by considering the period that each elevation in the profile experiences wave attack. Wave action causes flattening of the shore profile, whilst sea-level rise translates the zone of wave attack to higher elevations.

Each elevation in the profile is flattened less under higher rates of sea-level rise because the period it is exposed to wave attack is shorter.

These results might be compared with the Bruun model (1962) which assumes insensitivity of profile shape to sea-level rise. They do not contradict the Bruun model, which was conceived for deep beach shores, but does show that the assumption of an unchanging equilibrium form under accelerated sea-level rise is unrealistic for the shore type considered here.

4.5.2 Equilibrium Recession Rates under Sea-level Rise

The historic (equilibrium) recession rate (ε_1) is normally used when estimating future recession of a site because it represents the geological characteristics and sediment transport pathways in response to the imposed hydrodynamic loads. The future recession rate (ε_2) of a system *in dynamic equilibrium* may be assumed to be equal to ε_1 , but this is not the case under increased sea-level rise. ε_1 may still be used as a normalising factor, however, to account for geology and stationary hydrodynamic loads. Figure 4.19 shows the equilibrium recession rates from all of the parameter tests, whereas in Figure 4.20 the same data has been normalised to assumed historic rates.

For each test series (i.e. sequence of tests in which the amplification factors were held constant whilst the rate of sea-level rise was varied) it was assumed that the lowest rate of sea-level rise (2 mm/a) represented historic conditions (i.e. $S_1 = 2$ mm/a). This value was chosen simply because it is typical for southern Britain and many other regions during the 20th Century. Each value of ε was then divided by the value of ε resulting from this S_1 . Likewise, the rates of future sea-level rise were normalised to S_1 . This effectively removed the scatter in the data, as can be seen in Figure 4.20.

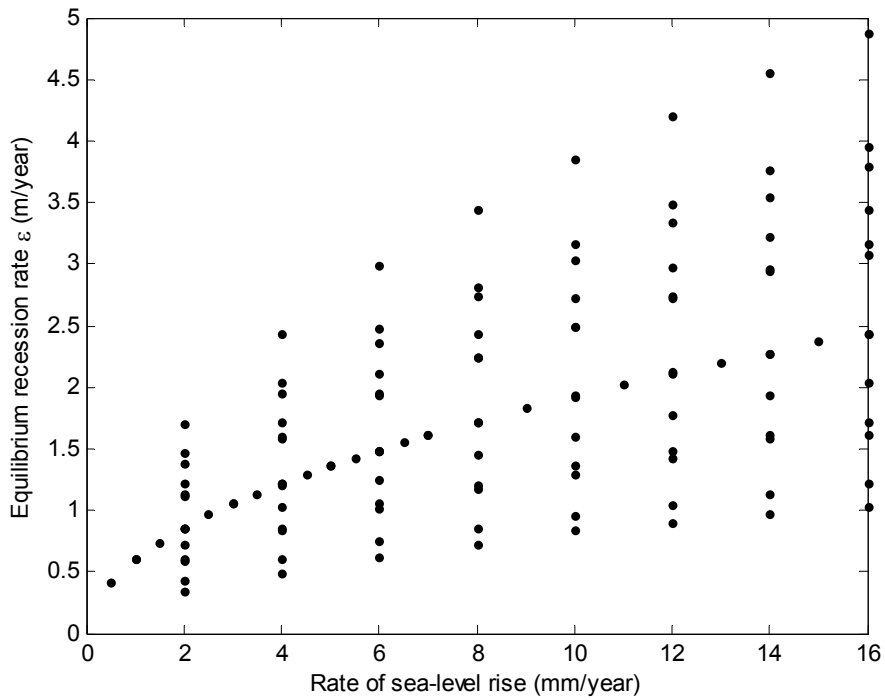


Figure 4.19. Equilibrium recession rates of the parameter tests.

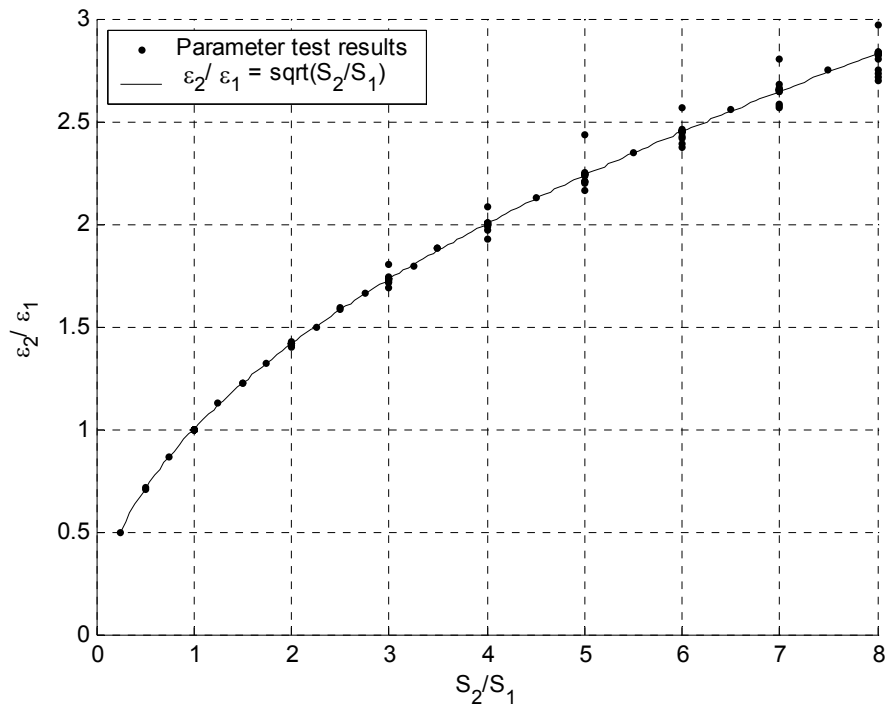


Figure 4.20. Normalised rates of sea-level rise and equilibrium recession.

The following expression fits the data in Figure 4.20 with a correlation coefficient of 0.98:

$$\frac{\varepsilon_2}{\varepsilon_1} = \left(\frac{S_2}{S_1} \right)^{0.5}$$

Equation 3

Hence, the model's response to increased sea-level rise, within the parameter space tested, for the case of an absent/small beach can be expressed as:

$$\varepsilon_2 = \varepsilon_1 \sqrt{\frac{S_2}{S_1}}$$

Equation 4

Equation 4 describes the relationship between future and historic equilibrium retreat rates. Equilibrium conditions take some time to emerge following a change in the rate of sea-level rise. The simulation passes through a transient stage, as illustrated in Figure 4.21 which shows results for one model, in which a step increase in sea-level rise from $S_1 = 2$ mm/a to $S_2 = 6$ mm/a was introduced at 6000 years. The results have been averaged within 100-year windows. It can be seen that the recession rates take around 1000 years to stabilise at approximately 1.47 m/a from the prior rate of approximately 0.85 m/a. However, approximately half of the total increase in retreat rate is achieved by the middle of the first century following the step change.

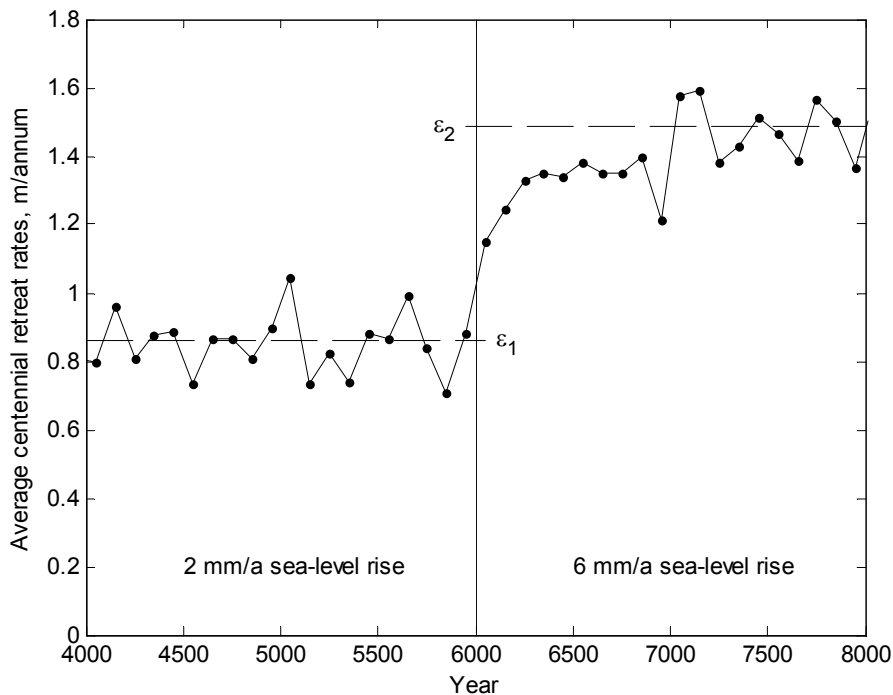


Figure 4.21. Example model recession rates before and after a step change in sea-level rise from 2mm/a to 6mm/a at 6000 years (averages of 100 year segments).

As stated above, these results describe the behaviour of shores with a low beach volume. It is difficult to estimate the proportion of shores at which this condition applies because coastal studies rarely observe beach volume or thickness. However, it is notable that shore platforms tend to mimic the slope of the beach overlying them (Kamphuis, 1987), such that beaches of relatively low volumes obscure a large platform area, perhaps the entire intertidal zone. Hence it is likely that many shores which meet this criteria, and therefore in behavioural terms are controlled by the dynamics of their shore platform, are probably currently being classified as 'beaches'.

Equation 4 does not describe future recession at sites with no historic sea-level rise. Results of SCAPE modelling not described here indicate that although such locations may recede they may not achieve a state of equilibrium, and so the concepts used to develop Equation 4 do not apply. Exploration of this condition will require further work, however the limitation that this constraint imposes on the applicability of Equation 4 is not severe since the average global sea-level is rising.

4.6 Summary of Key Findings from the Numerical Model Testing

The study site models proved rather less informative than the generic tests, but did produce some useful results. The Warden Point model indicated that biological weathering plays an important role in both shaping the foreshore profile and determining the overall shoreline recession rate.

The modelled rate of biological lowering (100 mm/annum maximum, 50 mm/annum average) may be an over-estimate if, as seems likely, the biological activity extends beyond the inter tidal zone. If this is so then the boring Piddocks would be able to amplify shoreline recession rates with lower rates of foreshore downwearing. Although this biological effect can not be proven with the limited data available it does provide an explanation for the high recession rates observed at Warden Point, which can not be attributed to the wave climate alone.

Difficulties in constructing and validating the Easington model revealed the importance of obtaining survey data of the sub-beach foreshore surface (and therefore beach volumes). Although this problem was compounded by the complexity of the beach behaviour at Easington, the need for foreshore surface data is generic especially when modelling sites with larger beaches. The need for good data on the foreshore form can also be inferred from the experiments on shore response to changes in either beach volume or sea-level rise. The consequences for the recession rate in both cases depend strongly on the current state of the foreshore.

The generic model tests showed that the cohesive shore platform/beach interaction is an important regulator of profile shape and shoreline recession. Cohesive shore platforms tend to steepen to mimic the shape of the beaches that overly them (Figure 4.11, Kamphuis, 1987, Walkden & Hall, 2005). Numerical simulations of beach building indicate that although recession rates temporarily cease, they begin to increase as the foreshore steepens, and the

beach thins (e.g. Figure 4.11). This implies that beach nourishment volumes would have to be increased over time to control shore retreat.

If a (natural or artificial) beach is sufficiently large then simulations indicate that it will reduce the shore's equilibrium recession rate (ε). In the simulations shown in Section 4.2 beaches had to be wide enough to reach beyond 1.5 MLWN in order to reduce ε . This may be understood by considering the shore erosion as occurring through a series of discrete erosion events, lasting for one tidal period. Each event removes material from a relatively wide tract of the shore as the surf zone is translated through the tidal cycle. To reduce the equilibrium recession rate a beach must defend against all of the erosion due to at least some of these events. The easiest events to defend against are driven by smaller combinations of wave height and tidal amplitude, since these are less aggressive (and so can be defended by a thinner beach) and occupy a narrow tract of the profile (therefore can be defended with a smaller width of beach). The tract eroded by the smallest event extends below mean water level to a limit (Z_{min}) which is approximately:

$$Z_{min} = \text{MSL} - \eta_{min} - H_{min}\gamma \quad \text{Equation 5}$$

where H_{min} is the smallest wave height able to erode material, η_{min} is the smallest tidal amplitude, MSL is the mean sea level and γ is the breaker depth ratio. For the models tested Z_{min} is somewhat below MLWN, which is probably fairly common for many locations.

Results presented in section 4.3 show that if a beach is allowed to deplete the foreshore becomes more gently sloping accompanied by high shoreline recession rates (e.g. Figures 4.16, and 4.17). This may occur if, for example, beach nourishment is not maintained or if the natural supply of beach material to a shore is cut off. The extreme erosion at Happisburgh in Norfolk may, in part, be an example of the latter case.

At sites where the beach volume falls due to a cessation of nourishment, the simulations indicate that the shoreline will try to 'catch-up' with where it would have been had the nourishment never been conducted. Whether or not there is some residual benefit once a new equilibrium form is established probably depends on the width of beach protection, i.e. whether the nourished beach extended beyond Z_{min} .

The exploration of shore response to accelerated sea-level rise indicated that the equilibrium profile form varies with the rate of sea level rise, with higher rates leading to steeper foreshores. The results for equilibrium recession rate under accelerates sea-level rise were found to be well represented with a simple relationship across all parameter values tested. This relationship is proposed as a means of rapidly estimating future equilibrium recession rates for soft rock shores overlain by a low volume (or absent) beach in which the profile is subjected to an increase in the rate of sea-level rise.

5 CONCLUSIONS AND PRELIMINARY MANAGEMENT GUIDANCE

5.1 Erosion and Weathering Processes of Cohesive Shore Platforms

Previously, little work existed on the relative importance of erosion and weathering processes on cohesive shore platforms. The field investigations and laboratory tests in this study have yielded the first direct measurements of key processes and parameters in such detail in the UK. Table 5.1 presents a summary of the key measurements.

Table 5.1. Summary Measurements for Field Investigations

Feature	Warden Point	Easington
Average platform downwearing rate (mm a ⁻¹)	17.63	41.93
Location of highest downwearing rate	Upper platform	Upper platform ²
Location of lowest downwearing rate	Lower platform	Lower platform
Triaxial test (kPa)	17.17	24.03
Gradient (ratio)	0.5	0.9
Wave energy (x10 ⁶ kJ/m)	20.2	162.6
Max wave height (m)	2.25	3.5
Most frequent wave height (m)	0-0.25	0.5-0.75
Biology	Abundant	Little
Platform surface morphology	Planar	Gullied

These results, together with the output from numerical model tests have been used to assign relative levels of importance (low, intermediate, high) to the factors involved in the downwearing of cohesive shore platforms (Table 5.2).

² Unconfirmed

Table 5.2. Relative Importance of the Factors Involved in Cohesive Shore Platform Downwearing, Based on the Findings at Warden Point and Easington.

Factor	Importance of Effect on Downwearing Rates	Reason
Boring organisms	Intermediate	Occurrence of piddocks at Warden Point does not coincide with areas of highest downwearing rates, but model tests demonstrate the importance of biological-related material weakening in profile development.
Protection of surface by non-boring organisms	Low	Does not appear to be a major factor on cohesive shore platforms.
Chemical weathering	Low	Does not appear to be a major factor on cohesive shore platforms.
Wetting-drying	Intermediate	Observed to occur on the upper platform at Warden Point.
Freeze-thaw	Low	Does not appear to be a major factor on cohesive shore platforms at present. Likely to remain of relatively low importance due to increasing winter temperatures associated with climate change.
Geotechnical properties	Intermediate	Geotechnical properties coincide with the platform downwearing at Warden Point but not at Easington.
Removal of overburdening cliff and expansion	Low	Does not appear to be a major factor on cohesive shore platforms.
Presence of a highly mobile beach	High	Movement of the extensive beach and sand bars at Easington actively erodes the platform. Elsewhere, thick upper beach deposits protect the platform.

Presence of fluid mud	Intermediate	Removal of fluid mud may result in sudden drops in surface elevation at a micro-scale.
Scour around objects	Intermediate	Observed to be a problem at Easington locally around protrusions.
Gulley or runnel downwearing	Intermediate	Depression or runnels erode more slowly than raised areas or ridges on both platforms at the micro-scale.
Wave conditions	High	Direct effect on the downwearing of the platform. Should be considered with platform elevation, width and gradient to determine location and period of wave attack (e.g. Easington's platform has an extremely low elevation making the period of wave attack only either side of low water).

It can be seen that whilst all of the listed factors contribute to overall platform downwearing in some way, it is the incident wave energy and presence (or absence) of a beach that are by far the most significant factors. The tidal range, which influences where wave activity impinges on a profile and also influences wetting-drying cycles across the platform, and both biological activity and material strength are all processes of some importance (e.g. in resisting wave activity or in weakening the material strength in advance of mechanical erosion by waves). However, even these processes can be deemed of considerably lesser significance than the dominating wave conditions and nature of a covering beach.

5.2 Platform/Beach/Cliff Interactions

From the field investigations, it is quite clear that interaction between the beach and the platform occurred at Easington, where the migrating sand bars covered the platforms during part of the field campaign. The effect of this was two-fold. Firstly the upper platform was covered by an extensive volume of material which did not move significantly during the experiments. Here, the platform is likely to have been well protected by the beach. Lower down the platform, the more mobile sand bar coverage is likely to have contributed to the high downwearing rates through abrasion of the platform by the non-cohesive material.

Numerical model testing has further investigated these interactions and has demonstrated that the shore platform/beach interaction is an important regulator of landward shoreline recession.

5.3 Preliminary Management Guidance

Cohesive shore platforms are formed by processes of erosion. As this happens, material is released that constitutes an important, and often overlooked, component of the coastal sediment budget.

These natural processes can, however, be problematic for coastal managers, who are faced with several issues related to the erosion of cohesive shore platforms. The erosion process can directly lead to loss of inter-tidal and sub-tidal habitat, which supports a range of faunal species, although it is recognised that such landforms are not as ecologically rich (in terms of either diversity or density) as other shore platform types (e.g. chalk, sandstone and other rock types) or other inter-tidal landforms (e.g. mudflats and salt marshes). Erosion processes can also expose and lead to the loss of sites of archaeological or geological importance. Further to this, erosion processes release material from the platform that constitutes an important, and often overlooked, component of the coastal sediment budget.

The erosion of cohesive shore platforms can also have negative consequences for coastal engineering interventions. Figure 5.1 demonstrates that continued platform lowering, in the absence of a substantial protective beach, can lead to exposure, and ultimately failure, of the foundation of coastal defence structures.



Figure 5.1 Exposure of Sheet Piling at the Toe of a Seawall

Elsewhere it is the consequences of the platform erosion on beach levels and cliff recession rates that are of concern to coastal managers.

In essence, the possible management responses to such problems are to:

- (i) Do nothing;
- (ii) Stop or limit the downwearing of the platform; or
- (iii) Manage the consequences of the platform downwearing.

The policy of ‘managed realignment’ (i.e. the removal of existing coastal defence structures) is also considered in the following discussion for completeness.

Do Nothing:

In situations where no cliff-top or foreshore assets are at risk from the processes, the irreversible downwearing of cohesive shore platforms does not necessarily cause a management concern, either directly or through its effects on beach levels or cliff recession rates. In such situations, the natural erosive processes should be allowed to continue since they release an important contribution of fine-grained material to the coastal sediment budget.

It is important to note that the adoption of a ‘Do Nothing’ policy will not, in the medium to long-term, necessarily result in a continuation of historic recession rates. This is because climate change, in particular accelerated sea-level rise, is expected to increase the erosion of cohesive shore platforms.

The use of predictive models, such as SCAPE, can provide managers with an indication of the scale of downwearing and cliff recession anticipated under different climate change scenarios so as to inform their decisions about whether or not the processes cause a longer-term risk to assets that are presently set-back from the current cliff edge. This predictive capacity can also be used to help inform land-use planning and development control activities.

Stop or Limit Downwearing of the Platform:

Where the downwearing of cohesive shore platforms, or the consequences of this process on beach levels or cliff recession, does cause a problem for cliff-top or foreshore assets, management efforts could be made to limit the downwearing rate. This is best achieved through the introduction of a protective covering of beach material across the platform. Such beach replenishment activities need to ensure a sufficient volume of material and regular maintenance (e.g. periodic ‘top-up’ replenishments) in order to remain protective and prevent enhanced erosion through processes of abrasion.

SCAPE modelling revealed that cohesive shore platforms respond dynamically to the introduction of a beach. This is important because it means that benefits seen shortly after beach building may not be sustained without increasing levels of investment. Over time the foreshore steepens, causing the beach to spread across it and become thinner. Ultimately the recession increases, and may return to pre-intervention rates.

The numerical models indicate that the critical threshold determining whether an artificial beach will reduce shoreline recession rates in the medium to long-term is how far it protects across the intertidal zone. If the beach provides some protection to the region between MLWN and MLWS and above then it will begin to have an effect on the equilibrium recession rate. If it does not extend this far then its benefits will only be transient. The further the beach extends beyond this level the more benefit it will bring.

Manage the Consequences of Platform Downwearing:

As an alternative to management of the platform downwearing process itself, a decision could be taken to manage its consequences using shoreline recession control structures. Typically, these may take the form of a seawall or revetment running along the toe of a sea cliff.

In such instances, it must be recognised that the downwearing of the fronting platform is likely to continue leading to:

- Increased wave loading on the defence structures as the water depth in front of them increases, due to both platform downwearing and sea level rise; and
- Decreased structural stability and increased risk of undermining of the foundations of the defence structures; and
- Narrowing of the intertidal zone, potentially leading to its disappearance.

When designing coastal defence structures, engineers incorporate an allowance in the design crest levels to account for predicted sea level rise over the design life of the scheme. Previous MAFF Flood and Coastal Defence Project Appraisal Guidance (MAFF, 1999) suggested an allowance be made of 6mm per year in the areas of the UK where cohesive shore platforms typically are located. More recent Defra Supplementary Guidance (Defra, 2006) has amended this linear allowance and recommends the following alternative arrangements for different future epochs for the east coast of England south of Flamborough Head (i.e. where both Easington and Warden Point are located):

- 1990 to 2025 4.0mm per year;
- 2025 to 2055 8.5mm per year;
- 2055 to 2085 12.0mm per year; and
- 2085 to 2115 15.0mm per year.

Such rates of sea level rise are often considered as significant when planning and designing coastal management responses, yet they are small in comparison to the rates of shore platform lowering measured at Warden Point and, particularly, Easington as part of the present study. Consequently, such downwearing rates should be incorporated into design aspects involving: (i) crest level design (e.g. through changes in overtopping volumes over time); (ii) calculation of wave loading forces on structures; and (iii) determination of foundation depths below existing, and predicted future, foreshore levels.

Managed Realignment:

If a decision is taken to cease or remove engineering interventions such as beach nourishment, groynes, seawalls or revetments to allow a coast to retreat the shoreline is likely to exhibit an initial 'catch-up'. Coastal managers should anticipate and account for these high rates of recession, which occur whilst a state of equilibrium with the governing processes is re-established.

When considering this question it is useful to first estimate the coastline's notional uninterrupted location, i.e. where it *would* be if the intervention had never been made. This can be found by multiplying the equilibrium recession rate prior to the intervention by the duration of the intervention. The numerical modelling work done within this study indicates the following:

- If the intervention protected the profile between MLWN and MLWS then the shoreline may not reach its uninterrupted location;
- If the intervention only protected higher elevations, *and* the coastal system is otherwise unchanged from its pre-intervention state then the shoreline is likely to catch up with its uninterrupted location; and
- The shoreline may retreat landward of its uninterrupted location if the coastal system has changed, for example if the beach volume has reduced, causing a more gently sloping foreshore.

The above issues are becoming increasingly relevant as the policy of managed realignment is now being more pro-actively considered in the second round of Shoreline Management Plans for the coastline of England and Wales.

6 REFERENCES

- Allen, J.R.L. and Duffy, M.J. (1998). "Medium-term sedimentation on high intertidal mudflats and salt marshes in the Severn Estuary, SW Britain: the role of wind and tide." Marine Geology **150**: 1-27.
- Amin, S.M.N. And Davidson-Arnott, R.G.D., 1997. A statistical analysis of the controls on shoreline erosion rates, Lake Ontario. Journal of Coastal Research, 13, 1093-1101.
- Amos, C.L., Van Wagoner, N.A. and Daborn, G.R. (1988). "The Influence of Subaerial Exposure on the Bulk Properties of Fine-grained Intertidal Sediment from Minas Basin, Bay of Fundy." Estuarine, Coastal and Shelf Science **27**: 1-13.
- Arulanandan, K.; Loganathan, P. And Krone, R.B., 1975. Pore and eroding fluid influences on surface erosion of soil. Journal of the Geotechnical Engineering Division, ASCE, 101, 51-66.
- Askin, R.W. and Davidson-Arnott, R.G.D. (1981). "Micro-erosion meter modified for use under water." Marine Geology, **40**: M45-M48.
- Bale, A.J., Morris, A.W. and Howland, R.J.M. (1985). "Seasonal sediment movement in the Tamar estuary." Oceanologica Acta **8** (1): 1-6.
- Balson, P.S., Brew, D.S., Charman, R.O., Hobbs, P., Moses, C.A., Pearson, S., Walkden, M. and Williams, R.B.G. (2006) DEFRA conference on Flood and Coastal Erosion Risk Management 4th to 6th July 2006.
- Bath, A. H., Ross, C. A. M., Entwisle, D. C., Cave, M. R., Green, K. A., Reeder, S., & Fry, M. B. (1989a). Hydrochemistry of porewaters from London Clay, Lower London Tertiaries and Chalk at the Bradwell site (Safety Studies No. Nirex Safety Studies). NIREX.
- Bell, F.G., 2002. The geotechnical properties of some till deposits occurring along the coastal areas of eastern England. Engineering Geology, 63, 49-68.
- Bishop, C.; Skafel, M. And Nairn, R., 1993. Cohesive profile erosion by waves. In: EDGE, B.L. (ed.), Proceedings of the 23rd International Conference on Coastal Engineering, (Venice, Italy. American Society of Civil Engineers), pp. 2976-2989.
- Bishop, A. W., Webb, D. L. & Lewin, P. I. (1965) Undisturbed samples of London Clay from the Ashford common shaft: strength-effective stress relationships. Géotechnique, Vol.15, pp 1-31.

- Boumans and Day (1993). in DL Childers, FH Sklar, B Drake and T Jordan. (1993) Seasonal measurements of sediment elevation in 3 Mid-Atlantic estuaries. Journal of Coastal Research. **9**: 986-1003.
- Bray, M.J. And Hooke, J.M., 1997. Prediction of soft-cliff retreat with accelerating sea-level rise. Journal of Coastal Research, 13, 453-467.
- Brew, D.S., 2003. Understanding and predicting beach morphological change processes associated with the erosion of cohesive foreshores – scoping report. Defra/Environment Agency Technical Report FD1915.
- Brew, D.S. (2004). Understanding and Predicting Beach Morphological Change: Processes Associated with the Erosion of Cohesive shore platforms. Scoping Report. DEFRA/Environment Agency Flood and Coastal Defence R&D Programme. Technical Report FD1915.
- Brew, D.S.; Balson, P.S.; Pearson, S.; Hobbs, P.; Williams, R.; Robinson, D.; Moses, C. And Walkden, M., 2004. The implications of cohesive shore platform erosion for coastal management. Proceedings of Littoral 2004, Vol 2 (Aberdeen, Scotland), pp. 590-595.
- Bruun, P. 1954. Coast erosion and the development of beach profiles. Beach erosion board technical memo 44, U.S. Army Corps of Engineers.
- Bruun, P.: 1962, 'Sea-level rise as a cause of shore erosion'. Journal of Waterways and Harbours Division ASCE. 88, 117-130.
- Burnett, A. D., & Fookes, P. G. (1974). A regional engineering geological study of the London Clay in the London and Hampshire Basins. Quart. J. Eng. Geol., 7, 257-295.
- Cahoon, D.R., Lynch, J.C., Hensel, P., Boumans, R., Perez, B.C., Segura, B. and Day, J.W. (2002). "High-precision measurements of wetland sediment elevation: I. Recent improvements to the sedimentation-erosion table." Journal of Sedimentary Research **72** (5): 730-733.
- Carter, M.C. (2003). "*Hiatella arctica*. Wrinkled rock borer." Marine Life Information network: Biology and Sensitivity Key Information Sub-programme. Plymouth. Marine Biological Association of the United Kingdom. On-line: www.marlin.ac.uk/species.
- Christie, M.C., Dyer, K.R. and Turner, P. (1999). "Sediment flux and bed level measurements from a macro tidal mudflat." Estuarine Coastal and Shelf Science **49**: 667-688.
- Coakley, J.P.; Rukavina, N.A. And Zeman, A.J., 1986. Wave-induced subaqueous erosion of cohesive tills: preliminary results. In: SKAFEL, M.G. (ed.), Proceedings of the Symposium on Cohesive Shores (Burlington, Ontario. Associate Committee for Research on Shoreline

- Erosion and Sedimentation, National Research Council, Canada), pp. 120-136.
- Couperthwaite, J.S., Mitchell, S.B., West, J.R. and Lawler, D.M. (1998). "Cohesive Sediment Dynamics on an Inter-tidal Bank on the Tidal Trent, UK." Marine Pollution Bulletin **37** (3): 144-154.
- Cripps, J.C. & Taylor, R.K. (1981) The engineering properties of mudrocks. *Q. J. Eng. Geol.*, Vol. 14, pp325-346.
- Croad, R.N., 1981. Physics of erosion of cohesive soils. University of Auckland, Ph.D. thesis.
- Culshaw, M.G. & Crummy, J. A. (1991) S-W Essex, M25 corridor: Engineering geology. *British Geological Survey*, Technical Report No. WN/90/2
- Dade, W.B.; Nowell, A.R.M. And Jumars, P.A., 1992. Predicting erosion resistance of muds. Marine Geology, 105, 285-297.
- Davidson-Arnott, R.G.D. and Askin, R.W., 1980. Factors controlling erosion of the nearshore profile in overconsolidated till, Grimsby, Lake Ontario. Proceedings of the Canadian Coastal Conference 1980 (National Research Council of Canada), pp. 185-199.
- Davidson-Arnott, R.G.D., 1986a. Rates of erosion of till in the nearshore zone. Earth Surface Processes and Landforms, 11, 53-58.
- Davidson-Arnott, R.G.D., 1986b. Erosion of the nearshore profile in till: rates, controls, and implications for shoreline protection. In: Skafel, M.G. (ed.), Proceedings of the Symposium on Cohesive Shores (Burlington, Ontario. Associate Committee for Research on Shoreline Erosion and Sedimentation, National Research Council, Canada), pp. 137-149.
- Davidson-Arnott, R.G.D. And Ollerhead, J., 1995. Nearshore erosion on a cohesive shoreline. Marine Geology, 122, 349-365.
- Davidson-Arnott, R.; Van Proosdij, D.; Ollerhead, J. And Langham, D., 1999. Rates of erosion of till in the nearshore zone on Lakes Huron and Ontario. Proceedings of the Canadian Coastal Conference 1999 (National Research Council of Canada), pp. 627-636.
- Davidson-Arnott, R.G.D. And Langham, D.R.J., 2000. The effects of softening on nearshore erosion of a cohesive shoreline. Marine Geology, 166, 145-162.
- Dawson, A.G., 1980. Shore erosion by frost: an example from the Scottish Lateglacial. In: Gray, J.M. and Lowe, J.J. (eds.), Studies in the Late-Glacial of North West Europe. Pergamon, Oxford, pp. 45-53.

- Defra, 2006. *Supplementary Note to Operating Authorities – Sea Level Rise*. October 2006.
- Deloffre, J., Lafite, R., Lesueur, P., Lesourd, S., Verney, R. and Guezennec, L. (2005). "Sedimentary processes on an intertidal mudflat in the upper macrotidal Seine estuary, France." Estuarine Coastal and Shelf Science **64** (4): 710-720.
- Dixon, M.J., and Tawn, J.A., 1997. Estimates of extreme sea conditions: spatial analysis for the UK coast. Ministry of Agriculture, Fisheries and Food.
- Dixon, N. & Bromhead, E.N. (2002) Landsliding in London Clay coastal cliffs Q. J. Eng. Geol., Vol. 35, pp327-343.
- Duval, D.M. (1963): "The biology of *Petricola pholadiformis* Lamark (Lamellibranchiata Petricolidae)." Journal of Molluscan Studies **35**, 69-100.
- Ellison, R.A. (1983) Facies distribution in the Woolwich and Reading Beds of the London Basin, England. Proc. Geol. Assoc., Vol. 94, pp311-319.
- Falcke, W. E., & Bath, A. H. (1989). Evaluation of vertical changes in groundwater chloride and stable isotope compositions in coastal London Clay No. WE/89/90). British Geological Survey.
- Fookes, P.G. & Parrish, D.G. (1969) Observations on small-scale structural discontinuities in the London Clay and their relation to regional geology. Quart. Journ. Eng. Geol., pp217-240.
- Fookes, P.G. et al. (2006) Industrial uses of clay. Geological Society Special Publication.
- Foote, Y.L.M., Plessis, E., Robinson, D.A., Hénaff, A. and Costa, S. (2006) "Rates and patterns of downwearing of chalk shore platforms of the Channel: comparisons between France and England". Zeitschrift für Geomorphologie, Supplementband **144**: 93-115.
- Forster, A. (1997) The engineering geology of the London area. 1:50,000 Geological sheets 256, 257, 270, & 271. British Geological Survey, Technical Report No. WN/97/27.
- Frostick, L.E. and McCave, I.N. (1979). "Seasonal Shifts of Sediment Within an Estuary Mediated by Algal Growth." Estuarine and Coastal Marine Science **9**: 569-576.
- Gutkuhn, J. (pers. comm). Creator of the Argus Surface Meter IV, communication in Brighton, UK, 2005.
- Harris W.B. and Ralph, K.J. (1980) "Coastal engineering problems at Clacton-on-Sea, Essex." Quarterly Journal of Engineering Geology **13**: 97-104.

- Hayward, P.J., Isaac, M.J., Makings, P., Moyse, J., Naylor, E. and Smaldon, G. (1995a) Crustaceans in P.J. Hayward and J.S. Ryland (Eds) Handbook of the Marine Fauna of North-West Europe, Oxford University Press: 289-461.
- Hayward, P.J., Wigham, G.D. and Yonow, N. (1995b) Molluscs in P.J. Hayward and J.S. Ryland (Eds) Handbook of the Marine Fauna of North-West Europe, Oxford University Press: 484-628.
- Hewitt, R.A. (1986) Bioturbation in the Upper London Clay Formation of Southend-on-Sea (Essex, England) Tertiary Research, Vol. 8 (1), pp7-15.
- Hénaff, A., Lageat, A. and Costa, S. (2006) "Geomorphology and shaping processes of chalk shore platforms of the Channel coasts". Zeitschrift für Geomorphologie, Supplementband 144: 61-91.
- High, C.J. and Hanna, F.K. (1970). "A method for direct measurement of erosion on rock surfaces." British Geomorphological Research Group Technical Bulletin, 5: 1-25.
- Hight, D.W., McMillan, F., Powell, J.J.M., Jardine, R.J. & Allenou, C.P. (2002). Some characteristics of London Clay. In: Tan et al. (eds.) *Characterisation and Engineering Properties of Natural Soils* (2)851-908. Singapore: A.A. Balkema.
- Hill, J.M. (2006). "Pholas dactylus. Common piddock." Marine Life Information network: Biology and Sensitivity Key Information Sub-programme. Plymouth. Marine Biological Association of the United Kingdom. On-line: www.marlin.ac.uk/species.
- Hobbs, P.R.N., Waine, P.J., & Hallam, J.R. (1990) Holly Hill Landslide Investigation British Geological Survey Technical Report No. WN/90/9C (for British Gas Plc, South-Eastern).
- Hutchinson, J.N., 1986. Cliffs and shores in cohesive materials: geotechnical and engineering geological aspects. In: SKAFEL, M.G. (ed.), Proceedings of the Symposium on Cohesive Shores (Burlington, Ontario. Associate Committee for Research on Shoreline Erosion and Sedimentation, National Research Council, Canada), pp. 1-44.
- Irving, R. (1998). Sussex marine life. East Sussex County Council, Lewes.
- Jassesnee.de web page (2006). <http://www.jassesnee.de/blog/index.php?m=200505> Accessed: 17/09/2006.
- Kamphuis, J.W. And Hall, K.R., 1983. Cohesive material erosion by unidirectional current. Journal of the Hydraulic Engineering, ASCE, 109, 49-61.

- Kamphuis, J.W., 1983. On the erosion of consolidated clay material by a fluid containing sand. Canadian Journal of Civil Engineering, 10, 213-231.
- Kamphuis, J.W., 1987. Recession rate of glacial till bluffs. Journal of Waterway, Port, Coastal and Ocean Engineering, 113, 60-73.
- Kamphuis, J.W., 1990. Influence of sand or gravel on the erosion of cohesive sediment. Journal of Hydraulic Research, 28, 43-53.
- Kirby, R., 1990. "The sediment budget of the erosional intertidal zone of the Medway Estuary, Kent." Proceedings of the Geologist's Association **101** (1): 63 - 77.
- Knight-Jones, E.W., Knight-Jones, P. and Nelson-Smith, A. (1995) Annelids in P.J. Hayward and J.S. Ryland (Eds) Handbook of the Marine Fauna of North-West Europe, Oxford University Press: 165-277.
- Larsen, E. And Holtedahl, H., 1985. The Norwegian strandflat: a reconstruction of its age and origin. Norsk Geologisk Tidsskrift, 65, 247-254.
- Lee, K.L. And Focht, J.A. Jr., 1976. Strength of clay subjected to cycling loading. Marine Geotechnology, 1, 165-185.
- Lefebvre, G. And Rohan, K., 1986. On the principal factors controlling erosivity of undisturbed clay. In: SKAFEL, M.G. (ed.), Proceedings of the Symposium on Cohesive Shores (Burlington, Ontario. Associate Committee for Research on Shoreline Erosion and Sedimentation, National Research Council, Canada), pp. 170-195.
- Lick, W. And Mcneil, J., 2001. Effects of sediment bulk properties on erosion rates. Science of the Total Environment, 266, 41-48.
- MAFF, 1999. *Flood and Coastal Defence Project Appraisal Guidance*. MAFF Publications.
- Matthews, J.A.; Dawson, A.G. And Shakesby, R.A., 1986. Lake shoreline development, frost weathering and rock platform erosion in an alpine periglacial environment, Jotunheimen, southern Norway. Boreas, 15, 33-50.
- Mcgreal, W.S., 1979. Marine erosion of glacial sediments from a low-energy cliffline environment near Kilkeel, Northern Ireland. Marine Geology, 32, 89-103.
- Mitchener, H. And Torfs, H., 1996. Erosion of mud/sand mixtures. Coastal Engineering, 29, 1-25.
- Nairn, R.B.; Pinchin, B.M. And Philpott, K.L., 1986. Cohesive profile development model. In: Skafel, M.G. (ed.), Proceedings of the Symposium

- on Cohesive Shores (Burlington, Ontario. Associate Committee for Research on Shoreline Erosion and Sedimentation, National Research Council, Canada), pp. 246-261.
- Nairn, R.B., & Southgate, H.N., (1993) Deterministic profile modelling of nearshore processes. Part 2. Sediment transport and beach profile development. *Coastal Engineering*, 19, 57-96.
- Nicholls, R.J., Dredge, A. and Wilson, T. (2000) Shoreline change and fine-grained sediment input: Isle of Sheppey coast, Thames Estuary, UK. in Pye, K. and Allen, J.R.L. (eds) Coastal and Estuarine Environments: sedimentology, geomorphology and geoarchaeology. Special Publication of the Geological Society, **175**: 305-315.
- O' Brien, D., Whitehouse, R. and A, C. (2000). "The cyclic development of a macrotidal mudflat on varying timescales." Continental Shelf Research **20**: 1593-1619.
- Panagiotopoulos, I.; Voulgaris, G. And Collins, M.B., 1997. The influence of clay on the threshold of movement of fine sandy beds. Coastal Engineering, 32, 19-43.
- Petley, D.N. & Allison, R.J. (1997) The mechanics of deep-seated landslides. Earth Surface Processes & Landforms. 22, 8, pp747-758. *Wiley & Sons, UK*.
- Perez Alberti, A.; Costa Casais, M. And Blanco Chao, R., 2002. Stability of sedimentary cliffs in the coast of Galicia (NW Spain): long-term inheritance influence in rocky coastal systems. Proceedings of Littoral 2002, Vol 3 (Porto. EUROCOAST-Portugal), pp. 281-285.
- Pringle, A.W., 1985 Holderness coast erosion and the significance of ords. Earth Surface Processes and Landforms 10:107-124
- Raudkivi, A.J. And Hutchison, D.L., 1974. Erosion of kaolinite clay by flowing water. Proceedings of the Royal Society of London, A337, 537-554.
- Royal Haskoning, March 2005. Strategic monitoring of the East Riding of Yorkshire Coastline. Project Appraisal Report.
- Russell, D.J. & Eyles, N. (1984) geotechnical characteristics of weathering profiles in British over-consolidated clays (Carboniferous to Pleistocene) *In: Geomorphology and Soils* (eds. K.S. Richards, R.R. Arnett, & S. Ellis) *George Allen & Unwin*, London.
- Shennan, I, Lambeck, K., Horton, B., Innes, J., Lloyd, J., McArthur, J & Rutherford, M., (2000). Holocene isostasy and relative sea-level changes

- on the east coast of England. Geographical Society, London, Special Publications, 166, 275-298.
- Skafel, M.G. And Bishop, C.T., 1994. Flume experiments on the erosion of till shores by waves. Coastal Engineering, 23, 329-348.
- Skafel, M.G., 1995. Laboratory measurement of nearshore velocities and erosion of cohesive sediment (Till) shorelines. Technical note. Coastal Engineering 24, 343–349.
- Skempton, A. W. (1948) The rate of softening of stiff fissured clays with special reference to London Clay. *Proc. 2nd I.C.S.M.* Rotterdam, Vol 2, pp 50-53.
- Skempton, A. W., Schuster, R. L., & Petley, D. J. (1969). Joints and fissures in the London Clay at Wraysbury and Edgware. Geotech., 19.
- Skempton, A. W. & DeLory, F. A. (1957) Stability of natural slopes in London Clay. *Proc. 4th I.C.S.M.F.E.*, Vol 2, pp 378-381.
- Schrottke, K. (2001). Rückgangsdynamik schleswig-holsteinischer Steilküsten unter besonder Betrachtung submariner Abrasion und Restsedimentmobilität (Retreat dynamics of Schleswig-Holstein's cliff-coast with special regard to submarine abrasion and residual sediment mobility). Berichte – Reports, Institu für Geowissenschaften, Christian-Albrechts-Universität zu Kiel (ISSN 0175-9302).
- Schrottke, K. Schwarzer, K. Kohlhase, S., Frohle, P. Riemer, J. and Mohr K. (2003). “Dynamics of cliff-coast retreat at the southern Baltic Sea: influence of short-term wave and water level fluctuations.” (abstract). International Conference on Coastal Sediments 2003: 59-60.
- Schwarzer, K., Schrottke, K., Kohlhase, S., Frohle,, P. Riemer, J. and Mohr, K. (2003). “What are the forcing functions for cliff retreat?” (abstract). International Conference on Coastal Sediments 2003: 447-448.
- Seawater.no web site, 2006. <http://www.seawater.no/fauna/Leddyr/fjarerur.htm>
Accessed: 17/09/2006.
- Stephenson, W.J., 2000. Shore platforms: a neglected coastal feature? Progress in Physical Geography, 24, 311-327.
- Sunamura, T. And Kraus, N.C., 1985. Prediction of average mixing depth of sediment in the surf zone. Marine Geology, 62, 1-12.
- Sunamura, T.,1992. Geomorphology of Rocky Coasts. John Wiley & Sons.
- Swantesson, J.O.H., Moses, C.A., Berg, G.E. and Jansson K.M. (2006) “Methods for measuring shore platform micro erosion: A comparison of the

- micro-erosion meter and laser scanner. Zeitschrift fur Geomorphologie, Supplementband 144: 1-17.
- Tebble, N., 1966. British Bivalve Seashells. British Museum (Natural History), London
- Trenhaile, A.S. And Rudakas, P.A., 1981. Freeze-thaw and shore platform development in Gaspé, Quebec. Geographie Physique et Quaternaire, 35 , 171-181.
- Trudgill, S.T., High, C. and Hannah F.K. (1981) "Improvements to the micro-erosion meter." British Geomorphological Research Group Technical Bulletin 29: 3-17.
- US Army Corps Of Engineers, 2002. Coastal Engineering Manual – Part III, Chapter 5. Erosion, Transport, and Deposition of Cohesive Sediments. US Army Corps of Engineers Publication EM1110-2-1100.
- Walkden. M.J.A. and Hall. J.W. (2002) A model of soft cliff and platform erosion (SCAPE). Proc. 28th International Conference on Coastal Engineering, Cardiff, pp. 3333-3345.
- Walkden. M.J.A. and Hall. J.W. (2005) A predictive mesoscale model of the erosion and profile development of soft rock shores. Coastal Engineering 52, 535-563.
- Ward, W. H., Marsland, A., & Samuels, S. E. (1965). Properties of the London Clay at the Ashford Common shaft: in situ and undrained strength tests. Geotechnique, 15, 321-344.
- Ward, H., Samuels, S. G. & Butler, M. E. (1959) Further studies of the properties of London Clay. Géotechnique, Vol. 9, No 2, pp 33-58.
- Williams, R.B.G, Swantesson, J.O.H and Robinson, D.A. (2000). "Measuring rates of surface downwearing and mapping microtopoography: the use of micro-erosion meters and laser scanners in rock weather studies." Zeitschrift fur Geomorphologie, Supplementband 120: 51-66.
- Yonge, C.M and Thompson, T.E. (1976). Living marine molluscs. Collins, London.

APPENDICES

APPENDIX A
BIOLOGICAL COUNTING RESULTS FROM WARDEN POINT

BIOLOGICAL COUNTING RESULTS FROM WARDEN POINT: JULY 2005

Upper Shore Platform: Sampling Point A1

Quadrat number	Number of cells with <i>Corophium</i> "perforations"	Number of open piddock holes	Number of "craters" concealing buried piddocks	Number of <i>Ulva</i> individuals	Number of filamentous red algae individuals	Number of cells with significant (>10%) shell content
1	0	4	1	0	3	0
2	48	7	0	0	1	0
3	58	1	0	0	1	0
4	53	0	0	0	0	0

Upper Shore Platform: Sampling Point A2

Quadrat number	Number of cells with <i>Corophium</i> "perforations"	Number of open piddock holes	Number of "craters" concealing buried piddocks	Number of <i>Ulva</i> individuals	Number of filamentous red algae individuals	Number of cells with significant (>10%) shell content
5	27	2	0	0	0	1
6	50	0	0	1	8	0
7	75	2	0	0	15	0
8	29	0	0	0	12	0

Top-of-Middle Shore Platform: Sampling Point B1

Quadrat number	Number of cells with <i>Corophium</i> "perforations"	Number of open piddock holes	Number of "craters" concealing buried piddocks	Number of <i>Ulva</i> individuals	Number of filamentous red algae individuals	Number of cells with significant (>10%) shell content
1	0	3	0	0	3	16
2	0	0	0	3	7	7
3	0	0	0	0	0	2
4	0	0	0	2	4	4

Top-of-Middle Shore Platform: Sampling Point B2

Quadrat number	Number of cells with <i>Corophium</i> "perforations"	Number of open piddock holes	Number of "craters" concealing buried piddocks	Number of <i>Ulva</i> individuals	Number of filamentous red algae individuals	Number of cells with significant (>10%) shell content
5	0	0	0	1	0	7
6	0	3	0	2	18	4
7	0	0	0	0	4	4
8	0	1	0	0	0	4

Bottom-of-Middle Shore Platform: Sampling Point C1

Quadrat number	Number of cells with <i>Corophium</i> "perforations"	Number of open piddock holes	Number of "craters" concealing buried piddocks	Number of <i>Ulva</i> individuals	Number of filamentous red algae individuals (plus number of brown seaweeds)	Number of cells with significant (>10%) shell content
1	0	18	0	6	4	9
2	0	3	0	10	6	7
3	0	24	0	11	5 (+8)	7
4	0	11	5	5	5	4

Bottom-of-Middle Shore Platform: Sampling Point C2

Quadrat number	Number of cells with <i>Corophium</i> "perforations"	Number of open piddock holes	Number of "craters" concealing buried piddocks	Number of <i>Ulva</i> individuals	Number of filamentous red algae individuals (plus number of brown seaweeds)	Number of cells with significant (>10%) shell content
5	0	39	17	1	0	4
6	0	2	0	5	7(+3)	3
7	0	22	8	3	3	9
8	0	20	7	5	8(+1)	6

Lower Shore Platform: Sampling Point D1

Quadrat number	Number of cells with <i>Corophium</i> "perforations"	Number of open piddock holes	Number of "craters" concealing buried piddocks	Number of <i>Ulva</i> individuals	Number of filamentous red algae individuals (plus number of brown seaweeds)	Number of cells with significant (>10%) shell content
1	0	42	9	0	0	52
2	0	3	6	0	0 (+1)	20
3	0	41	11	0	0	30
4	0	13	6	1	0	25

Lower Shore Platform: Sampling Point D2

Quadrat number	Number of cells with <i>Corophium</i> "perforations"	Number of open piddock holes (plus number of bristleworms)	Number of "craters" concealing buried piddocks	Number of <i>Ulva</i> individuals	Number of filamentous red algae individuals (plus number of brown seaweeds)	Number of cells with significant (>10%) shell content
5	0	11 (+0)	2	6	0	18
6	0	74 (+1)	12	0	0	23
7	0	1 (+0)	16	1	0 (+5)	80
8	0	3 (+3)	10	4	0	31

Lower Shore Platform: Sampling Point E1

Quadrat number	Number of cells with <i>Corophium</i> "perforations"	Number of open piddock holes (plus number of bristleworms)	Number of "craters" concealing buried piddocks	Number of <i>Ulva</i> individuals	Number of filamentous red algae individuals	Number of cells with significant (>10%) shell content
1	0	77 (+2)	23	1	1	22
2	0	2 (+6)	0	0	1	22
3	0	3 (+37)	2	4	3	23
4	0	27 (+2)	12	2	1	18

Lower Shore Platform: Sampling Point E2

Quadrat number	Number of cells with <i>Corophium</i> "perforations"	Number of open piddock holes (plus number of bristleworms)	Number of "craters" concealing buried piddocks	Number of <i>Ulva</i> individuals	Number of filamentous red algae individuals (plus number of brown seaweeds)	Number of cells with significant (>10%) shell content
5	0	0 (+1)	10	4	0	26
6	0	1 (+4)	7	0	2	19
7	0	17 (+8)	23	4	1	44
8	0	11 (+12)	34	4	1 (+4)	28

APPENDIX B
BIOLOGICAL COUNTING RESULTS FROM WARDEN POINT
FEBRUARY 2006

BIOLOGICAL COUNTING RESULTS FROM WARDEN POINT: FEBRUARY 2006

Upper Shore Platform: Sampling Point A1

Quadrat number	Number of cells with <i>Corophium</i> "perforations"	Number of open piddock holes	Number of "craters" concealing buried piddocks	Number of <i>Ulva</i> individuals	Number of filamentous red algae individuals	Number of cells with significant (>10%) shell content
1	100	0	0	1	19	1
2	98	0	0	0	14	0
3	92	0	0	0	0	0
4	9	0	0	0	0	0

Upper Shore Platform: Sampling Point A2

Quadrat number	Number of cells with <i>Corophium</i> "perforations"	Number of open piddock holes	Number of "craters" concealing buried piddocks	Number of <i>Ulva</i> individuals	Number of filamentous red algae individuals	Number of cells with significant (>10%) shell content
7	92	0	0	0	0	0
8	25	0	0	0	0	0
9	83	0	0	0	1	0
10	87	0	0	0	5	0

Top-of-Middle Shore Platform: Sampling Point B1

Quadrat number	Number of cells with <i>Corophium</i> "perforations"	Number of open piddock holes	Number of "craters" concealing buried piddocks	Number of <i>Ulva</i> individuals	Number of filamentous red algae individuals	Number of cells with significant (>10%) shell content
1	0	0	0	4	abundant	16
2	0	2	0	3	abundant	11
3	0	0	0	1	abundant	4
4	1	1	0	2	abundant	11

Top-of-Middle Shore Platform: Sampling Point B2

Quadrat number	Number of cells with <i>Corophium</i> "perforations"	Number of open piddock holes	Number of "craters" concealing buried piddocks	Number of <i>Ulva</i> individuals	Number of filamentous red algae individuals	Number of cells with significant (>10%) shell content
5	64	0	3	0	abundant	4
6	28	0	0	0	abundant	2
7	67	4	3	0	abundant	2
8	75	2	9	0	abundant	2

Bottom-of-Middle Shore Platform: Sampling Point C1

Quadrat number	Number of cells with <i>Corophium</i> "perforations"	Number of open piddock holes	Number of "craters" concealing buried piddocks	Number of <i>Ulva</i> individuals	Number of filamentous red algae individuals (plus number of brown seaweeds)	Number of cells with significant (>10%) shell content
1	0	3	0	7	abundant	10
2	0	4	6	6	abundant	0
3	2	9	61	2	abundant (+8)	14
4	2	12	1	3	abundant	4

Bottom-of-Middle Shore Platform: Sampling Point C2

Quadrat number	Number of cells with <i>Corophium</i> "perforations"	Number of open piddock holes	Number of "craters" concealing buried piddocks	Number of <i>Ulva</i> individuals	Number of filamentous red algae individuals	Number of cells with significant (>10%) shell content
5	0	3	4	21	abundant	9
6	2	16	10	18	abundant	16
7	0	15	3	12	abundant	13
8	0	1	0	8	abundant	3

Lower Shore Platform: Sampling Point D

Quadrat number	Number of cells with <i>Corophium</i> "perforations"	Number of open piddock holes	Number of "craters" concealing buried piddocks	Number of <i>Ulva</i> individuals	Number of filamentous red algae individuals	Number of cells with significant (>10%) shell content
1	0	22	89	3	abundant	29
2	0	22	112	1	abundant	34
3	0	23	97	9	abundant	19
4	0	12	98	4	abundant	25

Lower Shore Platform: Sampling Point E

Quadrat number	Number of cells with <i>Corophium</i> "perforations"	Number of open piddock holes (plus number of bristleworms)	Number of "craters" concealing buried piddocks	Number of <i>Ulva</i> individuals	Number of filamentous red algae individuals (plus no. of barnacles on small stones)	Number of cells with significant (>10%) shell content
1	0	10	152	5	0 (+24)	41
2	0	8	163	1	0	31
3	19 ³	26	184	0	0 (+220)	24
4	22	30 (+2)	262	1	0 (+34)	42

³ Holes 2 mm in diameter, unpaired.

APPENDIX C
BEACH SURVEY DATA FROM WARDEN POINT
JULY 2005

BEACH SURVEY DATA FROM WARDEN POINT: JULY 2005

Point Id	Easting	Northing	Orth. Height	Co-ord. Quality	Description
base1	601864.21	172553.74	16.81	0.00	Base station
cp4	602078.82	172526.83	-1.34	0.01	Cone penetrometer test
cp5	602078.83	172526.83	-1.34	0.01	Cone penetrometer test
cp6	602078.82	172526.84	-1.35	0.01	Cone penetrometer test
cp3	602082.80	172528.53	-1.42	0.01	Cone penetrometer test
cp1	602086.57	172530.25	-1.42	0.01	Cone penetrometer test
cp2	602090.22	172532.58	-1.49	0.02	Cone penetrometer test
bp1	602268.79	172629.44	-2.23	0.01	Platform profile (shore normal)
bp2	602262.81	172624.50	-2.24	0.01	Platform profile (shore normal)
bp3	602256.74	172620.57	-2.10	0.01	Platform profile (shore normal)
bp4	602249.58	172616.11	-2.12	0.01	Platform profile (shore normal)
bp5	602242.57	172611.51	-2.05	0.01	Platform profile (shore normal)
bp6	602235.05	172607.33	-2.00	0.01	Platform profile (shore normal)
bp7	602227.68	172602.89	-2.08	0.01	Platform profile (shore normal)
bp8	602219.99	172598.44	-2.05	0.01	Platform profile (shore normal)
bp9	602212.39	172593.83	-2.05	0.01	Platform profile (shore normal)
bp10	602205.04	172589.61	-1.98	0.01	Platform profile (shore normal)
bp11	602197.55	172585.43	-1.99	0.01	Platform profile (shore normal)
bp12	602190.47	172581.15	-2.04	0.02	Platform profile (shore normal)
bp13	602183.20	172577.26	-2.02	0.02	Platform profile (shore normal)
bp14	602169.07	172568.79	-1.94	0.01	Platform profile (shore normal)
bp15	602162.77	172564.16	-1.97	0.02	Platform profile (shore normal)
bp16	602154.65	172559.59	-1.89	0.01	Platform profile (shore normal)
bp17	602147.01	172555.45	-1.90	0.01	Platform profile (shore normal)
bp18	602140.01	172551.82	-1.84	0.01	Platform profile (shore normal)
bp19	602131.67	172547.39	-1.77	0.01	Platform profile (shore normal)
bp20	602123.59	172543.08	-1.72	0.01	Platform profile (shore normal)
bp21	602115.00	172538.51	-1.79	0.02	Platform profile (shore normal)
bp22	602106.70	172534.42	-1.61	0.01	Platform profile (shore normal)
bp23	602098.57	172529.97	-1.50	0.01	Platform profile (shore normal)
bp24	602090.41	172525.77	-1.44	0.01	Platform profile (shore normal)
bp25	602081.95	172521.61	-1.30	0.01	Platform profile (shore normal)
bp26	602073.54	172517.71	-1.18	0.01	Platform profile (shore normal)
bp27	602065.78	172514.56	-1.11	0.01	Platform profile (shore normal)
bp28	602054.29	172509.74	-1.08	0.01	Platform profile (shore normal)
bp29	602045.69	172506.03	-1.06	0.01	Platform profile (shore normal)
bp30	602037.94	172501.52	-0.91	0.01	Platform profile (shore normal)
bp31	602030.49	172497.11	-0.77	0.01	Platform profile (shore normal)
bp32	602022.69	172493.06	-0.59	0.01	Platform profile (shore normal)
bp33	602015.02	172489.28	-0.35	0.01	Platform profile (shore normal)
bp34	602007.81	172485.00	-0.08	0.01	Platform profile (shore normal)
bp35	602001.42	172480.36	0.03	0.01	Platform profile (shore normal)
bp36	601995.22	172475.90	0.42	0.01	Platform profile (shore normal)
bp37	601988.97	172471.25	1.05	0.01	Platform profile (shore normal)
bp38	601983.22	172466.23	2.07	0.01	Platform profile (shore normal)
u1	602087.99	172528.15	-1.40	0.01	Triaxial sample site SHEP1
base2	601864.25	172553.79	16.82	0.00	Base station
ea1	600228.76	172523.23	41.25	0.00	EA benchmark P23006
ea2	602368.77	171805.10	7.62	0.00	EA benchmark P23007
cp7	602074.03	172524.51	-1.21	0.00	Cone penetrometer test
cp8	602070.36	172521.33	-1.18	0.00	Cone penetrometer test
cp9	602065.91	172518.44	-1.15	0.00	Cone penetrometer test
cp10	602058.66	172514.66	-1.04	0.01	Cone penetrometer test
cp11	602051.35	172511.08	-1.01	0.00	Cone penetrometer test
D(1)	602144.63	172565.73	-1.81	0.02	University Sussex yellow post
D(2)	602144.64	172565.72	-1.82	0.02	University Sussex yellow post
D(3)	602144.64	172565.73	-1.82	0.02	University Sussex yellow post
C1	602084.93	172532.21	-1.37	0.00	University Sussex erosion beam
B1	602042.88	172509.24	-0.92	0.01	University Sussex erosion beam
B2	602039.94	172514.37	-0.84	0.01	University Sussex erosion beam
cp12	602044.35	172507.18	-0.95	0.00	Cone penetrometer test
cp13	602037.49	172502.60	-0.85	0.00	Cone penetrometer test
A1	601995.88	172496.46	-0.03	0.00	University Sussex erosion beam
A2	601992.87	172506.30	-0.12	0.00	University Sussex erosion beam
C2	602079.92	172535.64	-1.30	0.01	University Sussex erosion beam
bc1	602001.85	172435.58	2.59	0.04	Base of cliff
bc2	602001.26	172437.20	2.51	0.03	Base of cliff
bc3	602000.05	172438.56	2.42	0.03	Base of cliff
bc4	601998.23	172439.38	2.60	0.04	Base of cliff
bc5	601996.48	172440.47	2.82	0.04	Base of cliff
bc6	601995.22	172441.79	2.83	0.04	Base of cliff

bc7	601994.36	172443.11	2.92	0.05	Base of cliff
bc8	601993.90	172445.10	2.60	0.03	Base of cliff
bc9	601991.53	172446.22	2.78	0.08	Base of cliff
bc10	601990.27	172447.66	2.90	0.06	Base of cliff
bc11	601990.51	172450.50	2.74	0.02	Base of cliff
bc12	601988.97	172452.97	2.90	0.02	Base of cliff
bc13	601987.07	172454.41	3.06	0.02	Base of cliff
bc14	601987.11	172456.15	2.86	0.02	Base of cliff
bc15	601985.84	172457.41	2.95	0.02	Base of cliff
bc16	601984.53	172459.16	3.15	0.02	Base of cliff
bc17	601984.04	172461.44	2.75	0.02	Base of cliff
bc18	601982.74	172463.23	2.71	0.02	Base of cliff
bc19	601979.21	172465.91	2.45	0.02	Base of cliff
bc20	601977.21	172468.20	2.37	0.02	Base of cliff
bc21	601974.73	172466.02	3.05	0.02	Base of cliff
bc22	601971.96	172467.76	2.92	0.02	Base of cliff
bc23	601969.78	172468.27	3.00	0.02	Base of cliff
bc24	601967.68	172468.79	3.04	0.03	Base of cliff
bc25	601965.62	172469.88	3.02	0.02	Base of cliff
bc26	601964.20	172471.44	2.92	0.03	Base of cliff
bc27	601961.97	172471.62	3.15	0.02	Base of cliff
bc28	601960.71	172473.51	3.09	0.03	Base of cliff
bc29	601959.36	172475.18	2.99	0.02	Base of cliff
bc30	601958.34	172476.56	2.94	0.02	Base of cliff
bc31	601956.62	172477.29	3.08	0.04	Base of cliff
bc32	601955.56	172478.89	3.09	0.06	Base of cliff
bc33	601954.42	172480.36	3.05	0.07	Base of cliff
bc34	601954.12	172482.06	2.86	0.03	Base of cliff
bc35	601952.89	172483.00	2.81	0.05	Base of cliff
bc36	601951.20	172484.58	2.84	0.05	Base of cliff
bc37	601949.78	172485.90	2.88	0.04	Base of cliff
bc38	601948.54	172487.31	2.94	0.03	Base of cliff
bc39	601947.67	172489.28	2.75	0.04	Base of cliff
bc40	601946.43	172491.32	2.72	0.03	Base of cliff
bc41	601945.53	172493.21	2.55	0.03	Base of cliff
bc42	601944.02	172495.50	2.53	0.04	Base of cliff
bc43	601943.04	172497.83	2.50	0.04	Base of cliff
bc44	601942.20	172500.24	2.48	0.03	Base of cliff
bc45	601940.75	172501.62	2.55	0.03	Base of cliff
bc46	601940.04	172503.12	2.57	0.07	Base of cliff
bc47	601939.98	172505.30	2.50	0.04	Base of cliff
bc48	601940.37	172506.90	2.31	0.05	Base of cliff
bc49	601940.89	172508.31	2.41	0.04	Base of cliff
bc50	601940.56	172509.71	2.56	0.03	Base of cliff
u2	602029.23	172509.37	-0.74	0.00	Triaxial sample site SHEP2
cp14	602030.71	172497.57	-0.76	0.01	Cone penetrometer test
e1	601962.59	172475.91	2.54	0.02	Beach sediment sample
e2	601967.63	172477.75	1.97	0.01	Beach sediment sample
e3	601971.24	172480.27	1.51	0.02	Beach sediment sample
w1	601955.10	172484.77	2.39	0.02	Beach sediment sample
w2	601958.66	172488.29	1.83	0.02	Beach sediment sample
w3	601963.56	172490.47	1.26	0.01	Beach sediment sample
t1	601958.06	172477.67	2.76	0.01	Profile in trench through beach
t2	601958.25	172477.80	2.74	0.02	Profile in trench through beach
t3	601958.41	172477.92	2.71	0.02	Profile in trench through beach
t4	601958.58	172478.09	2.68	0.02	Profile in trench through beach
t5	601958.71	172478.20	2.65	0.02	Profile in trench through beach
t6	601958.94	172478.40	2.59	0.01	Profile in trench through beach
t7	601959.16	172478.58	2.54	0.02	Profile in trench through beach
t8	601959.33	172478.69	2.50	0.01	Profile in trench through beach
t9	601959.46	172478.83	2.46	0.02	Profile in trench through beach
t10	601959.66	172478.99	2.45	0.02	Profile in trench through beach
t11	601959.88	172479.17	2.43	0.02	Profile in trench through beach
t12	601960.07	172479.34	2.39	0.02	Profile in trench through beach
t13	601960.29	172479.50	2.37	0.02	Profile in trench through beach
t14	601960.49	172479.68	2.32	0.01	Profile in trench through beach
t15	601960.69	172479.88	2.26	0.02	Profile in trench through beach
t16	601960.91	172480.05	2.24	0.01	Profile in trench through beach
t17	601961.13	172480.24	2.20	0.02	Profile in trench through beach
t18	601961.36	172480.43	2.18	0.02	Profile in trench through beach
t19	601961.69	172480.63	2.12	0.01	Profile in trench through beach
t20	601961.98	172480.80	2.07	0.02	Profile in trench through beach
t21	601962.29	172481.00	2.04	0.01	Profile in trench through beach
t22	601962.56	172481.15	2.00	0.01	Profile in trench through beach
t23	601962.86	172481.30	1.99	0.02	Profile in trench through beach
t24	601963.15	172481.50	1.97	0.02	Profile in trench through beach

t25	601963.37	172481.67	1.95	0.01	Profile in trench through beach
t26	601963.64	172481.86	1.90	0.01	Profile in trench through beach
t27	601963.92	172482.05	1.88	0.02	Profile in trench through beach
t28	601964.14	172482.24	1.85	0.01	Profile in trench through beach
ts1	601958.09	172478.00	2.84	0.02	Profile on beach near trench
ts2	601958.24	172478.09	2.80	0.01	Profile on beach near trench
ts3	601958.41	172478.28	2.76	0.01	Profile on beach near trench
ts4	601958.56	172478.33	2.73	0.02	Profile on beach near trench
ts5	601958.84	172478.51	2.68	0.02	Profile on beach near trench
ts6	601959.01	172478.70	2.63	0.02	Profile on beach near trench
ts7	601959.19	172478.80	2.59	0.02	Profile on beach near trench
ts8	601959.36	172479.04	2.57	0.01	Profile on beach near trench
ts9	601959.50	172479.18	2.53	0.01	Profile on beach near trench
ts10	601959.72	172479.49	2.49	0.02	Profile on beach near trench
ts11	601959.94	172479.47	2.46	0.01	Profile on beach near trench
ts12	601960.13	172479.72	2.44	0.02	Profile on beach near trench
ts13	601960.29	172479.88	2.39	0.02	Profile on beach near trench
ts14	601960.63	172480.13	2.36	0.02	Profile on beach near trench
ts15	601960.82	172480.29	2.31	0.02	Profile on beach near trench
ts16	601961.12	172480.45	2.27	0.02	Profile on beach near trench
ts17	601961.30	172480.70	2.23	0.02	Profile on beach near trench
ts18	601961.57	172480.92	2.21	0.02	Profile on beach near trench
ts19	601961.88	172481.10	2.16	0.02	Profile on beach near trench
ts20	601962.19	172481.28	2.08	0.02	Profile on beach near trench
ts21	601962.42	172481.40	2.08	0.02	Profile on beach near trench
ts22	601962.72	172481.58	2.03	0.02	Profile on beach near trench
ts23	601963.05	172481.73	1.99	0.01	Profile on beach near trench
ts24	601963.34	172481.93	1.97	0.01	Profile on beach near trench
ts25	601963.78	172482.29	1.91	0.01	Profile on beach near trench
ts26	601964.07	172482.43	1.89	0.02	Profile on beach near trench
ts27	601964.29	172482.57	1.88	0.02	Profile on beach near trench
base3	601864.25	172553.69	16.83	0.00	Base station
bb1	602009.68	172444.09	1.26	0.02	Base of beach
bb2	602007.87	172446.05	1.28	0.02	Base of beach
bb3	602006.39	172447.47	1.33	0.02	Base of beach
bb4	602004.68	172449.36	1.32	0.02	Base of beach
bb5	602002.94	172452.11	1.30	0.02	Base of beach
bb6	602001.46	172454.23	1.25	0.02	Base of beach
bb7	602000.47	172456.44	1.23	0.02	Base of beach
bb8	601999.63	172458.84	1.13	0.02	Base of beach
bb9	601998.57	172461.01	1.10	0.02	Base of beach
bb10	601996.92	172463.11	1.08	0.02	Base of beach
bb11	601996.54	172465.27	0.93	0.02	Base of beach
bb12	601995.51	172466.98	0.91	0.02	Base of beach
bb13	601994.84	172468.91	0.82	0.03	Base of beach
bb14	601992.99	172470.52	0.88	0.03	Base of beach
bb15	601990.81	172472.14	0.90	0.03	Base of beach
bb16	601988.16	172473.38	0.99	0.03	Base of beach
bb17	601985.18	172474.34	1.06	0.02	Base of beach
bb18	601983.22	172475.38	1.17	0.02	Base of beach
bb19	601981.13	172477.00	1.15	0.02	Base of beach
bb20	601979.06	172478.03	1.15	0.02	Base of beach
bb21	601977.50	172480.45	1.08	0.02	Base of beach
bb22	601975.39	172480.52	1.19	0.02	Base of beach
bb23	601973.48	172481.40	1.22	0.03	Base of beach
bb24	601971.48	172482.53	1.30	0.02	Base of beach
bb25	601969.47	172483.49	1.41	0.03	Base of beach
bb26	601967.71	172485.37	1.37	0.02	Base of beach
bb27	601966.83	172487.02	1.29	0.02	Base of beach
bb28	601966.49	172489.84	1.07	0.02	Base of beach
bb29	601965.55	172492.59	0.95	0.02	Base of beach
bb30	601964.28	172494.89	0.88	0.02	Base of beach
bb31	601962.61	172496.40	0.89	0.02	Base of beach
bb32	601962.26	172498.20	0.79	0.02	Base of beach
bb33	601961.09	172500.73	0.73	0.02	Base of beach
bb34	601959.30	172502.81	0.70	0.03	Base of beach
bb35	601957.80	172504.48	0.69	0.02	Base of beach
bb36	601957.23	172506.89	0.61	0.02	Base of beach
bb37	601957.13	172509.45	0.51	0.02	Base of beach
bb38	601957.11	172511.38	0.44	0.02	Base of beach
bb39	601957.02	172513.00	0.38	0.02	Base of beach
bb40	601956.73	172514.94	0.35	0.02	Base of beach
bta	601959.30	172502.01	0.76	0.02	Beach profile a (shore normal)
bta1	601958.70	172501.43	0.82	0.02	Beach profile a (shore normal)
bta2	601957.67	172500.35	0.98	0.02	Beach profile a (shore normal)
bta3	601956.50	172499.40	1.14	0.02	Beach profile a (shore normal)

bta4	601955.26	172498.32	1.34	0.02	Beach profile a (shore normal)
bta5	601954.07	172497.20	1.56	0.01	Beach profile a (shore normal)
bta6	601953.03	172496.22	1.71	0.02	Beach profile a (shore normal)
bta7	601951.76	172495.06	1.88	0.02	Beach profile a (shore normal)
bta8	601950.69	172494.04	2.03	0.02	Beach profile a (shore normal)
bta9	601949.50	172493.10	2.22	0.02	Beach profile a (shore normal)
bta10	601948.21	172492.00	2.42	0.02	Beach profile a (shore normal)
btb1	601961.15	172476.49	2.61	0.03	Beach profile b (shore normal)
btb2	601963.60	172478.34	2.22	0.02	Beach profile b (shore normal)
btb3	601965.46	172479.85	1.97	0.02	Beach profile b (shore normal)
btb4	601967.38	172481.07	1.77	0.03	Beach profile b (shore normal)
btb5	601969.21	172482.19	1.54	0.03	Beach profile b (shore normal)
btb6	601970.85	172483.20	1.31	0.02	Beach profile b (shore normal)
btb7	601972.19	172484.58	1.10	0.02	Beach profile b (shore normal)
btb8	601973.05	172485.31	0.98	0.02	Beach profile b (shore normal)
btb9	601974.45	172486.28	0.82	0.02	Beach profile b (shore normal)
btc1	602025.34	172439.54	0.53	0.01	Platform profile c (shore normal)
btc2	602028.60	172441.67	0.53	0.02	Platform profile c (shore normal)
btc3	602031.88	172443.99	0.16	0.01	Platform profile c (shore normal)
btc4	602034.76	172446.38	-0.02	0.01	Platform profile c (shore normal)
btc5	602038.06	172449.53	-0.26	0.01	Platform profile c (shore normal)
btc6	602040.52	172452.21	-0.36	0.01	Platform profile c (shore normal)
btc7	602042.87	172454.60	-0.43	0.01	Platform profile c (shore normal)
btc8	602045.75	172457.18	-0.70	0.01	Platform profile c (shore normal)
btc9	602049.86	172460.59	-0.69	0.01	Platform profile c (shore normal)
btc10	602053.64	172464.74	-0.76	0.01	Platform profile c (shore normal)
btc11	602057.71	172468.32	-0.75	0.01	Platform profile c (shore normal)
btc12	602062.27	172471.93	-0.84	0.01	Platform profile c (shore normal)
btc13	602067.72	172476.01	-0.99	0.01	Platform profile c (shore normal)
btc14	602073.87	172481.20	-1.17	0.01	Platform profile c (shore normal)
btc15	602078.83	172485.94	-1.30	0.02	Platform profile c (shore normal)
btc16	602083.56	172490.34	-1.27	0.01	Platform profile c (shore normal)
btc17	602089.17	172495.40	-1.30	0.01	Platform profile c (shore normal)
btc18	602094.50	172500.34	-1.42	0.01	Platform profile c (shore normal)
btc19	602099.45	172505.23	-1.36	0.01	Platform profile c (shore normal)
btc20	602104.18	172509.63	-1.53	0.01	Platform profile c (shore normal)
btc21	602108.95	172514.85	-1.61	0.01	Platform profile c (shore normal)
btc22	602112.34	172519.72	-1.74	0.01	Platform profile c (shore normal)
btc23	602117.99	172524.30	-1.66	0.01	Platform profile c (shore normal)
btc24	602123.40	172528.77	-1.64	0.01	Platform profile c (shore normal)
btc25	602129.10	172533.07	-1.71	0.01	Platform profile c (shore normal)
btc26	602135.39	172537.49	-1.81	0.01	Platform profile c (shore normal)
btc27	602141.00	172541.36	-1.76	0.01	Platform profile c (shore normal)
btc28	602147.22	172545.35	-1.87	0.01	Platform profile c (shore normal)
btc29	602154.35	172549.65	-1.78	0.02	Platform profile c (shore normal)
btc30	602160.62	172553.60	-1.79	0.02	Platform profile c (shore normal)
btc31	602165.90	172557.46	-1.82	0.01	Platform profile c (shore normal)
btc32	602172.46	172561.75	-2.00	0.01	Platform profile c (shore normal)
btc33	602176.90	172565.26	-1.93	0.02	Platform profile c (shore normal)
btc34	602182.80	172568.93	-1.94	0.01	Platform profile c (shore normal)
btc35	602188.85	172571.80	-2.03	0.01	Platform profile c (shore normal)
btc36	602195.16	172575.26	-1.89	0.01	Platform profile c (shore normal)
btc37	602200.93	172578.60	-1.94	0.02	Platform profile c (shore normal)
btc38	602206.89	172582.13	-1.93	0.01	Platform profile c (shore normal)
btc39	602213.71	172585.98	-1.95	0.01	Platform profile c (shore normal)
btc40	602219.40	172590.37	-1.93	0.01	Platform profile c (shore normal)
btc41	602224.49	172595.48	-1.97	0.01	Platform profile c (shore normal)
btc42	602230.26	172601.18	-2.02	0.01	Platform profile c (shore normal)
btc43	602235.22	172605.91	-1.99	0.01	Platform profile c (shore normal)
btc44	602240.32	172610.58	-2.00	0.01	Platform profile c (shore normal)
btc45	602245.76	172615.73	-2.02	0.02	Platform profile c (shore normal)
btc46	602249.09	172619.96	-2.05	0.01	Platform profile c (shore normal)
E	602197.46	172600.68	-2.00	0.00	University Sussex encrusted post
btd1	602182.33	172630.01	-2.07	0.01	Platform profile d (shore normal)
btd2	602175.80	172625.27	-2.00	0.01	Platform profile d (shore normal)
btd3	602169.21	172620.72	-1.99	0.01	Platform profile d (shore normal)
btd4	602162.75	172616.86	-1.98	0.01	Platform profile d (shore normal)
btd5	602155.79	172612.62	-2.00	0.01	Platform profile d (shore normal)
btd6	602149.17	172607.32	-1.97	0.01	Platform profile d (shore normal)
btd7	602142.15	172602.09	-2.01	0.02	Platform profile d (shore normal)
btd8	602135.40	172597.44	-1.98	0.01	Platform profile d (shore normal)
btd9	602129.00	172592.63	-1.86	0.01	Platform profile d (shore normal)
btd10	602122.21	172587.63	-1.94	0.01	Platform profile d (shore normal)
btd11	602114.92	172582.77	-1.90	0.01	Platform profile d (shore normal)
btd12	602107.82	172577.82	-1.81	0.01	Platform profile d (shore normal)
btd13	602101.28	172572.78	-1.74	0.01	Platform profile d (shore normal)

btd14	602094.73	172568.16	-1.77	0.02	Platform profile d (shore normal)
btd15	602087.77	172563.19	-1.79	0.01	Platform profile d (shore normal)
btd16	602080.44	172558.03	-1.68	0.01	Platform profile d (shore normal)
btd17	602073.64	172552.65	-1.60	0.01	Platform profile d (shore normal)
btd18	602065.93	172549.07	-1.60	0.01	Platform profile d (shore normal)
btd19	602057.96	172544.61	-1.31	0.01	Platform profile d (shore normal)
btd20	602050.39	172540.55	-1.22	0.02	Platform profile d (shore normal)
btd21	602042.54	172536.16	-1.13	0.01	Platform profile d (shore normal)
btd22	602035.72	172532.06	-1.06	0.01	Platform profile d (shore normal)
btd23	602028.63	172527.95	-0.92	0.01	Platform profile d (shore normal)
btd24	602021.45	172523.37	-0.78	0.01	Platform profile d (shore normal)
btd25	602014.67	172519.21	-0.63	0.01	Platform profile d (shore normal)
btd26	602007.44	172514.69	-0.51	0.01	Platform profile d (shore normal)
btd27	602000.48	172510.54	-0.33	0.01	Platform profile d (shore normal)
btd28	601993.36	172505.68	-0.11	0.01	Platform profile d (shore normal)
btd29	601985.35	172500.86	0.09	0.01	Platform profile d (shore normal)
btd30	601978.60	172496.23	0.35	0.01	Platform profile d (shore normal)
btd31	601972.70	172491.41	0.61	0.01	Platform profile d (shore normal)
btd32	601966.29	172487.02	1.35	0.01	Platform profile d (shore normal)
btd33	601960.01	172482.42	2.20	0.02	Platform profile d (shore normal)
btd34	601955.98	172478.51	2.95	0.02	Platform profile d (shore normal)
bte1	601962.12	172473.48	2.81	0.02	Platform profile e (shore normal)
bte2	601968.84	172477.33	1.93	0.02	Platform profile e (shore normal)
bte3	601976.55	172481.64	1.03	0.02	Platform profile e (shore normal)
bte4	601984.94	172485.97	0.44	0.01	Platform profile e (shore normal)
bte5	601993.03	172490.37	0.15	0.01	Platform profile e (shore normal)
bte6	602001.03	172494.85	-0.07	0.01	Platform profile e (shore normal)
bte7	602008.94	172498.91	-0.30	0.02	Platform profile e (shore normal)
bte8	602016.65	172502.87	-0.44	0.01	Platform profile e (shore normal)
bte9	602024.38	172506.91	-0.61	0.02	Platform profile e (shore normal)
bte10	602032.28	172511.04	-0.82	0.01	Platform profile e (shore normal)
bte11	602043.05	172516.81	-0.92	0.02	Platform profile e (shore normal)
bte12	602051.15	172519.70	-1.02	0.01	Platform profile e (shore normal)
bte13	602060.20	172522.69	-1.11	0.01	Platform profile e (shore normal)
bte14	602068.11	172525.55	-1.17	0.01	Platform profile e (shore normal)
bte15	602076.76	172530.07	-1.30	0.01	Platform profile e (shore normal)
bte16	602084.81	172535.46	-1.44	0.02	Platform profile e (shore normal)
bte17	602093.49	172540.35	-1.63	0.02	Platform profile e (shore normal)
bte18	602102.45	172545.04	-1.64	0.01	Platform profile e (shore normal)
bte19	602110.20	172549.46	-1.68	0.01	Platform profile e (shore normal)
bte20	602118.32	172553.93	-1.77	0.01	Platform profile e (shore normal)
bte21	602126.17	172558.10	-1.73	0.01	Platform profile e (shore normal)
bte22	602134.37	172561.26	-1.75	0.01	Platform profile e (shore normal)
bte23	602142.05	172564.58	-1.79	0.02	Platform profile e (shore normal)
bte24	602151.47	172568.76	-1.79	0.01	Platform profile e (shore normal)
bte25	602159.72	172572.57	-1.87	0.01	Platform profile e (shore normal)
bte26	602167.75	172577.24	-1.94	0.01	Platform profile e (shore normal)
bte27	602174.56	172581.06	-1.95	0.02	Platform profile e (shore normal)
bte28	602183.12	172584.53	-2.01	0.02	Platform profile e (shore normal)
bte29	602191.15	172587.79	-2.06	0.02	Platform profile e (shore normal)
bte30	602199.66	172591.13	-1.97	0.01	Platform profile e (shore normal)
bte31	602207.30	172595.30	-1.99	0.01	Platform profile e (shore normal)
bte32	602216.28	172600.63	-1.98	0.01	Platform profile e (shore normal)
bte33	602223.36	172604.54	-1.95	0.01	Platform profile e (shore normal)
bte34	602231.86	172607.97	-1.97	0.01	Platform profile e (shore normal)
bte35	602239.28	172610.87	-1.99	0.01	Platform profile e (shore normal)
bte36	602247.68	172614.27	-2.07	0.01	Platform profile e (shore normal)
bte37	602254.81	172618.49	-2.06	0.01	Platform profile e (shore normal)
bte38	602260.53	172623.71	-2.16	0.02	Platform profile e (shore normal)
bte39	602267.50	172629.37	-2.20	0.01	Platform profile e (shore normal)
bcta1	602066.38	172507.45	-1.19	0.01	Platform profile a (shore parallel)
bcta2	602064.26	172511.08	-1.07	0.01	Platform profile a (shore parallel)
bcta3	602061.31	172514.96	-1.05	0.01	Platform profile a (shore parallel)
bcta4	602058.71	172518.03	-1.06	0.01	Platform profile a (shore parallel)
bcta5	602055.70	172520.87	-1.08	0.01	Platform profile a (shore parallel)
bcta6	602052.51	172524.04	-1.06	0.01	Platform profile a (shore parallel)
bcta7	602048.87	172527.27	-1.09	0.01	Platform profile a (shore parallel)
bcta8	602045.50	172530.53	-1.10	0.01	Platform profile a (shore parallel)
bcta9	602041.67	172533.94	-1.10	0.02	Platform profile a (shore parallel)
bcta10	602038.09	172537.12	-1.14	0.01	Platform profile a (shore parallel)
bcta11	602035.22	172540.17	-1.20	0.01	Platform profile a (shore parallel)
bcta12	602033.15	172542.27	-1.32	0.01	Platform profile a (shore parallel)
bctb1	602013.92	172529.65	-1.03	0.01	Platform profile b (shore parallel)
bctb2	602016.06	172525.72	-0.82	0.01	Platform profile b (shore parallel)
bctb3	602018.21	172521.73	-0.73	0.01	Platform profile b (shore parallel)
bctb4	602020.33	172517.93	-0.67	0.01	Platform profile b (shore parallel)

bctb5	602022.67	172513.43	-0.67	0.01	Platform profile b (shore parallel)
bctb6	602024.93	172509.17	-0.65	0.01	Platform profile b (shore parallel)
bctb7	602027.55	172504.63	-0.67	0.01	Platform profile b (shore parallel)
bctb8	602030.35	172500.38	-0.71	0.01	Platform profile b (shore parallel)
bctb9	602032.80	172496.72	-0.80	0.01	Platform profile b (shore parallel)
bctb10	602034.55	172494.41	-0.94	0.01	Platform profile b (shore parallel)

**APPENDIX D
BEACH SURVEY DATA FROM WARDEN POINT
FEBRUARY 2006**

BEACH SURVEY DATA FROM WARDEN POINT: FEBRUARY 2006

Point Id	Easting	Northing	Orth. Height	Coordinate Quality	Description
EA2	602368.77	171805.05	7.6	0.00	Base station
bcta12	602033.17	172542.04	-1.38	0.02	Platform profile a (shore parallel)
bcta11	602035.91	172539.15	-1.28	0.02	Platform profile a (shore parallel)
bcta10	602038.24	172536.67	-1.2	0.02	Platform profile a (shore parallel)
bcta9	602040.49	172534.19	-1.22	0.02	Platform profile a (shore parallel)
bcta8	602042.78	172531.62	-1.13	0.02	Platform profile a (shore parallel)
bcta7	602045.31	172529.07	-1.13	0.02	Platform profile a (shore parallel)
bcta6	602048.26	172525.91	-1.17	0.02	Platform profile a (shore parallel)
bcta5	602050.83	172523.06	-1.12	0.02	Platform profile a (shore parallel)
bcta4	602053.45	172520.39	-1.11	0.02	Platform profile a (shore parallel)
bcta3	602056	172517.77	-1.06	0.02	Platform profile a (shore parallel)
bcta2	602059.12	172514.65	-1.12	0.02	Platform profile a (shore parallel)
bcta1	602061.83	172511.87	-1.12	0.02	Platform profile a (shore parallel)
bcta0	602063.8	172510.47	-1.13	0.02	Platform profile a (shore parallel)
bcta	602066.33	172507.48	-1.26	0.02	Platform profile a (shore parallel)
bctb1	602013.76	172529.76	-1.15	0.02	Platform profile b (shore parallel)
bctb2	602015.52	172526.52	-0.92	0.02	Platform profile b (shore parallel)
bctb3	602017.2	172523.38	-0.83	0.01	Platform profile b (shore parallel)
bctb4	602018.89	172520.33	-0.76	0.01	Platform profile b (shore parallel)
bctb5	602020.81	172516.89	-0.75	0.01	Platform profile b (shore parallel)
bctb6	602022.46	172513.91	-0.73	0.02	Platform profile b (shore parallel)
bctb7	602024.31	172510.72	-0.74	0.02	Platform profile b (shore parallel)
bctb8	602025.96	172507.97	-0.74	0.02	Platform profile b (shore parallel)
bctb9	602027.6	172505.17	-0.74	0.01	Platform profile b (shore parallel)
bctb10	602029.37	172502.19	-0.75	0.01	Platform profile b (shore parallel)
bctb11	602031.18	172499.17	-0.81	0.02	Platform profile b (shore parallel)
bctb12	602032.86	172496.48	-0.84	0.02	Platform profile b (shore parallel)
bctb13	602034.42	172494.46	-1.03	0.02	Platform profile b (shore parallel)
bc1	602001.12	172435.15	2.42	0.03	Base of cliff
bc2	601997.02	172438.88	2.42	0.04	Base of cliff
bc3	601993.89	172442.89	2.39	0.04	Base of cliff
bc4	601987.15	172449.93	2.37	0.03	Base of cliff
bc5	601983.66	172454.25	2.31	0.02	Base of cliff
bc6	601979.34	172458.57	2.34	0.02	Base of cliff
bc7	601974.67	172463.16	2.3	0.02	Base of cliff
bc8	601969.98	172465.87	2.51	0.02	Base of cliff
bc9	601965.27	172469.15	2.61	0.02	Base of cliff
bc10	601961.15	172472.88	2.67	0.08	Base of cliff
bc11	601957.11	172477.47	2.64	0.02	Base of cliff
bc12	601953.44	172481.3	2.72	0.02	Base of cliff
bc13	601949.66	172485.54	2.66	0.04	Base of cliff
bc14	601945.56	172489.7	2.82	0.05	Base of cliff
bc15	601942.57	172494.74	2.63	0.03	Base of cliff
bc16	601940.26	172499.35	2.54	0.04	Base of cliff
bc17	601938.75	172504.24	2.55	0.03	Base of cliff

bc18	601939.68	172509.01	2.45	0.04	Base of cliff
bc19	601938.62	172512.76	2.45	0.01	Base of cliff
bb1	601948.81	172508.57	1.05	0.03	Base of beach
bb2	601952.3	172505.16	0.92	0.02	Base of beach
bb3	601956.17	172501.08	0.88	0.02	Base of beach
bb4	601958.34	172496.5	1.01	0.01	Base of beach
bb5	601960.95	172492.54	1.14	0.01	Base of beach
bb6	601965.24	172488.49	1.08	0.02	Base of beach
bb7	601968.25	172484.51	1.13	0.01	Base of beach
bb8	601971.16	172480.73	1.22	0.01	Base of beach
bb9	601975.37	172476.79	1.22	0.01	Base of beach
bb10	601978.8	172473.45	1.22	0.01	Base of beach
bb11	601980.87	172467.19	1.51	0.02	Base of beach
bb12	601984.02	172462.28	1.62	0.02	Base of beach
bb13	601987.73	172458.78	1.57	0.01	Base of beach
bb14	601991.88	172455.4	1.49	0.01	Base of beach
bb15	601995.63	172451.35	1.55	0.01	Base of beach
bb16	601999.17	172447.09	1.56	0.02	Base of beach
bb17	602002.8	172442.99	1.58	0.01	Base of beach
bb18	602005.1	172438.32	1.71	0.01	Base of beach
bb19	602009.05	172435.17	1.53	0.02	Base of beach
bb20	602013.54	172431.18	1.39	0.01	Base of beach
2w	601958.62	172488.23	1.59	0.04	Beach sediment sample position
3w	601963.47	172490.38	1.07	0.02	Beach sediment sample position
1e	601962.63	172475.92	2.31	0.04	Beach sediment sample position
2e	601967.65	172477.66	1.72	0.02	Beach sediment sample position
3e	601971.25	172480.2	1.28	0.02	Beach sediment sample position
1w	601955.11	172484.61	2.22	0.03	Beach sediment sample position
bta	601959.17	172502	0.67	0.02	Beach profile a (shore normal)
bta1	601957.63	172500.78	0.82	0.02	Beach profile a (shore normal)
bta2	601955.85	172499.18	1.03	0.02	Beach profile a (shore normal)
bta3	601954.1	172497.66	1.25	0.02	Beach profile a (shore normal)
bta4	601952.82	172496.36	1.42	0.02	Beach profile a (shore normal)
bta5	601951.95	172495.61	1.56	0.02	Beach profile a (shore normal)
bta6	601951.14	172494.84	1.69	0.02	Beach profile a (shore normal)
bta7	601950.33	172494.06	1.92	0.02	Beach profile a (shore normal)
bta8	601949.59	172493.28	2.02	0.03	Beach profile a (shore normal)
bta9	601948.72	172492.58	2.16	0.02	Beach profile a (shore normal)
bta10	601948.16	172492.05	2.25	0.03	Beach profile a (shore normal)
bta11	601946.67	172491.15	2.46	0.03	Beach profile a (shore normal)
bta12	601945.36	172490.29	2.77	0.03	Beach profile a (shore normal)
btb9	601974.41	172486.27	0.72	0.04	Beach profile b (shore normal)
btb8	601973.18	172485.41	0.83	0.03	Beach profile b (shore normal)
btb7	601971.45	172484.19	0.96	0.04	Beach profile b (shore normal)
btb6	601969.61	172482.85	1.15	0.04	Beach profile b (shore normal)
btb5	601968	172481.61	1.36	0.04	Beach profile b (shore normal)
btb4	601966.3	172480.4	1.59	0.04	Beach profile b (shore normal)
btb3	601964.72	172479.23	1.75	0.05	Beach profile b (shore normal)
btb2	601963.28	172478.25	2.03	0.04	Beach profile b (shore normal)

btb1	601961.13	172476.47	2.33	0.04	Beach profile b (shore normal)
btb	601959.49	172475.17	2.74	0.03	Beach profile b (shore normal)
bp1	602268.73	172629.43	-2.28	0.02	Platform profile (shore normal)
bp2	602260.5	172624.74	-2.25	0.02	Platform profile (shore normal)
bp3	602252.07	172619.88	-2.15	0.01	Platform profile (shore normal)
bp4	602243.23	172614.69	-2.12	0.02	Platform profile (shore normal)
bp5	602234.51	172609.45	-2.13	0.02	Platform profile (shore normal)
bp6	602225.83	172604.41	-2.09	0.02	Platform profile (shore normal)
bp7	602216.68	172599.41	-2.09	0.02	Platform profile (shore normal)
bp8	602207.36	172594.06	-2.04	0.01	Platform profile (shore normal)
bp9	602198.23	172589.06	-2.05	0.02	Platform profile (shore normal)
bp10	602189.22	172584.05	-2.08	0.02	Platform profile (shore normal)
bp11	602180.48	172579.34	-2.07	0.02	Platform profile (shore normal)
bp12	602172.52	172574.65	-2.04	0.02	Platform profile (shore normal)
bp13	602165.13	172570.44	-2.02	0.02	Platform profile (shore normal)
bp14	602157.42	172565.97	-1.98	0.02	Platform profile (shore normal)
bp15	602148.41	172561.11	-1.87	0.02	Platform profile (shore normal)
bp16	602139.8	172556.18	-1.84	0.02	Platform profile (shore normal)
bp17	602131.34	172551.24	-1.87	0.02	Platform profile (shore normal)
bp18	602122.1	172546.16	-1.81	0.02	Platform profile (shore normal)
bp19	602113.31	172541.18	-1.76	0.02	Platform profile (shore normal)
bp20	602104.41	172535.97	-1.66	0.02	Platform profile (shore normal)
bp21	602095.56	172531.05	-1.55	0.02	Platform profile (shore normal)
bp22	602086.17	172525.89	-1.42	0.02	Platform profile (shore normal)
bp23	602077.87	172521.28	-1.31	0.02	Platform profile (shore normal)
bp24	602068.56	172515.86	-1.17	0.02	Platform profile (shore normal)
bp25	602059.1	172510.78	-1.13	0.02	Platform profile (shore normal)
bp26	602049.88	172505.93	-1.32	0.02	Platform profile (shore normal)
bp27	602040.3	172500.46	-1.1	0.02	Platform profile (shore normal)
bp28	602030.81	172495.14	-0.82	0.02	Platform profile (shore normal)
bp29	602021.78	172489.84	-0.57	0.02	Platform profile (shore normal)
bp30	602013.58	172485.11	-0.32	0.02	Platform profile (shore normal)
bp31	602005.17	172480.16	-0.23	0.02	Platform profile (shore normal)
bp32	602001.55	172477.92	0.06	0.02	Platform profile (shore normal)
bp33	601999.51	172476.64	0.3	0.02	Platform profile (shore normal)
bp34	601997.49	172475.22	0.35	0.02	Platform profile (shore normal)
bp35	601995.66	172474.25	0.51	0.02	Platform profile (shore normal)
bp36	601993.41	172472.86	0.47	0.02	Platform profile (shore normal)
bp37	601991.26	172471.39	0.49	0.02	Platform profile (shore normal)
bp38	601989.15	172470.16	0.82	0.02	Platform profile (shore normal)
bp39	601987.44	172468.89	0.98	0.02	Platform profile (shore normal)
bp40	601985.57	172467.81	1.14	0.02	Platform profile (shore normal)
bp41	601983.13	172466.46	1.34	0.02	Platform profile (shore normal)
bp42	601981.08	172465.38	1.61	0.02	Platform profile (shore normal)
bp43	601978.95	172463.99	1.9	0.01	Platform profile (shore normal)
bp44	601977.02	172462.15	2.25	0.02	Platform profile (shore normal)
bp45	601975.63	172460.95	2.64	0.03	Platform profile (shore normal)
btc1	602249.03	172619.99	-2.11	0.01	Platform profile c (shore normal)
btc2	602240.76	172613.48	-2.15	0.02	Platform profile c (shore normal)

btc3	602232.72	172606.93	-2.07	0.02	Platform profile c (shore normal)
btc4	602224.16	172600.13	-2.06	0.01	Platform profile c (shore normal)
btc5	602215.45	172593.35	-2.04	0.01	Platform profile c (shore normal)
btc6	602206.97	172586.56	-1.99	0.01	Platform profile c (shore normal)
btc7	602198.17	172579.96	-2.04	0.02	Platform profile c (shore normal)
btc8	602189.9	172573.52	-2.04	0.02	Platform profile c (shore normal)
btc9	602182.09	172567.12	-2.08	0.01	Platform profile c (shore normal)
btc10	602174.66	172561.31	-2.09	0.01	Platform profile c (shore normal)
btc11	602166.2	172554.85	-1.89	0.02	Platform profile c (shore normal)
btc12	602157.7	172548.09	-1.99	0.02	Platform profile c (shore normal)
btc13	602149.57	172541.73	-1.93	0.02	Platform profile c (shore normal)
btc14	602141.06	172535.18	-1.87	0.02	Platform profile c (shore normal)
btc15	602132.48	172528.37	-1.83	0.02	Platform profile c (shore normal)
btc16	602124.73	172522.12	-1.79	0.02	Platform profile c (shore normal)
btc17	602116.54	172515.81	-1.77	0.02	Platform profile c (shore normal)
btc18	602108.46	172509.26	-1.61	0.02	Platform profile c (shore normal)
btc19	602100.76	172503.04	-1.42	0.01	Platform profile c (shore normal)
btc20	602092.43	172496.41	-1.44	0.02	Platform profile c (shore normal)
btc21	602085.12	172490.41	-1.44	0.02	Platform profile c (shore normal)
btc22	602077.03	172483.69	-1.33	0.02	Platform profile c (shore normal)
btc23	602069.34	172477.53	-1.18	0.01	Platform profile c (shore normal)
btc24	602061.21	172470.78	-0.85	0.01	Platform profile c (shore normal)
btc25	602053.05	172463.89	-0.81	0.02	Platform profile c (shore normal)
btc26	602045.77	172457.76	-0.79	0.01	Platform profile c (shore normal)
btc27	602043.7	172456.28	-0.63	0.01	Platform profile c (shore normal)
btc28	602041.77	172454.67	-0.4	0.01	Platform profile c (shore normal)
btc29	602039.94	172453.08	-0.45	0.01	Platform profile c (shore normal)
btc30	602037.83	172451.37	-0.48	0.01	Platform profile c (shore normal)
btc31	602035.7	172449.54	-0.24	0.01	Platform profile c (shore normal)
btc32	602033.93	172447.73	-0.11	0.01	Platform profile c (shore normal)
btc33	602032.21	172446.19	0.03	0.01	Platform profile c (shore normal)
btc34	602030.38	172444.65	0.16	0.01	Platform profile c (shore normal)
btc35	602028.4	172442.61	0.4	0.01	Platform profile c (shore normal)
btc36	602026.84	172441.19	0.47	0.02	Platform profile c (shore normal)
btc37	602025.2	172439.64	0.49	0.02	Platform profile c (shore normal)
btc38	602023.33	172438.28	0.5	0.02	Platform profile c (shore normal)
btc39	602021.36	172436.6	0.78	0.02	Platform profile c (shore normal)
btc40	602019.48	172435.06	0.93	0.02	Platform profile c (shore normal)
btc41	602017.6	172433.55	1.07	0.01	Platform profile c (shore normal)
btc42	602015.67	172432.01	1.19	0.02	Platform profile c (shore normal)
btc43	602013.72	172430.58	1.4	0.02	Platform profile c (shore normal)
btc44	602011.91	172429.3	1.67	0.02	Platform profile c (shore normal)
btc45	602010.09	172427.81	1.9	0.02	Platform profile c (shore normal)
btc46	602008.67	172426.77	2.19	0.02	Platform profile c (shore normal)
btc47	602007.19	172425.76	2.53	0.02	Platform profile c (shore normal)
btd1	602182.22	172630.02	-2.16	0.02	Platform profile d (shore normal)
btd2	602173.46	172624.42	-2.04	0.02	Platform profile d (shore normal)
btd3	602164.71	172618.64	-2.06	0.02	Platform profile d (shore normal)
btd4	602156.45	172613.3	-2.1	0.02	Platform profile d (shore normal)

btd5	602148.05	172607.7	-2.08	0.02	Platform profile d (shore normal)
btd6	602139.75	172602.14	-2.03	0.02	Platform profile d (shore normal)
btd7	602131.72	172596.99	-1.94	0.02	Platform profile d (shore normal)
btd8	602123.55	172591.4	-1.96	0.02	Platform profile d (shore normal)
btd9	602114.76	172585.65	-2.02	0.02	Platform profile d (shore normal)
btd10	602106.13	172580.12	-1.9	0.02	Platform profile d (shore normal)
btd11	602096.91	172573.94	-1.82	0.02	Platform profile d (shore normal)
btd12	602088.91	172568.49	-1.89	0.02	Platform profile d (shore normal)
btd13	602080.75	172563	-1.72	0.01	Platform profile d (shore normal)
btd14	602072.68	172557.74	-1.7	0.01	Platform profile d (shore normal)
btd15	602064.64	172552.04	-1.66	0.02	Platform profile d (shore normal)
btd16	602056.42	172546.43	-1.43	0.01	Platform profile d (shore normal)
btd17	602048.24	172540.97	-1.28	0.02	Platform profile d (shore normal)
btd18	602040.46	172535.58	-1.2	0.01	Platform profile d (shore normal)
btd19	602032.76	172530.46	-1.09	0.01	Platform profile d (shore normal)
btd20	602025	172525.28	-0.97	0.01	Platform profile d (shore normal)
btd21	602017.39	172520.11	-0.78	0.01	Platform profile d (shore normal)
btd22	602009.9	172514.93	-0.6	0.01	Platform profile d (shore normal)
btd23	602002.01	172509.73	-0.39	0.01	Platform profile d (shore normal)
btd24	601994.06	172504.57	-0.2	0.01	Platform profile d (shore normal)
btd25	601985.85	172499.12	0.06	0.02	Platform profile d (shore normal)
btd26	601978.26	172494.16	0.36	0.02	Platform profile d (shore normal)
btd27	601974.78	172491.71	0.48	0.02	Platform profile d (shore normal)
btd28	601971.52	172489.38	0.66	0.02	Platform profile d (shore normal)
btd29	601969.37	172488.36	0.83	0.02	Platform profile d (shore normal)
btd30	601967.47	172487.06	1	0.02	Platform profile d (shore normal)
btd31	601965.43	172485.74	1.27	0.01	Platform profile d (shore normal)
btd32	601963.42	172484.19	1.53	0.01	Platform profile d (shore normal)
btd33	601961.29	172482.76	1.8	0.01	Platform profile d (shore normal)
btd34	601959.24	172481.37	2.1	0.02	Platform profile d (shore normal)
btd35	601957.32	172479.9	2.4	0.03	Platform profile d (shore normal)
btd36	601955.84	172478.73	2.67	0.03	Platform profile d (shore normal)
btd37	601954.91	172478.02	2.9	0.03	Platform profile d (shore normal)
bte1	601962.13	172473.5	2.52	0.03	Platform profile e (shore normal)
bte2	601964.71	172474.66	2.2	0.02	Platform profile e (shore normal)
bte3	601966.98	172475.76	1.91	0.02	Platform profile e (shore normal)
bte4	601969.51	172477	1.61	0.02	Platform profile e (shore normal)
bte5	601971.83	172478.08	1.38	0.02	Platform profile e (shore normal)
bte6	601973.57	172479.05	1.23	0.02	Platform profile e (shore normal)
bte7	601975.45	172479.91	1.06	0.02	Platform profile e (shore normal)
bte8	601977.58	172481.02	0.91	0.02	Platform profile e (shore normal)
bte9	601979.62	172482.04	0.77	0.02	Platform profile e (shore normal)
bte10	601981.72	172483.11	0.56	0.01	Platform profile e (shore normal)
bte11	601983.98	172484.17	0.45	0.01	Platform profile e (shore normal)
bte12	601992.47	172488.31	0.11	0.01	Platform profile e (shore normal)
bte13	602001.56	172492.76	-0.16	0.01	Platform profile e (shore normal)
bte14	602010.76	172497.06	-0.31	0.01	Platform profile e (shore normal)
bte15	602020.05	172501.59	-0.56	0.01	Platform profile e (shore normal)
bte16	602029.47	172506.03	-0.75	0.01	Platform profile e (shore normal)

bte17	602038.65	172510.37	-0.91	0.01	Platform profile e (shore normal)
bte18	602047.76	172515.02	-1.01	0.01	Platform profile e (shore normal)
bte19	602057.13	172519.56	-1.12	0.01	Platform profile e (shore normal)
bte20	602066.54	172524.17	-1.22	0.01	Platform profile e (shore normal)
bte21	602075.93	172528.93	-1.31	0.01	Platform profile e (shore normal)
bte22	602085.24	172533.53	-1.5	0.01	Platform profile e (shore normal)
bte23	602094.44	172537.94	-1.68	0.01	Platform profile e (shore normal)
bte24	602103.87	172542.58	-1.8	0.01	Platform profile e (shore normal)
bte25	602113.16	172547.24	-1.79	0.01	Platform profile e (shore normal)
bte26	602122.65	172552.15	-1.86	0.01	Platform profile e (shore normal)
bte27	602131.41	172556.7	-1.81	0.01	Platform profile e (shore normal)
bte28	602140.76	172561.62	-1.81	0.01	Platform profile e (shore normal)
bte29	602149.92	172566.35	-1.87	0.01	Platform profile e (shore normal)
bte30	602159.07	172571.32	-1.94	0.01	Platform profile e (shore normal)
bte31	602167.93	172575.99	-1.98	0.01	Platform profile e (shore normal)
bte32	602175.35	172580.01	-2.01	0.01	Platform profile e (shore normal)
bte33	602184.39	172584.54	-2.02	0.01	Platform profile e (shore normal)
bte34	602192.86	172589.06	-2.04	0.01	Platform profile e (shore normal)
bte35	602201.81	172593.69	-2.04	0.01	Platform profile e (shore normal)
bte36	602210.89	172598.41	-2.05	0.02	Platform profile e (shore normal)
bte37	602219.82	172603.22	-2.07	0.01	Platform profile e (shore normal)
bte38	602228.9	172608.07	-2.09	0.01	Platform profile e (shore normal)
bte39	602237.75	172612.78	-2.1	0.01	Platform profile e (shore normal)
bte40	602246.55	172617.39	-2.1	0.01	Platform profile e (shore normal)
bte41	602254.91	172621.98	-2.17	0.01	Platform profile e (shore normal)
bte42	602262.9	172626.64	-2.24	0.02	Platform profile e (shore normal)
bte43	602267.48	172629.43	-2.27	0.02	Platform profile e (shore normal)

APPENDIX E
BEACH SURVEY DATA FROM EASINGTON
JULY 2005

BEACH SURVEY DATA FROM EASINGTON: JULY 2005

Point Id	Easting	Northing	Orth. Height	Co-ord. Quality	Description
base2	539777.14	420768.53	3.65	0.00	Base station
cp1	539847.66	420835.18	-2.48	0.01	Cone penetrometer test
bar1	539868.39	420910.93	-2.98	0.02	Sand bar profile
bar2	539869.35	420911.99	-2.87	0.01	Sand bar profile
bar3	539870.60	420913.50	-2.85	0.01	Sand bar profile
bar4	539872.00	420914.60	-2.70	0.02	Sand bar profile
bar5	539873.51	420915.75	-2.70	0.01	Sand bar profile
bar6	539874.86	420916.81	-2.59	0.01	Sand bar profile
bar7	539876.49	420917.76	-2.64	0.02	Sand bar profile
bar8	539878.24	420918.81	-2.53	0.01	Sand bar profile
bar9	539880.11	420919.66	-2.55	0.01	Sand bar profile
bar10	539882.21	420920.87	-2.48	0.01	Sand bar profile
bar11	539883.98	420921.73	-2.48	0.02	Sand bar profile
bar12	539885.90	420922.68	-2.49	0.01	Sand bar profile
bar13	539887.93	420923.75	-2.39	0.01	Sand bar profile
bar14	539890.27	420924.78	-2.47	0.02	Sand bar profile
bar15	539892.30	420925.50	-2.37	0.02	Sand bar profile
bar16	539894.68	420926.42	-2.39	0.02	Sand bar profile
bar17	539897.13	420927.44	-2.28	0.02	Sand bar profile
bar18	539899.57	420928.40	-2.43	0.02	Sand bar profile
bar19	539902.06	420929.30	-2.51	0.02	Sand bar profile
bar20	539904.19	420929.96	-2.43	0.02	Sand bar profile
bar21	539906.86	420930.69	-2.50	0.01	Sand bar profile
bar22	539908.76	420931.35	-2.34	0.02	Sand bar profile
bar23	539911.60	420932.36	-2.31	0.01	Sand bar profile
bar24	539914.72	420933.18	-2.31	0.02	Sand bar profile
bar25	539917.71	420934.02	-2.37	0.01	Sand bar profile
bar26	539920.82	420934.72	-2.30	0.01	Sand bar profile
bar27	539923.93	420935.72	-2.30	0.01	Sand bar profile
bar28	539927.36	420936.48	-2.34	0.02	Sand bar profile
bar29	539930.48	420937.95	-2.31	0.01	Sand bar profile
bar30	539933.84	420939.07	-2.40	0.01	Sand bar profile
bar31	539937.14	420940.57	-2.41	0.02	Sand bar profile
bar32	539938.38	420941.05	-2.84	0.01	Sand bar profile
bar33	539940.44	420941.81	-2.45	0.02	Sand bar profile
bar34	539943.85	420943.23	-2.49	0.02	Sand bar profile
bar35	539946.86	420944.74	-2.57	0.01	Sand bar profile
bar36	539950.07	420946.12	-2.59	0.01	Sand bar profile
bar37	539953.15	420947.24	-2.60	0.01	Sand bar profile
bar38	539956.05	420949.00	-2.66	0.01	Sand bar profile
bar39	539959.28	420950.51	-2.72	0.01	Sand bar profile
bar40	539962.62	420952.37	-2.74	0.01	Sand bar profile
bar41	539965.80	420954.55	-2.81	0.01	Sand bar profile
bb1	539692.01	420957.26	-1.46	0.02	Base of beach
bb2	539696.21	420952.13	-1.54	0.02	Base of beach
bb3	539700.80	420947.37	-1.60	0.02	Base of beach
bb4	539705.13	420942.17	-1.57	0.02	Base of beach
bb5	539710.22	420936.85	-1.63	0.02	Base of beach
bb6	539715.01	420931.56	-1.68	0.02	Base of beach
bb7	539720.14	420926.78	-1.74	0.02	Base of beach
bb8	539725.28	420920.74	-1.74	0.02	Base of beach
bb9	539730.24	420914.53	-1.75	0.02	Base of beach
bb10	539734.66	420909.08	-1.73	0.01	Base of beach
bb11	539738.70	420904.32	-1.75	0.02	Base of beach
bb12	539743.63	420898.38	-1.81	0.02	Base of beach
bb13	539750.37	420890.65	-1.73	0.03	Base of beach
bb14	539756.60	420889.52	-1.85	0.02	Base of beach
bb15	539762.99	420887.18	-2.10	0.03	Base of beach
bb16	539765.36	420880.80	-1.93	0.02	Base of beach
bb17	539768.68	420873.99	-1.93	0.02	Base of beach
bb18	539773.94	420869.47	-2.03	0.02	Base of beach
bb19	539778.16	420863.85	-2.04	0.02	Base of beach
bb20	539781.66	420858.09	-1.99	0.03	Base of beach
bb21	539785.37	420852.75	-1.89	0.02	Base of beach
bb22	539787.70	420845.98	-1.87	0.02	Base of beach
bb23	539791.37	420839.30	-1.74	0.01	Base of beach
bb24	539796.02	420833.73	-1.77	0.02	Base of beach
bb25	539799.50	420827.60	-1.81	0.02	Base of beach
bb26	539804.21	420822.73	-1.78	0.02	Base of beach
bb27	539808.11	420817.83	-1.78	0.02	Base of beach
bb28	539811.14	420812.64	-1.72	0.02	Base of beach

bb29	539816.34	420807.06	-1.73	0.03	Base of beach
bb30	539820.64	420802.21	-1.74	0.02	Base of beach
bb31	539824.84	420796.04	-1.68	0.02	Base of beach
bb32	539829.00	420790.83	-1.62	0.02	Base of beach
bb33	539833.46	420785.23	-1.58	0.02	Base of beach
bb34	539838.18	420779.49	-1.61	0.02	Base of beach
bb35	539842.79	420774.03	-1.56	0.02	Base of beach
bb36	539847.04	420767.50	-1.51	0.02	Base of beach
bb37	539851.43	420761.90	-1.47	0.02	Base of beach
bb38	539855.90	420756.48	-1.47	0.02	Base of beach
bb39	539860.32	420751.27	-1.59	0.02	Base of beach
bb40	539864.47	420745.36	-1.47	0.01	Base of beach
bb41	539868.69	420739.55	-1.44	0.02	Base of beach
bb42	539873.66	420734.56	-1.52	0.02	Base of beach
bb43	539877.38	420729.12	-1.47	0.02	Base of beach
bb44	539881.46	420723.24	-1.42	0.01	Base of beach
bb45	539883.42	420716.98	-1.33	0.02	Base of beach
bb46	539887.22	420711.67	-1.28	0.01	Base of beach
bb47	539890.28	420706.80	-1.23	0.01	Base of beach
bba1	539939.17	420722.12	-2.54	0.01	Beach/platform contact
bba2	539934.52	420725.98	-2.59	0.02	Beach/platform contact
bba3	539928.25	420729.18	-2.53	0.02	Beach/platform contact
bba4	539921.38	420731.81	-2.43	0.01	Beach/platform contact
bba5	539914.75	420734.24	-2.35	0.01	Beach/platform contact
bba6	539908.11	420736.50	-2.29	0.01	Beach/platform contact
bba7	539899.11	420736.70	-2.07	0.02	Beach/platform contact
bba8	539891.86	420742.13	-2.12	0.01	Beach/platform contact
bba9	539885.90	420744.89	-2.03	0.02	Beach/platform contact
bba10	539880.96	420749.57	-2.15	0.01	Beach/platform contact
bba11	539876.94	420754.52	-2.07	0.02	Beach/platform contact
bba12	539872.79	420760.85	-2.06	0.02	Beach/platform contact
bba13	539867.21	420764.06	-1.92	0.02	Beach/platform contact
bba14	539865.11	420771.98	-2.07	0.02	Beach/platform contact
bba15	539858.94	420774.54	-1.96	0.02	Beach/platform contact
bba16	539854.41	420780.74	-2.03	0.02	Beach/platform contact
bba17	539847.04	420784.55	-1.95	0.02	Beach/platform contact
bba18	539841.84	420790.04	-1.89	0.02	Beach/platform contact
bba19	539835.73	420795.87	-1.86	0.03	Beach/platform contact
bba20	539832.36	420802.46	-1.89	0.02	Beach/platform contact
bba21	539827.40	420806.85	-1.96	0.01	Beach/platform contact
bba22	539820.36	420807.14	-1.80	0.02	Beach/platform contact
bba23	539814.09	420809.34	-1.66	0.02	Beach/platform contact
cp2	539842.32	420829.67	-2.31	0.00	Cone penetrometer test
cp3	539836.81	420825.65	-2.21	0.00	Cone penetrometer test
cp4	539829.02	420821.87	-2.08	0.00	Cone penetrometer test
cp6	539827.84	420837.19	-2.22	0.01	Cone penetrometer test
cp7	539832.87	420831.43	-2.18	0.02	Cone penetrometer test
cp8	539841.18	420816.75	-2.24	0.01	Cone penetrometer test
cp5	539820.69	420816.01	-1.91	0.01	Cone penetrometer test
cp9	539847.24	420807.75	-2.23	0.00	Cone penetrometer test
u1	539838.84	420831.72	-2.47	0.01	Triaxial sample site EAS1
u2	539829.87	420819.94	-2.12	0.02	Triaxial sample site EAS2
bc1	539830.82	420688.52	4.02	0.03	Base of cliff
bc2	539824.61	420691.00	4.27	0.02	Base of cliff
bc3	539818.50	420690.99	4.84	0.02	Base of cliff
bc4	539815.46	420697.55	4.49	0.02	Base of cliff
bc5	539811.61	420702.71	4.56	0.03	Base of cliff
bc6	539806.91	420706.74	4.68	0.02	Base of cliff
bc7	539801.48	420709.42	4.98	0.02	Base of cliff
bc8	539798.81	420716.55	4.76	0.02	Base of cliff
bc9	539797.75	420722.67	4.57	0.02	Base of cliff
bc10	539798.14	420727.00	4.32	0.02	Base of cliff
bc11	539792.60	420729.67	4.52	0.02	Base of cliff
bc12	539788.68	420734.76	4.66	0.02	Base of cliff
bc13	539784.82	420740.86	4.67	0.03	Base of cliff
bc14	539781.34	420746.39	4.60	0.03	Base of cliff
bc15	539777.41	420751.40	4.65	0.02	Base of cliff
bc16	539775.09	420758.04	4.44	0.03	Base of cliff
bc17	539771.05	420763.14	4.51	0.02	Base of cliff
bc18	539769.05	420769.00	4.36	0.02	Base of cliff
bc19	539768.42	420774.87	3.90	0.02	Base of cliff
bc20	539763.79	420780.25	3.97	0.02	Base of cliff
bc21	539759.93	420786.01	3.90	0.03	Base of cliff
bc22	539753.78	420789.19	4.30	0.02	Base of cliff
bc23	539749.70	420794.66	4.26	0.02	Base of cliff
bc24	539745.86	420801.34	4.11	0.02	Base of cliff

bc25	539743.41	420807.84	3.94	0.02	Base of cliff
bc26	539738.67	420812.47	4.12	0.03	Base of cliff
bc27	539733.47	420816.23	4.31	0.02	Base of cliff
bc28	539732.95	420823.00	3.97	0.04	Base of cliff
bc29	539730.05	420828.64	3.87	0.03	Base of cliff
bc30	539726.10	420834.95	3.81	0.03	Base of cliff
bc31	539721.76	420840.65	3.80	0.04	Base of cliff
bc32	539717.90	420847.53	3.74	0.02	Base of cliff
bc33	539713.64	420851.43	3.73	0.02	Base of cliff
bc34	539708.82	420856.32	3.92	0.03	Base of cliff
bc35	539704.58	420860.86	3.98	0.03	Base of cliff
bc36	539701.52	420866.68	3.81	0.02	Base of cliff
bc37	539696.54	420870.99	3.96	0.03	Base of cliff
bc38	539692.41	420875.57	3.93	0.03	Base of cliff
bc39	539687.61	420878.55	4.20	0.04	Base of cliff
bc40	539683.91	420881.79	4.15	0.03	Base of cliff
bpa1	539738.71	420813.43	4.00	0.03	Beach profile a (shore normal)
bpa2	539742.40	420815.44	3.61	0.03	Beach profile a (shore normal)
bpa3	539745.84	420817.55	3.34	0.03	Beach profile a (shore normal)
bpa4	539749.17	420819.66	3.04	0.03	Beach profile a (shore normal)
bpa5	539753.11	420822.00	2.60	0.02	Beach profile a (shore normal)
bpa6	539756.98	420824.18	2.13	0.03	Beach profile a (shore normal)
bpa7	539761.26	420826.92	1.57	0.02	Beach profile a (shore normal)
bpa8	539765.32	420829.23	1.08	0.03	Beach profile a (shore normal)
bpa9	539768.79	420831.49	0.63	0.03	Beach profile a (shore normal)
bpa10	539772.05	420833.57	0.22	0.03	Beach profile a (shore normal)
bpa11	539775.74	420836.01	-0.27	0.02	Beach profile a (shore normal)
bpa12	539778.97	420838.25	-0.67	0.03	Beach profile a (shore normal)
bpa13	539782.35	420840.21	-1.07	0.03	Beach profile a (shore normal)
bpa14	539785.49	420842.05	-1.47	0.03	Beach profile a (shore normal)
bpa15	539788.29	420843.91	-1.81	0.03	Beach profile a (shore normal)
bbp1	539820.98	420798.98	-1.61	0.03	Beach profile b (shore normal)
bbp2	539817.71	420796.60	-1.18	0.03	Beach profile b (shore normal)
bbp3	539814.32	420794.16	-0.76	0.03	Beach profile b (shore normal)
bbp4	539810.73	420791.52	-0.30	0.03	Beach profile b (shore normal)
bbp5	539807.03	420788.58	0.19	0.03	Beach profile b (shore normal)
bbp6	539803.21	420786.06	0.66	0.03	Beach profile b (shore normal)
bbp7	539799.52	420783.60	1.14	0.03	Beach profile b (shore normal)
bbp8	539795.58	420780.91	1.60	0.03	Beach profile b (shore normal)
bbp9	539791.73	420778.26	2.13	0.03	Beach profile b (shore normal)
bbp10	539787.57	420775.15	2.59	0.03	Beach profile b (shore normal)
bbp11	539783.58	420772.17	3.08	0.03	Beach profile b (shore normal)
bbp12	539779.16	420769.08	3.48	0.02	Beach profile b (shore normal)
bbp13	539775.35	420766.45	3.80	0.03	Beach profile b (shore normal)
bbp14	539772.38	420764.67	4.25	0.03	Beach profile b (shore normal)
bbp15	539770.90	420763.58	4.48	0.03	Beach profile b (shore normal)
bpc1	539792.62	420727.40	4.80	0.04	Beach profile c (shore normal)
bpc2	539796.49	420730.11	4.22	0.03	Beach profile c (shore normal)
bpc3	539799.96	420732.87	3.87	0.02	Beach profile c (shore normal)
bpc4	539804.08	420736.05	3.60	0.03	Beach profile c (shore normal)
bpc5	539807.93	420738.84	3.25	0.03	Beach profile c (shore normal)
bpc6	539811.62	420741.67	2.80	0.02	Beach profile c (shore normal)
bpc7	539815.36	420743.98	2.37	0.03	Beach profile c (shore normal)
bpc8	539819.73	420746.75	1.90	0.02	Beach profile c (shore normal)
bpc9	539824.12	420749.41	1.37	0.03	Beach profile c (shore normal)
bpc10	539828.69	420752.11	0.83	0.03	Beach profile c (shore normal)
bpc11	539833.08	420754.65	0.32	0.02	Beach profile c (shore normal)
bpc12	539837.35	420757.29	-0.24	0.03	Beach profile c (shore normal)
bpc13	539841.55	420759.91	-0.70	0.02	Beach profile c (shore normal)
bpc14	539844.96	420762.32	-1.06	0.03	Beach profile c (shore normal)
bpc15	539848.08	420764.55	-1.45	0.02	Beach profile c (shore normal)
bpc16	539851.47	420767.12	-1.59	0.03	Beach profile c (shore normal)
bpc17	539855.59	420769.71	-1.72	0.02	Beach profile c (shore normal)
bpc18	539859.16	420772.17	-1.91	0.03	Beach profile c (shore normal)
bpc19	539860.81	420773.29	-1.98	0.03	Beach profile c (shore normal)
base3	539893.03	420516.54	19.02	0.00	Base station
n1	539799.11	420823.81	-1.55	0.01	Beach sediment sample
n2	539787.53	420817.50	-0.25	0.01	Beach sediment sample
n3	539777.84	420811.63	1.10	0.00	Beach sediment sample
s3	539796.05	420782.83	1.46	0.01	Beach sediment sample
s2	539807.13	420790.02	0.01	0.01	Beach sediment sample
s1	539817.01	420797.32	-1.19	0.00	Beach sediment sample
plata1	539821.63	420807.81	-1.82	0.01	Platform profile a (shore normal)
plata2	539824.96	420809.73	-1.91	0.01	Platform profile a (shore normal)
plata3	539828.10	420811.48	-1.93	0.01	Platform profile a (shore normal)
plata4	539831.36	420813.49	-2.05	0.02	Platform profile a (shore normal)

plata5	539834.61	420815.41	-2.07	0.02	Platform profile a (shore normal)
plata6	539836.85	420817.35	-2.14	0.01	Platform profile a (shore normal)
plata7	539838.89	420818.71	-2.14	0.01	Platform profile a (shore normal)
plata8	539841.01	420820.10	-2.25	0.02	Platform profile a (shore normal)
plata9	539843.85	420821.87	-2.30	0.02	Platform profile a (shore normal)
plata10	539846.45	420823.51	-2.35	0.01	Platform profile a (shore normal)
plata11	539848.96	420826.32	-2.34	0.01	Platform profile a (shore normal)
plata12	539850.89	420828.24	-2.40	0.02	Platform profile a (shore normal)
plata13	539852.75	420829.87	-2.42	0.01	Platform profile a (shore normal)
plata14	539854.82	420831.77	-2.43	0.02	Platform profile a (shore normal)
plata15	539856.90	420833.98	-2.49	0.01	Platform profile a (shore normal)
plata16	539859.14	420836.28	-2.52	0.01	Platform profile a (shore normal)
plata17	539860.76	420838.34	-2.51	0.01	Platform profile a (shore normal)
plata18	539862.44	420840.19	-2.57	0.01	Platform profile a (shore normal)
b1	539914.00	420904.49	-2.21	0.01	Bar sediment sample
b2	539931.95	420920.61	-2.25	0.00	Bar sediment sample
b3	539836.34	421007.03	-2.13	0.00	Bar sediment sample
b4	539760.71	421079.37	-1.96	0.00	Bar sediment sample
btna1	539599.69	421160.72	-2.47	0.02	Platform profile @ northern end of beach: a
btna2	539596.46	421157.95	-2.49	0.02	Platform profile @ northern end of beach: a
btna3	539592.95	421155.62	-2.38	0.03	Platform profile @ northern end of beach: a
btna4	539589.12	421152.35	-2.17	0.02	Platform profile @ northern end of beach: a
btna5	539585.48	421149.84	-2.16	0.02	Platform profile @ northern end of beach: a
btna6	539581.76	421146.27	-2.27	0.02	Platform profile @ northern end of beach: a
btna7	539577.49	421143.97	-2.08	0.03	Platform profile @ northern end of beach: a
btna8	539573.91	421141.21	-1.95	0.03	Platform profile @ northern end of beach: a
btna9	539570.83	421137.99	-1.87	0.02	Platform profile @ northern end of beach: a
btna10	539567.01	421135.22	-1.85	0.02	Platform profile @ northern end of beach: a
btna11	539563.41	421132.78	-1.83	0.03	Platform profile @ northern end of beach: a
btna12	539559.75	421130.01	-1.64	0.02	Platform profile @ northern end of beach: a
btna13	539555.65	421127.21	-1.36	0.02	Platform profile @ northern end of beach: a
btna14	539553.31	421125.77	-1.17	0.03	Platform profile @ northern end of beach: a
btna15	539551.25	421124.41	-0.93	0.03	Platform profile @ northern end of beach: a
btna16	539548.92	421122.89	-0.70	0.02	Platform profile @ northern end of beach: a
btna17	539546.70	421121.36	-0.41	0.02	Platform profile @ northern end of beach: a
btna18	539545.01	421120.19	-0.19	0.02	Platform profile @ northern end of beach: a
btna19	539543.40	421119.02	-0.02	0.02	Platform profile @ northern end of beach: a
btbn1	539589.72	421133.67	-2.15	0.02	Platform profile @ northern end of beach: b
btbn2	539586.40	421131.23	-2.06	0.02	Platform profile @ northern end of beach: b
btbn3	539583.03	421128.47	-1.90	0.02	Platform profile @ northern end of beach: b
btbn4	539579.31	421125.69	-1.93	0.02	Platform profile @ northern end of beach: b
btbn5	539575.87	421123.21	-1.89	0.01	Platform profile @ northern end of beach: b
btbn6	539571.22	421120.26	-1.71	0.02	Platform profile @ northern end of beach: b
btbn7	539567.66	421117.86	-1.55	0.01	Platform profile @ northern end of beach: b
btbn8	539564.50	421115.69	-1.44	0.02	Platform profile @ northern end of beach: b
btbn9	539562.61	421114.36	-1.25	0.01	Platform profile @ northern end of beach: b
btbn10	539560.95	421113.16	-1.07	0.02	Platform profile @ northern end of beach: b
btbn11	539558.94	421111.77	-0.86	0.01	Platform profile @ northern end of beach: b
btbn12	539556.83	421110.32	-0.63	0.02	Platform profile @ northern end of beach: b
btbn13	539554.52	421108.73	-0.34	0.02	Platform profile @ northern end of beach: b
btbn14	539552.86	421107.36	-0.09	0.02	Platform profile @ northern end of beach: b
btbn15	539551.10	421105.98	0.16	0.01	Platform profile @ northern end of beach: b
btbn16	539549.48	421104.60	0.29	0.02	Platform profile @ northern end of beach: b
btbn17	539543.33	421100.38	0.99	0.02	Platform profile @ northern end of beach: b
u3	539830.05	420819.98	-2.22	0.00	Triaxial sample site EAS3
platb1	539810.40	420813.26	-1.71	0.03	Platform profile b (shore normal)
platb2	539814.08	420816.07	-1.79	0.03	Platform profile b (shore normal)
platb3	539818.29	420818.66	-1.93	0.04	Platform profile b (shore normal)
platb4	539822.96	420820.82	-1.99	0.02	Platform profile b (shore normal)
platb5	539828.10	420823.08	-2.12	0.02	Platform profile b (shore normal)
platb6	539833.11	420825.65	-2.20	0.03	Platform profile b (shore normal)
platb7	539837.97	420827.92	-2.32	0.03	Platform profile b (shore normal)
platb8	539841.82	420831.97	-2.33	0.03	Platform profile b (shore normal)
platb9	539845.89	420834.67	-2.47	0.02	Platform profile b (shore normal)
platb10	539850.03	420836.57	-2.51	0.02	Platform profile b (shore normal)
platb11	539854.20	420838.76	-2.52	0.02	Platform profile b (shore normal)
platb12	539859.19	420841.02	-2.60	0.02	Platform profile b (shore normal)
platb13	539861.68	420843.52	-2.67	0.02	Platform profile b (shore normal)
platoba1	539900.84	420764.98	-2.50	0.02	Platform profile (shore parallel)
platoba2	539894.67	420771.10	-2.36	0.02	Platform profile (shore parallel)
platoba3	539888.26	420777.44	-2.33	0.03	Platform profile (shore parallel)
platoba4	539882.34	420784.78	-2.37	0.02	Platform profile (shore parallel)
platoba5	539876.19	420791.61	-2.36	0.02	Platform profile (shore parallel)
platoba6	539870.65	420798.66	-2.38	0.02	Platform profile (shore parallel)
platoba7	539864.85	420805.28	-2.36	0.02	Platform profile (shore parallel)
platoba8	539859.35	420811.52	-2.30	0.02	Platform profile (shore parallel)

platoba9	539853.85	420818.60	-2.30	0.02	Platform profile (shore parallel)
platoba10	539846.62	420827.76	-2.47	0.02	Platform profile (shore parallel)
platoba11	539839.95	420834.79	-2.39	0.02	Platform profile (shore parallel)
platoba12	539833.17	420841.55	-2.31	0.02	Platform profile (shore parallel)
platoba13	539827.49	420848.23	-2.24	0.02	Platform profile (shore parallel)
platoba14	539822.53	420853.76	-2.27	0.02	Platform profile (shore parallel)
platoba15	539817.37	420859.12	-2.22	0.02	Platform profile (shore parallel)
platoba16	539812.86	420866.40	-2.38	0.02	Platform profile (shore parallel)
platoba17	539806.55	420873.33	-2.41	0.02	Platform profile (shore parallel)
platoba18	539800.34	420879.54	-2.26	0.02	Platform profile (shore parallel)
platoba19	539793.72	420885.91	-2.42	0.02	Platform profile (shore parallel)
platoba20	539788.24	420891.24	-2.45	0.02	Platform profile (shore parallel)
platac1	539796.09	420832.59	-1.71	0.02	Platform profile c (shore normal)
platac2	539801.83	420835.24	-1.81	0.02	Platform profile c (shore normal)
platac3	539807.75	420837.69	-1.93	0.02	Platform profile c (shore normal)
platac4	539814.28	420840.64	-2.06	0.02	Platform profile c (shore normal)
platac5	539820.07	420843.86	-2.17	0.02	Platform profile c (shore normal)
platac6	539825.51	420846.83	-2.23	0.03	Platform profile c (shore normal)
platac7	539831.10	420850.25	-2.32	0.03	Platform profile c (shore normal)
platac8	539836.74	420854.22	-2.46	0.02	Platform profile c (shore normal)
platac9	539840.75	420858.90	-2.52	0.02	Platform profile c (shore normal)
platac10	539844.08	420862.37	-2.66	0.03	Platform profile c (shore normal)
p1	539838.31	420847.85	-2.56	0.00	Platform sand sample
p2	539824.89	420869.85	-2.51	0.00	Platform sand sample
A	539828.41	420826.35	-1.96	0.02	University Sussex erosion beam
B	539819.52	420863.62	-2.19	0.02	University Sussex erosion beam
C	539835.98	420864.36	-2.38	0.02	University Sussex erosion beam
pedestal	539902.55	420776.72	-2.34	0.01	Pedestal ('earth pillar')

APPENDIX F
BEACH SURVEY DATA FROM EASINGTON
MARCH 2006

BEACH SURVEY DATA FROM EASINGTON: MARCH 2006

Point Id	Easting	Northing	Orth. Height	Coordinate Quality	Description
station1	539893	420515.19	19.08	0	Base Station
bb1	539898	420763.92	-2.42	0.01	Base of beach
bb2	539895	420768.74	-2.45	0.01	Base of beach
bb3	539891	420772.69	-2.29	0.02	Base of beach
bb4	539890	420778.43	-2.34	0.02	Base of beach
bb5	539891	420783.29	-2.39	0.02	Base of beach
bb6	539888	420787.88	-2.47	0.01	Base of beach
bb7	539884	420790.75	-2.41	0.02	Base of beach
bb8	539880	420790.52	-2.33	0.02	Base of beach
bb9	539876	420794.18	-2.41	0.02	Base of beach
bb10	539872	420798.12	-2.45	0.01	Base of beach
bb11	539868	420802.18	-2.34	0.02	Base of beach
bb12	539863	420805.08	-2.42	0.01	Base of beach
bb13	539858	420808.4	-2.31	0.02	Base of beach
bb14	539854	420812.46	-2.23	0.02	Base of beach
bb15	539852	420817.9	-2.34	0.01	Base of beach
bc1	539613	420976.84	2.9	0.02	Base of cliff
bc2	539612	420969.4	3.84	0.02	Base of cliff
bc3	539618	420963.14	3.48	0.02	Base of cliff
bc4	539623	420956.58	3.73	0.02	Base of cliff
bc5	539628	420948.84	3.91	0.02	Base of cliff
bc6	539637	420942.27	3.55	0.01	Base of cliff
bc7	539642	420934.17	3.6	0.04	Base of cliff
bc8	539650	420928.55	3.15	0.02	Base of cliff
bc9	539656	420921.16	2.95	0.02	Base of cliff
bc10	539660	420911.2	3.22	0.03	Base of cliff
bc11	539665	420903.3	3.32	0.02	Base of cliff
bc12	539673	420894.24	3.39	0.03	Base of cliff
bc13	539679	420887.86	3.28	0.05	Base of cliff
bc14	539689	420879.97	2.94	0.05	Base of cliff
bc15	539695	420874.92	2.76	0.04	Base of cliff
bc16	539701	420867.81	2.75	0.02	Base of cliff
bc17	539706	420861.63	2.62	0.02	Base of cliff
bc18	539712	420853.87	2.65	0.01	Base of cliff
bc19	539718	420847.9	2.4	0.02	Base of cliff
bc20	539722	420843.08	2.42	0.02	Base of cliff
bc21	539728	420833.09	2.24	0.02	Base of cliff
bc22	539733	420825.11	2.21	0.02	Base of cliff
bc23	539738	420816.75	2.3	0.01	Base of cliff
bc24	539742	420813.46	2.09	0.02	Base of cliff
bc25	539745	420809.5	2.01	0.03	Base of cliff
bc26	539747	420804.58	1.99	0.04	Base of cliff
bc27	539749	420799.21	2.16	0.02	Base of cliff
bc28	539753	420794.49	2.05	0.02	Base of cliff
bc29	539757	420790.37	1.99	0.02	Base of cliff
bc30	539761	420786.26	1.95	0.02	Base of cliff

bc31	539764	420782.06	1.95	0.01	Base of cliff
bc32	539768	420777.44	1.93	0.02	Base of cliff
bc33	539770	420772.76	2.02	0.01	Base of cliff
bc34	539773	420767.92	1.97	0.02	Base of cliff
bc35	539775	420762.61	2.1	0.02	Base of cliff
bc36	539779	420758.13	2.06	0.02	Base of cliff
bc37	539782	420753.8	2.08	0.02	Base of cliff
bc38	539785	420749.37	1.98	0.02	Base of cliff
bc39	539789	420745.7	1.86	0.02	Base of cliff
bc40	539791	420740.34	1.92	0.02	Base of cliff
bc41	539794	420736.33	1.92	0.02	Base of cliff
bc42	539796	420730.71	2.42	0.02	Base of cliff
bc43	539799	420727.11	2.45	0.02	Base of cliff
bc44	539802	420723.04	2.31	0.02	Base of cliff
bc45	539800	420719.19	2.86	0.02	Base of cliff
bc46	539799	420714.28	3.19	0.02	Base of cliff
bc47	539804	420710.98	3.09	0.02	Base of cliff
bc48	539810	420708.04	2.98	0.02	Base of cliff
bc49	539814	420704.41	2.93	0.02	Base of cliff
bc50	539817	420699.28	3.18	0.03	Base of cliff
bc51	539818	420693.5	3.76	0.02	Base of cliff
bc52	539823	420693.66	3.22	0.02	Base of cliff
bc53	539832	420689.85	2.69	0.02	Base of cliff
bc54	539836	420682.55	2.86	0.02	Base of cliff
bc55	539839	420676.49	2.95	0.02	Base of cliff
bc56	539840	420669.04	3.58	0.03	Base of cliff
bc57	539844	420660.49	3.83	0.02	Base of cliff
bc58	539847	420653.33	4.01	0.03	Base of cliff
bc59	539851	420645.82	4.04	0.04	Base of cliff
bc60	539857	420639.35	3.7	0.03	Base of cliff
barc	539928	420817.85	-2.47	0.02	Sand bar cross-profile
barc1	539929	420818.95	-2.16	0.02	Sand bar cross-profile
barc2	539933	420821.84	-2.05	0.02	Sand bar cross-profile
barc3	539937	420825.02	-2.04	0.01	Sand bar cross-profile
barc4	539941	420827.79	-2.12	0.02	Sand bar cross-profile
barc5	539946	420830.7	-2.2	0.02	Sand bar cross-profile
barc6	539950	420833.42	-2.35	0.02	Sand bar cross-profile
barc7	539953	420835.71	-2.48	0.02	Sand bar cross-profile
bpa1	539739	420813.43	3.76	0.02	Beach profile a (shore normal)
bpa2	539740	420814.41	2.17	0.02	Beach profile a (shore normal)
bpa3	539746	420817.02	1.68	0.02	Beach profile a (shore normal)
bpa4	539750	420819.81	1.23	0.01	Beach profile a (shore normal)
bpa5	539755	420822.59	0.95	0.02	Beach profile a (shore normal)
bpa6	539759	420825.38	0.84	0.02	Beach profile a (shore normal)
bpa7	539764	420828.1	0.69	0.02	Beach profile a (shore normal)
bpa8	539768	420830.88	0.55	0.02	Beach profile a (shore normal)
bpa9	539772	420833.68	0.36	0.02	Beach profile a (shore normal)
bpa10	539777	420836.27	0.23	0.01	Beach profile a (shore normal)
bpa11	539781	420838.88	0.04	0.02	Beach profile a (shore normal)

bpa12	539785	420841.56	-0.15	0.01	Beach profile a (shore normal)
bpa13	539789	420843.8	-0.3	0.02	Beach profile a (shore normal)
bpa14	539793	420846.5	-0.52	0.02	Beach profile a (shore normal)
bpa15	539798	420848.98	-0.71	0.02	Beach profile a (shore normal)
bpa16	539802	420851.54	-0.9	0.02	Beach profile a (shore normal)
bpa17	539806	420854.21	-1.11	0.02	Beach profile a (shore normal)
bpa18	539811	420856.83	-1.29	0.02	Beach profile a (shore normal)
bpa19	539815	420859.44	-1.48	0.02	Beach profile a (shore normal)
bpa20	539819	420862.22	-1.71	0.02	Beach profile a (shore normal)
bpa21	539824	420864.87	-2.01	0.02	Beach profile a (shore normal)
bpa22	539828	420867.72	-2.01	0.02	Beach profile a (shore normal)
bpa23	539833	420870.43	-2.11	0.02	Beach profile a (shore normal)
bpa24	539837	420873.15	-2.28	0.02	Beach profile a (shore normal)
bpa25	539842	420875.76	-2.37	0.02	Beach profile a (shore normal)
bpa26	539846	420878.36	-2.36	0.02	Beach profile a (shore normal)
bpa27	539850	420880.87	-2.35	0.02	Beach profile a (shore normal)
bpa28	539854	420883.64	-2.64	0.02	Beach profile a (shore normal)
bbp1	539916	420864.02	-2.57	0.02	Beach profile b (shore normal)
bbp2	539912	420860.72	-2.41	0.02	Beach profile b (shore normal)
bbp3	539907	420857.73	-2.29	0.02	Beach profile b (shore normal)
bbp4	539903	420855.09	-2.09	0.02	Beach profile b (shore normal)
bbp5	539898	420852.02	-2.06	0.02	Beach profile b (shore normal)
bbp6	539894	420849.13	-2.04	0.02	Beach profile b (shore normal)
bbp7	539890	420846.29	-2.01	0.02	Beach profile b (shore normal)
bbp8	539885	420843.24	-1.97	0.02	Beach profile b (shore normal)
bbp9	539881	420840.07	-1.96	0.02	Beach profile b (shore normal)
bbp10	539877	420837.05	-1.99	0.02	Beach profile b (shore normal)
bbp11	539872	420833.9	-2.06	0.01	Beach profile b (shore normal)
bbp12	539868	420831.1	-2.11	0.02	Beach profile b (shore normal)
bbp13	539864	420828.18	-2.4	0.02	Beach profile b (shore normal)
bbp14	539859	420824.8	-2.3	0.02	Beach profile b (shore normal)
bbp15	539854	420821.84	-2.35	0.02	Beach profile b (shore normal)
bbp16	539851	420819.46	-2.32	0.02	Beach profile b (shore normal)
bbp17	539847	420816.5	-1.77	0.02	Beach profile b (shore normal)
bbp18	539843	420813.46	-1.5	0.02	Beach profile b (shore normal)
bbp19	539838	420810.64	-1.25	0.02	Beach profile b (shore normal)
bbp20	539834	420807.55	-1.01	0.02	Beach profile b (shore normal)
bbp21	539830	420804.92	-0.79	0.02	Beach profile b (shore normal)
bbp22	539826	420802.11	-0.53	0.02	Beach profile b (shore normal)
bbp23	539822	420799.4	-0.3	0.02	Beach profile b (shore normal)
bbp24	539818	420796.51	-0.08	0.02	Beach profile b (shore normal)
bbp25	539813	420793.9	0.18	0.02	Beach profile b (shore normal)
bbp26	539809	420791	0.37	0.02	Beach profile b (shore normal)
bbp27	539805	420788.19	0.59	0.02	Beach profile b (shore normal)
bbp28	539801	420785.28	0.73	0.02	Beach profile b (shore normal)
bbp29	539797	420782.4	0.87	0.02	Beach profile b (shore normal)
bbp30	539793	420779.45	0.99	0.02	Beach profile b (shore normal)
bbp31	539788	420776.33	1.17	0.02	Beach profile b (shore normal)
bbp32	539783	420772.8	1.41	0.02	Beach profile b (shore normal)

bpb33	539779	420769.68	1.69	0.02	Beach profile b (shore normal)
bpb34	539775	420766.54	1.94	0.02	Beach profile b (shore normal)
bpb35	539771	420763.59	2.5	0.02	Beach profile b (shore normal)
bpb36	539771	420763.52	2.51	0.02	Beach profile b (shore normal)
bpc1	539793	420727.42	5	0.02	Beach profile c (shore normal)
bpc2	539794	420728.23	4.14	0.01	Beach profile c (shore normal)
bpc3	539795	420728.88	2.77	0.02	Beach profile c (shore normal)
bpc4	539800	420731.82	1.95	0.02	Beach profile c (shore normal)
bpc5	539804	420734.81	1.73	0.02	Beach profile c (shore normal)
bpc6	539809	420737.63	1.61	0.02	Beach profile c (shore normal)
bpc7	539813	420740.7	1.43	0.02	Beach profile c (shore normal)
bpc8	539818	420743.72	1.2	0.01	Beach profile c (shore normal)
bpc9	539822	420746.66	0.98	0.01	Beach profile c (shore normal)
bpc10	539827	420749.59	0.72	0.02	Beach profile c (shore normal)
bpc11	539831	420752.78	0.44	0.01	Beach profile c (shore normal)
bpc12	539836	420755.92	0.18	0.02	Beach profile c (shore normal)
bpc13	539841	420758.95	-0.06	0.02	Beach profile c (shore normal)
bpc14	539845	420762.12	-0.31	0.02	Beach profile c (shore normal)
bpc15	539849	420765	-0.51	0.01	Beach profile c (shore normal)
bpc16	539854	420768.06	-0.76	0.02	Beach profile c (shore normal)
bpc17	539858	420771	-0.98	0.02	Beach profile c (shore normal)
bpc19	539861	420773.28	-1.11	0.02	Beach profile c (shore normal)
bpc20	539865	420776.19	-1.32	0.02	Beach profile c (shore normal)
bpc21	539870	420779.23	-1.52	0.01	Beach profile c (shore normal)
bpc22	539874	420782.19	-1.79	0.02	Beach profile c (shore normal)
bpc23	539879	420785.19	-2.18	0.02	Beach profile c (shore normal)
bpc24	539883	420788.15	-2.4	0.02	Beach profile c (shore normal)
bpc25	539886	420790.69	-2.45	0.01	Beach profile c (shore normal)
btnc1	539578	421141.7	-2.04	0.01	Platform profile @ northern end of beach: c
btnc2	539573	421138.93	-1.98	0.01	Platform profile @ northern end of beach: c
btnc3	539569	421136.42	-1.86	0.02	Platform profile @ northern end of beach: c
btnc4	539564	421133.27	-1.78	0.01	Platform profile @ northern end of beach: c
btnc5	539561	421130.77	-1.69	0.01	Platform profile @ northern end of beach: c
btnc6	539557	421128.19	-1.23	0.02	Platform profile @ northern end of beach: c
btnc7	539552	421125.56	-0.91	0.01	Platform profile @ northern end of beach: c
btnc8	539548	421122.75	-0.57	0.02	Platform profile @ northern end of beach: c
btnc9	539543	421119.12	-0.19	0.02	Platform profile @ northern end of beach: c
btnc10	539539	421116.13	0.17	0.02	Platform profile @ northern end of beach: c
btnc11	539535	421112.77	0.61	0.02	Platform profile @ northern end of beach: c
btnc12	539530	421109.69	1.1	0.01	Platform profile @ northern end of beach: c
btnc13	539527	421106.73	1.58	0.02	Platform profile @ northern end of beach: c
btnc14	539523	421103.86	2.19	0.02	Platform profile @ northern end of beach: c
btnc15	539519	421101.15	2.78	0.01	Platform profile @ northern end of beach: c
btnc16	539517	421099.68	3.17	0.02	Platform profile @ northern end of beach: c
platoba1	539919	420761.11	-2.64	0.05	Platform profile (shore parallel)
platoba2	539915	420767.59	-2.56	0.04	Platform profile (shore parallel)
platoba3	539912	420771.6	-2.55	0.04	Platform profile (shore parallel)
platoba4	539909	420774.98	-2.61	0.02	Platform profile (shore parallel)
platoba5	539905	420779.15	-2.54	0.02	Platform profile (shore parallel)

platoba6	539901	420783.25	-2.58	0.01	Platform profile (shore parallel)
platoba7	539897	420787.81	-2.53	0.02	Platform profile (shore parallel)
platoba8	539895	420790.69	-2.56	0.02	Platform profile (shore parallel)
platoba9	539891	420795.21	-2.62	0.01	Platform profile (shore parallel)
platoba10	539889	420798.64	-2.55	0.02	Platform profile (shore parallel)
platoba11	539884	420803.52	-2.61	0.02	Platform profile (shore parallel)
platoba12	539879	420808.64	-2.65	0.02	Platform profile (shore parallel)
platoba13	539876	420811.57	-2.6	0.02	Platform profile (shore parallel)
platoba14	539875	420818.72	-2.53	0.02	Platform profile (shore parallel)
platoba15	539873	420821.93	-2.54	0.02	Platform profile (shore parallel)
platoba16	539873	420825.59	-2.58	0.02	Platform profile (shore parallel)
platoba17	539873	420827.69	-2.63	0.01	Platform profile (shore parallel)
n1	539799	420823.83	-0.02	0.02	Beach sediment sample position
n2	539788	420817.5	0.42	0.02	Beach sediment sample position
n3	539778	420811.63	0.65	0.02	Beach sediment sample position
s1	539817	420797.31	-0.07	0.02	Beach sediment sample position
s2	539807	420790.02	0.49	0.02	Beach sediment sample position
s3	539796	420782.87	0.89	0.02	Beach sediment sample position

APPENDIX G
BEACH SURVEY DATA FROM EASINGTON
JULY 2006

BEACH Survey data from EASINGTON: July 2006

Point Id	Easting	Northing	Orth. Height	Coordinate Quality	Description
Station1	539893.46	420515.19	19.08	0	Base station
btnc1	539634.87	421190.4	-2.36	0.01	Beach/platform profile (shore normal)
btnc2	539630.87	421187.11	-2.29	0.01	Beach/platform profile (shore normal)
btnc3	539626.88	421183.76	-2.18	0.02	Beach/platform profile (shore normal)
btnc4	539622.99	421180.7	-2.08	0.02	Beach/platform profile (shore normal)
btnc5	539619.16	421177.52	-1.98	0.02	Beach/platform profile (shore normal)
btnc6	539615.3	421174.04	-1.88	0.02	Beach/platform profile (shore normal)
btnc7	539611.42	421170.73	-1.74	0.02	Beach/platform profile (shore normal)
btnc8	539607.59	421167.21	-1.61	0.02	Beach/platform profile (shore normal)
btnc9	539603.35	421163.62	-1.49	0.01	Beach/platform profile (shore normal)
btnc10	539599.27	421160.13	-1.33	0.01	Beach/platform profile (shore normal)
btnc11	539595.17	421156.51	-1.16	0.02	Beach/platform profile (shore normal)
btnc12	539591.09	421152.98	-1.02	0.01	Beach/platform profile (shore normal)
btnc13	539586.92	421149.44	-0.87	0.01	Beach/platform profile (shore normal)
btnc14	539582.88	421146	-0.73	0.02	Beach/platform profile (shore normal)
btnc15	539578.96	421142.63	-0.58	0.02	Beach/platform profile (shore normal)
btnc16	539574.78	421139.15	-0.43	0.02	Beach/platform profile (shore normal)
btnc17	539570.86	421135.95	-0.29	0.01	Beach/platform profile (shore normal)
btnc18	539566.71	421132.7	-0.15	0.02	Beach/platform profile (shore normal)
btnc19	539562.68	421129.43	-0.03	0.02	Beach/platform profile (shore normal)
btnc20	539558.68	421126.2	0.09	0.02	Beach/platform profile (shore normal)
btnc21	539554.68	421122.76	0.21	0.02	Beach/platform profile (shore normal)
btnc22	539550.71	421119.39	0.3	0.02	Beach/platform profile (shore normal)
btnc23	539546.83	421116.01	0.36	0.02	Beach/platform profile (shore normal)
btnc24	539542.98	421112.71	0.47	0.01	Beach/platform profile (shore normal)
btnc25	539538.98	421109.2	0.48	0.01	Beach/platform profile (shore normal)
btnc26	539534.9	421105.49	0.73	0.01	Beach/platform profile (shore normal)
btnc27	539530.88	421101.81	1.21	0.02	Beach/platform profile (shore normal)
btnc28	539528.93	421099.68	1.68	0.02	Beach/platform profile (shore normal)
bc1	539612.42	420976.75	1.57	0.02	Base of cliff
bc2	539613.58	420971.45	1.85	0.01	Base of cliff
bc3	539617.18	420967.11	1.81	0.02	Base of cliff
bc4	539619.8	420961.46	1.93	0.01	Base of cliff
bc5	539624.86	420957.55	1.78	0.02	Base of cliff
bc6	539628.77	420953.66	1.74	0.02	Base of cliff
bc7	539631.5	420947.66	1.9	0.02	Base of cliff
bc8	539636.31	420943.25	1.86	0.02	Base of cliff
bc9	539639.48	420938.35	1.95	0.01	Base of cliff
bc10	539647.24	420933.94	1.64	0.02	Base of cliff

bc11	539649.51	420929.67	1.76	0.02	Base of cliff
bc12	539653.1	420925.48	1.76	0.02	Base of cliff
bc13	539655.98	420920.96	1.84	0.02	Base of cliff
bc14	539657.98	420915.22	2.06	0.03	Base of cliff
bc15	539660.75	420910.18	2.28	0.02	Base of cliff
bc16	539663.72	420905.86	2.38	0.02	Base of cliff
bc17	539666.64	420901.07	2.6	0.03	Base of cliff
bc18	539669.72	420896.43	2.76	0.02	Base of cliff
bc19	539674.31	420893.12	2.49	0.03	Base of cliff
bc20	539678.64	420889.14	2.5	0.02	Base of cliff
bc21	539681.4	420884.12	2.62	0.04	Base of cliff
bc22	539687.83	420882.4	1.99	0.05	Base of cliff
bc23	539690.62	420879.09	2.09	0.05	Base of cliff
bc24	539695.67	420876.48	1.83	0.05	Base of cliff
bc25	539697.81	420871.9	2.03	0.02	Base of cliff
bc26	539701.18	420868.36	2.03	0.02	Base of cliff
bc27	539704.53	420864.09	2.14	0.02	Base of cliff
bc28	539707.58	420859.84	2.2	0.04	Base of cliff
bc29	539711.07	420855.82	2.22	0.02	Base of cliff
bc30	539715.19	420852.25	2	0.02	Base of cliff
bc31	539718.09	420845.3	2.13	0.02	Base of cliff
bc32	539722.55	420841.46	2.18	0.03	Base of cliff
bc33	539723.96	420836.52	2.5	0.02	Base of cliff
bc34	539728.81	420833.06	2.34	0.02	Base of cliff
bc35	539731.04	420828.01	2.6	0.02	Base of cliff
bc36	539733.24	420823.65	2.81	0.02	Base of cliff
bc37	539733.85	420818.32	3.19	0.01	Base of cliff
bc38	539736.89	420815.31	3.31	0.02	Base of cliff
bc39	539739.63	420812.3	3.41	0.02	Base of cliff
bc40	539743.48	420809.31	3.34	0.01	Base of cliff
bc41	539744.21	420805.15	3.71	0.02	Base of cliff
bc42	539747.01	420801.23	3.87	0.02	Base of cliff
bc43	539747.96	420796.9	4.14	0.02	Base of cliff
bc44	539751.42	420793.54	4.04	0.02	Base of cliff
bc45	539753.84	420788.88	4.1	0.02	Base of cliff
bc46	539759.25	420786.03	3.89	0.02	Base of cliff
bc47	539760.75	420780.92	3.92	0.02	Base of cliff
bc48	539762.87	420776.26	3.95	0.04	Base of cliff
bc49	539768.27	420774.5	3.77	0.02	Base of cliff
bc50	539769.72	420770.21	3.65	0.02	Base of cliff
bc51	539769.59	420764.98	3.67	0.02	Base of cliff
bc52	539773.01	420761.43	3.57	0.02	Base of cliff
bc53	539775.02	420757.3	3.58	0.01	Base of cliff
bc54	539776.76	420752.99	3.5	0.02	Base of cliff
bc55	539779.31	420748.98	3.46	0.01	Base of cliff
bc56	539783.24	420745.98	3.35	0.02	Base of cliff
bc57	539785.9	420742.44	3.32	0.02	Base of cliff
bc58	539788.9	420737.72	3.29	0.01	Base of cliff
bc59	539791.87	420733.53	3.18	0.01	Base of cliff
bc60	539794.32	420729.33	3.26	0.01	Base of cliff
bc61	539798.76	420727.23	3.09	0.02	Base of cliff
bc62	539801	420723.28	3.09	0.02	Base of cliff
bc63	539799.35	420718.65	3.19	0.01	Base of cliff
bc64	539798.7	420714.12	3.51	0.02	Base of cliff
bc65	539801.66	420710.96	3.43	0.02	Base of cliff
bc66	539806.27	420709.48	3.22	0.02	Base of cliff
bc67	539810.16	420707.36	3.06	0.02	Base of cliff
bc68	539813.28	420703.4	3.13	0.01	Base of cliff
bc69	539816.03	420700.53	3.13	0.02	Base of cliff
bc70	539817.31	420697.57	3.21	0.02	Base of cliff
bc71	539819.24	420693.27	3.33	0.02	Base of cliff
bc72	539823.42	420694.22	2.89	0.02	Base of cliff

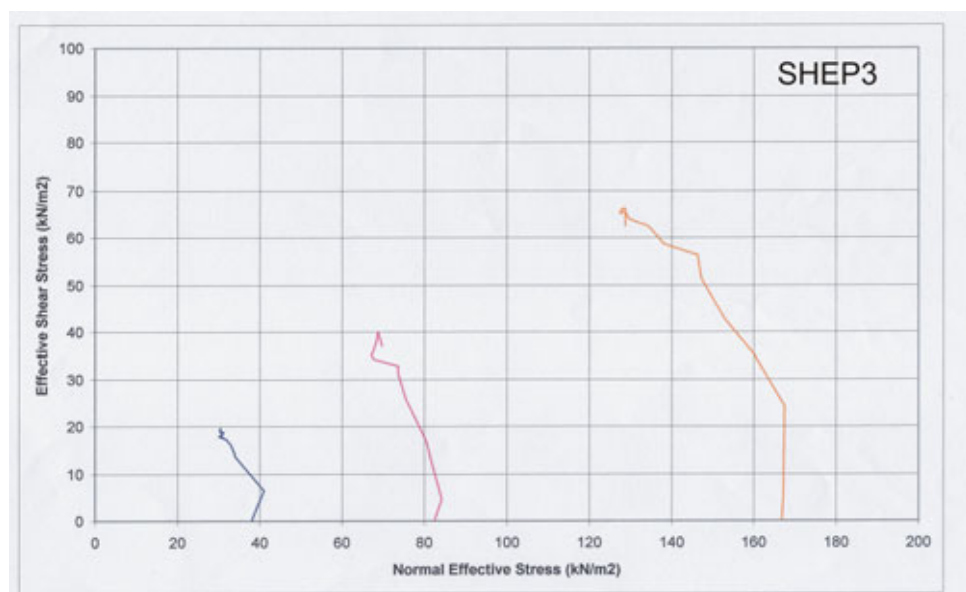
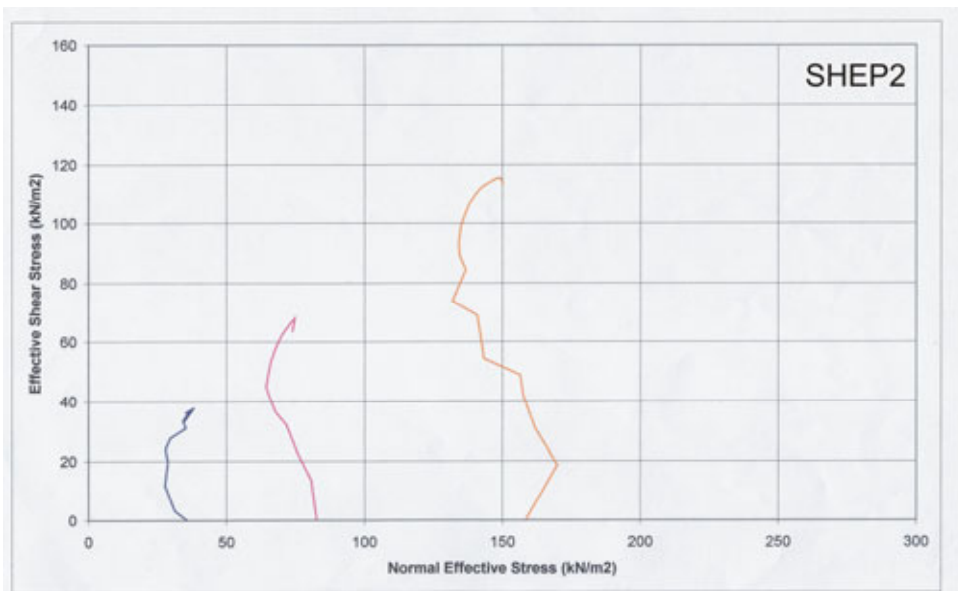
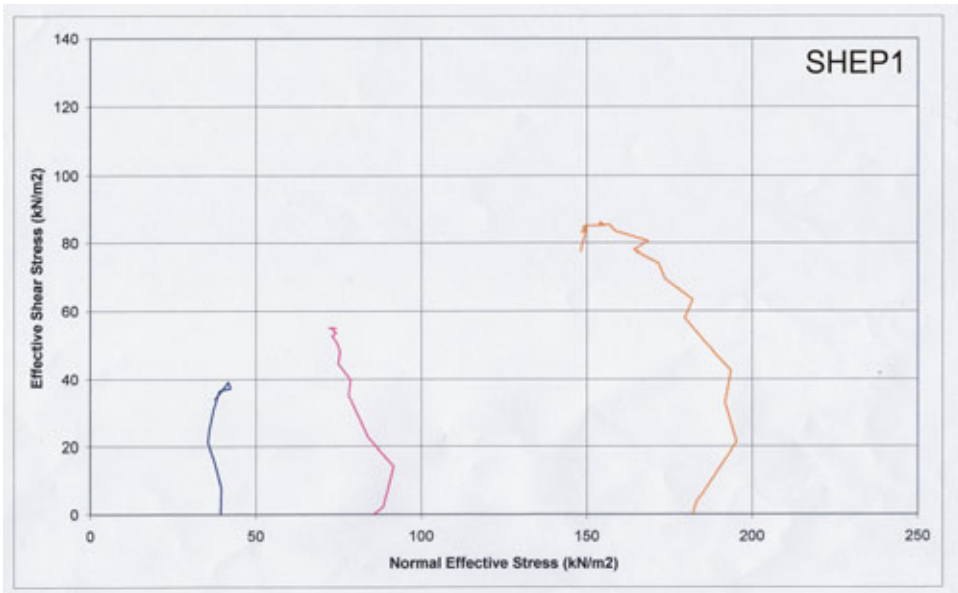
bc73	539826.45	420691.43	2.96	0.02	Base of cliff
bc74	539831.97	420689.8	2.75	0.01	Base of cliff
bc75	539834.54	420686.38	2.85	0.01	Base of cliff
bc76	539835.9	420682.19	2.84	0.02	Base of cliff
bc77	539839.05	420678.51	2.78	0.02	Base of cliff
bc78	539840.5	420673.42	2.7	0.02	Base of cliff
bc79	539841.45	420668.54	2.77	0.02	Base of cliff
bc80	539843.24	420663.78	2.65	0.02	Base of cliff
bc81	539845.05	420659.47	2.81	0.02	Base of cliff
bc82	539848.13	420655.75	2.71	0.02	Base of cliff
bc83	539848.06	420650.93	2.95	0.02	Base of cliff
bc84	539851.55	420647.49	2.85	0.02	Base of cliff
bc85	539855.01	420643.7	2.63	0.01	Base of cliff
bc86	539858.07	420640.2	2.59	0.02	Base of cliff
bpc1	539792.58	420727.4	4.8	0.02	Beach profile c (shore normal)
bpc2	539794.7	420728.85	3.24	0.02	Beach profile c (shore normal)
bpc3	539799.03	420731.4	3.12	0.02	Beach profile c (shore normal)
bpc4	539803.23	420733.94	3.19	0.02	Beach profile c (shore normal)
bpc5	539807.27	420736.47	3.19	0.02	Beach profile c (shore normal)
bpc6	539811.67	420739.22	2.72	0.02	Beach profile c (shore normal)
bpc7	539816.3	420742.22	2.33	0.02	Beach profile c (shore normal)
bpc8	539820.36	420744.85	1.92	0.02	Beach profile c (shore normal)
bpc9	539825.03	420747.91	1.44	0.02	Beach profile c (shore normal)
bpc10	539829.48	420750.83	0.93	0.02	Beach profile c (shore normal)
bpc11	539833.64	420753.71	0.4	0.02	Beach profile c (shore normal)
bpc12	539837.87	420756.64	-0.08	0.02	Beach profile c (shore normal)
bpc13	539842.32	420759.71	-0.49	0.02	Beach profile c (shore normal)
bpc14	539846.88	420762.9	-0.74	0.02	Beach profile c (shore normal)
bpc15	539851.64	420766.21	-1	0.02	Beach profile c (shore normal)
bpc16	539856.09	420769.46	-1.14	0.02	Beach profile c (shore normal)
bpc17	539860.88	420773.06	-1.32	0.02	Beach profile c (shore normal)
bpc18	539865.07	420775.66	-1.42	0.02	Beach profile c (shore normal)
bpc19	539869.31	420778.55	-1.59	0.02	Beach profile c (shore normal)
bpc20	539873.69	420781.28	-1.8	0.02	Beach profile c (shore normal)
bpc21	539878.04	420784.2	-1.99	0.02	Beach profile c (shore normal)
bpc22	539882.43	420787.16	-2.24	0.02	Beach profile c (shore normal)
bpc23	539886.72	420790.01	-2.45	0.02	Beach profile c (shore normal)
bpc24	539890.79	420792.78	-2.63	0.02	Beach profile c (shore normal)
bpc25	539894.85	420795.87	-2.75	0.02	Beach profile c (shore normal)
bpb1	539771	420763.1	3.59	0.02	Beach profile b (shore normal)
bpb2	539775.12	420765.69	3.51	0.02	Beach profile b (shore normal)
bpb3	539778.55	420768.18	3.4	0.02	Beach profile b (shore normal)
bpb4	539782.69	420771.15	2.9	0.02	Beach profile b (shore normal)
bpb5	539786.92	420774.13	2.45	0.02	Beach profile b (shore normal)
bpb6	539791.23	420777.17	1.98	0.02	Beach profile b (shore normal)
bpb7	539795.67	420780.32	1.49	0.02	Beach profile b (shore normal)
bpb8	539799.92	420783.45	1.02	0.02	Beach profile b (shore normal)
bpb9	539804.01	420786.54	0.47	0.02	Beach profile b (shore normal)
bpb10	539808.15	420789.71	-0.07	0.02	Beach profile b (shore normal)
bpb11	539812.27	420792.67	-0.56	0.02	Beach profile b (shore normal)
bpb12	539816.29	420795.59	-0.87	0.02	Beach profile b (shore normal)
bpb13	539820.23	420798.44	-1.07	0.02	Beach profile b (shore normal)
bpb14	539824.27	420801.26	-1.18	0.02	Beach profile b (shore normal)
bpb15	539828.72	420804.35	-1.37	0.02	Beach profile b (shore normal)
bpb16	539833.27	420807.41	-1.59	0.02	Beach profile b (shore normal)
bpb17	539837.71	420810.43	-1.79	0.02	Beach profile b (shore normal)
bpb18	539842.07	420813.45	-1.98	0.02	Beach profile b (shore normal)
bpb19	539846.42	420816.33	-2.18	0.02	Beach profile b (shore normal)
bpb20	539850.74	420819.46	-2.27	0.02	Beach profile b (shore normal)
bpb21	539854.54	420822.24	-2.36	0.02	Beach profile b (shore normal)
bpb22	539858.73	420825.18	-2.47	0.02	Beach profile b (shore normal)
bpb23	539863.18	420828.27	-2.5	0.02	Beach profile b (shore normal)

bpb24	539867.67	420831.49	-2.67	0.02	Beach profile b (shore normal)
bpb25	539871.92	420834.57	-2.81	0.02	Beach profile b (shore normal)
bpb26	539876.36	420837.84	-2.78	0.02	Beach profile b (shore normal)
bpb27	539880.64	420840.98	-2.83	0.02	Beach profile b (shore normal)
bpb28	539884.84	420844.28	-2.95	0.02	Beach profile b (shore normal)
bpb29	539888.21	420847.09	-3.07	0.02	Beach profile b (shore normal)
bpa1	539738.67	420813.5	3.73	0.02	Beach profile a (shore normal)
bpa2	539739.11	420813.79	3.28	0.02	Beach profile a (shore normal)
bpa3	539743.73	420816.47	2.6	0.01	Beach profile a (shore normal)
bpa4	539748.36	420819.29	1.99	0.02	Beach profile a (shore normal)
bpa5	539752.39	420821.8	1.55	0.02	Beach profile a (shore normal)
bpa6	539756.77	420824.43	1.09	0.02	Beach profile a (shore normal)
bpa7	539761.45	420827.25	0.6	0.02	Beach profile a (shore normal)
bpa8	539766.11	420830.14	0.05	0.01	Beach profile a (shore normal)
bpa9	539770.71	420832.97	-0.47	0.02	Beach profile a (shore normal)
bpa10	539775.11	420835.61	-0.84	0.01	Beach profile a (shore normal)
bpa11	539780.11	420838.7	-1.18	0.02	Beach profile a (shore normal)
bpa12	539784.6	420841.52	-1.41	0.02	Beach profile a (shore normal)
bpa13	539788.87	420844.24	-1.64	0.02	Beach profile a (shore normal)
bpa14	539793.47	420847.04	-1.84	0.02	Beach profile a (shore normal)
bpa15	539798.16	420849.95	-2.03	0.02	Beach profile a (shore normal)
bpa16	539802.62	420852.62	-2.22	0.02	Beach profile a (shore normal)
bpa17	539806.62	420855.1	-2.26	0.01	Beach profile a (shore normal)
bpa18	539810.49	420857.46	-2.26	0.02	Beach profile a (shore normal)
bpa19	539815.76	420860.82	-2.29	0.02	Beach profile a (shore normal)
bpa20	539820.32	420863.5	-2.38	0.01	Beach profile a (shore normal)
bpa21	539824.89	420866.42	-2.44	0.01	Beach profile a (shore normal)
bpa22	539829.57	420869.22	-2.58	0.01	Beach profile a (shore normal)
bpa23	539833.91	420872.08	-2.64	0.02	Beach profile a (shore normal)
bpa24	539838.26	420874.81	-2.73	0.02	Beach profile a (shore normal)
bpa25	539842.29	420877.34	-2.85	0.01	Beach profile a (shore normal)
bpa26	539846.38	420879.77	-2.8	0.01	Beach profile a (shore normal)
bara1	539871.95	420895.51	-3.04	0.01	Sand bar cross-profile a
bara2	539874.58	420896.96	-2.62	0.01	Sand bar cross-profile a
bara3	539878.3	420899.12	-2.39	0.02	Sand bar cross-profile a
bara4	539882.6	420901.79	-2.35	0.01	Sand bar cross-profile a
bara5	539886.91	420904.58	-2.4	0.01	Sand bar cross-profile a
bara6	539891.53	420907.36	-2.45	0.02	Sand bar cross-profile a
bara7	539895.93	420910.06	-2.47	0.01	Sand bar cross-profile a
bara8	539900.46	420912.85	-2.51	0.02	Sand bar cross-profile a
bara9	539904.93	420915.47	-2.56	0.01	Sand bar cross-profile a
bara10	539909.56	420918.26	-2.6	0.01	Sand bar cross-profile a
bara11	539914.09	420920.96	-2.66	0.01	Sand bar cross-profile a
bara12	539918.78	420923.79	-2.74	0.01	Sand bar cross-profile a
bara13	539923.54	420926.73	-2.74	0.01	Sand bar cross-profile a
bara14	539928.82	420929.9	-2.8	0.01	Sand bar cross-profile a
bara15	539933.64	420932.71	-2.81	0.01	Sand bar cross-profile a
bara16	539938.43	420935.53	-2.81	0.01	Sand bar cross-profile a
bara17	539943.25	420938.48	-2.76	0.02	Sand bar cross-profile a
bara18	539947.71	420941.19	-2.74	0.01	Sand bar cross-profile a
bara19	539952.18	420944.1	-2.71	0.01	Sand bar cross-profile a
bara20	539956.6	420946.99	-2.76	0.01	Sand bar cross-profile a
bara21	539961.12	420949.96	-2.76	0.01	Sand bar cross-profile a
barb1	539919.93	420869.66	-2.98	0.01	Sand bar cross-profile b
barb2	539922.05	420871.3	-2.66	0.01	Sand bar cross-profile b
barb3	539925.41	420873.75	-2.53	0.01	Sand bar cross-profile b
barb4	539929.78	420876.68	-2.55	0.01	Sand bar cross-profile b
barb5	539934.44	420879.88	-2.63	0.01	Sand bar cross-profile b
barb6	539938.79	420882.85	-2.67	0.01	Sand bar cross-profile b
barb7	539943.05	420885.77	-2.68	0.01	Sand bar cross-profile b
barb8	539947.55	420888.79	-2.69	0.01	Sand bar cross-profile b
barb9	539952	420891.77	-2.7	0.01	Sand bar cross-profile b

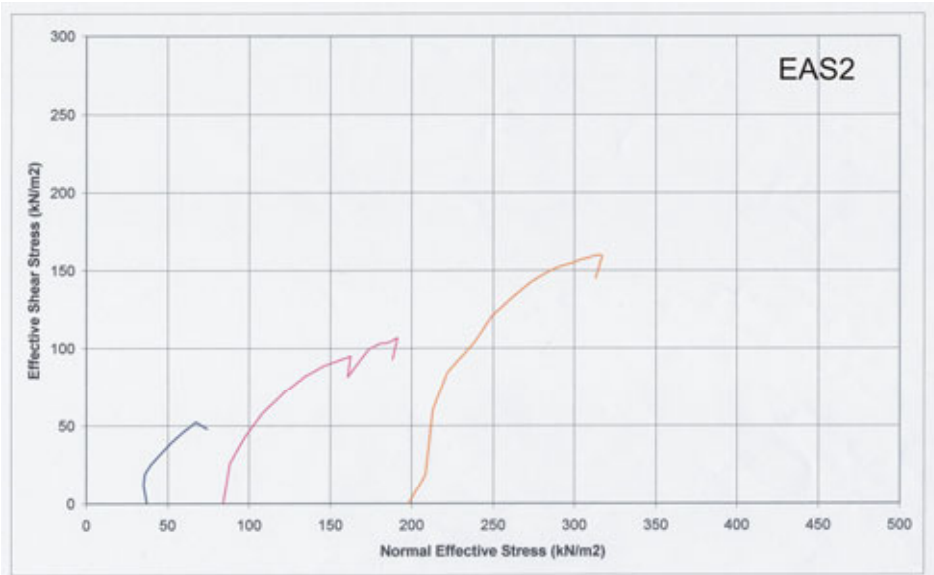
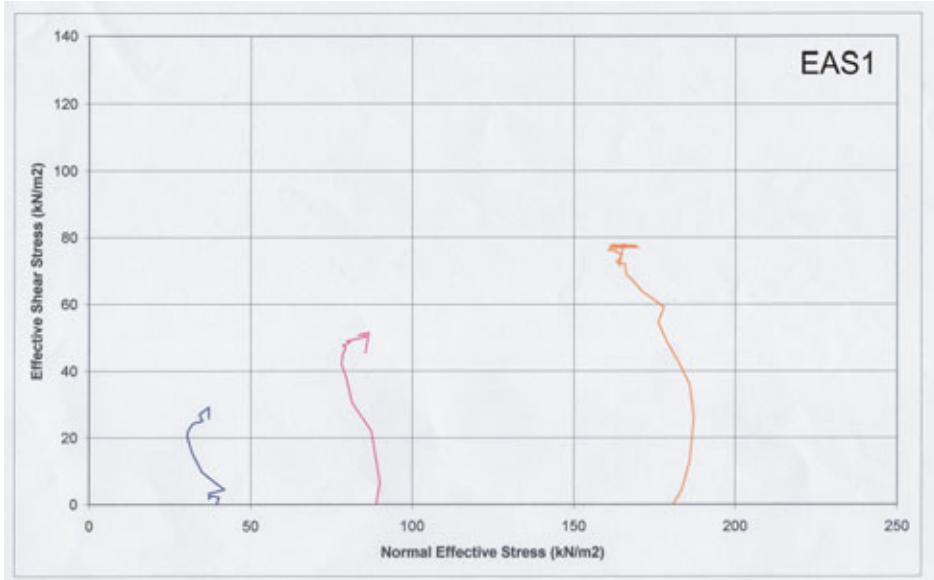
barb10	539956.48	420894.74	-2.74	0.01	Sand bar cross-profile b
barb11	539960.82	420897.74	-2.81	0.01	Sand bar cross-profile b
barb12	539965.04	420900.73	-2.9	0.01	Sand bar cross-profile b
barb13	539969.07	420903.65	-2.91	0.01	Sand bar cross-profile b
barb14	539973.19	420906.66	-2.87	0.01	Sand bar cross-profile b
barb15	539977.28	420909.71	-2.8	0.01	Sand bar cross-profile b
barb16	539981.26	420912.84	-2.77	0.01	Sand bar cross-profile b
barb17	539985.17	420916.09	-2.81	0.01	Sand bar cross-profile b
barb18	539989.73	420919.29	-2.87	0.01	Sand bar cross-profile b
barc1	539960.49	420839.77	-3.01	0.01	Sand bar cross-profile c
barc2	539962.44	420841.04	-2.79	0.01	Sand bar cross-profile c
barc3	539966.54	420843.66	-2.72	0.01	Sand bar cross-profile c
barc4	539970.92	420846.41	-2.73	0.01	Sand bar cross-profile c
barc5	539975.56	420849.33	-2.75	0.01	Sand bar cross-profile c
barc6	539980.12	420852.3	-2.8	0.01	Sand bar cross-profile c
barc7	539984.79	420855.44	-2.86	0.01	Sand bar cross-profile c
barc8	539989.36	420858.44	-2.89	0.01	Sand bar cross-profile c
barc9	539993.94	420861.58	-2.9	0.01	Sand bar cross-profile c
barc10	539998.54	420864.72	-2.89	0.01	Sand bar cross-profile c
barc11	540003.01	420867.95	-2.89	0.01	Sand bar cross-profile c
barc12	540007.4	420871.14	-2.87	0.01	Sand bar cross-profile c
barc13	540012.21	420874.23	-2.89	0.01	Sand bar cross-profile c
folad1	539887.93	420878.74	-2.79	0.01	Pholad concentration on platform
folad2	539882.05	420873.09	-2.79	0.01	Pholad concentration on platform
folad3	539877.02	420890.79	-2.83	0.01	Pholad concentration on platform
dc	539835.97	420864.36	-2.37	0.02	Univ Sussex erosion pin
db	539819.53	420863.62	-2.18	0.02	Univ Sussex erosion pin
da	539828.41	420826.37	-1.95	0.01	Univ Sussex erosion pin
bb1	539919.2	420755.6	-2.54	0.02	Base of beach
bb2	539913.64	420756.43	-2.43	0.01	Base of beach
bb3	539909.21	420759.1	-2.41	0.01	Base of beach
bb4	539908.42	420764.34	-2.58	0.01	Base of beach
bb5	539904.29	420767.77	-2.51	0.02	Base of beach
bb6	539900.03	420771.21	-2.46	0.02	Base of beach
bb7	539895.75	420773.91	-2.38	0.01	Base of beach
bb8	539893.2	420777.58	-2.46	0.01	Base of beach
bb9	539889.72	420781.19	-2.35	0.01	Base of beach
bb10	539889.33	420786.28	-2.46	0.01	Base of beach
bb11	539885.92	420791.03	-2.42	0.02	Base of beach
bb12	539885.54	420796.02	-2.54	0.01	Base of beach
bb13	539884.5	420800.72	-2.62	0.01	Base of beach
bb14	539885.76	420804.15	-2.68	0.01	Base of beach
bb15	539868.86	420816.19	-2.51	0.01	Base of beach
bb16	539862.93	420817.16	-2.35	0.01	Base of beach
bb17	539861.19	420822.37	-2.46	0.01	Base of beach
bb18	539857.36	420826.07	-2.43	0.01	Base of beach
bb19	539853.5	420829.85	-2.39	0.01	Base of beach
bb20	539844.72	420828.94	-2.4	0.01	Base of beach
bb21	539840.28	420830.95	-2.33	0.02	Base of beach
bb22	539835.43	420831.95	-2.27	0.02	Base of beach
bb23	539831.98	420834.5	-2.28	0.01	Base of beach
bb24	539828.43	420837.89	-2.32	0.01	Base of beach
bb25	539823.66	420840.7	-2.21	0.01	Base of beach
bb26	539819.36	420842.52	-2.19	0.01	Base of beach
bb27	539814.09	420843.41	-2.13	0.02	Base of beach
bb28	539809.1	420840.87	-2.01	0.01	Base of beach
bb29	539804.77	420840.27	-1.87	0.01	Base of beach
bb30	539802.52	420844.82	-1.97	0.01	Base of beach
bb31	539802.48	420849.88	-2.16	0.01	Base of beach
bb32	539799.74	420853.14	-2.14	0.01	Base of beach
bb33	539794.21	420854.64	-2.1	0.01	Base of beach
bb34	539788.84	420858.12	-2.09	0.01	Base of beach

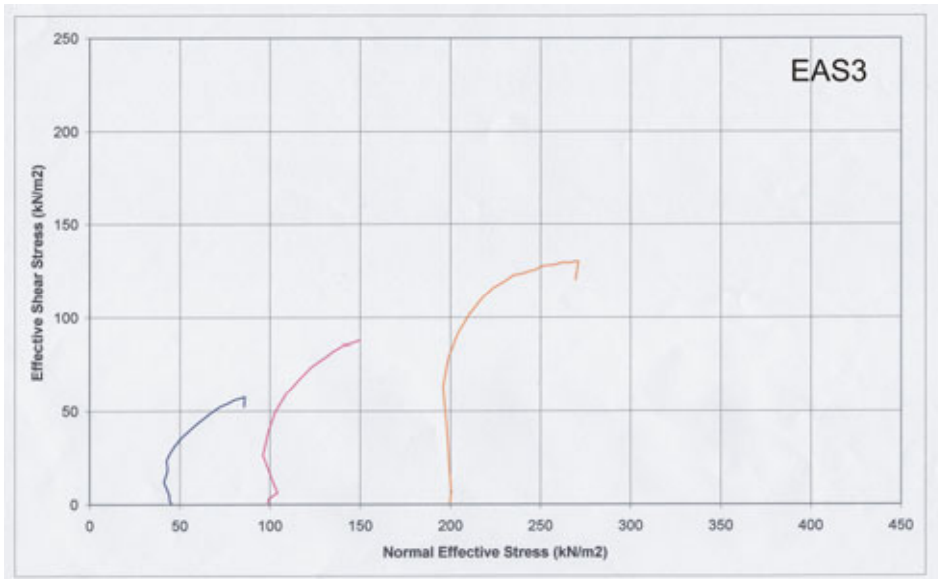
bb35	539785.1	420862.22	-2.11	0.01	Base of beach
bb36	539780.73	420865.06	-2.08	0.01	Base of beach
bb37	539775.79	420868.92	-2.12	0.01	Base of beach
bb38	539771.29	420870.35	-2.02	0.01	Base of beach
bb39	539767.18	420873.58	-1.9	0.01	Base of beach
bb40	539764.02	420877.62	-1.94	0.01	Base of beach
bb41	539759.82	420880.55	-1.83	0.01	Base of beach
bb42	539756.5	420884.18	-1.81	0.01	Base of beach
bb43	539752.98	420887.39	-1.77	0.01	Base of beach
bb44	539751.39	420892.1	-1.91	0.01	Base of beach
bb45	539748.32	420896.7	-1.88	0.01	Base of beach
bb46	539744.45	420900.2	-1.89	0.01	Base of beach
bb47	539740.16	420903.99	-1.83	0.01	Base of beach
bb48	539735.55	420906.28	-1.73	0.01	Base of beach
bb49	539731.02	420909.7	-1.67	0.02	Base of beach
bb50	539729.56	420914.26	-1.8	0.01	Base of beach
bb51	539729.46	420919.56	-1.94	0.01	Base of beach
bb52	539727.45	420924.1	-1.98	0.01	Base of beach
bb53	539724.44	420928.22	-1.89	0.01	Base of beach
bb54	539724.58	420934.96	-1.97	0.02	Base of beach
n1	539798.88	420823.8	-1.27	0.02	n1
n2	539787.39	420817.38	-0.54	0.02	n2
n3	539777.86	420811.63	0.56	0.02	n3
s3	539796.09	420782.78	1.31	0.02	s3
s2	539807.15	420790.01	-0.01	0.02	s2
s1	539817.02	420797.31	-0.94	0.02	s1
LaneBM	538318.6	420684.93	10.48	0.02	Ordnance Survey BM

APPENDIX H
TRIAxIAL STRESS-PATH PLOTS FROM WARDEN POINT



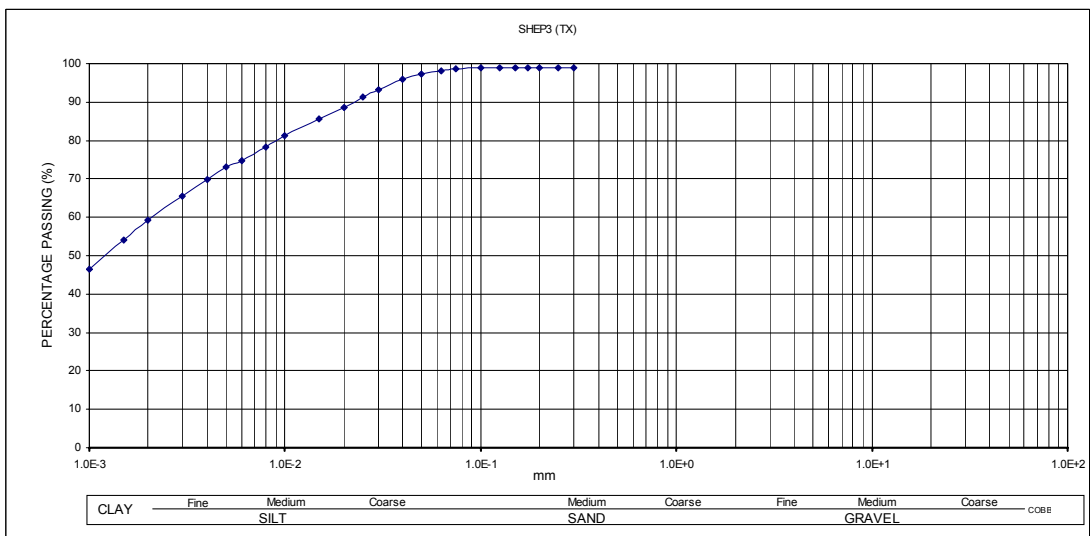
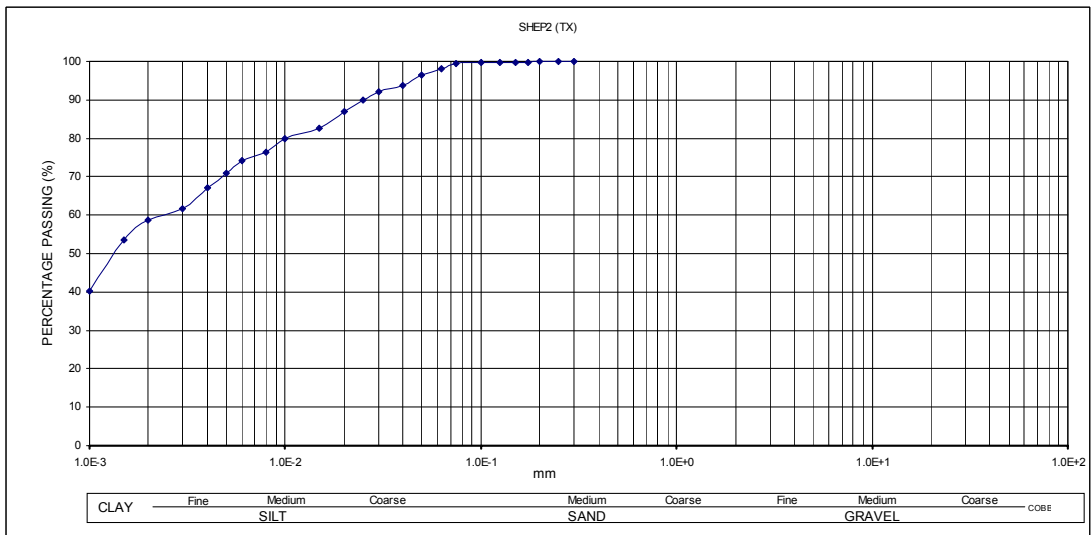
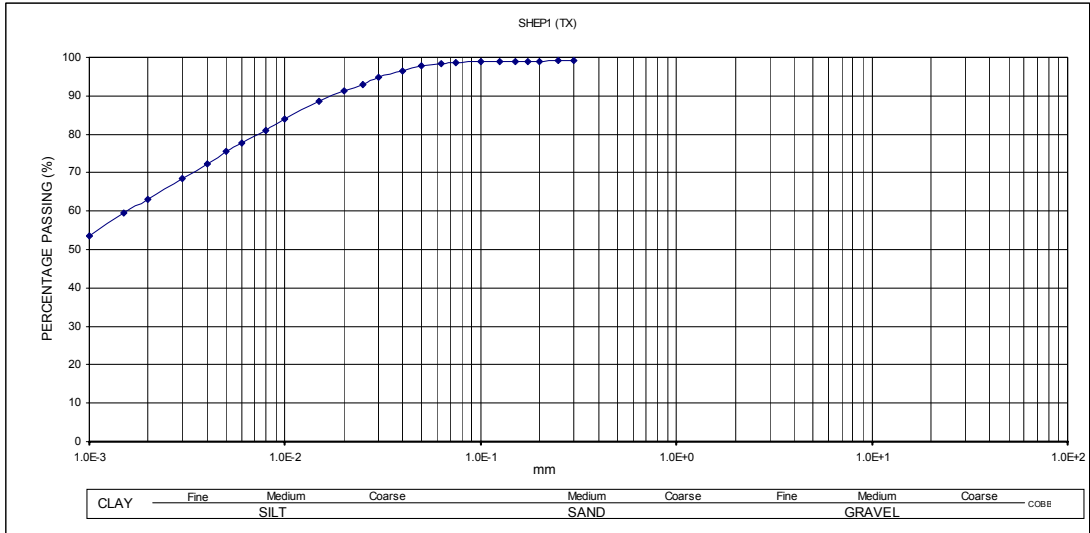
APPENDIX I
TRIAxIAL STRESS-PATH PLOTS FROM EASINGTON





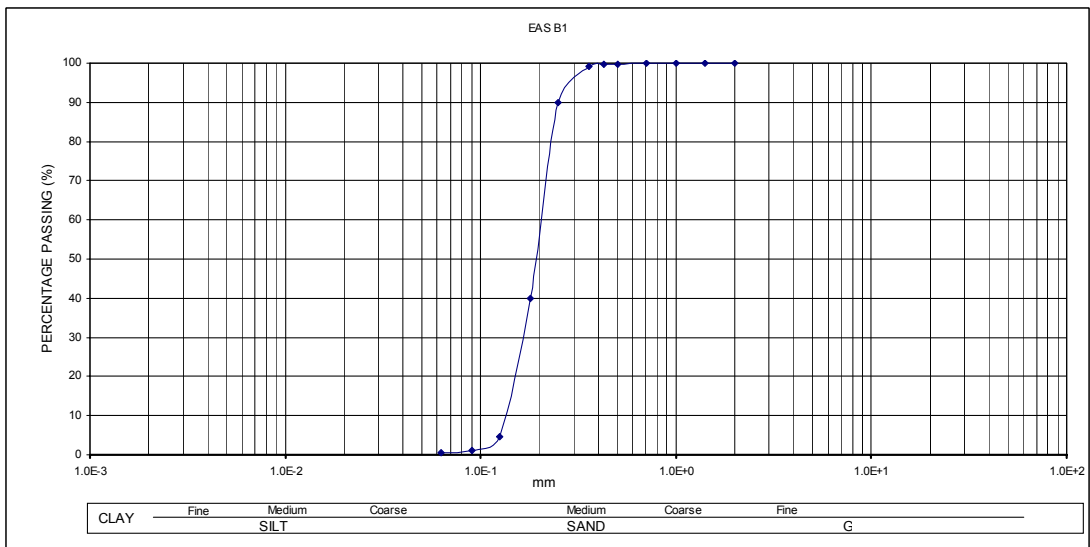
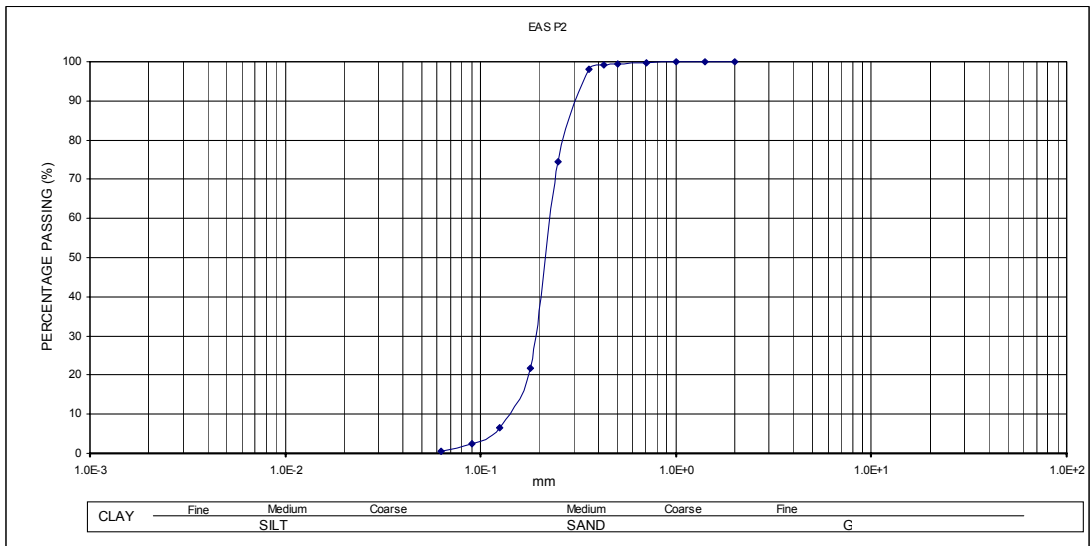
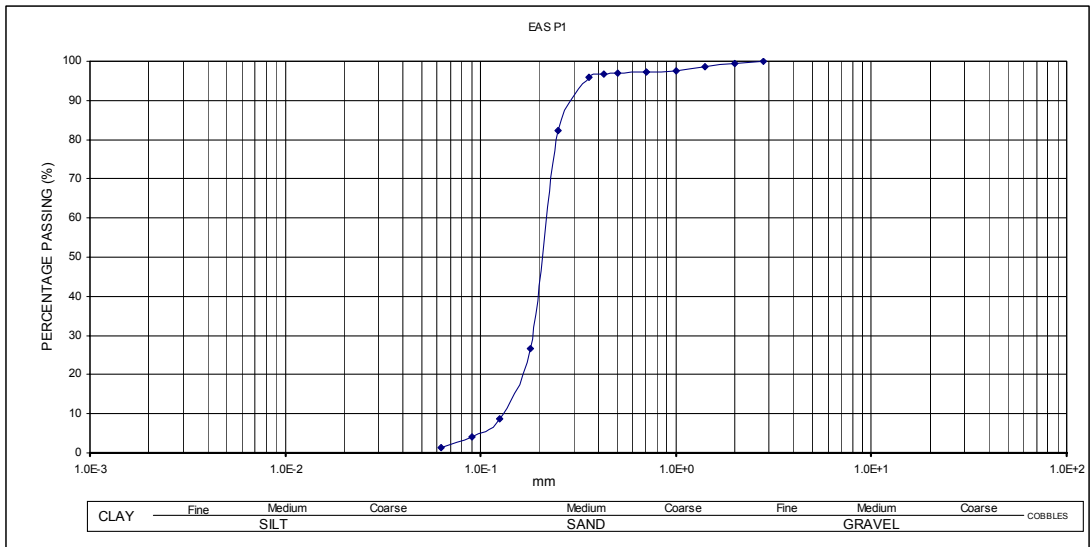
APPENDIX J
PARTICLE SIZE ANALYSIS RESULTS FROM WARDEN POINT

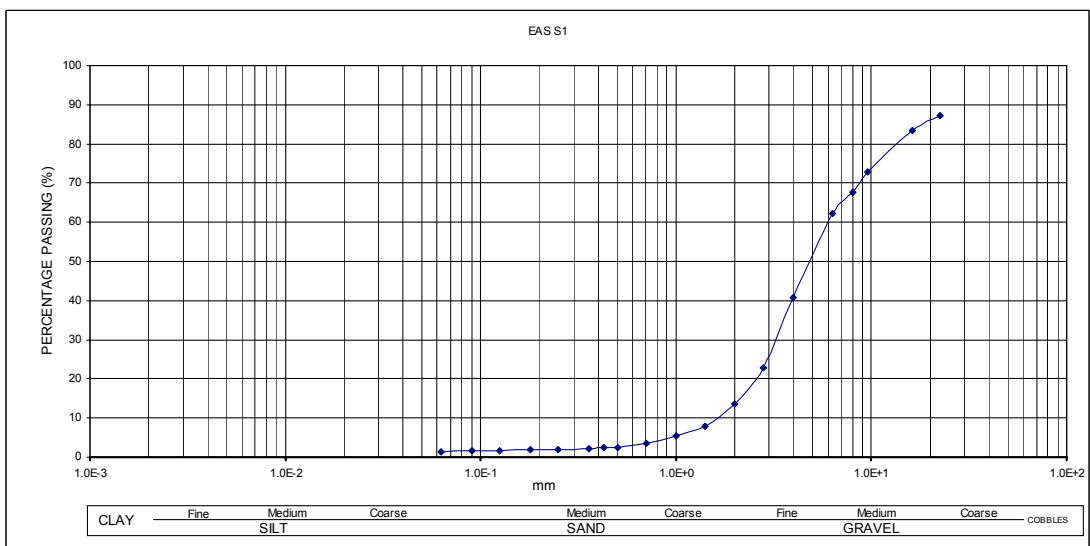
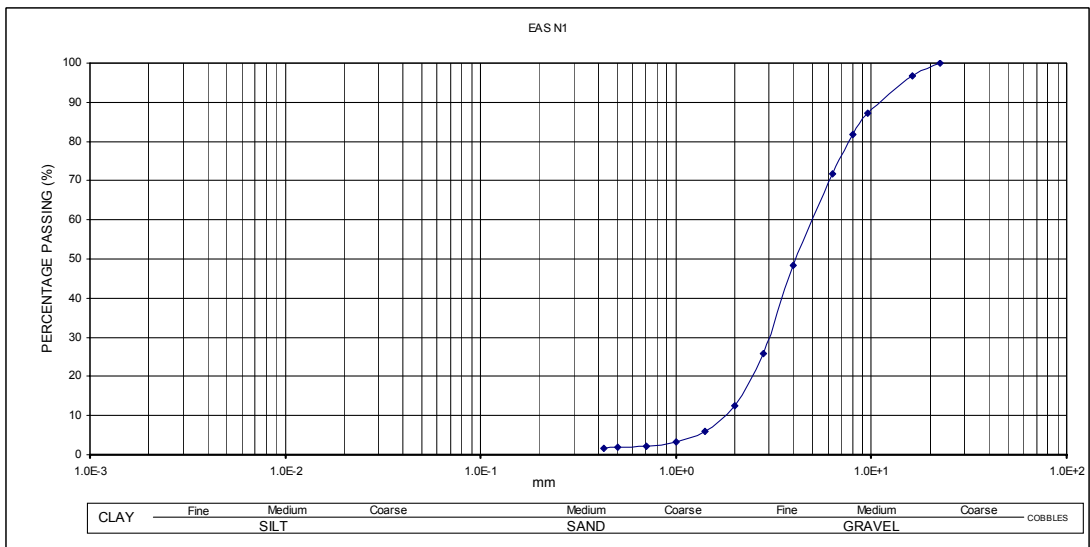
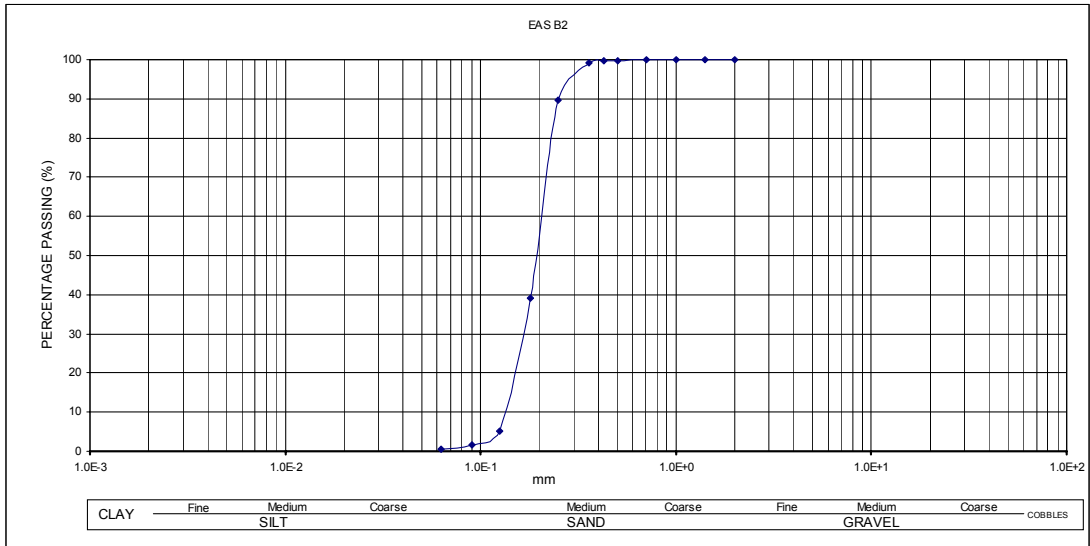
PARTICLE-SIZE ANALYSES: WARDEN POINT

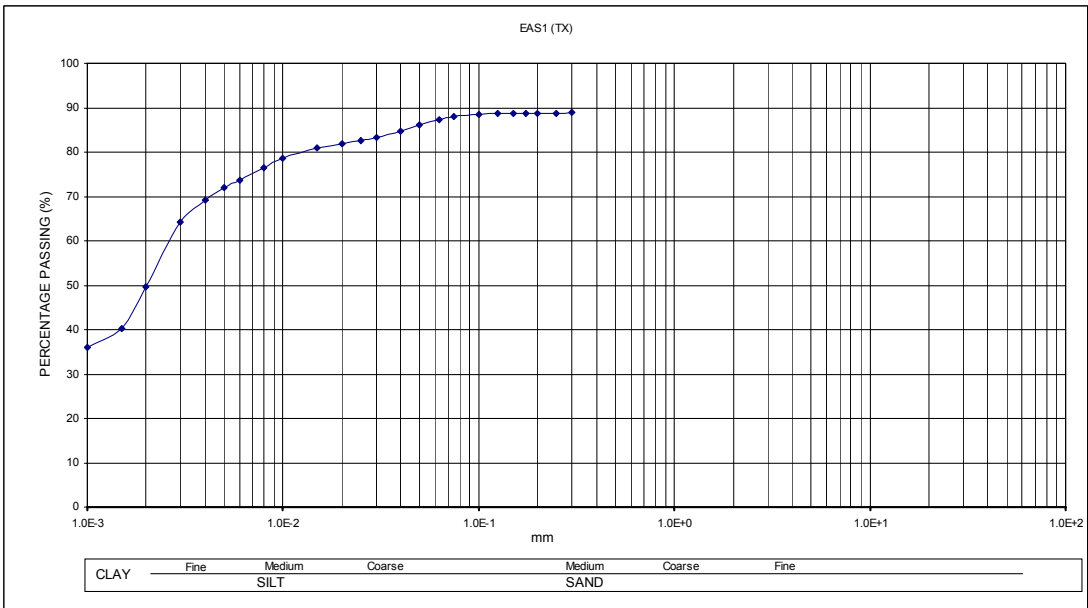
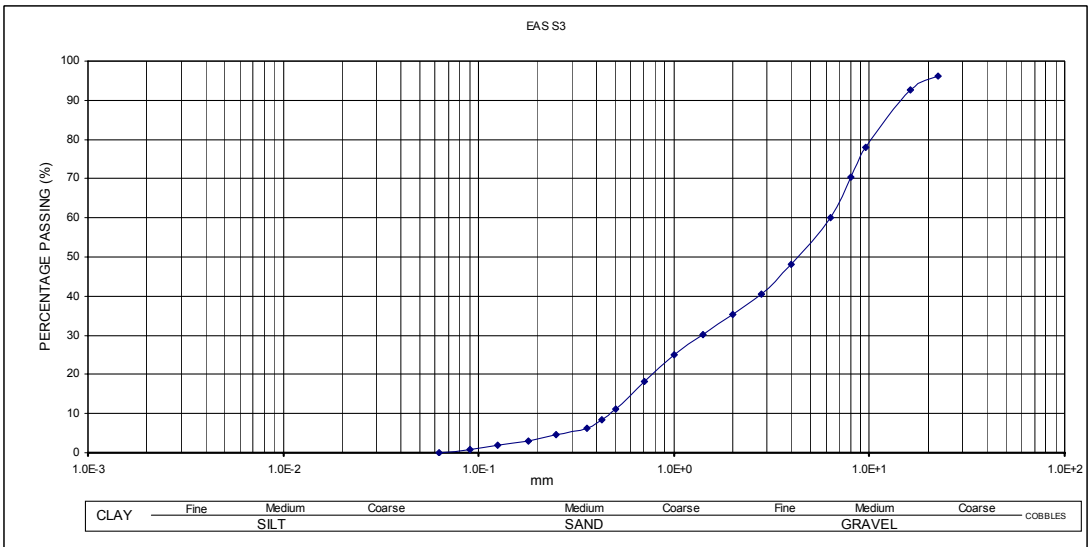
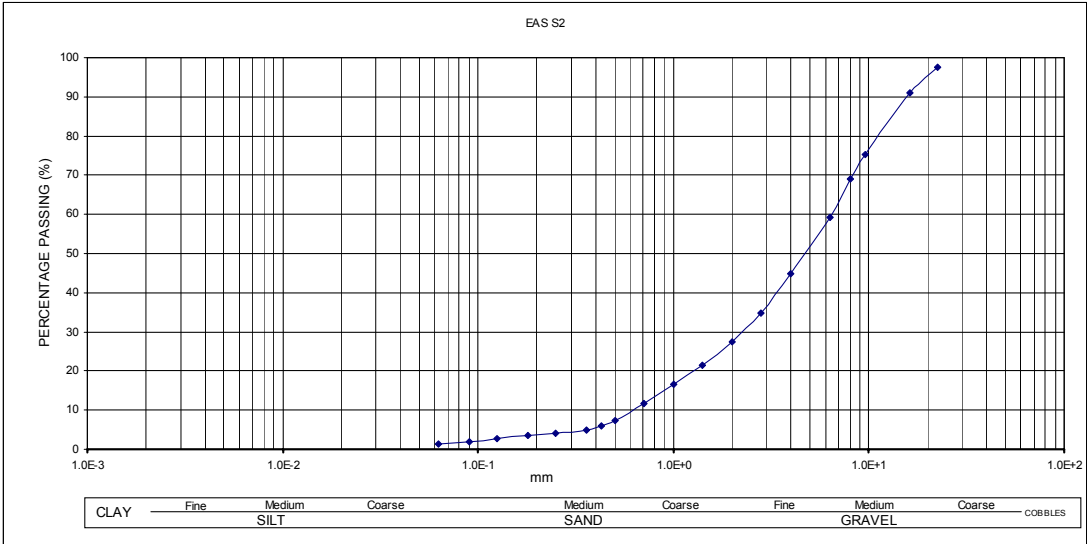


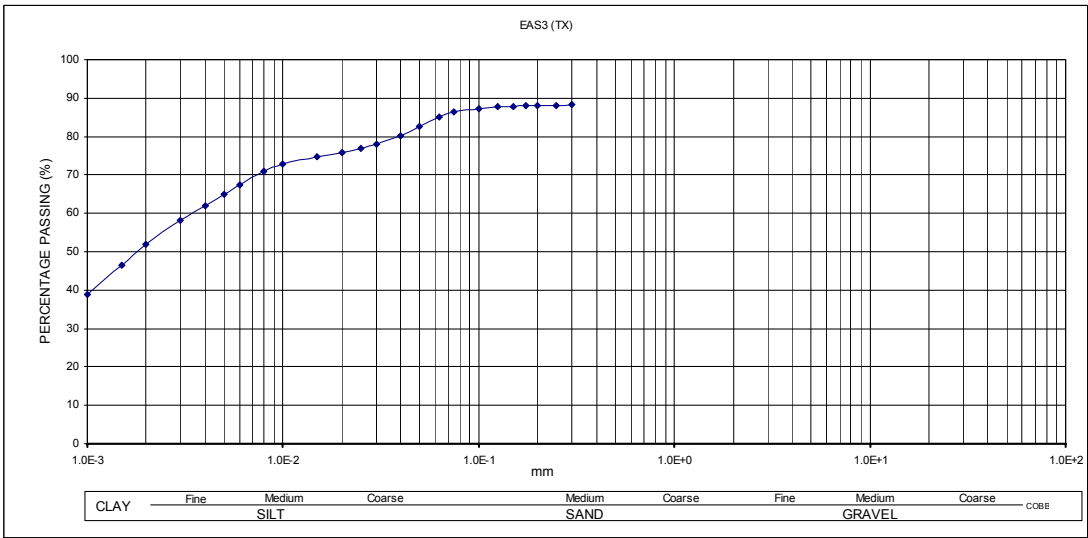
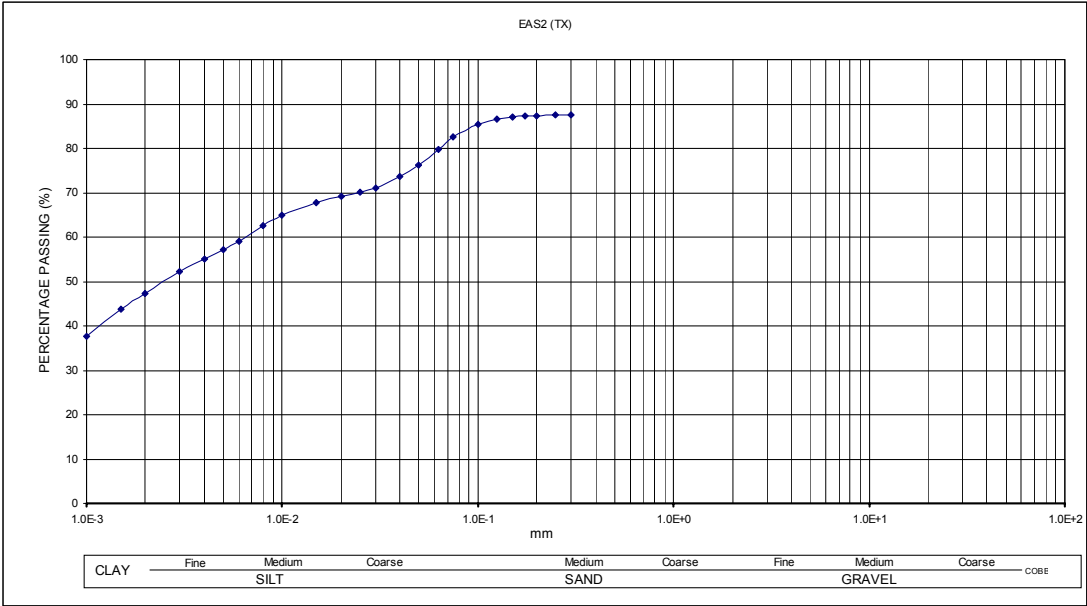
APPENDIX K
PARTICLE SIZE ANALYSIS RESULTS FROM EASINGTON

PARTICLE-SIZE ANALYSES: EASINGTON









PB 12807 TR

**Ergon House
Horseferry Road
London SW1P 2AL**

www.defra.gov.uk

